STEM CELLS AND SPERMATOGENIC LINEAGE DEVELOPMENT IN THE PRIMATE TESTIS

by

Adetunji Peter Fayomi

Doctor of Veterinary Medicine, University of Ibadan, 2008

Master of Veterinary Science, University of Ibadan, 2012

Submitted to the Graduate Faculty of

School of Medicine in partial fulfillment

of the requirements for the degree of

Doctor of Philosophy

University of Pittsburgh

2018

UNIVERSITY OF PITTSBURGH

SCHOOL OF MEDICINE

This thesis was presented

by

Adetunji Peter Fayomi

It was defended on

March 22, 2018

and approved by

Micheal Tsang (PhD), Associate Professor, Molecular Genetics and Developmental Biology

Neil Hukriede (PhD), Associate Professor, Molecular Genetics and Developmental Biology

Satdarshan Singh Monga (MD), Professor, Cellular and Molecular Pathology

Aleksander Rajkovic (MD, PhD), Professor, Molecular Genetics and Developmental Biology

Dissertation Advisor: Kyle E. Orwig (PhD), Professor, Molecular Genetics and Developmental Biology

STEM CELLS AND SPERMATOGENIC LINEAGE DEVELOPMENT IN THE PRIMATE TESTIS

Adetunji P. Fayomi, PhD

University of Pittsburgh, 2018

Stem cells in the primate testis, A_{dark} and A_{pale}, have been designated as "reserve" and "active" stem cells, respectively. It is not clear if A_{dark} participate in steady-state spermatogenesis; little is known about how these descriptions correlate with molecular markers or clone size and there are knowledge gaps on the potential use of primate stem cells for fertility preservation/restoration. We show that A_{dark} are mitotically active, slow-cycling, label-retaining cells during steady-state spermatogenesis, with evidence of self-renewal and differentiation. We found that UTF1, ENO2 and UCHL1 are markers of A_{dark} and A_{pale} spermatogonia during development and they mark undifferentiated spermatogonia in adult Rhesus Testis. We also demonstrate that undifferentiated spermatogonia (UTF1+/cKIT- cells) exist more frequently as clones of 1 or 2, less frequently as clones of 3 or 4, clones greater than 4 are rare. cKIT+ clones of 1 (~20%) and 2 (~15%) cells were also observed. Our novel approach to staging seminiferous epithelium through EDU staining revealed that cKIT+ clones of 1 or 2 cells are not stage dependent. Our data indicate that primate spermatogonia undergo both symmetric (undifferentiated) and asymmetric (differentiating) divisions during steady-state spermatogenesis. For cell-based application of primate stem cell, we show that the concentration of xenotranplantable stem cells was higher in neonatal testis. Using ITGA6, stem and progenitor population were enriched by 18-fold (FACS) and 9-fold (MACS) while stem cell activity was enriched by 5-fold (MACS). We established foundational primate SSC culture conditions. ITGA6-positive cells produced colonies with "grape-like" appearance in culture. ITGA6-positive cells retain phenotype of stem and progenitor

cells up to 14 days in culture. For tissue-based application of primate stem cell, we grafted fresh and frozen-thawed prepubertal testicular tissues in the subcutis of the back and scrotal skin. Volume of testicular tissue grafts increased in graft sites. Although weight of recovered tissue grafts from the scrotal area were higher than from the back, spermatogenesis was confirmed in grafts with spermatids/sperm cells in more than 70% of tissue cross-section. Millions of sperm were recovered per graft and sperm were competent to fertilize oocytes, resulting in hatching blastocyst in vitro and pregnancy following embryo transfer.

TABLE OF CONTENTS

LIST OF TABLES

LIST OF FIGURES

PREFACE

ACKNOWLEDGEMENT

Like spermatogenic lineage development, life is in cycle with stages. Some are long, others are short; some are rapidly productive, others are steady. I have gone through these stages, not alone. I give “all honor and glory to God forever and ever” for bringing me into the niche that provided guidance, support and inner strength for this stage of my development. He obviously accomplished these through many great people. The list is long, and if you are reading this, you are one of them. Thank you for being part of this project. To Elizabeth, my friend and wife, thank you for believing in my decision to go to graduate school and tolerating the plasticity of our intercytoplasmic bridge, long enough to extend from lab to home. To Comfort and Wisdom, the realities of my self-renewing potential, thanks for tolerating my attraction, which sometimes displace the attention you deserve. To Dr. Kyle E. Orwig, my mentor and Sertoli man, thanks for providing the platform and resources that facilitated my progress through various stages. To my lab mates at different times-Hanna, Jen, Karen, Meena, Sherin, Chatchanan, Payal, Sarah M., Sarah S., Kein, Yi sheng, Lu Lu, Lin Lin and many others, thanks for the paracrine factors you exuded that helped my development in this common seminiferous epithelium. To my thesis committee members-Dr. Hukriede, Dr. Tsang, Dr. Monga and Dr. Rajkovic, thanks for your exocrine inputs that shaped the morphology of my thoughts and studies. To my parents (Mr and Mrs Fayomi), family, in laws, classmates, friends and colleagues (in the United states and

Nigeria), present and former church members (RCCG Livingspring International, Pittsburgh and elsewhere) and acquaintances, thanks for the pains we shared together, the victories we celebrated together, the challenges we confronted together, the hopes we embraced together. We've embarked on this journey together and I have benefitted from your love, prayers and words of encouragement. We did it, thanks be to God, the Ultimate Stem Cell.

LIST OF ABBREVIATED MOLECULAR MARKERS*

SRY - sex determining region Y

SOX9 - SRY Box 9

PRDM – PR/SET domain

BMP – Bone morphogenetic protein

ID4 – Inhibitor of DNA binding 4

GFRA1 - Glial cell line derived neurotrophic factor family receptor alpha 1

PLZF - Promyelocytic leukemia zinc finger (also known as zinc finger and BTB domain containing 16 or ZBTB16)

PAX7 - paired box 7

EOMES - eomesodermin

BMI1 - BMI1 proto-oncogene

GFP – Green fluorescent protein

MAGEA4 – MAGE family member A4

SALL4 - Spalt like transcription factor 4

TRA – T-cell receptor alpha locus

SNAP91 - synaptosome associated protein 91

DSG2 – Desmoglein 2

CTAG1A - cancer/testis antigen 1A

OCT2 - organic cation/carnitine transporter 2

SSX - sister-of-Sex-lethal 2

SAGE1 - sarcoma antigen 1

GPR125 - G protein-coupled receptor 125

FGFR3 – Fibroblast growth factor receptor 3

EXOS10 – Exosome 10

THY-1 - Thymus cell antigen 1

cKIT – KIT proto-oncogene receptor kinase

SOHLH1- Spermatogenesis and oogenesis specific basic helix-loop-helix

NGN3 - Neurogenin 3

FOXO1 - Forkhead box O1

* List excludes names of markers that were not abbreviated and those that were written in full elsewhere in the Thesis.

1.0 INTRODUCTION

Some sections of this introductory chapter have been submitted, in part, for a book chapter (Fayomi et al., 2018) and a review paper (Fayomi & Orwig, In Press).

1.1 INTRODUCTORY OVERVIEW

Spermatogenesis is a highly organized process that produces millions of sperm each day in postpubertal mammals (Gupta et al., 2000; Sharpe, 1994; Thayer et al., 2001). This productivity depends on the activity of spermatogonial stem cells (SSCs), which are the adult tissue stem cells in the testes that balance self-renewing divisions with differentiating divisions to maintain the stem cell pool and fuel spermatogenesis, respectively (Clermont & Bustos-Obregon, 1968; de Rooij & Grootegoed, 1998; Huckins & Oakberg, 1978a; Tegelenbosch & de Rooij, 1993). SSCs development begin before birth. During postnatal life, they reside in a specialized niche in the seminiferous tubules where they are in direct contact with the basement membrane and Sertoli cells, which produce some of the paracrine factors required to regulate self-renewal and differentiation fate decisions (Chen & Liu, 2015). When SSCs differentiate, they give rise to progenitor spermatogonia that undergo a species-specific number of transit amplifying mitotic divisions, followed by two meiotic divisions and spermiogenesis (morphological transformation) to produce terminally differentiated sperm (Figure 1) (Fayomi et al., 2018; Valli et al., 2015b).

Stem, progenitor and differentiating spermatogonia are all located on the basement membrane of the seminiferous tubules. Differentiating spermatogonia give rise to spermatocytes that initiate meiosis, migrate off the basement membrane and give rise to secondary spermatocytes, spermatids and sperm cells (Huckins & Oakberg, 1978a; Phillips et al., 2010). Spermatogenesis occurs in a cyclic manner along the length of the seminiferous tubules, ensuring continuous sperm production throughout the postpubertal life of mammals (Oakberg, 1956b). The identity of the SSC pool is the subject of active research and debate. What is presently known about stem cells in mammalian testis, their role in spermatogenic development and their applications to male fertility/infertility are learnt using the rodent model (Brinster, 2007).

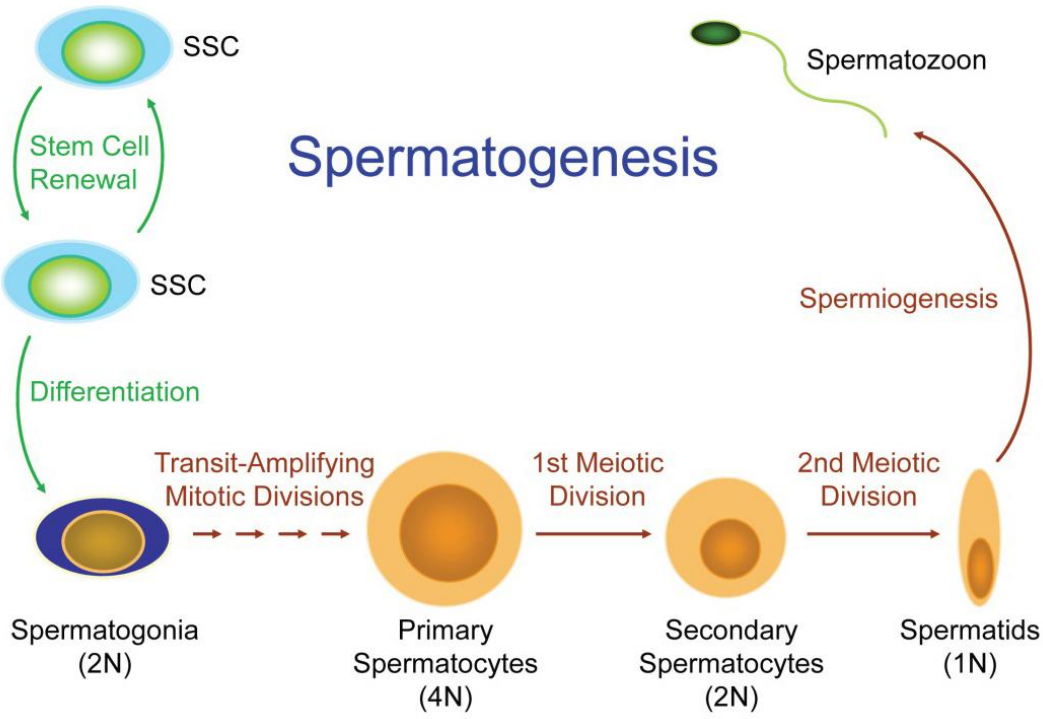

The spermatogonial stem cells (SSCs) pool, which are diploid, balance self-renewing divisions that maintain the stem cell pool with differentiating divisions that sustain continuous sperm production. SSCs that are committed to the next phase of lineage development undergo species-dependent transit amplifying division and modifications that give rise to undifferentiated progenitor and differentiating spermatogonia. Transit amplifying division facilitates yield of sperm cells from a single stem cell. Primary spermatocytes arise from the differentiating spermatogonia and they undergo two meiotic divisions to produce haploid spermatids, which in turn undergo spermiogenesis to produce sperm cells

Figure 1: Mammalian spermatogenesis

1.2 STEM CELLS AND SPERMATOGENIC DEVELOPMENT-LESSONS FROM RODENT

1.2.1 Precursors of the spermatogonial stem cells in rodent

In the mouse, expressions of PRDM1 and PRDM14 by cells in the proximal part of the epiblast first determine the fate of the primordial germ cells (PGCs)-precursors around 6.25 days post coitum (dpc). These cells then evolve to a small cluster of alkaline phosphatase-positive cells in the epiblast by 7-7.25 dpc and are specified as PGCs. Specification of PGC is dependent on the expression of BMP2, BMP4 and BMP8, which are secreted by the extraembryonic ectoderm (de Sousa Lopes et al., 2004; Ginsburg et al., 1990; Kurimoto et al., 2008; Lawson et al., 1999; Manku & Culty, 2015; Saitou, 2009; Ying et al., 2001). During allantois development, PGCs are passively displaced and incorporated into the epithelial wall of the hindgut. By 9.5 dpc, they begin to migrate through the hindgut reaching the dorsal mesentery by 10.5 dpc, and the genital ridge, which is on the dorsal body wall by 11.5 dpc (De Miguel et al., 2009; McLaren, 2003). The PGCs are then enclosed by the Sertoli cells, forming testicular cords by 12.5 dpc (Jameson et al., 2012). During PGCs migration, they also multiply, reaching about 3000 PGCs that colonize the genital ridge (Bendel-Stenzel et al., 1998).

The mouse PGCs (mPGCs) develop into gonocytes around 13.5 dpc. Gonocyte is used to describe cells that include the M-prospermatogonia, T1-prospermatogonia and T2-prospermatogonia. M-prospermatogonia undergo continuous mitotic division until around 16.5 dpc, and they are located away from the basement membrane at the middle of the testicular cord. These cells evolve into T1-spermatogonia which enter G_0 mitotic arrest (McCarrey, 1993; McLaren, 2003; Tohonen et al., 2003). About 1 week after birth, T1-prospermatogonia resume

proliferation as T2-prospermatogonia, and migrate to the basement membrane of the seminiferous tubules (Clermont & Perey, 1957). On the basement membrane, T2-prospermatogonia give rise to the first wave of spermatogenesis, and the massive pool of SSCs which sustain continuous spermatogenesis during postpubertal life (Kluin & Derooij, 1981; McCarrey, 1993; Yoshida et al., 2006).

1.2.2 Spermatogonial stem cell niche in rodent

SSC niche is a complex environment that includes cells as well as soluble factors that regulate SSC dynamics and spermatogenic lineage development (Valli et al., 2015b). The Sertoli, Leydig and peritubular myoid cells mainly constitute the cellular component of SSC niche in the adult testis. During fetal development in the mouse, expression of *Sry* (beginning from 10.5 dpc) in the bipotential gonadal ridge triggers the specification of pre-Sertoli cells. Expression of Sox 9 (around 11.5 dpc) induces proliferation of pre-Sertoli cells and facilitates their differentiation to Sertoli cells. Proliferation enables the emerged Sertoli cells to make stronger contact with germ cells as they contribute to the formation of testis cord by 12.5 dpc (Kashimada & Koopman, 2010; Nel-Themaat et al., 2009; Svingen & Koopman, 2013). Sertoli cell proliferation continues until around 15th postnatal day (15 pnd) (Vergouwen et al., 1991). The fetal Leydig cells (FLC) were first differentiated and identified by 12.5 dpc-13.5 dpc. After birth, they atrophy gradually and are replaced by the adult Leydig cells (ALC) 2-3 weeks after birth (Wen et al., 2016; Wen et al., 2014). Peritubular myoid cells (PMC) are first morphologically identified by 13.5 dpc in mice and their origin is yet to be determined (Jeanes et al., 2005; Svingen & Koopman, 2013).

During adult life, Sertoli cells (SCs) constitute the polarized epithelial cell whose roles include supporting the SSCs and differentiating germ cell during spermatogenic development. They do these by making direct contact with cells thereby 1) supplying nutrients to developing germ cells (Griswold, 1998), 2) functioning as the conduit for hormonal regulation of spermatogenesis (Meachem et al., 2005), 3) facilitating communication between germ cells and external signals (Griswold, 1998) and 4) enabling the movement of germ cells from the basal compartment into the adluminal compartment through the blood-testis barrier, which is important for regulation of germ cell differentiation (Cheng & Mruk, 2002; Smith & Braun, 2012). Sertoli cells produce glial cell line-derived neurotrophic factor (GDNF) which functions to maximize the proliferation of SSCs (Meng et al., 2000). They also act as "nurse" cells, directly facilitate SSC expansion and induce SSC differentiation (Zhang et al., 2007).

ALCs produce testosterone. Testosterone-mediated GDNF expression and action in PMC is important for the maintenance of SSC and undifferentiated spermatogonia pool in adult testis (Chen et al., 2014; Chen et al., 2016). ALC and PMC are also source of colony stimulating factor 1 (CSF1), which is important for SSC self-renewal (Oatley et al., 2009).

1.2.3 Clonal dynamics during Spermatogenic development in rodent

During steady state or post-pubertal life, spermatogenesis arises from a population of single spermatogonial cell (Figure 2). In the rodent, this population of cells are described as A_{single} spermatogonia (A_s) (Figure 2, red, top row), and they are located on the basement membrane of seminiferous tubules (de Rooij, 1973; Huckins, 1971a; Oakberg, 1971). A_s spermatogonia are rare, comprising 0.03% of all germ cells in the mouse testis; they are evenly distributed along the basement membrane of the seminiferous tubules; have a relatively large nuclear to cytoplasmic

ratio and diffuse chromatin (lacking heterochromatin) (Tegelenbosch & de Rooij, 1993). When A_s spermatogonia divide they produce A_{paired} (A_{pr}) spermatogonia (Figure 1.2, yellow, top row) that either complete cytokinesis to produce two new A_s spermatogonia (self-renewal) or stay connected via an intercytoplasmic bridge and produce a chain of four $A_{aligned}$ (A_{al4}) spermatogonia at the next division. Subsequent divisions of A_{al4} spermatogonia give rise to A_{al8} and A_{al16} spermatogonia (Figure 2, green, top row). A_s, A_{pr} and A_{al} are collectively termed, undifferentiated spermatogonia. A_s and A_{pr} are equally distributed along the length of the seminiferous tubules, while A_{al} are distributed in a stage-dependent manner with peak numbers in the mid-stages before the appearance of differentiating type A1 spermatogonia (Tegelenbosch & de Rooij, 1993). The transition to differentiating type A1 spermatogonia can occur from clones of A_s, A_{pr} or A_{al4}, but most frequently occurs from clones of A_{al8} or A_{al16} (de Rooij & Griswold, 2012; de Rooij & Russell, 2000; Griswold & Oatley, 2013; Nakagawa et al., 2010). Eight successive transit amplifying divisions from A1 spermatogonia in rodents give rise to differentiating spermatogonial types A2, A3, A4, Intermediate and B, followed by primary spermatocytes, secondary spermatocytes and round spermatids (Figure 2, top row). With a total of 10 transit amplifying mitotic divisions followed by two meiotic divisions, a single stem cell that commits to differentiate can theoretically produce 4096 sperm in rodents (Russell et al., 1990) (Figure 2, top row).

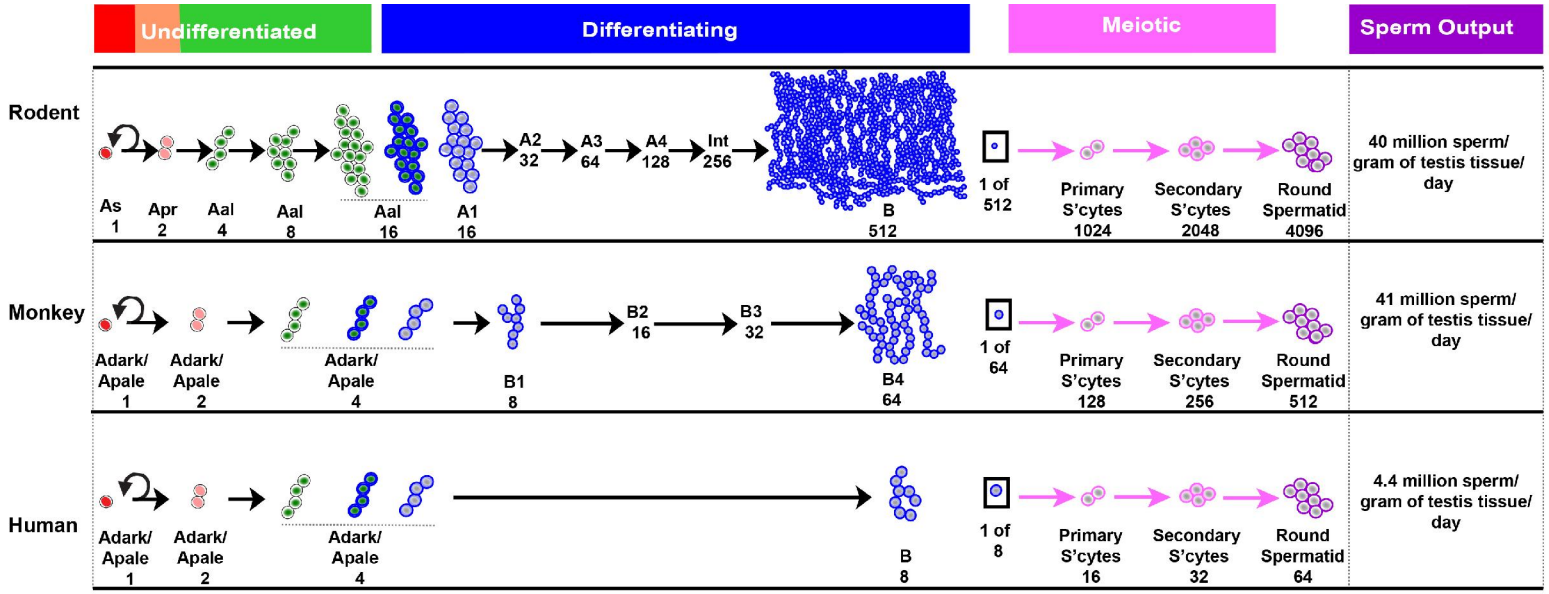

While the undifferentiated spermatogonia population are described either as A_s, A_{pr} or A_{al} in the rodent, they are described as A_{dark} and A_{pale} in monkey and Human. During spermatogenic development, SSC pool of A_s and A_{dark} and/or A_{pale} (red cell) undergo either a self-renewing division or give rise to a progenitor cell of clone size 2 (orange cells). The progenitor cell undergo further mitotic divisions (black arrow) to give rise to other progenior cell population (green cells). The undifferentiated progenitor cells then differentiate (blue cells) and undergo further mitotic divisions (black arrow) before becoming spermatocytes. The number of mitotic divisions of undifferentiated and differentating spermatogonia varies: 9 in rodent, 5 in monkey and 2 in human. Due to similar number of meiotic divisions (pink arrow) across these 3 species, variations in the mitotic divisions is believed to be responsible for the differences in the spermatogenic output.

Figure 2: Clone sizes of germ cell during development in rodent, monkey and human

1.2.4 The spermatogonial stem cells in rodent

A_s, A_{pr} and A_{al} spermatogonia all have an undifferentiated appearance with homogenous, diffuse chromatin. They can be distinguished by clone size, as revealed by molecular markers (see partial list in Figure 3), in whole mount preparations of seminiferous tubules but not in histological cross section. This distinction is important because there is general consensus that A_s spermatogonia comprise at least a part of the spermatogonial stem cell pool and that stem cell activity decreases with increasing clone size. In 2011, Oatley and colleagues identified for the first time, a molecular marker (ID4) with expression that was limited to A_s spermatogonia on the basement membrane of seminiferous tubules (Oatley et al., 2011). ID4 represents a subpopulation of A_s spermatogonia; it is co-expressed with GFRA1 and PLZF, but represents a subpopulation of GFRA1+ and PLZF+ cells (Figure 3A). ID4+ cells can be maintained and expanded in culture and regenerate spermatogenesis when transplanted into infertile recipients. Relative to $ID4^{bright}$ cells, transplantable stem cell activity is substantially reduced in $ID4^{dim}$ and $ID4^{-}$ cells, but not absent (Chan et al., 2014; Helsel et al., 2017; Oatley et al., 2011). Since 2011, PAX7 (Aloisio et al., 2014), BMI1 (Komai et al., 2014) and EOMES (Braun et al., 2017) have also emerged as markers restricted to A_s spermatogonia on the basement membrane of seminiferous tubules(Figure 3A). Each marker is expressed by a sub-population of GFRA1+ cells and a subpopulation of A_s spermatogonia (Figure 3A). Cells expressing each of these markers produce and maintain colonies of spermatogenesis after transplantation and/or in lineage tracing studies.

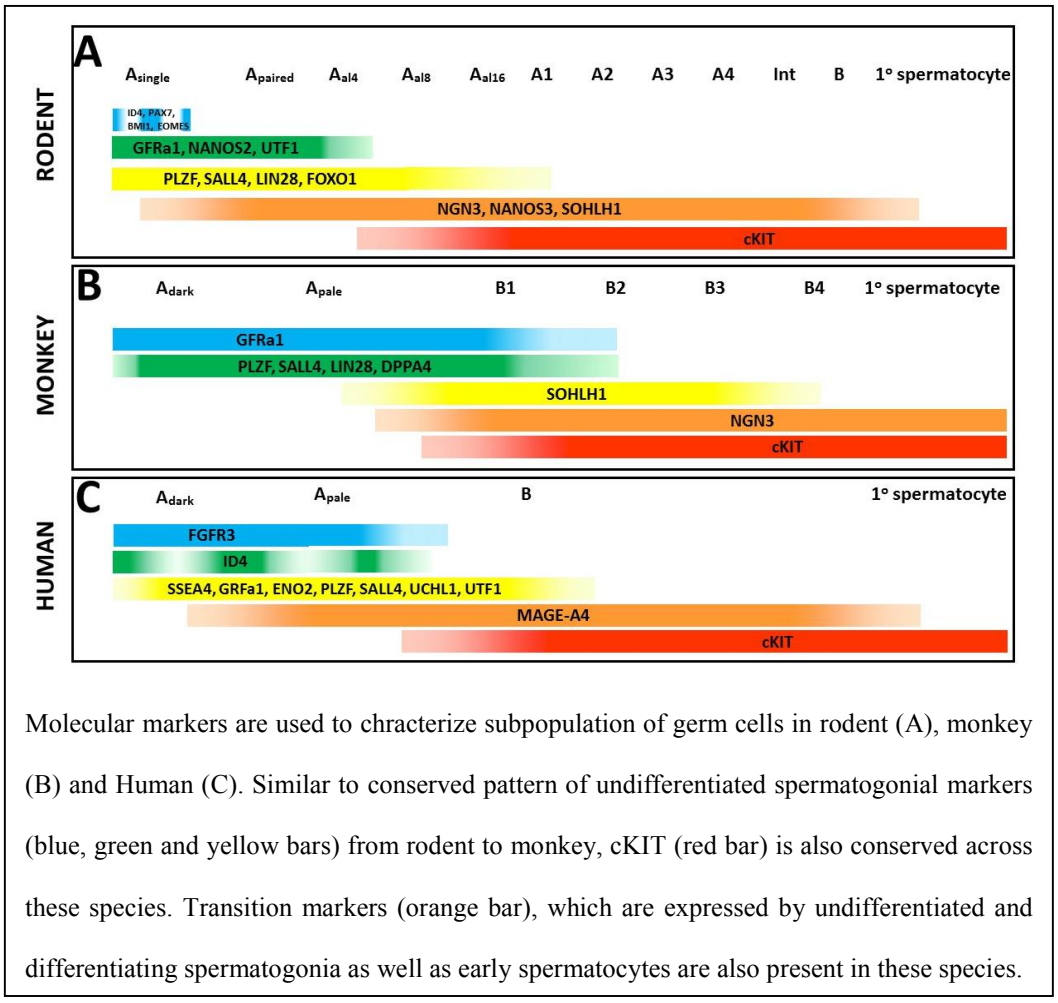

Molecular markers are used to chracterize subpopulation of germ cells in rodent (A), monkey (B) and Human (C). Similar to conserved pattern of undifferentiated spermatogonial markers (blue, green and yellow bars) from rodent to monkey, cKIT (red bar) is also conserved across these species. Transition markers (orange bar), which are expressed by undifferentiated and differentiating spermatogonia as well as early spermatocytes are also present in these species.

Figure 3: Partial list of markers expressed by rodent, monkey and human male germ cells

It seems reasonable to suppose that the stem cell pool also extends to some A_{pr} spermatogonia because A_s must transit through an A_{pr} state in the process of self-renewal (this concept is nicely reviewed in (de Rooij & Griswold, 2012)). In fact, self-renewal and differentiation could be precisely balanced if half of A_{pr} spermatogonia completed cytokinesis to produce two new A_s, while the other half produced chains of A_{al4} at the next division. However, pulse labelling of GFRA1+ cells indicated that the balance was skewed more toward the A_{pr} to A_{al4} transition than the A_{pr} to 2 A_s transition. To reconcile this apparent imbalance, Hara and colleagues provided live video imaging GFRA1-GFP spermatogonia data to suggest that clone fragmentation (eg., A_{al4} fragment to A_{al3} + A_s or A_{pr} + 2 A_s or 4 A_s) was an important contributor to maintenance of the A_s pool (Hara et al., 2014). While the fate of the fragmenting clones could not be documented in that study, clones of A_{al3} have been observed by others and apoptosis rarely occurs in undifferentiated spermatogonia (Gassei & Orwig, 2013; Suzuki et al., 2009). However, one concern with the clone fragmentation model is that it does not account for the contribution of GFRA1 negative cells to the pool of A_s (Gassei & Orwig, 2013; Suzuki et al., 2009) or the pool of transplantable stem cells (Garbuzov et al., 2018; Grisanti et al., 2009).

1.2.5 Cycle of seminiferous epithelium in rodent

During steady state, spermatogenesis, which arises from the pool of undifferentiated stem and progenitor spermatogonia, occurs in waves that are propagated along the length of the seminiferous tubules. This starts, proceeds and ends with a similar association of cells in the seminiferous epithelium (Clermont, 1972). A complete progression is known as a cycle, and seminiferous epithelium consists of repetitive and regular pattern of distinct cellular associations during spermatogenic development. There are 12 stages of seminiferous epithelial cycle in

mouse, and 8.6 days are required for a single segment of seminiferous tubule to progress through all 12 stages. Thus, each segment of seminiferous tubules releases a new batch of sperm into the lumen every 8.6 days and this occurs at stages VIII and IX (Oakberg, 1956a, 1956b, 1971). The number of A_s and A_{pr} spermatogonia are relatively constant across the different stages of the seminiferous epithelial cycle (Tegelenbosch & de Rooij, 1993). Larger A_{al} (8-, 16- and 32-cell) clones become differentiated A1 spermatogonia between stages IV to VII of seminiferous epithelial cycle (Oakberg, 1971). Apoptosis rarely occurs in undifferentiated stem and progenitor spermatogonia, but is more frequent in differentiated type A2-A4 spermatogonia, which reduces overall spermatogenic output by about 50% and may serve as a density-dependent control of spermatogenic output (de Rooij, 1998; De Rooij & Lok, 1987; Huckins, 1978a).

1.3 STEM CELLS AND SPERMATOGENIC DEVELOPMENT IN PRIMATE

1.3.1 Precursors of the spermatogonial stem cells in Primate

In human, time of PGCs (hPGCs) specification is unclear but it is thought to be between 2-3 weeks of gestation during gastrulation (Leitch et al., 2013). Observation of specified hPGCs was first made during early 4th week of gestation in the extraembryonic yolk sac around allantois, and this corresponds to the location of mPGCs by 8.0 dpc as reviewed by Tang et. al. (Tang et al., 2016). Migration of hPGCs occur from the 5th to 8th week of gestation (Aflatoonian & Moore, 2006). Gonadal hPGCs or gonocytes are mitotically active until about the tenth week of gestation when they become quiescent mitotically (Tang et al., 2016).

In the monkey (*Callithrix jacchus*), the primordial germ cells (mPGCs) can be identified in the caudal endoderm lining of both the primitive gut and yolk sac stalk. The location of future gonadal ridge is known by the 8th week (E50) of gestation. By the 10th week of gestation, monkey PGCs migrate to the indifferent gonad and the prospective testicular cord is formed by the 11th week (E75) of gestation (Aeckerle et al., 2015).

1.3.2 Primate spermatogonial stem cell niche

In the human fetal gonad, *Sry* expression was first detected in the pre-Sertoli cells around 6th-7th weeks of gestation, which then differentiates to Sertoli cells by 7-8th weeks of gestation (Hanley et al., 2000). After birth, human Sertoli cells continue to proliferate and undergo morphological changes until puberty but the proportion of testis space they occupied decrease over this time (Cortes et al., 1987; Nistal et al., 1982). Similar trend of Sertoli cell development was observed in Rhesus macaques during postnatal life (Marshall & Plant, 1996; Plant et al., 2005; Simorangkir et al., 2012).

In contrast to rodent Leydig cell maturation, primate Leydig cells' maturation is a triphasic process which includes the fetal, neonatal and pubertal phases (Prince, 2001; Teerds & Huhtaniemi, 2015). Human fetal Leydig cells differentiate from mesenchymal cells beginning from the 8th week of gestation. They grow between the 9th to 12th week of gestation reaching their highest number by 14th week of gestation. These cells then began to involute by 17th week of gestation (Holstein et al., 1971). Neonatal Leydig cells are believed to arise from the redifferentiation of fetal Leydig cells (Codesal et al., 1990; Teerds & Huhtaniemi, 2015), and the adult Leydig cells are believed to arise from fibroblast-like cells which respond to luteinizing hormone stimulation at the onset of puberty (Chemes et al., 1985). In the monkey, neonatal

Leydig cells are known to produce testosterone during the first three month of life (Fouquet & Raynaud, 1985; Verhagen et al., 2014).

While there is dearth of information on the development of peritubular myoid cells in the primate testis, it was reported that they were first morphologically identified during the 12^{th} week of gestation (Ostrer et al., 2007).

1.3.3 Stem, progenitor and differentiating spermatogonia in primate

Nonhuman primate and human testes contain two morphologically distinct types of undifferentiated spermatogonia, classified as A_{dark} and A_{pale} based on differences in nuclear morphology and staining with hematoxylin in histological cross sections (Clermont, 1966; Clermont & Leblond, 1959). Clermont initially proposed that A1 spermatogonia (A_{dark}) were the SSCs that gave rise to progressively more differentiated A2 (A_{pale}) and B spermatogonia. However, he later revised this model based on observations that A_{dark} failed to label after a single bolus injection of [^{3}H]-thymidine. Since A_{dark} did not appear to self-renew under steady state conditions, he proposed that A_{dark} and A_{pale} represented reserve and active stem cells, respectively (Clermont, 1969). In this reserve stem cell model, spermatogenesis is maintained by the "active" A_{pale} SSCs that self-renew to maintain the A_{pale} pool and differentiate to produce spermatogenesis. The "reserve" A_{dark} spermatogonia are quiescent and become active only when A_{pale} are depleted by noxious insult. This notion is supported by observations in nonhuman primates indicating that X-irradiation caused a rapid decline in the pool of A_{pale} spermatogonia, which were later replenished by the surviving A_{dark} spermatogonia (van Alphen et al., 1988). Whether A_{dark} are truly quiescent and reserve or slow cycling stem cells that contribute to steady state spermatogenesis is uncertain. Chronic or repetitive administrative of a mitotic labelling

reagent followed by a period of washout would identify slow cycling stem cells that retain label for an extended time, which is a classic feature of adult tissue stem cells. This is an experiment that has been performed to identify slow cycling, label retaining A_s stem cells in rats (Huckins, 1971b) and could be performed in nonhuman primates.

A_{dark} and A_{pale} spermatogonia are present in equal numbers on the basement membrane of the seminiferous tubules and together represent ~4% of germ cells in the testis, a frequency that is 100-fold greater than rodent A_s spermatogonia (0.03%), and 5-fold less than human A_{dark} and A_{pale} population (Figure 4). A_{dark} are evenly distributed along the length of the seminiferous tubules (Similar to rodent A_s and A_{pr}), while A_{pale} exhibit a stage-dependent distribution with peak numbers at mid-cycle (similar to rodent A_{al}) that precedes the appearance of differentiating type B1 spermatogonia (Figure 2, middle and bottom row). A_{dark} and A_{pale} are arranged predominantly as singles, pairs or chains of four (Figure 2, middle and bottom row) (Clermont, 1969), while differentiating B1 spermatogonia appear as clones of 4 or 8 (Figure 2, middle and bottom row), indicating that there are 1-2 transit amplifying divisions (following the initial self-renewing divisions) in the undifferentiated A_{dark} or A_{pale} spermatogonia before differentiating to B1 in the monkey (Ehmcke et al., 2005a). In monkeys, four additional transit-amplifying divisions from B1 produce differentiating spermatogonia types B2, B3 and B4, followed by primary spermatocytes (Figure 2, middle row). In human, only one transit amplifying division is believed to occur before the resulting B-type spermatogonia transit to spermatocytes (Figure 2, bottom row). Based on the expression of differentiation marker, cKIT, differentiating type B spermatogonia in monkeys and humans are equivalent to differentiating type A spermatogonia in rodents (Figure 3) (Valli et al., 2015b). In contrast to rodents, which have a small stem cell pool and many transit amplifying divisions to produce 40 x 10^6 sperm per gram of testicular

parenchyma per day (Figure 2A and 4A), nonhuman primates achieve a similar sperm output (41 x 10^6/gram/day) with a relatively larger stem cell pool and fewer transit amplifying divisions (Figure 2B and 4B). Sperm output in human is lower than rodent's or monkey's and this can be attributed to one generation of differentiating type B spermatogonia in human (Figure 2C and 4C).

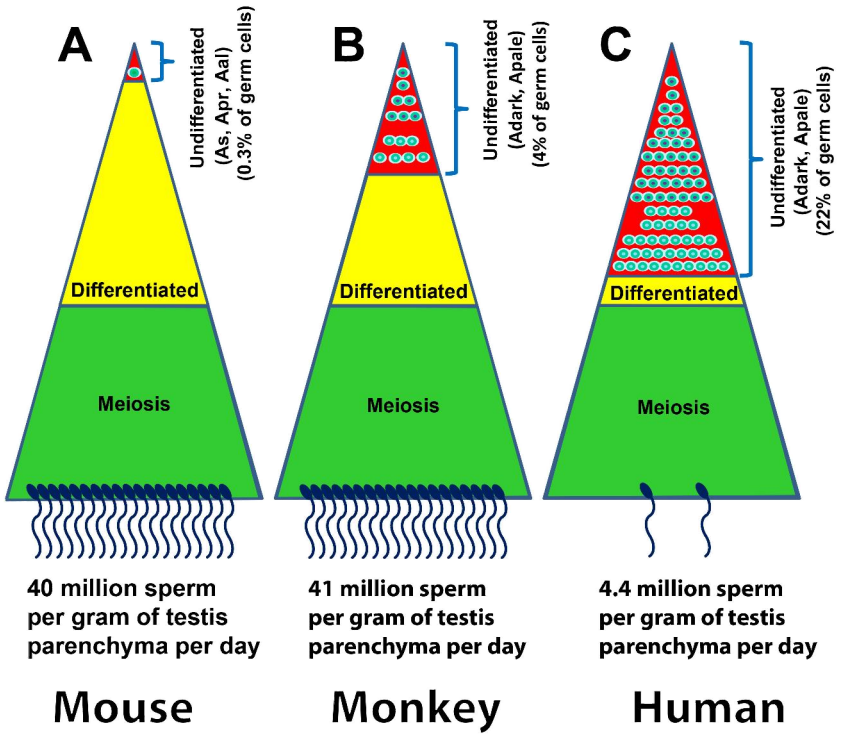

The undifferentiated spermatogonia pool (red) is least in the mouse (A); spermatogenic output (blue) in the mouse is similar to monkeys', which is about 8-fold more than in human. Extensive spermatogenic output in the mouse may be associated with 6 amplifying differentiation divisions (A, yellow) which are superior to 4 in the monkey (B, yellow) and 1 in human (C, yellow). Spermatogenic output in monkey at the level comparable to mouse may be associated with compensation from higher undifferentiated spermatogonia-4% (B, red) in monkey when compared with mouse-0.3% (A, red). Human use the highest pool of undifferentiated spermatogonia-22% (C, red) to compensate for its only one amplifying differentiation divisions (yellow). Events in the meiotic phase (green) of spermatogenesis appear to be conserved from mouse to human.

Figure 4: Schematics of the comparative spermatogenic output in mouse, monkey and human

1.3.4 Molecular markers of undifferentiated and differentiating spermatogonia in the primate

In different primate species, molecular markers including PLZF, ENO2, UCHL1, UTF1, MAGEA4 (*Homo sapiens*) (Di Persio et al., 2017; Valli et al., 2014b; von Kopylow et al., 2010), LIN28 (*Macaca mulatta, Macaca silenus, Papio anubis*) (Aeckerle et al., 2012), SALL4 (*C Jachus, Homo sapiens)* (Eildermann et al., 2012), SSEA-4 and TRA-1-81 (*M mulatta, C jachus*), TRA-1-160 (*C jacchus*) (Muller et al., 2008), SNAP91, DSG2, CTAG1A, CBL, OCT2, SSX, SAGE1,GPR125, FGFR3 and EXOS10 (*H sapiens*) (Izadyar et al., 2011; Lim et al., 2011; von Kopylow et al., 2010; von Kopylow et al., 2012a; von Kopylow et al., 2012b) have been used to characterize spermatogonial populations that include the undifferentiated spermatogonia (see partial list in Figure 3B and C). Similarly, expression of surface markers including GFRA1 (*M mulatta, H sapiens*), Alpha 6 integrin (ITGA6) (*M mulatta, H sapiens*), Beta1 integrin, SSEA-4 (*H sapiens*), THY-1 (*H sapiens, M mulatta*) (Di Persio et al., 2017; Gassei et al., 2010; Hermann et al., 2007; Hermann et al., 2009; Izadyar et al., 2011; Maki et al., 2009) have also been used to characterize the undifferentiated spermatogonia, or use to isolate a fraction of the testis cell that is enriched for SSCs. cKIT is a marker of differentiating spermatogonia that is conserved in monkey and human (Di Persio et al., 2017; Hermann et al., 2009; Valli et al., 2014b). Recent studies have identified SOHLH1, NGN3 (in monkey) and MAGEA4 (in monkey and human) as transition markers with coverage across the undifferentiated and differentiating spermatogonia) (Figure 3B and 3C). Molecular markers that are specifically expressed by the stem cell pool in

the primate testis have neither been identified nor functionally evaluated and little is known about how these markers correlate with classical descriptions of spermatogonia in primates.

1.3.5 Cycle of the seminiferous epithelium in primate

Twelve distinct events or stages constitute one cycle of the seminiferous epithelium in the Rhesus macaque (Clermont & Leblond, 1959). A segment of seminiferous tubule continuously progresses through all 12 stages of the seminiferous epithelium in a repetitive 10.5-day cycle. By extension, a segment of the seminiferous epithelium releases new batch of sperm into the lumen every 10.5 days, and this occurs by stage VI of the cycle (de Rooij et al., 1986). Previous studies indicate that A_{pale} divide between stages VII and IX of the cycle of the seminiferous epithelium (Clermont, 1969; Clermont & Antar, 1973; Ehmcke et al., 2005b; Fouquet & Dadoune, 1986; Plant, 2010; Simorangkir et al., 2009a). In some studies, this division appears bimodal, and there is disagreement in the models available in the field as to whether A_{pale} divide once (Clermont, 1969; Clermont & Leblond, 1959; Plant, 2010; Simorangkir et al., 2009a) or twice (Clermont & Antar, 1973; Ehmcke et al., 2005a; Fouquet & Dadoune, 1986) during a cycle of the seminiferous epithelium. Cycle of seminiferous epithelium was thought to be 6 stages in human but recent studies have demonstrated the presence of 12 stages of the seminiferous epithelium, similar to the number in other primate species (Clermont, 1963; Muciaccia et al., 2013). It takes 16 days for a segment of the human seminiferous epithelium to complete a cycle (Heller & Clermont, 1963).

1.4 EXPERIMENTAL TOOL BOX AND POTENTIAL APPLICATIONS

1.4.1 Experimental tool box in rodent

Spermatogonial stem cells are rare in rodent testes because they are outnumbered by the progenitor and differentiating spermatogonia, spermatocytes and spermatids that they produce; and this challenges efforts to understand the molecular regulation of SSC function. Therefore, to learn the molecular features of SSCs, it was necessary to 1) study testes early in development prior to spermatogonial differentiation (Shima et al., 2004); 2) study testes in which differentiating germ cells were depleted (Orwig et al., 2008); 3) enrich transplantable SSCs by fluorescence activated cell sorting (FACS) or magnetic activated cell sorting (MACS) techniques (Hermann et al., 2015) or 4) modulating growth factors in SSC culture (Oatley et al., 2006). Each of these approaches identified molecules expressed by stem and progenitor spermatogonia and provided clues about pathways that regulate SSC self-renewal and differentiation. However, gene expression data generated from these approaches should be interpreted with caution because the cell populations were heterogeneous and approaches 1, 2 and 4 do not represent the steady state condition with homeostatic balance of self-renewal and differentiation.

It is tempting to speculate that a pure population of stem cells could be isolated from the adult testis (with steady state spermatogenesis) by sorting cells that express ID4, PAX7, BMI1 or EOMES. However, that approach could provide an incomplete picture because it is not certain that these four molecules mark the same cell population or that they capture the entire population of SSCs. It is possible, and perhaps likely, that the stem cell pool is dynamic and molecularly heterogeneous; reflecting changes that occur 1) at different stages of the cell cycle, 2) during

development, 3) through the stages of the seminiferous epithelium or 4) under conditions of stress.

A new generation of single cell sequencing technologies (Fluidigm, drop-seq and 10X genomics) now allow researchers to study the heterogeneous mammalian testis and SSC pool with a throughput and resolution that was not previously possible (Guo et al., 2017; Hermann et al., 2015). Furthermore, the drop-seq and 10X platforms can process hundreds of thousands of cells in a single run, which means it is possible to study all cell populations in the mammalian testis without the bias of preselection enrichment. These approaches will certainly expand the list of spermatogonial stem cell markers and may identify subpopulations of spermatogonia that were not previously recognized. So, how should researchers validate the expanding list of SSC markers?

The simplest and least stringent approach to validate candidate markers of undifferentiated stem/progenitor spermatogonia is by real time polymerase chain reaction (RT-PCR) technique or immunocytochemical (ICC) staining of an experimental cell population with known markers of undifferentiated spermatogonia (e.g., ID4, GFRA1, PLZF). A more stringent approach is to examine the pattern of candidate marker expression in situ by immunohistochemical (IHC) analysis in histological cross-section. A marker that is restricted to stem and/or progenitor spermatogonia should be expressed by a subpopulation of cells located on the basement membrane of seminiferous tubules. Co-staining in histological cross-section helps to establish whether the candidate marker is expressed by undifferentiated spermatogonia (e.g., co-stain with PLZF or GFRA1), differentiating spermatogonia (e.g., co-stain with cKIT) or both, but does not provide any information about clone size. Immunohistochemical analyses in whole mount preparations of seminiferous tubules provide the same basement membrane localization

and co-expression information as histological cross section as well as information about the clonal arrangement of marked cells. Unfortunately, markers that work well in histological cross section do not always work well in whole mount preparations of seminiferous tubules and vice versa. Each marker needs to be tested empirically in each approach with the appropriate negative and positive controls.

The descriptive methods described above are useful, but cannot demonstrate the biological potential of cell population to produce and maintain spermatogenesis, which is the hallmark of SSCs. Ralph Brinster and colleagues pioneered the method of SSC transplantation, which demonstrates the potential of an experimental cell population to regenerate spermatogenesis in the testes of infertile recipients (Brinster & Avarbock, 1994; Brinster & Zimmermann, 1994). More than 2 decades after the initial reports, SSC transplantation remains the "gold standard" bioassay of spermatogonial stem cells. This approach may also have application for the treatment of some cases of infertility especially those that are due to gonadotoxic exposures following chemotherapy or radiation treatments. (Gassei & Orwig, 2016; Valli et al., 2015a; Valli et al., 2014a).

In recent years lineage tracing has emerged as a powerful tool that also demonstrates the in vivo capacity of marker-positive cells to produce and sustain spermatogenesis over a long period of time (Aloisio et al., 2014; Hara et al., 2014; Komai et al., 2014; Nakagawa et al., 2007). Lineage tracing results can be a little more difficult to quantify than transplantation, but have the advantage that stem cell potential can be assayed in the steady state condition of the adult testis.

Rodent SSCs express surface markers including THY1, ITGA6 and others. These surface markers are not restricted to SSCs, but can be used to isolate and enrich SSCs using FACS and

MACS techniques (Kubota et al., 2003a; Shinohara et al., 1999). These techniques facilitate effective separation of undifferentiated spermatogonia from more differentiated germ cells and somatic cells of the testis, which is a critical step in the establishment of rodent SSC culture system (Kubota et al., 2004a; Nagano et al., 1998). Other critical steps for culturing mouse SSCs included addition of growth factors (GDNF, basic fibroblast growth factor (bFGF)) and use of feeders (for example, Sandos Inbred Mice (SIM) Thioguanine/Ouabain-resistant mouse fibroblast line (STO) cells) or feederless (for example, laminin) platform on which SSCs can be maintained and expanded in number (Kubota & Brinster, 2008). Although SSC culture does not represent steady state spermatogenesis, it has served as a powerful tool to dissect the mechanisms that regulate SSC self-renewal, differentiation and transplantation potential (Chapman et al., 2015; Lee et al., 2007; Oatley et al., 2006; Yeh et al., 2011).

1.4.2 Experimental tool box for monkeys and humans with potential application

Many markers of undifferentiated and differentiating spermatogonia are conserved from rodents to nonhuman primates to humans (see partial list in Figure 3). While some markers appear species-specific, this could also reflect lack of experimentation or antibody availability. Nonetheless, several good markers of undifferentiated, transitioning and differentiating spermatogonia are available and can be used during of RT-PCR, ICC or IHC analyses. High throughput single cell sequencing is as accessible for monkey and human studies as it is for rodent, assuming the availability of normal tissues (Guo et al., 2017). Experimental tool box with potential application for fertility preservation

1.4.2.1 Spermatogonial stem cell transplantation

Primate-to-primate SSC transplantation is technically feasible and can demonstrate the potential of an experimental cell population to produce and maintain spermatogenesis, long-term (Hermann et al., 2012). However, this approach is not practicable or accessible to most researchers as a routine bioassay and it is presently impossible for human application. Monkey-to-monkey SSC transplantation has been demonstrated in *Callithrix jacchus* (autologous (Schlatt et al., 2002a)) and *Macaca mulatta* (autologous (Jahnukainen et al., 2011) and allogeneic (Hermann et al., 2012)). This approach is valuable for the proof of principle experiment and its use as routine bioassay may be limited by extensive variabilities within and between primate species, sample-size limitation, experimental cost, technical know-how and difficulty in differentiating the endogenous cells from transplanted cells. However, regeneration of spermatogenesis following SSCs transplantation in Rhesus macaque (Hermann et al., 2012) opened a potential pipeline for the possibility of using this technique to treat certain cases of infertility. As developmental studies begin to elucidate on the developmental dynamics of the stem and progenitor cells in primate, the required knowledge for predicting the behavior of endogenous and/or transplanted human SSCs becomes plausible. This approach may eventually provide the technique that will help us to identify and understand the molecular pathways of SSCs self-renewal, survival or maintenance, which are unique to primates that can be pharmacologically targeted to treat certain cases of infertility or for contraceptive purposes.

Primate-to-mouse xenotransplantation has emerged as a valuable surrogate assay of monkey and human SSCs. SSCs from higher primates do not produce complete spermatogenesis in mouse seminiferous tubules. However, they do recapitulate several aspects of spermatogonial function that are not shared with other cell types: 1) they migrate through Sertoli cells to engraft

the basement membrane of seminiferous tubules; 2) they proliferate to produce chains and clusters of cells with typical spermatogonial-like appearance and 3) they persist for long period of time. One day it may be possible to recapitulate complete spermatogenesis from monkey or human cells in organoid cultures, as previously described for mice (Zhou et al., 2016). However, the mouse results still need to be replicated to establish a robust assay and translation to monkeys and humans will likely require a source of monkey and/or human fetal gonadal cells that are not widely available, if at all.

1.4.2.2 Testicular Tissue Grafting

Testicular tissue grafting or transplantation pre-dated the era of SSCs transplantation or its potential use for fertility purposes. Testicular tissue grafting was being used to study the endocrine effects of the testis, to evaluate secondary sex characteristics and to restore the recipient's vigor until the middle 20th century. Although this began with John Hunter who performed the first undocumented autologous transplantation of testicular tissue to chicken's comb in 1767 (as reviewed by Setchell) (Setchell, 1990), but it was first documented by Berthold in 1849 (Berthold, 1894). Progress by Cevelotto (1909), Steinach (1910) and Sand (1919) in autologous or allogeneic transplantation results in the successful grafting of viable rodent testis tissue without observing sperm cell or spermatid (Cevelotto, 1909; Sand, 1919; Steinach, 1910). By 1924, Moore first identified spermatid (complete spermatogenesis) from autologous grafts placed in the scrotum (Moore, 1924). Subsequently, complete spermatogenesis was identified from autologous, ectopic grafting of rodent's testicular tissue into scrotal skin (Richter, 1928), anterior chamber of the eye (Dameron, 1951; Turner, 1938) and "transparent chambers" in the ear (Williams, 1949, 1950). However, one of the challenges of the early scientists (including

Crisler (1929) and Browman (1937)) was their inability to successful recover viable testis tissues and/or testis with complete spermatogenesis from xenografted mice to rats testis, and vice versa (Browman, 1937; Crisler, 1929).

In higher mammals, Lespinasse (1913) and Lydston (1914) used allogeneic grafting of testicular tissue into human subject in their attempt to treat impotence and psoriasis respectively (Lespinasse, 1913; Lydston, 1914). Xenogeneic grafting of monkey and ram testicular tissue was being used to restore patients' vitality by Voronoff (1910s-1920s) and Stanley (1920) respectively (Hamilton, 1986; Stanley, 1920).

Progress was made in 1974 with the introduction of immunodeficient recipient mice which facilitated the recovery of viable testis tissue and gonocytes from xenografted human fetal testis tissue (Povlsen et al., 1974; Skakkebaek et al., 1974). The potential use of testicular tissue grafting for fertility preservation became realizable in 2002 when complete spermatogenesis was observed from xenografted goat and pig fetal testis tissues (Honaramooz et al., 2002). Subsequently, this success has been repeated in several animal species with donor derived offspring in some cases as reviewed elsewhere (Arregui & Dobrinski, 2014). This is a potential fertility preservation option for prepubertal boys undergoing gonadotoxic treatments that are cryopreserving their testicular tissues in anticipation that they could be used one day for fertility purposes.

1.5 CONCLUDING REMARKS

While different vocabulary is used to describe stem, progenitor and differentiating spermatogonia in rodents, nonhuman primates and humans, some aspects of spermatogenic lineage development are conserved. A_s spermatogonia mostly constitute the stem cell pool in rodent and the A_{pale} is presumed to constitute the stem and progenitor population in primates. The contribution of A_{dark} to steady-state spermatogenesis is unclear. Undifferentiated spermatogonia, including SSCs, exist as individual cells or small clones of interconnected cells. Transit-amplifying divisions lead to larger clones that are progressively more differentiated. Key differences in spermatogenic lineage development between rodents and higher primates include the size of the stem cell pool and the number of transit-amplifying divisions that precede meiosis. Many markers of undifferentiated spermatogonia are conserved from mice to monkeys to humans (e.g GFRA1, PLZF). This is true also for transitioning spermatogonia (e.g., SOHLH1, NGN3) and differentiating spermatogonia (e.g., cKIT). It is important to understand how molecular markers of spermatogonia in monkeys and humans correspond with clone size and dark and pale descriptions of nuclear morphology. This knowledge will help to link contemporary studies with the classic literature and identifies parallels between rodents, monkeys and humans. This is particularly important because few modern-day investigators have the experience or patience to conduct classic morphometric studies that were common in the 1950s to 1970s. Since SSCs are described differently in rodent and primates, potential applications for fertility preservation and/or restoration should be optimized and/or validated in nonhuman primate models which have testis anatomy and physiology similar to humans.

2.0 REVISITING THE CONCEPT OF A_{DARK} AS RESERVE AND A_{PALE} AS ACTIVE STEM CELLS IN THE ADULT PRIMATE TESTIS

This chapter is being submitted, as a primary research article, to the journal of "Human Reproduction".

2.1 INTRODUCTION

Continuous, steady-state spermatogenesis in postpubertal males is dependent on spermatogonial stem cells (SSCs), which balance self-renewing divisions that maintain stem cell pool with differentiating divisions that sustain continuous production of mature sperm cells (de Rooij & Grootegoed, 1998; Huckins, 1971a, 1978a; Tegelenbosch & de Rooij, 1993; Valli et al., 2015b)

In the rodent, A_{single} spermatogonia (A_s) are at the foundation of spermatogenesis and comprise a major portion of functional SSCs (Huckins, 1971a, 1978b) which was demonstrated by transplantation or lineage tracing of ID4-, PAX7- and BMI1-positive, A_s spermatogonia (Aloisio et al., 2014; Chan et al., 2014; Komai et al., 2014; Oatley et al., 2011). A_s spermatogonia divide once every 3 days in the adult mouse testis (Huckins & Oakberg, 1978b). The A_s can either divide to become two new A_s (self-renewal), or remain attached following a mitotic division to become a pair of cells (A_{paired} spermatogonia (A_{pr})) joined by an intercytoplasmic bridge. A_{pr} undergo further mitotic divisions to produce chains of $A_{aligned}$

spermatogonia (A_{al}) in clones of 4 (A_{al4}), 8 (A_{al8}), and 16 (A_{al16}) cells (Huckins & Oakberg, 1978b; Phillips et al., 2010; Tegelenbosch & de Rooij, 1993). Nakagawa and colleagues have suggested that A_{pr} and smaller clones of A_{al} can sometimes fragment and may contribute to maintenance of the pool of A_s spermatogonia. This phenomenon occurs more frequently under conditions where spermatogenesis has been destroyed by toxic insult (Nakagawa et al., 2010). The A_{al} spermatogonia differentiate to A_1 spermatogonia in a stage-dependent manner and this transition is marked by the onset of cKIT expression (de Rooij, 1998; de Rooij & Russell, 2000; Griswold & Oatley, 2013; Manova et al., 1990; Phillips et al., 2010; Schrans-Stassen et al., 1999; Yoshinaga et al., 1991). Morphometric analyses revealed that A_s spermatogonia are rare in rodent testis, comprising only 0.03% of all testicular germ cells, and they are evenly distributed along the length of the seminiferous tubules (Huckins, 1971a; Huckins & Oakberg, 1978a, 1978b; Tegelenbosch & de Rooij, 1993).

The description of stem, progenitor and differentiated spermatogonia; the size of the stem cell pool and the dynamics of spermatogenic development in rodent are different than higher primates (Hermann et al., 2010; Marshall & Plant, 1996; Valli et al., 2015b). Clermont and Leblond initially described two morphologically distinct types of undifferentiated spermatogonia in the testes of the Rhesus macaque (*Macaca mulatta*) in 1959 and designated these cells as A_1 and A_2 (Clermont & Leblond, 1959), which were later renamed A_{dark} and A_{pale}, respectively (Clermont, 1963). Clermont initially proposed that A_1/A_{dark} were the stem cells that undergo self-renewing divisions to maintain the stem cell pool and also give rise to A_{pale}, which eventually differentiate to type B spermatogonia (Clermont & Leblond, 1959). Ten years later, Clermont revised this model based on observations in the Vervet monkey (*Cercopithecus aethiops*) that A_{dark} failed to label after a bolus of ^{3}H-thymidine was injected (i.e., they did not appear to self-

renew). A_{pale} did incorporated ^{3}H-thymidine, so Clermont proposed that A_{dark} and A_{pale} represent "reserve" and "active" stem cells, respectively (Clermont, 1969). According to the "reserve and active stem cell" model, spermatogenesis is maintained by the "active" pool of A_{pale} SSCs during steady state, and the quiescent pool of A_{dark} is only mobilized to regenerate spermatogenesis when spermatogenesis (including the pool of A_{pale}) is destroyed by gonadotoxic insults (e.g., radiation) (van Alphen & de Rooij, 1986).

Since 1969, six studies have reported the mitotic labeling index of A_{dark} and A_{pale} spermatogonia after a single bolus administration of ^{3}H-thymidine or 5-Bromo-2$^{'}$-deoxyuridine (BrdU) in various nonhuman primate species. While three studies reported that no labeling was observed in the A_{dark} spermatogonia (Clermont, 1969; Fouquet & Dadoune, 1986; Simorangkir et al., 2009a), three studies reported a wide (0.06% to 18%) range of A_{dark} labeling (Clermont & Antar, 1973; Ehmcke et al., 2005b; Kluin et al., 1983). Similarly, there is a lack of consensus on the mitotic properties of A_{dark} spermatogonia during pre-adult life. While one study showed robust (14.1%-22.4%) labeling of A_{dark} spermatogonia in Rhesus less than 18 months old (Simorangkir et al., 2005), another study observed a prepubertal labeling index that is similar to postpubertal labeling index (1.5%) (Kluin et al., 1983). It has been argued that the low mitotic index and regenerative capacity of A_{dark} are consistent with the characteristics of a "true stem cell," and the regular proliferation of A_{pale} is indicative of "renewing progenitors" (Ehmcke & Schlatt, 2006). Of course, a true stem cell must also contribute to steady-state spermatogenesis, and whether A_{dark} divide under steady state conditions is the subject of debate (Hermann et al., 2010). Therefore, it is time to re-examine the A_{dark} (reserve)/A_{pale} (active) stem cell model now that it is possible to reflect on decades of experimentation on self-renewing stem cells in adult tissues. Since typical cell division takes about 16-24 hours and S-phase only last for about 6-8

hours, true stem cells, which have long G_0 phase (Li & Bhatia, 2011), would unlikely be labelled following a bolus of BrdU. We hypothesize that A_{dark} are slow-cycling, active (not reserve) stem cells, which participate in steady-state spermatogenesis in primate testis.

Primate models may be most suited for evaluating this hypothesis because in addition to cellular level differences, rodents lack the extended prepubertal and pubertal stages of development that are characteristic of nonhuman primates and humans. Direct investigation of stem cells and spermatogenic development in humans is possible but limited by the availability of normal testicular tissues and the types of experimental manipulations that can be performed. Nonhuman primates (including Rhesus macaques) have identifiable prepubertal and pubertal stages of development; they are amenable to *in vivo* experimental manipulations that are not possible in humans; they have undifferentiated A_{dark} and A_{pale} spermatogonia as well as testis anatomy and physiology that are similar to humans (Hermann et al., 2010; Hermann et al., 2007; Marshall & Plant, 1996; Plant, 2006). Therefore, we used long-term BrdU labeling in Rhesus macaques to test our hypothesis.

2.2 MATERIALS AND METHODS

2.2.1 Experimental Animals

Experiments involving the use of Rhesus macaques and nonhuman primate tissues were approved by the Institutional Animal care and Use Committee of Magee-Womens Research Institute and the University of Pittsburgh, and they were performed according to the National Institutes of Health's *Guide for the Care and Use of Laboratory Animals*. Seven adult Rhesus

macaques (Age: 72 to 108 months) and four prepubertal (Age: 35 to 40 months) housed in the nonhuman Primate vivarium of Magee-Womens Research Institute under a 12-hour cycle of light and darkness were used for this experiment. Monkeys were randomly divided into four groups: one bolus group and three groups got BrdU in drinking water for 3 weeks followed by 0, 5 or 9 weeks of wash out (Figure 5).

2.2.2 BrdU bolus

One adult and one prepubertal Rhesus macaques were mildly sedated for venipuncture and intravenous BrdU administration. Then, 33 mg/kg of BrdU (Sigma-Aldrich, B5002, St. Louis, MO) was diluted in sterile normal saline and injected intravenously as previously described (Simorangkir et al., 2009a). Testis tissues were collected 3 hours after the injection.

2.2.3 BrdU in drinking water

All animals were conditioned to Kool-Aid® flavored drinking water, and a favorite flavor for each individual monkey was identified before commencing the experiment. BrdU (Sigma-Aldrich, B5002, St. Louis, MO) was added (1mg/ml) to the Kool-Aid flavored drinking water and offered to each monkey *ad libitum* (Walls et al., 2012). Consumption of Kool-Aid® flavored drinking water with BrdU was monitored and recorded each day to obtain the precise quantity of BrdU consumed by each animal. Testis was collected from each animal at the end of experimental period.

2.2.4 Testicular tissue processing for anti-BrdU staining

Collected testis tissues were cut into small pieces and fixed in Bouin's fluid in a 24-hour (hr) fixation. Fixed testis tissues were washed in 70% ethanol (3×1 hr), embed in paraffin wax block and sectioned (5μm per section). To avoid counting a cell twice, every fifth section was used for quantitative analysis.

2.2.5 Colorimetric BrdU staining in testis tissue sections

Sections were deparaffinized in xylene (2×15 minutes (mins)), rehydrated in graded ethanol series (2×100% for 10 mins, 1×95% for 5 mins, 1×80% for 5 mins, 1×70% for 5 mins, 1×50% for 5 mins, 1×25% for 5 mins) and washed in 1X Gibco® Dulbecco's phosphate-buffered saline (DPBS; Life Technologies, 14200-166, Grand Island, NY) for 3 mins. Sections were then incubated in peroxidase block (3% hydrogen peroxide in methanol) for 15 mins, washed in 1X DPBS (3×5 mins) and stained with mouse anti-BrdU, formalin grade (1:30, Roche Diagnostics, 11170376001, Indianapolis, IN), at 4°C overnight. The next day, sections were washed in 1X DPBS (3×5 mins) and then incubated with horseradish peroxidase-conjugated secondary antibody (1:200, Santa Cruz, SC-2055, Dallas, TX) for 45mins at room temperature. After washing in 1X DPBS (3×5 mins), metal enhanced 3, 3'-diaminobenzidine (DAB) substrate solution (ThermoFisher, 34065, Waltham, MA) was then added to detect and develop positive signal for 5 mins. Sections were then washed in distilled water (dH_2O) for 5 mins and stained with sufficient drops of periodic acid (Cancer Diagnostics, SS1011, Durham, NC) for 7 mins. Sections were washed in tap H_2O for 3 mins, dipped in dH_2O and then stained with sufficient drops of Schiff's reagent (Cancer Diagnostics, SS1011, Durham, NC) for 10 mins. Sections were

washed in tap H_2O for 10 mins, followed by washing in dH_2O for 5 mins and dipping in deionized, distilled water (ddH_2O). Next, sections were counterstained with Gill's number 3 hematoxylin (Sigma-Aldrich, GHS332, St Louis, MO) for 30 secs and washed in tap H_2O for 10 mins, followed by dipping into acid rinse (2% glacial acetic acid in water) 10 times and dipping into H_2O 10 times. Sections were briefly dipped in bluing solution (0.1% sodium bicarbonate) for 1 min and washed in tap H_2O for 1 min. Tissue sections were then dehydrated in graded ethanol series (1×70% for 3 min, 1×95% for 3 min, 2×100% for 5 mins each, 2× xylene for 5 min each) and mounted with permount® (ThermoFisher, SP15, Grand Island, NY).

2.2.6 Colorimetric Ki67, cKIT or caspase 3 staining in testis tissue sections

Testis tissues used for these experiments were fixed in 4% paraformaldehyde (PFA) solution (at 4°C) for 24 hours. PFA-fixed testis tissues were then washed in DPBS (3×1 hour). Tissues were then embedded in paraffin wax block and sectioned (5μm). To avoid counting a cell twice, every fifth section was acquired and analyzed. Tissue sections were deparaffinized in xylene (2×15 mins). Deparaffinized sections were rehydrated in graded ethanol series (2×100% for 10 mins, 1×95% for 5 mins, 1×80% for 5 mins, 1×70% for 5 mins, 1×50% for 5 mins, 1×25% for 5 mins) and washed in 1× DPBS (1×3 mins). Antigen retrieval was performed by incubating slides in sodium citrate buffer (10 mM sodium citrate, 0.05% Tween-20, pH 6) for 30 mins at 97.5°C. Slides in retrieval buffer were left on the bench to cool to room temperature. This was followed by washing twice in DBPS-T (0.1% Tween-20 in 1× DPBS) for 2 mins each. Goat blocking buffer (1X DPBS containing 3% bovine serum albumin, 0.1% Triton X-100 and 5% normal goat serum) was then used to block non-specific antigenic sites in tissue sections for 30 mins at room temperature. Mouse anti-human Ki67 (BD Biosciences, 550609, San Jose, CA) or rabbit anti-

human cKIT (1:100, Agilent, A4502, Santa Clara, CA) or rabbit anti-human caspase 3 (1:100, Abcam, AB13847, Cambridge, MA) primary antibodies were diluted in goat blocking buffer, and sufficient drops were added to tissue sections for 90 mins at room temperature. Sections were then washed in DPBS-T (3×5 mins) and incubated in peroxidase block for 15 mins. This was followed by another wash in DPBS-T (3×5 min). Sections were then washed in 1X DPBS (3×5 mins) and then incubated with goat anti-mouse IgG horseradish peroxidase-conjugated secondary antibody (1:200, Santa Cruz, SC-2055, Dallas, TX) for 45 min at room temperature. (Subsequent periodic acid, Schiff's reagent and hematoxylin staining, as well as washing and mounting steps, were exactly as described in **Colorimetric BrdU staining in testis tissue section**, above).

2.2.7 Quantification of labeled germ cells and statistical analysis

Quantification of germ cells with or without BrdU, Ki67, cKIT and activated caspase 3 expressions involved counting events in round seminiferous tubule cross-sections in multiple (except otherwise stated, usually 7-8) tissue sections from each biological replicate. Number of biological replicates used for the experiments is indicated in each result section. Quantitative observations from biological replicates are presented as mean ± standard error of the mean (SEM). Two quantitative variables were compared using independent-sample student's T-test analysis, while quantitative variables greater than 2 were compared with one-way analysis of variance (ANOVA) method. If significantly different F-value was obtained (*-$P<0.05$; **-$P<0.01$), multiple paired-wise comparison was then performed, by simultaneously using Scheffé multiple comparison test, Tukey's honest significant difference (HSD) test and Bonferroni and Holm's multiple comparison test, to identify variables with relative significant difference. All

statistical analyses were performed using freely available online (as at 03/30/2018) statistical tool at http://astatsa.com/OneWay_Anova_with_TukeyHSD/.

2.3 RESULTS

2.3.1 Long-term BrdU labeling reveals mitotically active A_{dark} and A_{pale} spermatogonia in adult testis

We designed experiment in which adult Rhesus macaques were either administered an intravenous bolus (33mg/kg) of BrdU (Simorangkir et al., 2009a), which was meant to replicate Clermont's experiment (Clermont, 1969) or 1 mg/ml of BrdU (Walls et al., 2012) continuously in drinking water for two cycles of the seminiferous epithelium (21 days or 3 weeks) to label slow-cycling cells that may not be labeled by administration of BrdU bolus (Figure 5A). To the best of our knowledge, this approach has never been used to evaluate the cycling activity of A_{dark} or A_{pale} during steady state spermatogenic development. BrdU labeling was detected in germ cells (including A_{dark} and A_{pale} spermatogonia) of adult Rhesus macaque through colorimetric immunohistochemistry assay (Figure 5B-D). In this study, A_{dark} spermatogonia were identified as "relatively small, spherical or slightly ovoid" cells on the basement membrane, having dark, dense chromatin in their "uniformly stained" nucleus (Clermont & Antar, 1973; Clermont & Leblond, 1959). A_{pale} spermatogonia were identified as "relatively larger, oval" or almost round cells on the basement membrane of the seminiferous tubules, having pale, elongated nuclei with "coarser" or more "granular chromatin (Clermont & Antar, 1973; Clermont & Leblond, 1959). B-type spermatogonia were identified by their relatively larger spherical size, location on or

close to the basement membrane of the seminiferous tubules, and clear nuclei. Granulations and density of heterochromatin staining differentiate one generation of B-type spermatogonia from the other. B1 spermatogonia are least heterochromatic and B4 spermatogonia are most heterochromatic(Clermont & Antar, 1973; Clermont & Leblond, 1959). Quantification of BrdU-labeled spermatogonial cells revealed that 2.6% of A_{dark} and 24.7% of A_{pale} were labeled following a bolus of BrdU (Figure 5E). The B-type spermatogonia and preleptotene were also labeled following a bolus of BrdU (Appendix A, Figure 33A-C). While the proportion of labeled A_{pale} was similar to those previously reported (Clermont, 1969, 1972; Clermont & Antar, 1973; Ehmcke et al., 2005b; Kluin et al., 1983; van Alphen & de Rooij, 1986), we wondered if the A_{dark} labeling was true, steady state labeling or whether it was negligible enough to be considered an artefact. We postulate that prolonged BrdU-labeling will reveal higher proportion of labeled A_{dark} spermatogonia at steady state. Following continuous administration of BrdU to Rhesus macaques in drinking water for 3 weeks, we observed that 11.7% of A_{dark} and 55.5% of A_{pale} spermatogonia incorporated the label (Figure 5E), which demonstrates the presence of cyclically active A_{dark} and A_{pale} spermatogonia in adult Rhesus testes. This also demonstrates the presence of a relatively quiescent subpopulation of A_{pale} spermatogonia in the testis of adult Rhesus macaques. Indeed, phenomena of A_{dark} at different stages of mitotic division were observed (Appendix A, Figure 33D and E). Labeled spermatocytes were also observed following continuous administration of BrdU for 3 weeks (Appendix A, Figure 33F).

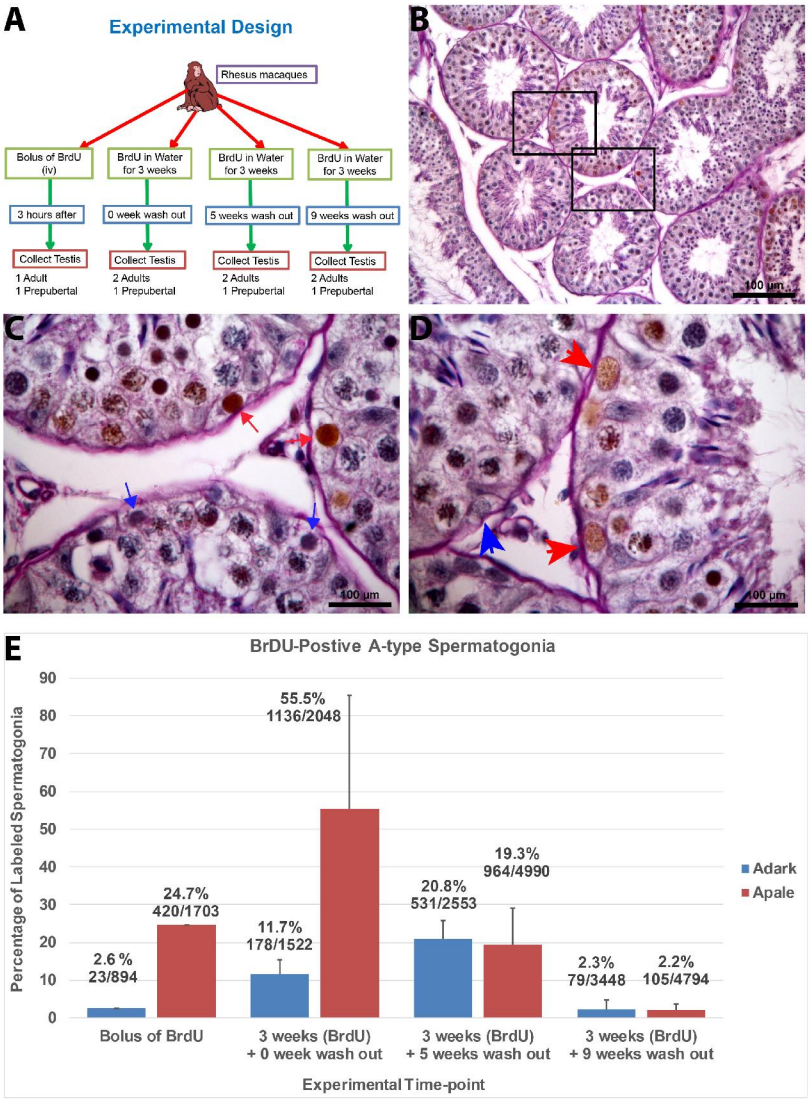

Experimental design for the assessment of mitotic labeling and label-retention of A_{dark} and A_{pale} Spermatogonia (A). BrdU staining of the seminiferous tubules cross-section during PAS-H experiment revealed incorporation of BrdU into testis cells (B). Higher magnification of the insert (bottom rectangle in B) revealed labeled A_{dark}-red small arrow and unlabeled A_{dark}-blue small arrow (C) Higher magnification of the insert (top rectangle in B) revealed labeled A_{pale}-red big arrow and unlabeled A_{pale}-blue big arrow (D). Quantification of BrdU labeling demonstrates that both A_{dark} and A_{pale} are mitotically active and label-retaining cells (E). Quantification analysis was normalized from animal to animal by counting cells in 500 cross sections of seminiferous epithelium. Scale bar=100um

Figure 5: Active A_{dark} and A_{pale} spermatogonia in adult testis

A classical approach for identifying adult stem cells is based on their ability to retain label. Slow-cycling stem cells will retain label since more rapidly dividing, normal cycling cells will rapidly dilute out their label (Alison & Islam, 2009). Therefore, we further hypothesize that (similarly to other adult stem cells in mammalian tissue) A_{dark} and/or A_{pale} are label-retaining cells in Rhesus macaque testis. To test the hypothesis, we allowed for 5 weeks of wash out or 9 weeks of wash out before testis collection (Figure 5A). Five weeks wash out was allowed so that the labeled spermatogonia would have had the opportunity to go through at least three cycles of the seminiferous epithelium (31.5 days, a cycle=10.5days) (de Rooij et al., 1986). For the 9 weeks of wash out, A_{dark} and A_{pale}, would have had the opportunity to go through 6 cycles of the seminiferous epithelium and all previously labeled B-type spermatogonia and cells in subsequent stages of development would have completely gone through the seminiferous epithelium (de Rooij et al., 1986). After continuous administration of Brdu for 3 weeks, with 5 weeks of wash out, the proportion of labeled A_{dark} increased to 20.8%, while the proportion of labeled A_{pale} decreased to 19.3% (Figure 5E). These suggest that A_{dark} and A_{pale} divided again during the 5 weeks of wash out. Following 9 weeks of wash out after three weeks of continuous oral BrdU administration, the proportion of labeled A_{dark} and A_{pale} was reduced to 2.3% and 2.2%, respectively, (Figure 5E). These results indicate that both A_{dark} and A_{pale} include subpopulation of label-retaining cells. No other testis germ cell types retain label (Appendix A, Figure 33G-H).

2.3.2 Long-term BrdU labeling reveals mitotically active A_{dark} with A_{pale} spermatogonia in prepubertal pestis

Next, we asked whether BrdU-labeling would reveal similar trend of cycling activity of A_{dark} and A_{pale} spermatogonia in the prepubertal Rhesus as observed in the adult. To address this question, prepubertal Rhesus monkeys (age: 35-40 months) were given either a bolus of BrdU (33mg/kg) or BrdU in drinking water for 3 weeks, followed by 0, 5 or 9 weeks of wash out (Figure 5A). BrdU incorporation was detected in the A_{dark} and A_{pale} spermatogonia when BrdU was administered either as a bolus, or continuously in drinking water for 3 weeks followed by 0 or 9 weeks of wash out (Figure 6A-B). During experimentation, the testis of the monkey allocated to the 5 weeks of wash out group underwent rapid growth and reached a size with similar gonadosomatic index as adult Rhesus and it was excluded from the analysis (Table 1).

Following administration of BrdU bolus to prepubertal Rhesus macaques, we observed label in 11.2% A_{pale} and in 0% A_{dark} (Figure 6C). After continuous administration of BrdU in drinking water for 3 weeks followed by 0 week wash out, we observed label in 14.7% A_{dark} and 22.8% A_{pale} (Figure 6C). After 9 weeks of wash out, BrdU labeling was detected in 0.7% A_{dark} and 2.4% A_{pale} (Figure 6C). These results indicate that the cycling activity of A_{dark} and A_{pale} spermatogonia in prepubertal Rhesus macaque is similar to that observed in adults (Figure 5).

Table 1: Selected Parameters of Experimental Animals

Identification	Experimental Group	Age at Onset of Experiment (Month)	Start Weight (Kg)	End Weight (Kg)	Average Testicular Weight (Gram)	Gonado-somatic Index ($*10^{-3}$)
55T	BrdU for 3 Weeks, 9 weeks wash out	108	11.2	11.4	27.5	2.41
6C7	BrdU for 3 Weeks, 9 weeks wash out	72	9.1	8.8	12.4	1.41
6G8	BrdU for 3 Weeks, 9 weeks wash out	35	5.2	5.6	1.6	0.29
71T	BrdU for 3 Weeks, 5 weeks wash out	108	12	12.4	35.9	2.9
7B8	BrdU for 3 Weeks, 5 weeks wash out	74	11.6	12.2	24.3	1.99
4G4	BrdU for 3 Weeks, 5 weeks wash out	39	7.0	8.0	15.7	1.96
9B5	BrdU for 3 Weeks, 0 weeks wash out	73	9.6	9.4	21.5	2.29
8A4	BrdU for 3 Weeks, 0 weeks wash out	81	9.8	9.4	14.6	1.55
1H2	BrdU for 3 Weeks, 0 weeks wash out	38	6.2	7.0	1.9	0.27
50Z	BrdU Bolus	85	8.2	8.2	13.2	1.61
O12	BrdU Bolus	40	4.2	4.2	1.7	0.4

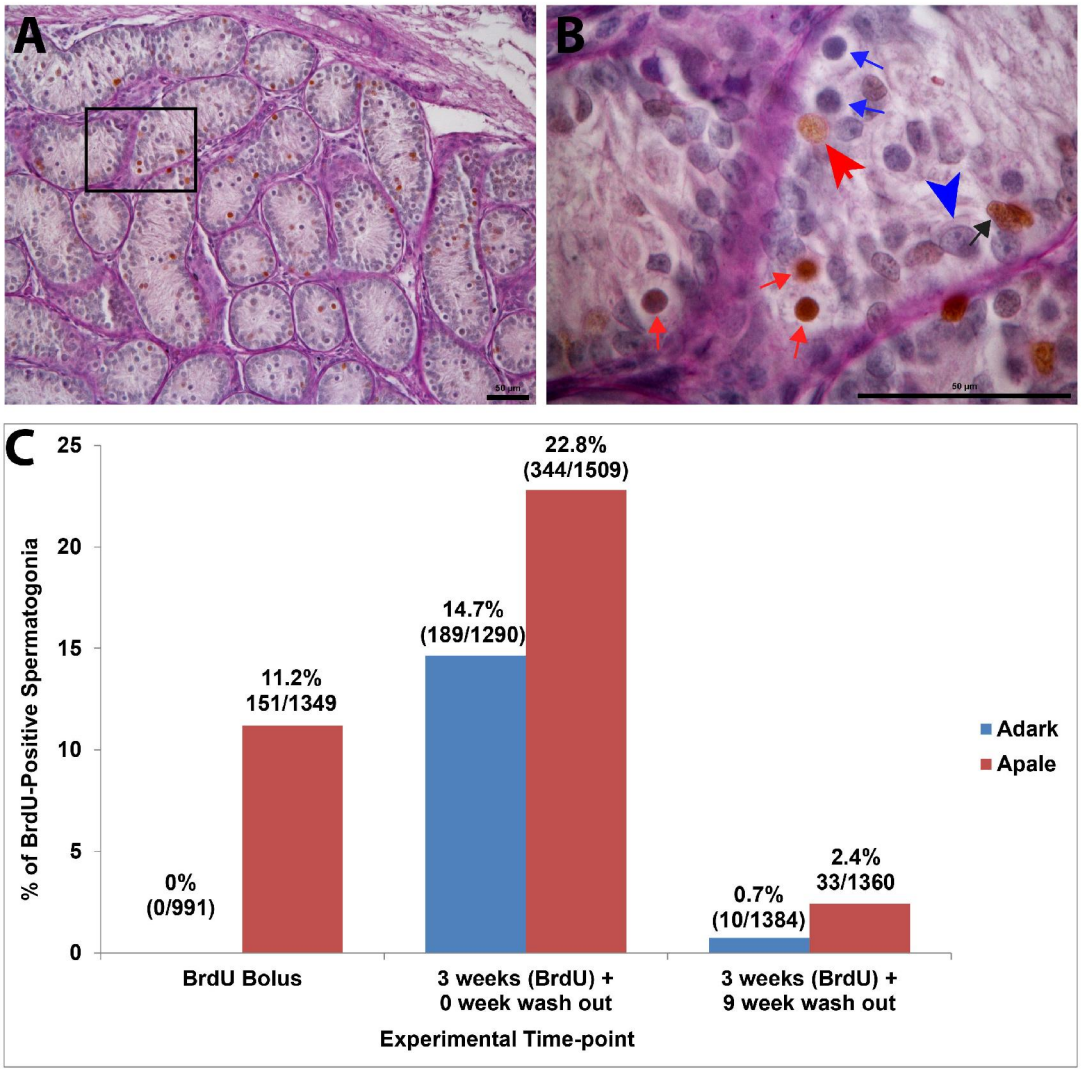

BrdU staining of the seminiferous tubules cross-section during PAS-H experiment revealed incorporation of BrdU into testis cells after administration of BrdU (A). Higher magnification of the insert (black rectangle in A) revealed unlabeled A_{dark}-blue small arrow, labeled A_{dark}-red small arrow, labeled A_{pale}-red big arrow and unlabeled A_{pale}-blue big arrow (B). Quantification of BrdU labeling demonstrates that both A_{dark} and A_{pale} are mitotically active and label-retaining cells (G). Quantification analysis was normalized from animal to animal by counting cells in 500 cross sections of seminiferous epithelium. Scale bar=50um

Figure 6: Active A_{dark} and A_{pale} in prepubertal testis

2.3.3 Proliferating A_{dark} and A_{pale} spermatogonia in monkey testis

Next, we evaluated momentary cycling status of A_{dark} and A_{pale} spermatogonia in Rhesus testis during development and at steady state using Ki67 expression. Ki67 marks cells in the active (G_1, S, G_2 and Mitosis (M)) phases, but not those in the resting or quiescent (G_0) phase of the cell cycle (Scholzen & Gerdes, 2000). Ki67 expression was detected in A_{dark} and A_{pale} spermatogonia (Figure 7A-B). Quantification of momentary Ki67-positive spermatogonia during development revealed that 2.4% of A_{dark} and 18.8% of A_{pale} were positive in adult; while 8.1% of A_{dark} and 12.9% of A_{pale} were Ki67-positive in the neonatal Rhesus testis and 4.6% of A_{dark} and 8.2% of A_{pale} in the prepubertal testis during development (Figure 7C). The proportion of Ki67-positive A_{dark} in neonate was statistically greater ($P<0.01$) than in adult testis. In adult life or during steady state, spermatogenic development occurs as a systematic progression of events, which starts, proceeds and ends with similar association of cells in the seminiferous epithelium (Clermont, 1972). A complete progression is known as a cycle, and 12 distinct events or stages constitute one cycle of the seminiferous epithelium in the Rhesus macaque (Clermont & Leblond, 1959). A segment of seminiferous tubule progresses through all 12 stages of the seminiferous epithelium in a repetitive 10.5-day cycle. Evaluation of the stage-specific cycling activity of A_{dark}, A_{pale} and B1 spermatogonia revealed that Ki67-Positive $A_{d\ ark}$ spermatogonia were seen in stages IX to IV (Figure 7D). Quantitatively, following lack of Ki67 expression in A_{dark} spermatogonia from stages V-VIII, the proportion of Ki67-positive A_{dark} begins to rise from stage IX (1.4%), peaks by stage X (5.8%) and is sustained at relatively comparable proportions during stages XI (4.4%) and XII (5.2%) (Figure 7D). Relatively fewer A_{dark} spermatogonia were Ki67 positive during stages I (1.8%), II (2.1%), III (3.4%) and IV (1.6%) (Figure 7D). Similarly, the A_{pale} spermatogonia were Ki67-positive during all stages of the seminiferous epithelium

except during stage V (Figure 7D). Ki67-positive A_{pale} spermatogonia are almost constant from stage I (9.2%) to II (9.5%). The proportion declines by stage III (3.8%) but rises remarkably by stage IV (15.0%). The proportion of Ki67-positive A_{pale} spermatogonia becomes robust from stage VII (23.7%), peaking by stage IX (42.0%), and gradually declines from stage X (37.2%) to stage XII (17.8%) (Figure 7D). Ki67-positive B1 spermatogonia were observed beginning from stage IX. Not less than 90% of B1 spermatogonia from stages IX-XII were Ki67-postive. Almost all B2-B4 spermatogonia and some spermatocytes were Ki67-positive (Appendix B, Figure 34A).

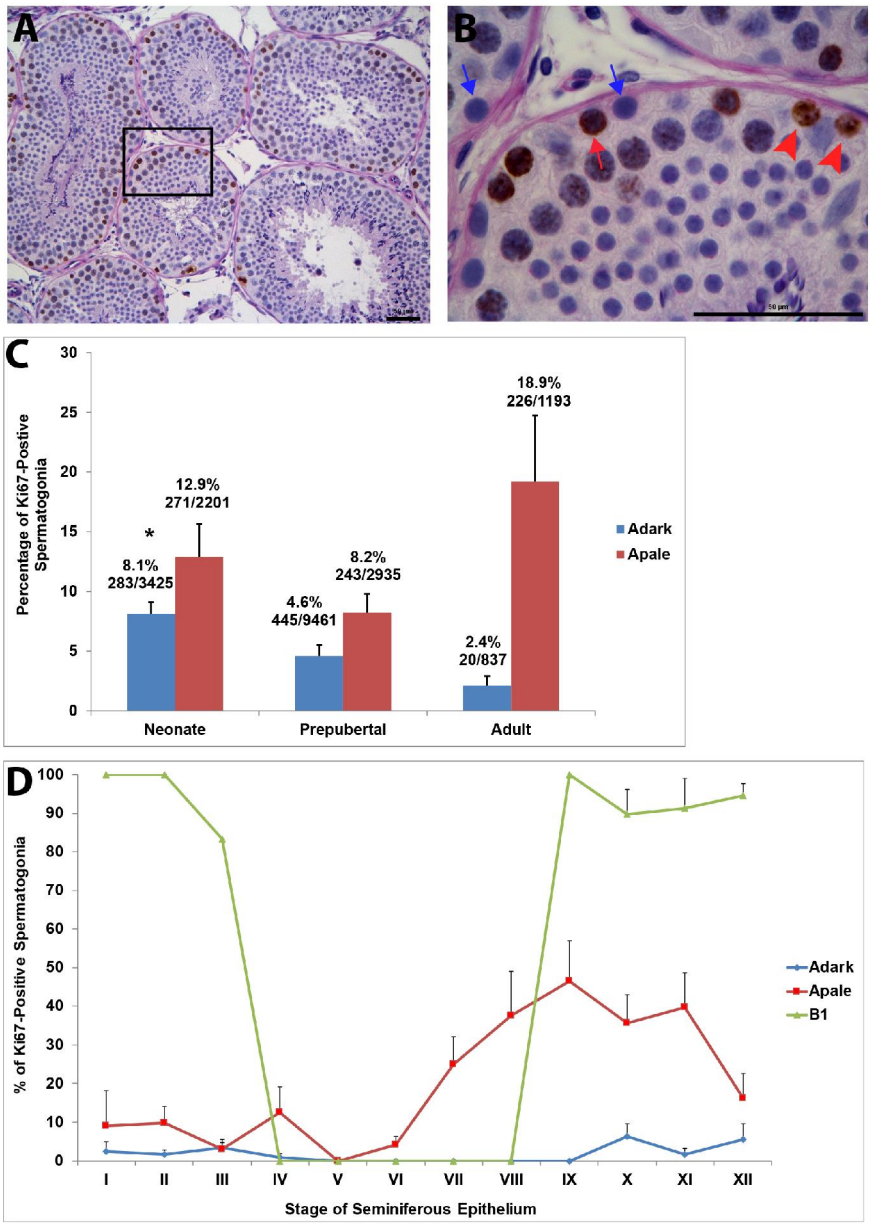

Ki67 expression in testis during steady state (A). Higher magnification of the insert (black rectangle in A) revealed labeled A_{dark}-red small arrow, unlabeled A_{dark}-blue small arrow, labeled A_{pale}-red big arrow (B). Quantification of Ki67-postive cells during development (C). Quantification of Ki67 expression by A_{dark}, A_{pale} and B1 across stages of seminiferous epithelium (D) (n=4), Observation were normalized by counting cells in round cross sections of seminiferous epithelium in 8 different testis sections per animal. Scale bar=50um

Figure 7: Proliferating A_{dark} and A_{pale} spermatogonia in monkey testis

2.3.4 Proliferating A_{dark} and A_{pale} spermatogonia in human testis

Next, we assessed the expression of Ki67 in A_{dark} and A_{pale} spermatogonia in Human testis during development (Figure 8A-E). Quantification of momentary Ki67 expression revealed that 2.3% of A_{dark} and 3.5% of A_{pale} were positive in infant (1.5-year old); while 0.8% of A_{dark} and 3.7% of A_{pale} were Ki67-positive in the (5-year old) prepubertal boys. Higher frequency of Ki67-postive A_{dark} (4.0%) and A_{pale} (13.5%) were observed in the older (12 to 13-year old) prepubertal boys. In the adult 14.9% of A_{dark} and 17% of A_{pale} were ki67-postive (Figure 8E).

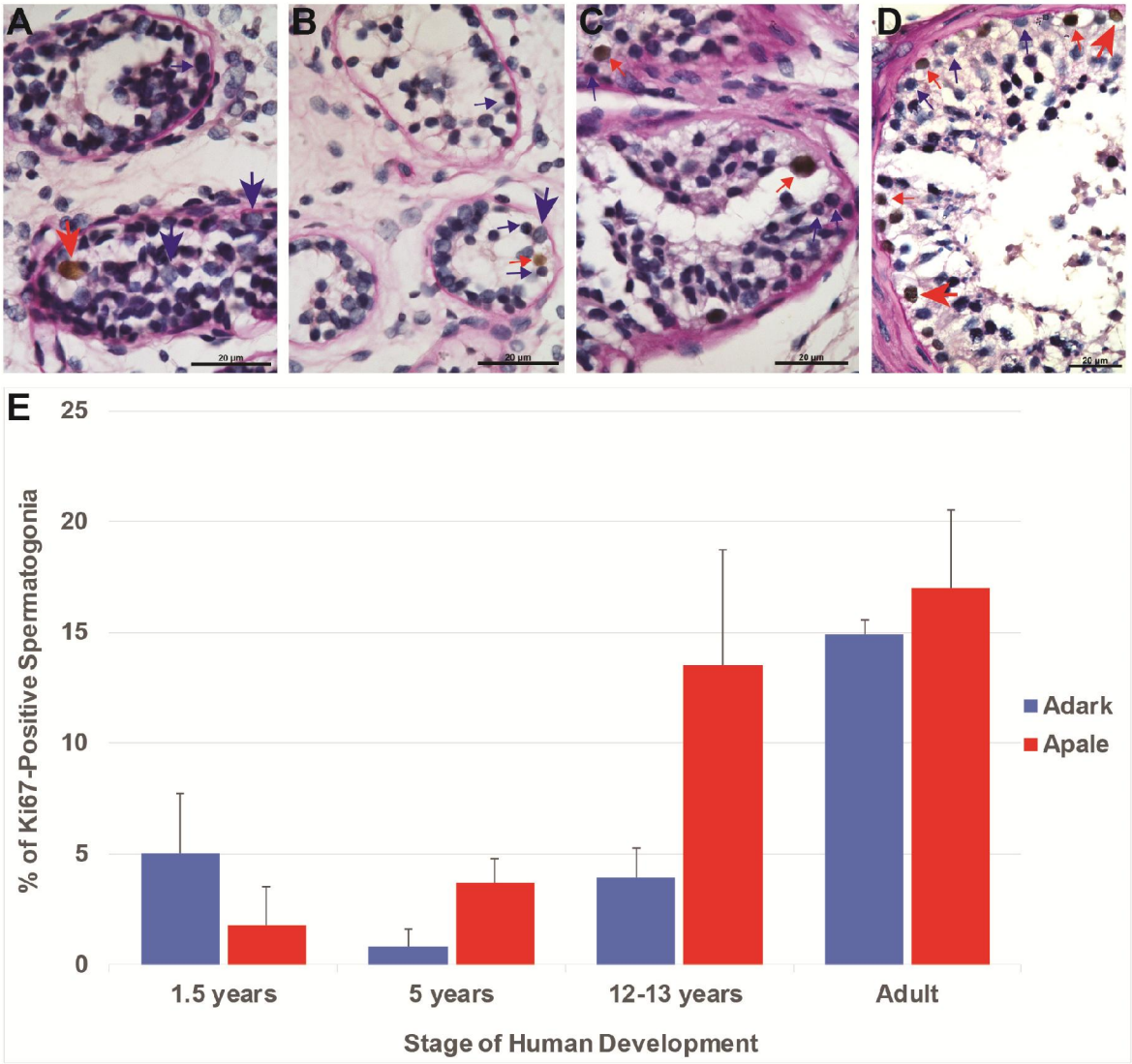

Ki67 staining in the seminiferous tubules cross-section during colorimetric PAS-H experiment reveals Ki67 expression in labeled A_{pale}-red big arrow with unlabeled A_{pale}-blue big arrow in a 1.5-year old boy (A), labeled A_{dark}-red small arrow with unlabeled A_{dark}-blue small arrow with unlabeled A_{pale}-blue big arrow in 5-year old boy (B), labeled A_{dark}-red small arrow with unlabeled A_{dark}-blue small arrow in a 12-year old boy (C), and labeled A_{dark}-red small arrow with unlabeled A_{dark}-blue small arrow alongside labeled A_{pale}-red big arrow in cross section of adult (D) testes. Quantification of Ki67 expression by A_{dark} and A_{pale} in Human testis during development (n=2), Observation were normalized by counting cells in all the cross sections in a tissue section. Scale bar=20um

Figure 8: Proliferating A_{dark} and A_{pale} spermatogonia in human testis

2.3.5 Differentiating A_{dark} and A_{pale} spermatogonia in adult Testis

We next evaluated fate of proliferating A_{dark} and A_{pale} spermatogonia during steady-state spermatogenesis. There are three possibilities during steady-state spermatogenesis: self-renewal, cell differentiation and/or cell death. Findings in our BrdU experiment after 5 and 9 weeks of wash out (Figure 5E) suggest presence of self-renewed subpopulation of A_{dark} and A_{pale} spermatogonia following cell division. Kinetics of differentiating A_{dark} and A_{pale} spermatogonia was evaluated by staining adult Rhesus macaque testis sections with cKIT in colorimetric immunohistochemistry experiment. cKIT, a marker of differentiating spermatogonia, is conserved in rodents, human and nonhuman primate (Hermann et al., 2009; Manova et al., 1990; Schrans-Stassen et al., 1999; Valli et al., 2014b). Colorimetric staining revealed that cKIT is expressed by A_{pale} (Figure 9A-B) and surprisingly by A_{dark} spermatogonia (Figure 9A and C). Evaluation of differentiating spermatogonia by stage of the seminiferous epithelium revealed that the proportion of cKIT-positive A_{dark} was approximately 3% during stages I (3.3%), II (3.1%) and III (2.9%) (Figure 9D). While no cKIT-positive A_{dark} spermatogonia was observed during stages IV, VIII, IX and XII, approximately 2.2–2.6% A_{dark} was labeled during stages V (2.4%), VI (2.2%) and VII (2.6%) (Figure 9D). cKIT expression in A_{dark} spermatogonia peaked by stage X (3.8%), and this proportion decreased to 1.4% by stage XI (Figure 9D). cKIT-positive A_{pale} were observed in every stage of the seminiferous epithelium (Figure 9D). The proportion of this cell-type was 9.4% in stage I of the seminiferous epithelium, which gradually increased during stages II (12.0%) and III (12.9%) and increased rapidly during stages IV (20.6%) and V (21.7%). While there was a little dip in the trend of cKIT-positive A_{pale} in stages VI (16.5%) and VIII (30.0%), the trend appears to peak by stage VII (42.4%) and gradually declined from stage IX (38.5%), through X (34.4%), XI (24.7%) and XII (11.5%) (Figure 9D). Almost all B1

spermatogonia arising from stage VIII through to stage XII are cKIT-positive (Appendix B, Figure 34B). Other B-type (B2-B4) spermatogonia were cKIT-positive during steady state spermatogenic development (Appendix B, Figure 34B).

To evaluate if elevated proportion of cKIT-positive cells in the middle stages (IV-VI) is associated with proliferation of cKIT-positive cells or expression of cKIT in previously cKIT-negative cells, testis tissue from BrdU-treated monkey was stained for cKIT expression. Most of the BrdU-positive A_{pale} spermatogonia were cKIT-positive (Appendix C, Figure 35A-D). However, BrdU-negative cKIT-negative A_{pale} spermatogonia were also detected in these cross sections (Appendix C, Figure 35B). Also seen were BrdU-negative cKIT-positive A_{pale} spermatogonia (Appendix C, Figure 35C) as well as BrdU-positive cKIT-negative A_{pale} spermatogonia (Appendix C, Figure 35D).

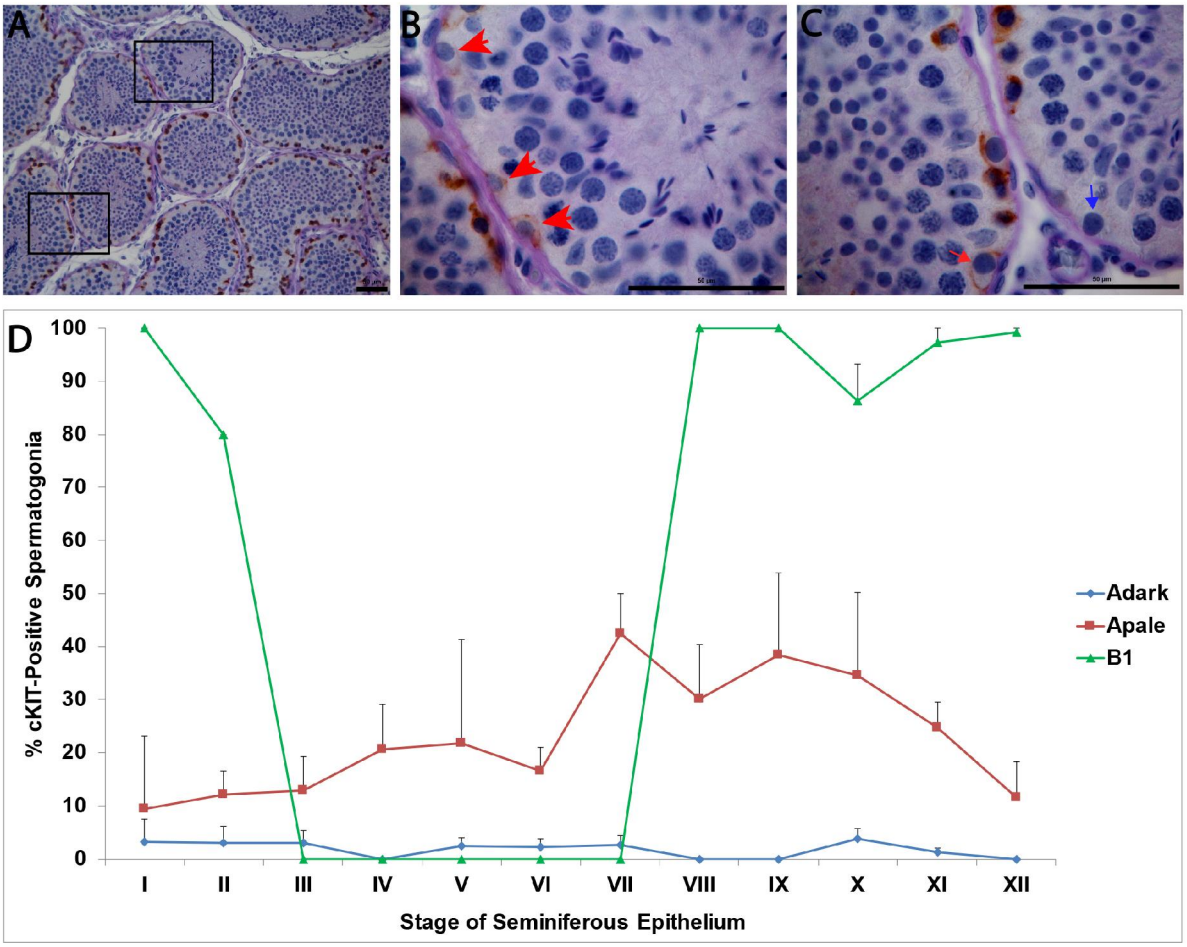

cKIT staining in the seminiferous tubules cross-section during colorimetric PAS-H experiment revealed cKIT expression in adult testis during steady state (A). Higher magnification of the insert (top right rectangle in A) revealed labeled A_{pale}-red big arrow (B), and higher magnification of the insert (bottom left rectangle in A) revealed labeled A_{dark}-red small arrow and unlabeled A_{dark}-blue small arrow (C). Quantification of cKIT-postive cells showing the proportion of positive A_{dark}, A_{pale} and B1 spermatogonia (D). Pattern of cKIT expression by A_{dark}, A_{pale} and B1 spermatogonia across stages of seminiferous epithelium was evaluated and presented as proportion of total cell (E). Normalized by counting cells in round cross sections of seminiferous epithelium in 8 different testis sections per animal, (n=4). Scale bar=50um

Figure 9: Differentiating A_{dark} and A_{pale} spermatogonia in adult testis

2.3.6 Apoptosis in germ cells in adult Rhesus testis

We then investigated how apoptosis might regulate proliferation of A_{dark} and A_{pale} spermatogonia in Rhesus macaque testis during steady-state spermatogenic development. Caspase 3 is an executioner enzyme that is activated for cell apoptosis (Parrish et al., 2013). Expression of activated/cleaved caspase 3 in germ cells is conserved from rodent to human (Almeida et al., 2011; Narisawa et al., 2002) but, to the best of our knowledge, has not been demonstrated/evaluated in Rhesus macaque testis. Expression of activated caspase 3 were mostly seen in the pachytene spermatocyte (49.4%) (Figure 10A-C) and round spermatid (46.7%) (Figure 10C). However, expressions of activated caspase 3 was also detected in A_{dark} (4.9%), A_{pale} (3.9%), preleptotene (2.7%), leptotene (3.0%), Zygotene (1.8%) and elongated spermatids (5.6%) (Figure 10C). Stage-specific analysis of activated caspase 3 expression revealed that higher proportion (> 59%) of caspase 3-positive pachytene was seen from stage V-XI, while the proportion of activated caspase 3-positive pachytene in other stages (XII-IV) were less than 30% (Figure 10D). Similarly, caspase 3-positive round spermatid (31%-61%) was more frequent during stages I-VII but not in other stages (Figure 10D). While about 30% of elongating spermatids of stage VIII were caspase 3-positive, expression of this marker was not seen in spermatids during other stages of the seminiferous epithelium (Figure 10D). Among the spermatogonia population, while activated caspase 3 was not expressed by A_{dark} in stage II, remarkable proportion (10%) of A_{dark} were caspase 3-postive by stage IV while the marker expression in A_{dark} stood at 2.0% (I), 3.0% (III), 1.4% (V), 4.8% (VI), 5.3% (VII), 4.8% (VIII), 4.2% (IX) and 4.2% (XII) during other stages of seminiferous epithelium (Figure 10E). In the A_{pale} spermatogonia, except for stages VI (9.3%), X (5.1%) and XII (7.1%), the proportion of activated caspase 3 expression was generally less than 5%, and they were quantified to be 0.5%

(I), 1.8% (II), 3.3% (III), 4.2% (IV), 2.0% (V), 4.9% (VII), 3.7% (VIII), 3.0% (IX) and 1.0% (XI) during other stages of the seminiferous epithelium (Figure 10E). Activated caspase 3 was only observed in 2% of B-type spermatogonia in stage I and the marker expression was not detected in B-types in other stages (Figure 10E).

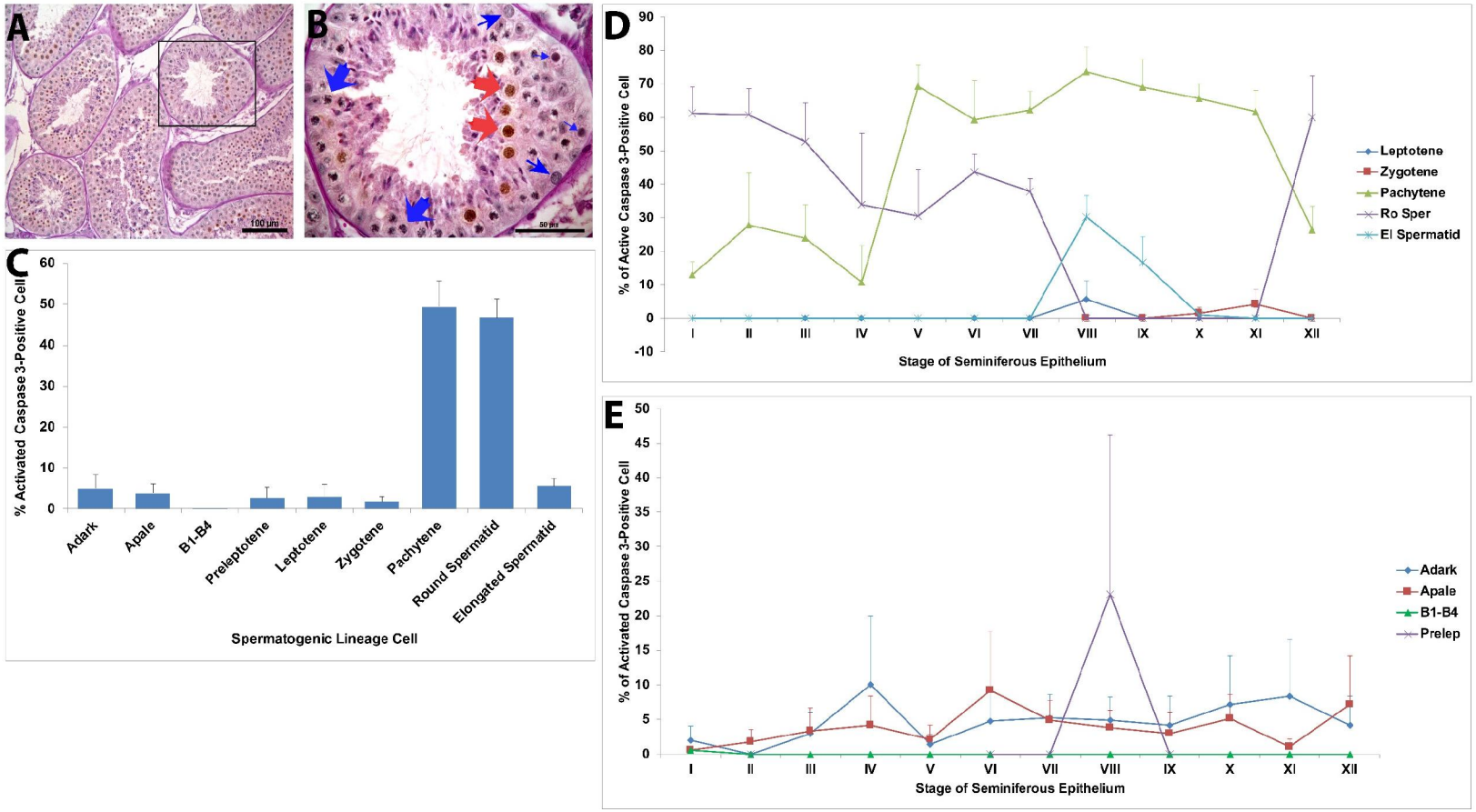

Activated caspase-3 staining in adult testis (A). Higher magnification of the insert (rectangle in A) (B). Quantification of proportion of activated caspase 3-postive cells in germ cells (C). Quantification of stage-specific dynamics of activated caspase 3 expression in germ cells (D) Quantification of stage-specific dynamics of activated caspase 3 expression in A_{dark}, A_{pale}, B-type spermatogonia and preleptotene (E). Quantitative assay was normalized by counting cells in round cross sections of seminiferous epithelium in 3 testis sections per animal. (n=3). Scale bar=100um (A) and 50um (B).

Figure 10: Apoptosis in germ cells in adult Rhesus testis

2.4 DISCUSSION

This study demonstrates unequivocally that A_{dark} are label-retaining, slow cycling, active cells which are dividing during steady-state spermatogenesis. First, this is due to our observation of relatively high proportion of S phase-labeled A_{dark} spermatogonia following prolonged BrdU administration when compared to the proportion of labeled cells from monkey treated with bolus of BrdU. Second, the proportion of labeled A_{dark} spermatogonia appears to increase after 5 weeks of wash out, which suggest self-renewing divisions during the wash out period. Third, the proportion of labeled A_{dark} spermatogonia appears to decline after 9 weeks of wash out, which further suggests mitotic divisions (beyond five weeks of wash out) that result in the dilution of incorporated BrdU. Fourth, the detection of label-retaining A_{dark} and A_{pale}, a classical characteristics of adult stem cells, indicate that they are slow cycling cells. Since the phenotype of every BrdU-labeled A_{dark} spermatogonia was not known at the time of labeling, we cannot rule out the possibility of labeled cells of another phenotype transitioning to A_{dark} spermatogonia during the wash out period. In primate testis, SSCs and progenitor cells are still being described as A_{dark} and A_{pale}; therefore, the genetic and lineage-tracing experiments necessary to address this question is presently difficult. However, since A_{dark} and A_{pale} spermatogonia were the only cell-type retaining labels after 5 weeks of wash out, BrdU-positive cells (after 9 weeks of wash out) might not have been from other cell-types. It has been reported that A_{pale} spermatogonia arise from A_{dark} (van Alphen & de Rooij, 1986), and no known data have suggested otherwise. Our observation of rare events indicate that daughter A_{dark} arise from mother A_{dark} undergoing mitotic divisions. Taken together, our data indicate that A_{dark} are mitotically active during steady-state

spermatogenesis resulting in production of other A_{dark}, which is a self-renewal division (Figure 11).

These observations are very similar to those made during prepubertal spermatogenic development. The proportions of labeled A_{dark} and A_{pale} following administration of BrdU as a bolus or for 3 weeks in drinking water followed by 0 or 9 weeks of wash out are similar to those in the adult study. Our observation of a relatively lower proportion of labeled A_{pale} during prepubertal development (compared to that in adult testis) is consistent with previous reports that fewer A_{pale} incorporate labels during infant and prepubertal development (Kluin et al., 1983; Simorangkir et al., 2005). These results also suggest that, at least, the S-phase duration of A_{pale} during prepubertal development is relatively longer than during adult or steady state spermatogenic development.

During evaluation of steady state events, the results of our pulse-labeling (BrdU and Ki67) experiments of A_{dark} are similar to those previously reported (Clermont & Antar, 1973; Ehmcke et al., 2005b; Fouquet & Dadoune, 1986; Kluin et al., 1983). The differences among previous conclusions (e.g., by some studies that A_{dark} are "reserve stem cells"(Clermont, 1969; Ehmcke et al., 2005b; Schlatt & Weinbauer, 1994; Simorangkir et al., 2009a)) may arise from variations in the species of primate used for the experiment (*Cercopithecus aethiops* vs. *Macaca arctiodes* vs. *Macaca fascicularis* vs. *Macaca mulata*), time to analysis (1 hour vs. 2.5 hours vs. 3 hours vs. 11.1 days vs. 12.1 days vs. 9-10 days), the compound used for analysis (^{3}H thymidine vs. BrdU) and the number of testis cross sections evaluated. Importantly, our study indicates that A_{dark} are not just cells that might be labeled when they come into cell cycle once in a long time, but they are cells that cycle regularly, albeit slowly.

Also, the proportion of labeled A_{pale} during our pulse-labeling experiments is similar to previous observations(Clermont, 1969; Clermont & Antar, 1973; de Rooij et al., 1986; Ehmcke et al., 2005b; Kluin et al., 1983; Schlatt & Weinbauer, 1994; Simorangkir et al., 2009a). The proportion of labeled A_{pale} after 3 weeks of BrdU loading suggest that A_{pale} either divide more frequently and/or have longer S-phase duration than A_{dark}. However, as discussed above, we cannot rule out the possibility of the high proportion of labeled A_{pale} after 3 weeks of loading being due to transition of other cell types to A_{pale}.

Ki67 expression reveals momentary proliferation of A_{dark} and A_{pale} during development. In the Rhesus, proliferation of A_{dark} and A_{pale} spermatogonia during neonatal and prepubertal phase of life is due to the self-renewing divisions that accompany post-natal testis development, and this is continuous across all stages of prepubertal life (Simorangkir et al., 2005). However, significant difference between the proportion of momentarily cycling A_{dark} during neonatal and adult life suggest that cell cycle of A_{dark} is differentially regulated during development with proliferative activity lowest during adult life in Rhesus macaque. This observation also demonstrates that irrespective of the age group, high proportion of A_{dark} are in G0 phase at any point in time irrespective of stage of development. Adult stem cells are expected to divide very slowly, and the proportion of Ki67-positive A_{dark} is similar to the proportion of labeled A_{dark} from BrdU bolus. Conversely, proportion of cycling A_{pale} appears to be highest in the adult life during which differentiated spermatogonia and other cell-types in spermatogenic development are needed to drive complete spermatogenesis. These give credence to the theory that A_{dark} are the stem cells while A_{pale} are the progenitor cells (Ehmcke & Schlatt, 2006). Proportion of proliferating spermatogonia in preadolescent boys appears to be similar to that of prepubertal Rhesus macaque. However, just before puberty and in adult Human testis, there is apparent

difference in the proportion of proliferating A_{dark}. Conversely, the proportion of proliferating A_{pale} is similar in these species at steady state. This is similar to observation from Bergmann group that 22.1% of A-type spermatogonia are Ki67-positive (Steger et al., 1998). Our study further resolves Ki67 expression in A_{dark} and A_{pale} spermatogonia, which are the cell type that constitute the A-type spermatogonia in Human testis (Clermont, 1963). We also show that fewer proliferating activity occurs in human testis during development. Higher number of proliferating A_{dark} is probably required during steady state to compensate for fewer amplifying divisions of B-type spermatogonia (Fayomi et al., 2018).

Previous studies in Rhesus have indicated that A_{pale} undergo mitotic division between stages VII-X (Clermont, 1969; Clermont & Antar, 1973; Simorangkir et al., 2009a), and we also observed higher proportions (23.7%-37.2%) of Ki67-positive A_{pale} between stages VII and X. This range is similar to the one observed by Clermont and Antar (25.6%-41.9%) following pulse-labeling with ^{3}H-thymidine (Clermont & Antar, 1973). A_{pale} were unlabeled in all other stages of the seminiferous epithelium in that experiment. Our data, like previous observations (Simorangkir et al., 2009a; van Alphen & de Rooij, 1986), indicate that A_{pale} do not all divide during every cycle of the seminiferous epithelium. Previous studies have also demonstrated that A_{pale} develop from A_{dark} (van Alphen & de Rooij, 1986) and B1 spermatogonia from A_{pale} (Clermont & Leblond, 1959). Therefore, it follows a logical sequence to speculate that label-retaining A_{pale} are products of transitioned daughter cells of divided, label-retaining A_{dark} during steady state. Using Ki67 expression to mark proliferating cells helps us to identify cells in the active (G_1, S, G_2 and Mitosis (M)) and quiescent (G_0) phases of the cell cycle (Scholzen & Gerdes, 2000). Ki67 expression alongside BrdU labeling reveals that at any giving stage of the seminiferous tubules, less than half of the total A_{pale} population are Ki67-positive (cycling)

despite the presence of A_{pale} in all stages of the seminiferous epithelium (Clermont & Leblond, 1959; Simorangkir et al., 2009a). Since A_{dark} are only completely Ki67-negative from stage V to VIII, which constitute 42%(Clermont & Antar, 1973) or 4.6 days(de Rooij et al., 1986) of the seminiferous epithelial cycle, we speculate that A_{dark} and A_{pale} quiescence is differentially regulated by stage-specific factors.

Rapid decline in the proportion of cycling A_{pale} from stage XI to I is associated with the transition of mitotically active A_{pale} to B1 spermatogonia (Clermont & Antar, 1973) (Figure 11). Exactly how B1 evolve from A_{pale} has been a subject of debate. It's been postulated that each A_{pale} division gives rise to another A_{pale} and a B1 spermatogonium (Clermont, 1969). Others have hypothesized that a proportion of A_{pale} self-renew while another proportion is simultaneously transiting to B1 spermatogonia (Ehmcke et al., 2005b; Simorangkir et al., 2009a). Per our data, since almost all B1 spermatogonia are cKIT-positive, then almost all A_{pale} spermatogonia transiting to B1 would be cKIT-positive. The gradual increase in the proportion of cKIT-positive A_{pale} spermatogonia from about 9% (stage I) to about 20% (stages IV-VI) may not be unconnected with proliferation or doubling just as there may be simultaneous addition through turning on of cKIT expression from cKIT-negative A_{pale}. We postulate that the rapid elevation in the proportion of cKIT-positive A_{pale} by stage VII is a result of the duplicating mitotic division of cKIT-positive A_{pale} at this stage. Transitioning to B1 or remaining as cKIT-positive A_{pale} are the only fate of cKIT-positive A_{pale} by stage IX. Thus, based on the estimate from our data, three out of every four cKIT-positive A_{pale} spermatogonia would have transited to B1 spermatogonia by stage XII provided cKIT expression was not activated in subpopulation of A_{pale} spermatogonia during the latter stages. Expression of cKIT by A_{dark} spermatogonia is a surprising finding, but this has also been reported in A_s, the spermatogonial stem cell equivalent in rodent (Gassei &

Orwig, 2013). Further experiment is required to identify and elucidate the fate of cKIT-positive A_{dark} spermatogonia.

This study demonstrates that A_{dark} spermatogonia at G_0 phase can commit to differentiate (by cKIT expression) or be targeted for apoptosis (by activated caspase 3 expression). Our data further suggest that the mechanisms targeting A_{dark} and A_{pale} spermatogonia for apoptosis do not depend on whether they are cycling or not. However, it is not impossible that apoptotic regulation plays a role in regulating the progression of events leading to the (required proportionate) contribution of A_{dark} and A_{pale} spermatogonia to spermatogenic development. Previously, Simorangkir et al. reported the presence of degenerating germ cells "on or near the basement membrane" of the seminiferous tubules in Rhesus macaque (Simorangkir et al., 2009a). Cell types on or near the basement membrane of the seminiferous tubules would include the A_{dark}, A_{pale} and all B-type spermatogonia and sometimes the preleptotene spermatocyte (Clermont & Leblond, 1959). Here, we have demonstrated that B2-B4 spermatogonia are rarely targeted for cell death in the Rhesus macaque testis. Unlike in the rodent, where up to 75% of their equivalence, A2-A4 spermatogonia, are targeted for cell death (Huckins, 1978a; Sinha Hikim et al., 2003).This suggests the presence of different mechanisms for the regulation of spermatogenic development in rodent and Rhesus macaque. The mechanism for spermatogenic output regulation in Rhesus testis appears to focus mainly on targeting roughly 50% of pachytene and round spermatids for apoptotic degradation (Figure 11), which is a less common event in rodents (Sinha Hikim et al., 2003). We observed that pachytene of older generations were mostly targeted for degradation, and this may have implications for "clearing out" older generations of pachytene that could increase the risk of mutation during spermatogenesis (Walter et al., 1998). Mechanisms for selection of each cell-type for apoptotic degradation are not yet understood.

Results from our BrdU-labeling experiment are cautiously and simply presented as the proportion of labeled events from total observation across 1 or 2 animals. Animal intractability and variability remain some of the challenges in the use of nonhuman primates as model animal, and these factors impact the sample size reported in this study. Future studies using multiple, subsequent pulse-labeling approach would help to dissect the subpopulations of cycling A_{dark} and A_{pale}, and may potentially give insight to their cell cycle duration/stages. Identification and/or characterization of A_{dark}- and A_{pale}-specific markers would provide tools for molecular evaluations of these cell-types during development and at steady state.

In conclusion, this study demonstrates that A_{dark} are mitotically active, slow-cycling cells that are dividing during steady-state spermatogenesis, and they have similar mitotic activity potential in adult and prepubertal Rhesus testis. We also demonstrate that subpopulations of both A_{dark} and A_{pale} possess the ability to self-renew, differentiate and retain label, thereby meeting the classical definition of stem cells. We also demonstrated that A_{dark} exist as Ki67-negative (G_0 phase) cells during stages V-VIII. A_{pale} do not divide during every cycle of the seminiferous epithelium, and they include subpopulation of differentiating spermatogonia which may undergo at least one mitotic division (VII-IX) before estimated three out of every four differentiating A_{pale} transit to B1 spermatogonia (X-XII). We propose that B1 spermatogonia arise (mostly) from cKIT-postive A_{pale} spermatogonia, and on few occasions, from cKIT-positive A_{dark} spermatogonia.

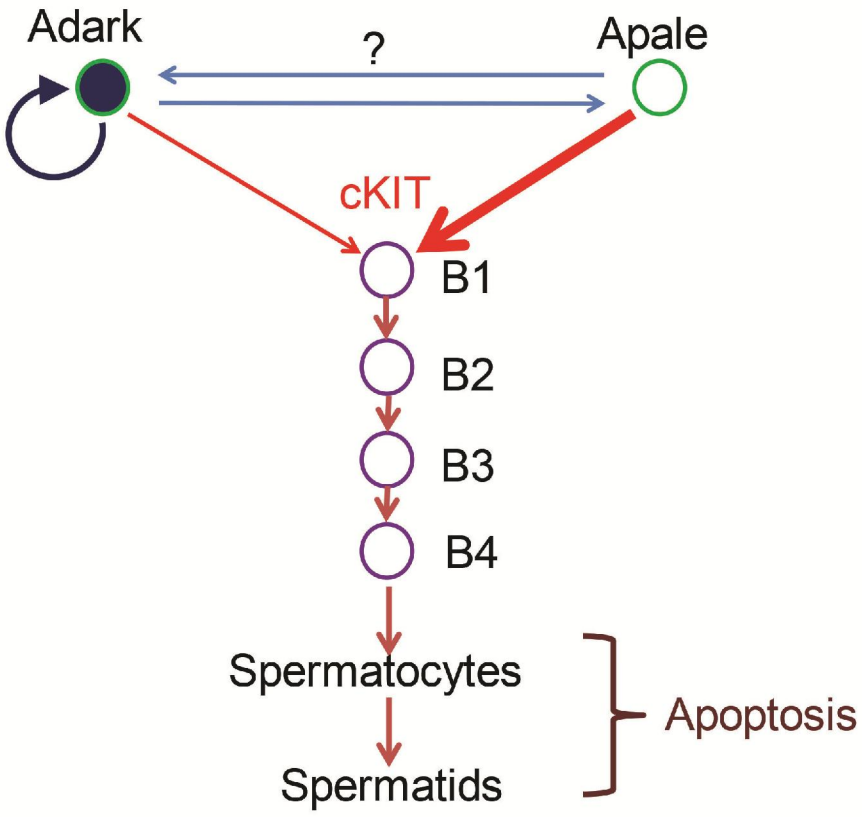

A_{dark} are mitotically active, slow-cycling, label-retaining cells that divides during steady-state spermatogenesis. A_{dark} and A_{pale} self-renew and differentiate, thereby fulfilling the definition of stem cells. cKIT-positive B1 spermatogonia mostly arise from A_{pale} spermatogonia, and from A_{dark} spermatogonia on few occasions. Apoptotic regulation of spermatogenic development mostly occurs in the pachytene and round spermatids in a stage-dependent manner

Figure 11: Revised model of spermatogenic development in Rhesus macaque

3.0 MOLECULAR MARKERS AND CLONAL DYNAMICS OF SPERMATOGONIA IN THE PRIMATE TESTIS

This chapter is being submitted as a research article to "Development" journal.

3.1 INTRODUCTION

The roles of spermatogonia in spermatogenic lineage development and male fertility are revealed mostly by decades of studies using rodent model (Brinster, 2007). In one of those studies, Huckins and Oakberg classically demonstrate the developmental dynamics of spermatogonia in rodents using histological evaluations of germ cell morphology and kinetics (Huckins, 1971a; Oakberg, 1971). These pioneering works, alongside the initial work of Clermont and Bustos-Obregon, which identified isolated type A spermatogonium that was later called A_{single} (Tegelenbosch & de Rooij, 1993), as the spermatogonial stem cell (Clermont & Bustos-Obregon, 1968) are the foundation of our present knowledge of spermatogonial development. According to these works, A_{single} spermatogonia (A_s) divides to either form two daughter A_s (self-renewal) or a pair of spermatogonia (A_{paired} (A_{pr})) connected by intercytoplasmic bridge. Mitotic division of A_{pr} results in the formation of $A_{aligned}$ spermatogonia (A_{al}) clone of 4. Subsequent mitotic divisions result in 8 and 16 or 32 clones of undifferentiated A_{al} spermatogonia. The A_s, A_{pr} and A_{al} collectively constitute the undifferentiated spermatogonia pool (Clermont & Bustos-Obregon,

1968; Huckins, 1971a; Oakberg, 1971). A_{al} spermatogonia give rise to differentiated type A_1 spermatogonia. Further sequential mitotic divisions produce type A_2, A_3, A_4, Intermediate and type B spermatogonia. The B-type spermatogonia then transit to preleptotene spermatocyte (Huckins, 1971a; Oakberg, 1971). Spermatocytes undergo 2 meiotic divisions, and the resulting spermatid undergo morphological differentiation (spermiogenesis) to produce terminally differentiated sperm (Roosen-Runge, 1962). Stem cell function is thought to reside in the population of A_s spermatogonia (de Rooij, 1998; Huckins & Oakberg, 1978a; Oatley & Brinster, 2006), but recent studies suggest that stem cell function may also be retained in some A_{pr} and A_{al} spermatogonia (Yoshida et al., 2004).

Contemporary approach to studying spermatogonial development involves the use of molecular markers including ID4, PAX7, BMI1, GFRA1, NANOS2, PLZF, SALL4, LIN28, NGN3, SOHLH1, SOHLH2, NANOS3, STRA8, cKIT and others, to identify and describe the molecular phenotype of different cell types (Aloisio et al., 2014; Buaas et al., 2004a; Chan et al., 2014; Costoya et al., 2004; Gassei & Orwig, 2013; Grasso et al., 2012; Hermann et al., 2011; Komai et al., 2014; Manova et al., 1990; Oatley et al., 2011; Oulad-Abdelghani et al., 1996; Sada et al., 2009; Suzuki et al., 2012; Suzuki et al., 2009; Yoshida et al., 2004; Zheng et al., 2009). Markers like ID4, PAX7 and BMI1 mark the A_s spermatogonia (Aloisio et al., 2014; Komai et al., 2014; Oatley et al., 2011) and the undifferentiated spermatogonia which include the A_s, A_{pr} and A_{al} spermatogonia are positive for markers that include GFRA1, PLZF, NGN3, NANOS2, SALL4 and others (Buaas et al., 2004a; Costoya et al., 2004; Gassei & Orwig, 2013; Grasso et al., 2012; Sada et al., 2009; Valli et al., 2015b; Yoshida et al., 2004). The tyrosine protein-kinase receptor, KIT (cKIT) is rarely expressed by A_s, A_{pr} and A_{al4} clones of spermatogonia, but cKIT expression increases in larger A_{al} clones of 8-cell, 16-cell and in all cells at later stages of

development (A_1-A_4, Intermediate and B spermatogonia). cKit expression defines the transition from undifferentiated A_{al} spermatogonia to differentiated A_1 spermatogonia and this transition typically occurs in clones of 8 and 16 cells in the rodent (Buaas et al., 2004b; Gassei & Orwig, 2013; Grasso et al., 2012; Schrans-Stassen et al., 1999; Tokuda et al., 2007; Yoshida et al., 2004).

In contrast, spermatogonia in higher (nonhuman and human) primates are described by their histological staining characteristics, morphology and morphometric position in the seminiferous tubules (Hermann et al., 2010). Classical study on Rhesus macaques' testis cells by Clermont and Leblond identified two types of morphologically distinct "spermatogonial stem cells" (A1 and A2) which were later called A_{dark} and A_{pale} respectively (Clermont, 1963; Clermont & Leblond, 1959). These cell-types are present in roughly equal numbers on the basement membrane of the seminiferous tubules (Marshall & Plant, 1996). Clermont and colleague proposed that A2 (A_{pale}) undergo one amplifying division before giving rise to differentiated type B1 spermatogonia. Subsequent divisions produce differentiated types B2, B3 and B4 spermatogonia, primary spermatocytes, secondary spermatocytes and spermatids that undergo spermiogenesis to produce mature sperm cells (Clermont & Leblond, 1959).

Over the years, different scientists have contributed towards understanding the clonal dynamics of primate spermatogonia during development. Clermont previously described the clonal distribution of A_{dark} and A_{pale} spermatogonia as "even number of cells" that are mostly (>60%) "pairs" and "tetrads" as revealed by topographical mapping approach in vervet monkey (Clermont, 1969). This observation might not give a complete picture as it may be difficult to define cellular clone size when cells' relative (clonal) position were not evaluated *in situ*. Also, the approach did not use intercytoplasmic bridges and the 25μm rule distance between clones

(Hermann et al., 2010; Huckins, 1971a). Relying on the morphological appearance of cells that was believed to be A_{pale}, Schlatt and colleagues determined that A_{pale} exist as 2 or 4 spermatogonial clones in the Rhesus testis (Ehmcke et al., 2005a). During the replenishment phase of an X-ray treated Rhesus seminiferous epithelium, de Rooij and colleagues observed A_{dark} and A_{pale} more frequently as clone sizes 1 (20%), 2 (37%), 4(25%) or 8 (14%) and less frequently as clones greater than 16. They also noted that both A_{dark} and A_{pale} clones clustered as a single colony with differentiated, B-type spermatogonia and more of A_{pale} than A_{dark} were seen as single spermatogonia (van Alphen et al., 1988). Whether this clonal distribution is consistent with clonal arrangement in steady state is an open question (Hermann et al., 2010). It is not known how and if these observations will translate to similar clonal distribution as seen in rodents using molecular markers.

Some molecular markers have been used to characterize the undifferentiated and differentiating spermatogonia in different primate. These include Lin28 (*Macaca mulatta, Macaca silenus, Papio anubis*) (Aeckerle et al., 2012), Sall4 (*Callithrix Jachus*) (Eildermann et al., 2012), SSEA-4 and TRA-1-81 (*M mulatta, C jachus*), TRA-1-160 (*C jacchus*) (Muller et al., 2008) and SOHLH1 (*M mulatta*) (Ramaswamy et al., 2014). It is not clear if the expressions of these markers partially or completely overlap with classically described primate spermatogonia. Our laboratory previously demonstrated that 100% of A_{dark} and 100% of A_{pale}, with some B1 and B2 express GFRA1 in the testis of Rhesus macaque (*M mulatta*). NGN3 and cKIT were expressed by about 50% and 20% of A_{pale}, respectively in the study (Hermann et al., 2007).

Spermatogenic development occurs as waves of distinct and regularly repetitive events along the length of the seminiferous tubules. Each distinct event is defined by distinct cellular associations with unique cellular morphologies at that “stage” of development. There are 12

stages in the seminiferous epithelial cycle in mouse, and 8.6 days are required for a single segment of seminiferous tubule to progress through all 12 stages (Oakberg, 1956a, 1956b, 1971). The number of A_s and A_{pr} spermatogonia are relatively constant across the stages of the seminiferous epithelial cycle. Mitotic division of A_s and A_{pr} could be seen at any stage across the length of the seminiferous tubules, but occur more frequently from stage IX to I. Larger A_{al} (8-, 16- and 32-cell) clones become differentiated A_1 spermatogonia between stages IV to VII of seminiferous epithelial cycle (Oakberg, 1971). Similar to mouse, 12 stages of the seminiferous epithelium have been described in Rhesus monkey and 10.5 days are required for a single segment of seminiferous tubule to transit through all 12 stages (Clermont & Leblond, 1959; de Rooij et al., 1986). While Clermont previously described 6 stages in human, a more recent study identified 12 stages in the human seminiferous epithelium and it takes 16 days for a segment of the seminiferous epithelium to run through a complete (Clermont, 1963; Heller & Clermont, 1963; Muciaccia et al., 2013). A_{dark} and A_{pale} spermatogonia are present in every stage of seminiferous epithelium in the Rhesus and human testis (Clermont, 1966; Clermont & Leblond, 1959; de Rooij et al., 1986; Muciaccia et al., 2013), and the stage of their clonal (self-renewing and differentiation) divisions using molecular markers have not been evaluated.

Available data indicate that the size of undifferentiated spermatogonia pool and cellular dynamics during spermatogenic development in rodent is different from primates' (Hermann et al., 2010). First, A_{dark} and A_{pale} spermatogonia represent 4% of germ cells in the Rhesus testis, which is much greater than the frequency of As or undifferentiated spermatogonial pool in the mouse testis (0.03% and 0.3% of germ cells respectively) (Hermann et al., 2009; Plant et al., 2005; Tegelenbosch & de Rooij, 1993). Second, based on available models, there are about 5-6 transit amplifying mitotic divisions before meiosis in monkey compared to about 9-10 mitotic

divisions in the rodent during spermatogenic development (Clermont & Leblond, 1959; Ehmcke & Schlatt, 2006; Ehmcke et al., 2006; Huckins, 1971a; Plant, 2010). There is limited information about how dark and pale descriptions of spermatogonial nuclear morphology in higher primates correlate with molecular phenotype or clone size (Hermann et al., 2010).

This knowledge gap has made it difficult to apply lessons learnt from decades of scientific observations in rodent to primate spermatogenic development. Steps towards understanding the molecular mechanisms regulating spermatogonial stem cell renewal and proliferation as well as spermatogonial development and differentiation in primates begin with re-defining the spermatogonial stem, progenitor and differentiating population in molecular terms. Evaluation of primate clonal dynamics might involve in vivo experiments, thus, performing these experiments directly in human might be difficult due to ethical reasons. However, these studies can be performed using Rhesus macaques which have stem cells, spermatogenic lineage development, testicular anatomy and prepubertal/pubertal development similar to humans. In addition, the Rhesus monkey is amenable to in vivo experimental manipulations that are not possible in humans. Functional studies (transplantation and fertilization assays) can also be performed if needed.

Therefore, the objectives of this study are to 1) use molecular markers to characterize the A_{dark} and A_{pale} spermatogonia in the Rhesus testis during development, 2) use molecular markers to characterize the clone sizes of undifferentiated and differentiating spermatogonia in Rhesus testis and to 3) evaluate steady state clonal dynamics of undifferentiated and differentiating spermatogonia across the stages of seminiferous epithelium in primate using Rhesus as a model.

3.2 MATERIALS AND METHODS

3.2.1 Experimental animals

Experiments involving the use of Rhesus macaques and nonhuman primate tissues were approved by the Institutional Animal care and Use Committee of Magee-Womens Research Institute and University of Pittsburgh, and performed according to the National Institutes of Health's *Guide for the Care and Use of Laboratory Animals*. Rhesus macaques used in this study were housed in the Nonhuman Primate Vivarium of Magee-Womens Research Institute under a 12-hour cycle of light and darkness. Testis tissue from 4 neonatal (Age=1-2days), 4 prepubertal (Age=30-38 months) and 4 adult (Age=72-168 months) Rhesus macaques were used for this study.

3.2.2 Testicular tissue preparation

Testis tissues were collected by castration, fixed in 4% Paraformaldehyde (PFA) solution either (at 4°C for 24 hours) for immunohistochemistry staining or (at 4°C for 3.5 hours) for whole mount staining. Fixed tissues were washed (3×1 hr) in 1X Dulbecco's phosphate buffer saline (D-PBS) (ThermoFisher Scientific, 14200-166, Grand Island, NY). Following embedment in paraffin wax block, tissues were sectioned (5µm per section) for immunohistochemistry and immunofluorescent staining.

3.2.3 Colorimetric immunohistochemistry staining

Fixed and sectioned testes tissues on glass slides were deparaffinized in xylene (2×15 mins). They were then rehydrated in graded ethanol series (2×100% for 10 mins, 1×95% for 5 mins, 1×80% for 5 mins, 1×70% for 5 mins, 1×50% for 5 mins, 1×25% for 5 mins) followed by washing in 1X Gibco® Dulbecco's phosphate-buffered saline (DPBS; ThermoFisher Scientific, 14200166, Grand Island, NY) for 3 min. For antigen retrieval, tissues were suspended in preheated Sodium Citrate buffer (10 mM Sodium Citrate, 0.05% Tween-20, pH 6) at 97.5°C in water bath. After allowing to cool down on bench, they were rinsed twice (2 mins each) in DPBS-T (0.1% Tween-20 in 1X DPBS). Non-specific antigenic sites were blocked using goat blocking buffer (1X DPBS containing 3% bovine serum albumin, 0.1% Triton X-100 and 5% normal goat serum) at room temperature for 30 mins This was followed by the addition of peroxidase block fluid (DAKO, K4010, Santa Clara, CA) for 5 mins. Drops of reconstituted primary antibody (UTF1: 1:100, Millipore, MAB 4337, Burlington, MA; ENO2: 1:20, LSBio, LS-B2890, Seattle, WA; cKIT: 1:250, DAKO, A4502, Santa Clara, CA; UCHL1: 1:500, Bio-rad, 7863-1004, Hercules, CA) in goat blocking buffer were added to each section and incubated for 90 mins at room temperature. After washing in DPBS-T (3×2 mins), drops of labelled anti-mouse or anti-rabbit fluid from DAKO kit (DAKO, K4010, Santa Clara, CA) was added and this was incubated for 30 mins at room temperature. After washing (2×2 mins in DPBS-T), drops of freshly prepared liquid 3, 3^{L}-diaminobenzidine (DAB) solution was added to tissue sections and development of positive signal was monitored under a light microscope. After washing, sections were stained with sufficient drops of periodic acid (Sigma-Aldrich, 395132, St Louis, MO) for 7 mins, washed in flowing tap water (7mins) and then stained with sufficient drops of Schiff's reagent (Sigma-Aldrich, 3952016, St Louis, MO) for 10 mins. Next, sections were

counterstained with Gill's number 3 hematoxylin (Sigma-Aldrich, GHS332, St Louis, MO) for 10 secs, washed in tap H_2O for 10 mins, followed by dipping into acid rinse (2% glacial acetic acid in water) 10 times and dipping into water 10 times. Sections were then placed in bluing solution (0.1% sodium bicarbonate) for 1 min and washed in tap water for 1 min. Tissue sections were dehydrated in graded ethanol series and xylene, and they were mounted with permount® (ThermoFisher Scientific, SP15, Grand Island, NY).

3.2.4 Immunofluorescence staining of Rhesus testis tissue section

Tissue sections on glass slides were deparaffinized, rehydrated and antigenic sites retrieved as described in the section above. Drops of donkey blocking buffer (1X DPBS containing 3% bovine serum albumin, 0.1% Triton X-100 and 5% normal donkey serum) was then added to each testis section for 30 min at room temperature to block non-specific antigenic sites in tissue sections. Drops of diluted primary antibodies (UTF1: 1:100, Millipore, MAB 4337, Burlington, MA; UTF1: 1:100, R&D, AF3958, Minneapolis, MN; ENO2: 1:20, LSBio, LS-B2890, Seattle, WA; cKIT: 1:250, DAKO, A4502, Santa Clara, CA; cKIT: 1:20, R&D, AF332, Minneapolis, MN; UCHL1: 1:500, Bio-rad, 7863-1004, Hercules, CA) in donkey blocking buffer were added to tissue sections and incubated for 90 mins at room temperature. Either of mouse (BD Bioscience, BDB557273, Franklin Lakes, NJ), rabbit (BD Bioscience, BDB550875, Franklin Lakes, NJ) or goat (R&D, AB-108-C, Minneapolis, MN) normal IgG at similar concentration as primary antibody, was used as substitute of primary antibody in negative controls. Excessive antibodies were removed by washing the slides in DPBS-T (3×5 mins). Drops of reconstituted secondary antibody (Alexa fluoro® Donkey anti-mouse 647: A31571; Alexa fluoro® anti-rabbit 488: A21206 and Alexa fluoro® anti-goat 568: A11057; Life technologies Inc, Eugene, OR) was

then used to conjugate primary antibody on tissue section for 45 min at room temperature. Tissue sections were then rinsed with DPBS-T (3×5 min) and DPBS (1×5 min). Mounting was performed using Vectashield mounting media (Vector Laboratories, H-1200, Burlingame, CA).

3.2.5 EDU in drinking water

Rhesus macaque was conditioned to Kool-Aid flavored drinking water before commencing EDU administration, 1 mg/ml of EDU (Santa Cruz, SC284628A, Santa Cruz, CA) was included in the Kool-Aid flavored drinking water and given to monkey *ad libitum* (Walls et al., 2012). Intake of Kool-Aid flavored drinking water with EDU was monitored each day. Testis was collected from the monkey after biphasic one-week EDU administration before and after a 3-week wash out period.

3.2.6 Whole mount immunofluorescent staining

Testicular tissue was digested enzymatically using 2mg/ml type IV Collagenase (Worthington, LS004188, Lakewood, NJ) with 1mg/ml of DNase I (Sigma-Aldrich, DN-25, St Louis, MO), and mechanically teased apart under a dissection microscope until the seminiferous tubules were observed as free strands. Tubules were then fixed in 4% Paraformaldehyde (PFA) (ThermoFisher Scientific, T353-500, Grand Island, NY) for 3.5 hours. After washing, tissue was dehydrated in gradient methanol series (25%, 50%, 75%, 95%, 2×100% methanol in DPBS) for 10 mins each. Tissue sample was then suspended in methanol, dimethylsulfoxide and hydrogen peroxide at ratio 4:1:1 for 3 hours. This was followed by tissue rehydration by suspending in gradient methanol series (50%, 25%, 2×0% methanol in DPBS) for 15 mins each. It was then blocked

with blotto milk (Santa Cruz, SC-2324, Dallas, TX) solution (20 mg of blotto dry powder milk/ml of D-PBS with 0.05%Triton-X). They were then stained with primary antibodies (UTF1: 1:100, Millipore, MAB 4337, Burlington, MA; cKIT: 1:20, R&D, AF332, Minneapolis, MN; ACROSIN: 1:300, Novus Biologicals, NBP1-85407, Littleton, CO) overnight at 4°C. Excess primary antibody was removed by washing with blotto milk solution (2×15 mins, 5×1 hour), and secondary antibodies (Alexa fluoro® Donkey anti-mouse 647: A31571; Alexa fluoro® anti-rabbit 488: A21206 and Alexa fluoro® anti-goat 568: A11057; Life technologies Inc, Eugene, OR) were then applied to detect the primary antibody in an overnight incubation at 4°C. After washing in blotto milk (2×15 mins, 5×1 hr), seminiferous tubules were mounted with mounting media containing DAPI ((Vector Laboratories, H-1200, Burlingame, CA). For whole mounts with EDU staining; after the initial wash in blotto milk (2×15 mins, 2×1 hr) following secondary antibody incubation, EDU was detected by suspending seminiferous tubules in Click iT® plus EDU imaging solution (ThermoFisher Scientific, C10637, Grand Island, NY) for 1 hr at room temperature. Sample was then washed (2×15mins) in DPBS followed by washing in blotto milk (2×1 hr) before mounting. For quantitative analysis, observations in sixty microscopic fields per replicate were analyzed.

3.2.7 Quantification of labeled germ cells and statistical analysis

Quantification of A_{dark}, A_{pale}, B-type spermatogonia and preleptotene spermatocytes with or without UTF1, ENO2, UCHL1 and cKIT expression in PAS-H colorimetric studies involved counting events in the seminiferous epithelium cross-section in a testis section. Quantification of UTF1-, ENO2-, UCHL1- and cKIT-positive cells following immunofluorescence staining involved counting observations in 100 round seminiferous tubules cross-section per biological

replicate. Number of biological replicates used for the experiments is indicated in each result section. Quantitative observations from biological replicates are presented as mean ± standard error of the mean (SEM). Variables were compared using one-way analysis of variance (ANOVA) method. If significantly different F-value was obtained (*-P<0.05; **-P<0.01), post-hoc analysis was then performed by using Tukey's honest significant difference (HSD) test, to identify variables with relative significant difference. All statistical analyses were performed using freely available online (as at 03/30/2018) statistical tool at http://astatsa.com/OneWay_Anova_with_TukeyHSD/.

3.3 RESULTS

We aimed to characterize undifferentiated embryonic cell transcription factor 1 (UTF1), Enolase 2 or gamma enolase (ENO2) and Ubiquitin carboxyl terminal hydrolase L1 (UCHL1) in this study. UTF1 is a chromatin-associated transcription repressor protein that is expressed by embryonic stem (ES) cells and it is important for the differentiation of ES cells (van den Boom et al., 2007). In the rodent, UTF1 is expressed by the gonocytes during development and the undifferentiated spermatogonia in the postnatal testis (van Bragt et al., 2008). ENO2 is an enzyme in the glycolytic and gluconeogenetic pathway, which catalysis the production of phosphoenolpyruvate from 2-phospho-D-glycerate in a dehydration reaction (Sanzey et al., 2015). The enzyme is highly expressed in neuronal and neuroendocrine cells. Its expression has also been detected in the breast, prostate, uterus, aorta and kidney (Haimoto et al., 1985). UCHL1 is an enzyme that facilitates the release of ubiquitin monomer from polyubiquitin chain

through its hydrolytic activities (Wilkinson et al., 1989). This enzyme is highly selectively expressed in the testis, ovary and brain cells (Kurihara et al., 2001; Shen et al., 1996).

These molecular markers (UTF1, ENO2 and UCHL1) are also expressed by undifferentiated spermatogonia in human testis (Di Persio et al., 2017; Kristensen et al., 2008; Valli et al., 2014b; von Kopylow et al., 2010). While a previous study had demonstrated the expression of UTF1 in the testis of involuted monkey (*Lemur catta*) (Aeckerle et al., 2012), molecular marker expressed by germ cells of other primate species (TRA-1-160 for example) might not be conserved in Rhesus macaque (Muller et al., 2008). We asked whether UTF1, ENO2 and UCHL1 are expressed by germ cells including putative SSCs in the Rhesus testis.

3.3.1 A_{dark} and A_{pale} expressed UTF1, ENO2 and UCHL1 in neonatal testis

Because neonatal germ cells, also known as gonocytes give rise to SSCs after birth (Culty, 2009) and SSCs are enriched in the prepubertal Rhesus testis (Chapter 4), we first evaluated the expression of UTF1, ENO2 and UCHL1 in the Rhesus testis during development and correlated their expressions to classical descriptions of "stem cells" in primate testis-A_{dark} and A_{pale}. We found that A_{dark} and A_{pale} in neonatal Rhesus testis expressed UTF1 (Figure 12A), ENO2 (Figure 12B) and UCHL1 (Figure 12C). Quantitative analysis revealed that 53% of A_{dark} and 59.5% of A_{pale} are UTF1+; 61% of A_{dark} and 64.8% of A_{pale} are ENO2+ and 69.5% of A_{dark} and 80.4% of A_{pale} are UCHL1+ in the neonatal Rhesus testis (Figure 12D). There is no significant difference ($P>0.05$) either in the proportion of A_{dark} expressing UTF1, ENO2 and UCHL1 or in the proportion of A_{pale} expressing UTF1, ENO2 and UCHL1 (Figure 12D).

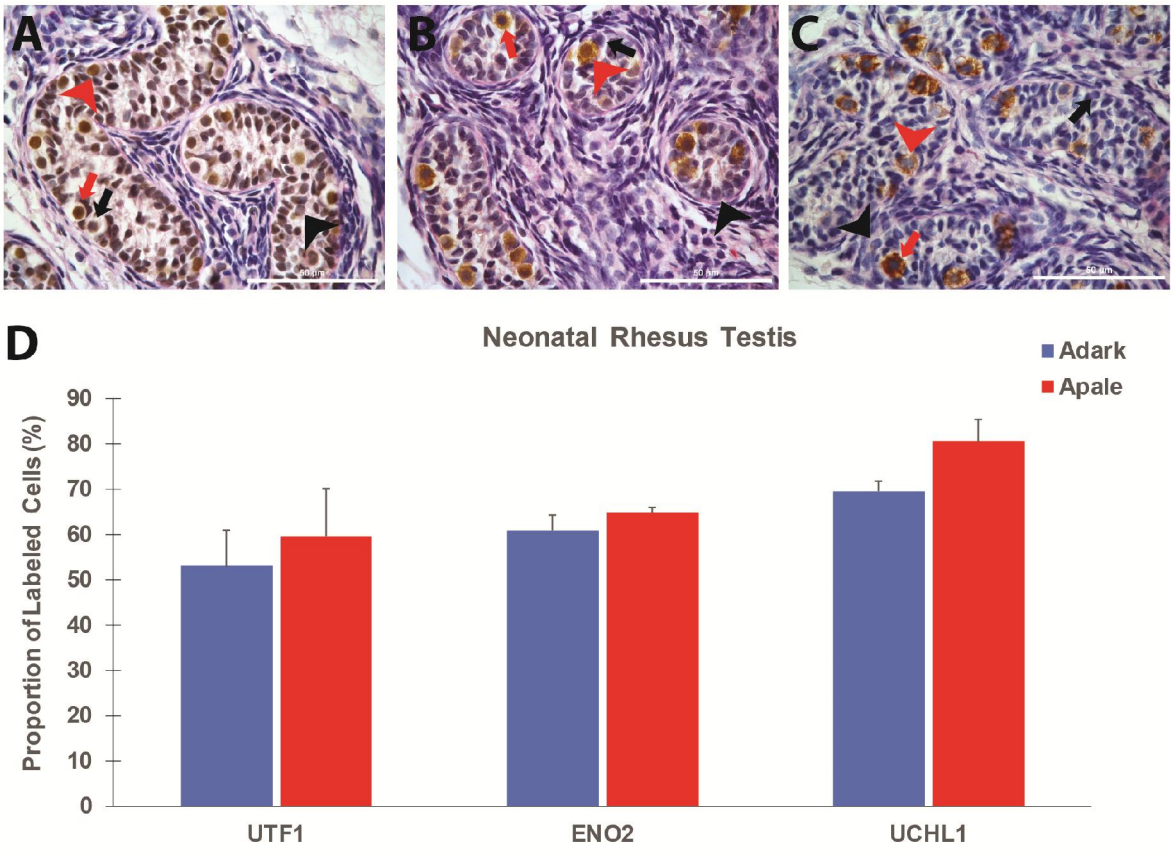

Colorimetric PAS-H staining for UTF1 (A), ENO2 (B) and UCHL1 (C) in neonatal testis revealed subpopulations of UTF1+ A_{dark} (A, small red arrow), UTF1- A_{dark} (A, small black arrow), UTF1+ A_{pale} (A, big red arrow) and UTF1- A_{pale} (A, big black arrow); ENO2+ A_{dark} (B, small red arrow), ENO2- A_{dark} (B, small black arrow), ENO2+ A_{pale} (B, big red arrow) and ENO2- A_{pale} (A, big black arrow) and UCHL1+ A_{dark} (C, small red arrow), UCHL1- A_{dark} (C, small black arrow), UCHL1+ A_{pale} (C, big red arrow) and UCHL1-A_{pale} (A, big black arrow). We quantified the proportion of A_{dark} and A_{pale} expressing these markers in neonatal testis cross section (D). Quantitative analysis was normalized by counting cells in a testis section per animal. Proportion of spermatogonia expressing molecular markers was compared using one-way ANOVA. (n=4). Scale bar=50µm.

Figure 12: Adark and Apale express UTF1, ENO2 and UCHL1 in neonatal testis

3.3.2 Adark and Apale expressed UTF1, ENO2 and UCHL1 in prepubertal testis

Similar evaluation in the testis of prepubertal Rhesus revealed that A_{dark} and A_{pale} express UTF1 (Figure 13A), ENO2 (Figure 13B) and UCHL1 (Figure 13C) during this stage of development. Quantification of the correlation of these expressions with classical description revealed that 34.9% of A_{dark} and 42.6% of A_{pale} are UTF1+, 49.0% of A_{dark} and 24.8% of A_{pale} are ENO2+ and 82.8% A_{dark} and 79.5% of A_{pale} are UCHL1+ (Figure 13D). The proportion of A_{dark} expressing UCHL1 in prepubertal testis is greater than those expressing UTF1 ($P<0.01$) and ENO2 ($P<0.05$). Similarly, the proportion of A_{pale} expressing UCHL1 is greater than those expressing UTF1 ($P<0.05$) and ENO2 ($P<0.01$) at this stage of development. Taken together, these results indicate that UTF1, ENO2 and UCHL1 are expressed by subpopulations of A_{dark} and A_{pale} in the prepubertal Rhesus testis with greater proportion of UCHL1expression in A_{dark} and A_{pale}.

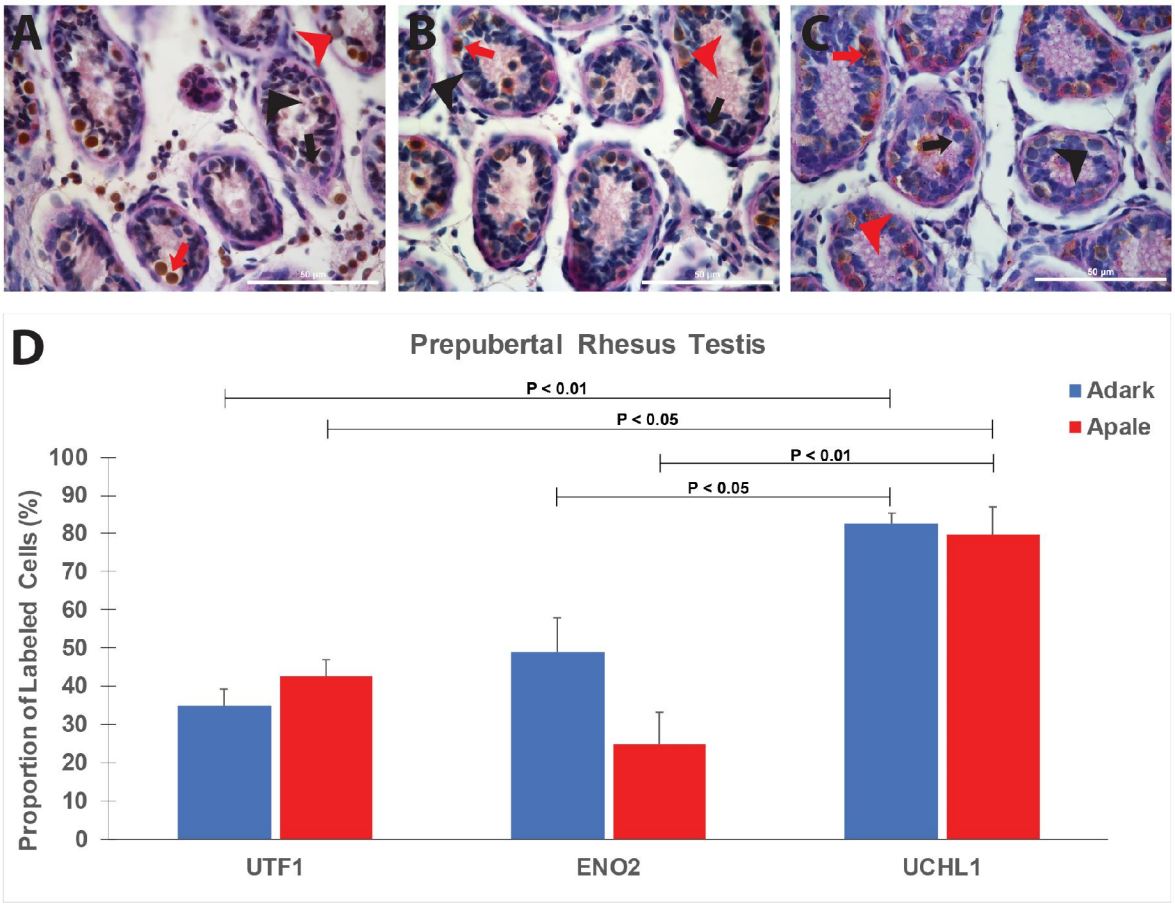

Colorimetric PAS-H staining for UTF1 (A), ENO2 (B) and UCHL1 (C) in prepubertal testis revealed subpopulations of UTF1+ A_{dark} (A, small red arrow), UTF1- A_{dark} (A, small black arrow), UTF1+ A_{pale} (A, big red arrow) and UTF1- A_{pale} (A, big black arrow); ENO2+ A_{dark} (B, small red arrow), ENO2- A_{dark} (B, small black arrow), ENO2+ A_{pale} (B, big red arrow) and ENO2- A_{pale} (A, big black arrow) and UCHL1+ A_{dark} (C, small red arrow), UCHL1- A_{dark} (C, small black arrow), UCHL1+ A_{pale} (C, big red arrow) and UCHL1-A_{pale} (A, big black arrow). We quantified the proportion of A_{dark} and A_{pale} expressing these markers in prepubertal testis cross section (D). Quantitative analysis was normalized by counting cells in a testis section per animal. Proportion of spermatogonia expressing molecular markers was compared using one-way ANOVA followed by post-hoc analysis with Tukey's HSD test. (n=3). Scale bar=50µm.

Figure 13: Adark and Apale express UTF1, ENO2 and UCHL1 in prepubertal testis

3.3.3 A_{dark} and A_{pale} expressed UTF1, ENO2, UCHL1 in adult testis

Next, we evaluated the expression and coverage of UTF1, ENO2 and UCHL1 in the stem and progenitor spermatogonia (A_{dark} and A_{pale}), differentiating spermatogonia (B-Type) and early spermatocytes (preleptotene) in the Rhesus testis during steady state by staining for these markers in adult Rhesus testis. Expressions of UTF1 (Figure 14A), ENO2 (Figure 14B) and UCHL1 (Figure 14C) were detected in subpopulation of A_{dark} and A_{pale} spermatogonia, as well as in subpopulation of B-type spermatogonia (Figure 14D). UCHL1 expression was also observed in a subpopulation of early spermatocytes (Figure 14D). Quantification analysis show that UTF1 was detected in 79.1% of A_{dark}, 51.4% of A_{pale} and 5.4% of B-type spermatogonia, ENO2 was detected in 50.5% of A_{dark}, 47.4% of A_{pale} and 9.1% of B-type spermatogonia while UCHL1 was detected in 55.2% of A_{dark}, 62.0% of A_{pale}, 28.5% of B-type spermatogonia and 15.9% of preleptotene spermatocytes. Greater proportion ($P<0.05$) of A_{dark} expressed UTF1 than ENO2 (Figure 14D). These results suggest that subpopulation of undifferentiated and differentiating spermatogonia in the Rhesus testis express UTF1, ENO2 and UCHL1.

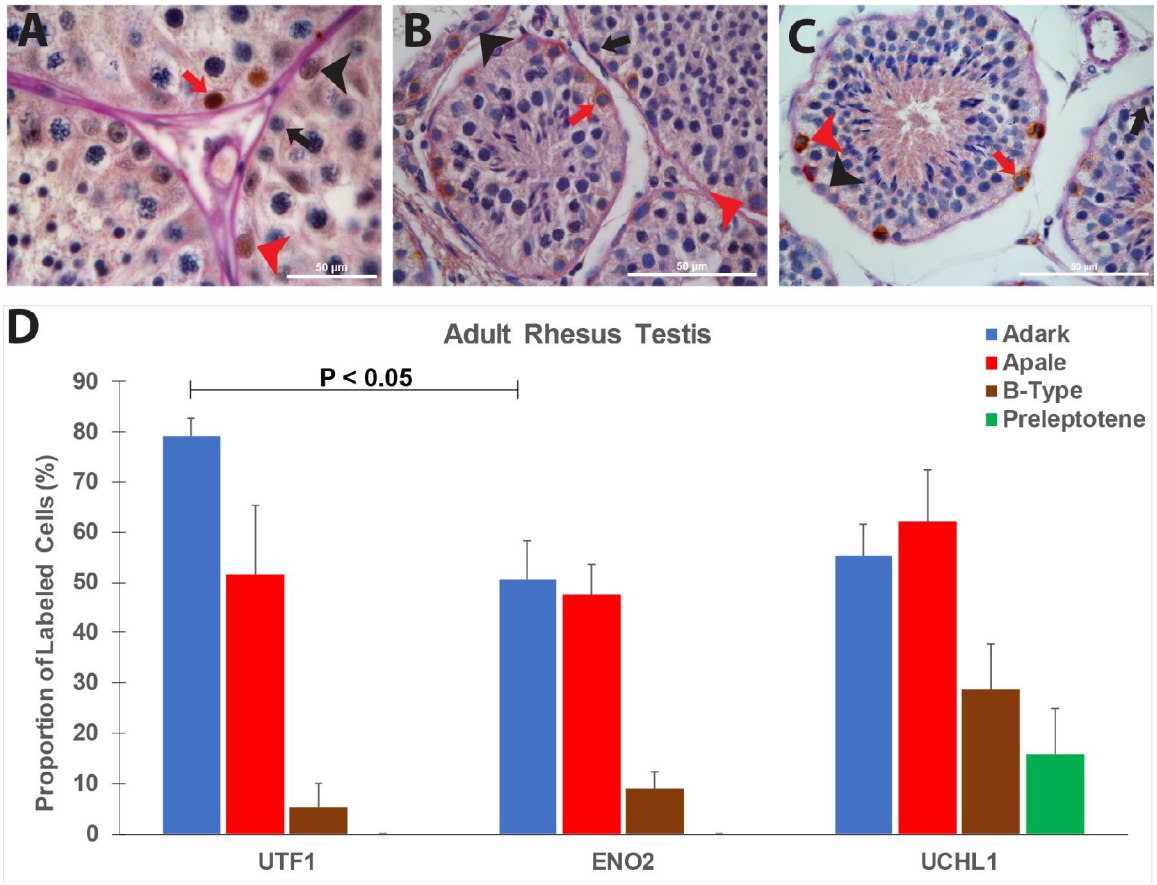

Colorimetric PAS-H staining for UTF1 (A), ENO2 (B) and UCHL1 (C) in adult Rhesus testis revealed subpopulations of UTF1+ A_{dark} (A, small red arrow), UTF1- A_{dark} (A, small black arrow), UTF1+ A_{pale} (A, big red arrow) and UTF1- A_{pale} (A, big black arrow); ENO2+ A_{dark} (B, small red arrow), ENO2- A_{dark} (B, small black arrow), ENO2+ A_{pale} (B, big red arrow) and ENO2- A_{pale} (A, big black arrow) and UCHL1+ A_{dark} (C, small red arrow), UCHL1- A_{dark} (C, small black arrow), UCHL1+ A_{pale} (C, big red arrow) and UCHL1-A_{pale} (A, big black arrow). We quantified the proportion of A_{dark} and A_{pale} expressing these markers in prepubertal testis cross section (D). Quantitative analysis was normalized by counting cells in a testis section per animal. Proportion of spermatogonia expressing molecular markers was compared using one-way ANOVA followed by post-hoc analysis with Tukey's HSD test. (n=3). Scale bar=50µm.

Figure 14: Adark and Apale express UTF1, ENO2 and UCHL1 in adult testis

3.3.4 Proportion of cKIT-positive A_{dark} and A_{pale} germ cells in the adult testis

To elucidate on the proportion of differentiating spermatogonia in these cell types, we used cKIT, a marker of differentiating spermatogonia that is also conserved in Rhesus macaque (Hermann et al., 2009), to evaluated the extent of cKIT expression in A_{dark}, A_{pale}, B-type, and preleptotene germ cells. cKIT expression was detected in subpopulation of each cell type (Figure 15A and B). Specifically, 1.9% of A_{dark}, 21.7% of A_{pale} and 95.9% of B-type spermatogonia as well as 96.7% of preleptotene spermatocytes are cKIT+ (Figure 15A and B). Taken together, these results demonstrate that UTF1, ENO2 and UCHL1 are expressed by subpopulations of A_{dark}, A_{pale} and B-type spermatogonia during steady state with UCHL1 expression also in the preleptotene spermatocytes, which are almost completely cKIT+.

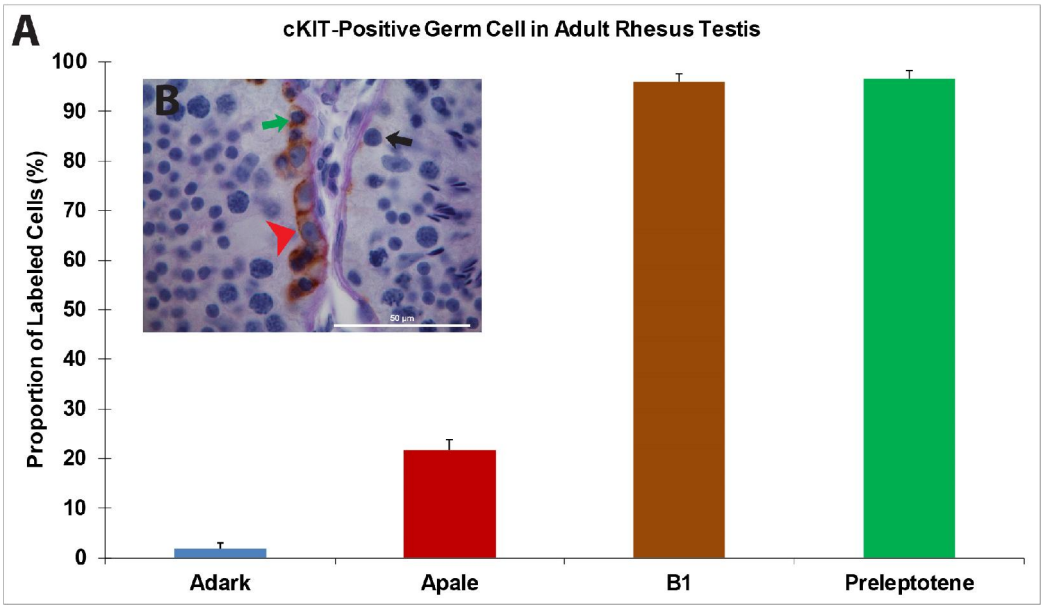

Using colorimetric PAS-H staining, we found that subpopulation of A_{dark}, $A_{pale,}$ and B-type spermatogonia as well as preleptotene spermatocytes express cKIT in adult testis (A and B). See ckit+ $A_{pale,}$ (B, big red arrow) and preleptotene spermatocytes (B, small green arrow) Quantitative analysis was normalized by counting cells in a testis section per animal. (n≥3). Scale bar=50µm.

Figure 15: Adark and Apale expressed UTF1, ENO2, UCHL1 and cKIT in adult testis

3.3.5 UTF1, ENO2 and UCHL1 are markers of undifferentiated spermatogonia

While cKIT expression in preleptotene is almost total, it is expected that this marker will overlap with UCHL1. However, since the addition of subpopulation of (A_{dark}, A_{pale} and B-type spermatogonia) cells expressing each marker and cKIT is less than 100%, it is not clear whether there would be overlap, and the extent of the overlap between UTF1, ENO2 and UCHL1, with cKIT in germ cells. To investigate these, we co-stained UTF1, ENO2 and UCHL1 with cKIT in immunofluorescence staining experiment. As expected, germ cells, positive for either or both of UTF1 and cKIT were seen on the basement membrane of the seminiferous tubules (Figure 16A-C). Quantification analysis, normalized to proportion of total labeled cells, revealed that 13.6% of these cells are UTF1+, 79.2% are cKIT+ and 7.2% of labeled cells are UTF1+/cKIT+ (Figure 16D). Following co-staining of ENO2 with cKIT, cells that are positive for either or both of ENO2 and cKIT were also observed on the basement membrane of the seminiferous tubules (Figure 16E-G). While 63.8% of quantified cells were cKIT+, 25.9% were ENO2+ and 10.3% expressed both markers (Figure 16H). Co-staining of UCHL1 and cKIT also revealed germ cells that are either UCHL1+, cKIT+ or both (Figure 16I-K). While UCHL1 expression alone (UCHL1+) is detected in 23.5% of labeled cells, cells expressing both markers (UCHL1+/cKIT+) are 67.9% and cells expressing only cKIT are 8.6% (Figure 16L). Since UTF1, ENO2 and cKIT are expressed by subpopulation of cKIT- spermatogonia. These results indicate that UTF1, ENO2 and UCHL1 are markers of undifferentiated spermatogonia in the Rhesus testis.

Next, we ask whether these markers of undifferentiated spermatogonia are expressed by the same or different germ cell population on the basement membrane of the seminiferous tubules. To address this, we co-stained UTF1 with ENO2 in an immunofluorescence staining

experiment. Cells expressing either or both markers were identified on the basement of the seminiferous tubules (Figure 16M-O). While there is 48.7% of double (UTF1+/ENO2+)-positive cells, 6.4% of labeled cells were UTF1+ and 44.9% were ENO2+ (Figure 16P). We also co-stained UTF1 with UCHL1. We found that these two markers mostly overlap on the basement membrane of the seminiferous tubules (Figure 16Q-S). Quantification revealed that only 0.7% of observed labeled cells were UTF1+, 19.5% of cells were UTF1+/UCHL1+ while 79.8% of labeled cells were UCHL1+ (Figure 16T). Taken together, these results indicate that UTF1 is the most restricted marker of undifferentiated spermatogonia of the three. ENO2 is a broader marker and UCHL1 coverage is widest compared to other markers in this study.

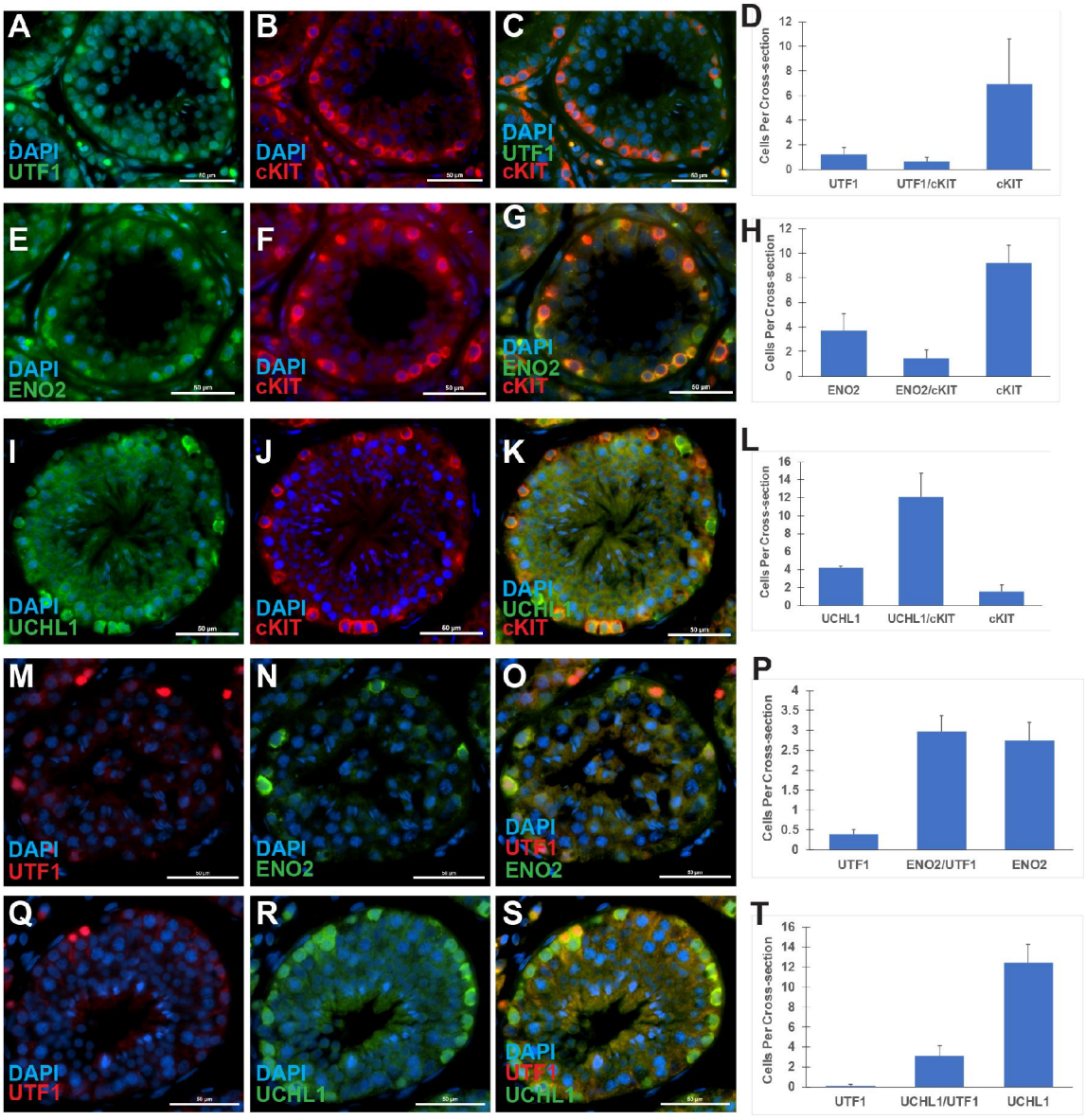

Immunofluorescence co-staining of UTF1 and cKIT (A-D), ENO2 and cKIT (E-H) and UCHL1 and cKIT (K-L) in the cross section of Rhesus seminiferous tubules revealed these markers as markers of undifferentiated spermatogonia. To determine the extent of overlap between UTF1, ENO and UCHL1, we co-stained UTF1 with ENO2 (M-P), and we identified UTF1+/ENO2-, UTF1+/ENO2+ and UTF1-/ENO2+ cells (O, P) in the cross sections of adult testis. Co-staining of UTF1 (Q) with UCHL1 (R) demonstrated the presence of very rare UTF1+/ UCHL1-, while the frequency of UTF1+/ UCHL1+ and UTF1-/ UCHL1+ cells (O, P) were relatively higher on the basement membrane of the seminiferous epithelium. Quantitative analysis was performed by counting positive cells in 100 cross-sections of seminiferous epithelium per animal. (n=3). Scale bar=50µm.

Figure 16: UTF1, ENO2 and UCHL1 are markers of undifferentiated spermatogonia

3.3.6 Clonal distribution of undifferentiated and differentiating spermatogonia

Next, we sought to use one of our markers of undifferentiated spermatogonia, co-stained with cKIT, in whole mount experiment to dissect clonal dynamics of undifferentiated and differentiating spermatogonia during development. We reasoned that use of a broad marker, like UCHL1, might capture very wide range of cells including preleptotene with clone sizes that may mask those of smaller clones of undifferentiated and differentiating spermatogonia. One possibility for limited expression of UTF1 is if it's expressed by spermatogonia during some stages of the seminiferous epithelium. To use UTF1 as a marker of undifferentiated spermatogonia, we first attempted to rule out the possibility of UTF1 expression being restricted to some stages of the seminiferous epithelium by staining UTF1 in periodic acid, Schiff's and hematoxylin (PAS-H) staining protocol. We showed that UTF1+ A_{dark} and A_{pale} spermatogonia are present in all stages of the seminiferous epithelium (Appendix D, Figure 36). It's interesting to note that UTF1 marks 64-89% of A_{dark} and 29-100% of A_{pale} depending on the stage of seminiferous epithelium. All A_{pale} spermatogonia in stage XI of seminiferous epithelium are UTF1+, while UTF1+ B-type spermatogonia were observed mainly in stage XII (Appendix D, Figure 36).

Co-staining of UTF1 with cKIT in the whole mount of Rhesus seminiferous tubules revealed distinctly recognizable clones of UTF1+ and cKIT+ spermatogonia (Figure 17A and Appendix E, Figure 37). We used stringent arbitrary rules to define a clone size and these include: (1) Cells are attached by intercytoplasmic bridges, (2) cells have similar nuclear or circumferential morphology, (3) cells have similar staining intensity, (4) cells are proximally within 25µm of the next and (5) clone size is finite. Using these rules, we quantified the frequency of UTF1+, UTF1+/cKIT+ and cKIT+ spermatogonial clones in sixty microscopic field

of whole mount per biological replicate. Observations in 3 biological replicates were quantified and the data were pooled (Table 2).

Table 2: Frequency of Undifferentiated and Differentiating Clones

Clone size	**1**	**2**	**3**	**4**	**5**	**6**	**7**	**8**	**>8**
UTF1+/cKIT-	1374	748	109	138	5	8	1	5	13
UTF1+/cKIT+	73	47	7	7	0	0	1	1	67
UTF1-/cKIT+	380	143	34	49	18	24	4	14	170
Asymmetric clones	0	23	9	8	7	13	3	7	0
	1828	**963**	**162**	**206**	**35**	**51**	**16**	**35**	**250**
% Asymmetry	0	2.4	5.6	3.9	20	25.5	18.8	20	0

Regions of dense and less dense cKIT+ spermatogonia of clone sizes lesser and greater than 8 were encountered (Figure 17A and Appendix E, Figure 37) and quantified when possible (Table 2). Relative proportion of UTF1+, UTF1+/cKIT+ and cKIT+ spermatogonial clone sizes not more than 8 are of interest in this study (Figure 17B). Quantitative analysis revealed that the proportion of UTF1+ clones of spermatogonial cells trend decreases as the clone sizes increases from 1 to 8; while the proportion of cKIT+ spermatogonial clones trend increases as the spermatogonial clone size increases from 1 to 8. Surprisingly, more than 15-20% of quantified spermatogonial cells of clone sizes 1 or 2 were cKIT+ (Figure 17B). Frequency of quantified observation revealed that UTF1+ cells spermatogonia are mostly seen as cells of clone sizes 1 (57.2%) or 2 (31.2%), and less frequently as cells of clone size 3 (4.5%) or 4 (5.7%) (Table 2). Frequency of cKIT+ spermatogonial clones also follow similar trend, which is, higher in cKIT+ spermatogonia of clone sizes 1 (45.5%) and 2 (17.1%) and relatively fewer in clone sizes 3

(4.1%) and 4 (5.9%) (Table 2). Clone sizes greater than 4 are rare (Table 2). Average frequency of asymmetric clones is 2.0%. UTF1+/cKIT+ and UTF1-/cKIT+ cells constitute 26.8% and 68% of spermatogonial clones >8 respectively (Table 2).

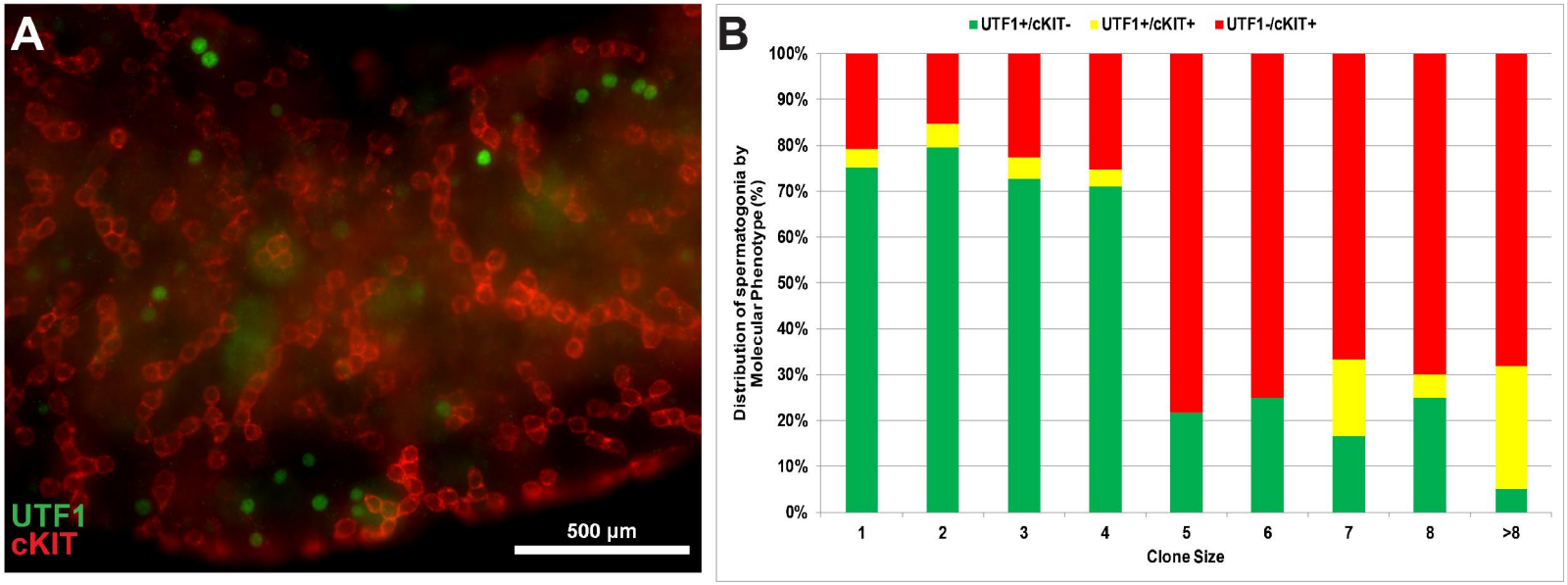

Co-staining of UTF1 and cKIT in whole mount seminiferous epithelium revealed clones of UTF1+ and cKIT+ cells (A). Quantification of the proportionate expression of marker per clone size (B) indicate that cells of clone size 1-4 are predominantly undifferentiated spermatogonia while cells of clone sizes greater than4 are predominantly differentiating cells.

Figure 17: Clonal Distribution of undifferentiated and differentiating spermatogonia

3.3.7 Staging seminiferous tubules in whole mount using Acrosin and EDU

Studies in rodent clonal development show that A_s, A_{pr} and A_{al} spermatogonia are present in all stages of seminiferous epithelium and that emergence of cKIT-positive differentiating spermatogonia and their clone sizes are stage-dependent (Ikami et al., 2015; Oakberg, 1971). We hypothesize that the relative distribution of undifferentiated (UTF1+) spermatogonial clones is stage-independent, and their transition to differentiating (cKIT+) spermatogonial clones is stage-dependent in the Rhesus testis. To address this, we co-stained UTF1, cKIT with ACROSIN in Rhesus whole mount seminiferous tubules. ACROSIN is a protein that is expressed during spermatid development. The site and shape of ACROSIN expression reveals the momentary morphological state of spermatid during development and this helps to identify stage of seminiferous epithelium (Leblond & Clermont, 1952; Muciaccia et al., 2013). This staining approach enabled us to observe and evaluate events in stages with round spermatids, for example stages II (Figure 18A-E). However, it was difficult to identify distinct stages of development in elongated spermatids using this approach in whole mount. Next, we developed a novel staining approach using 5-ethynyl-2'-deoxyuridine (EDU)-labeling in whole mount to mark cells at S-phase, thereby establishing a tool for staging nonhuman primate seminiferous tubules in whole mount. This approach effectively identifies unique morphological features on round spermatids that define a stage of the seminiferous epithelium. Stage of seminiferous epithelium with round spermatids including stage II (Figure 18F-J) and stage V (Figure 18K-O) were distinctly identified. This technique also revealed unique morphology of elongated spermatids (Figure 18P-T). We used unique morphology of spermatocytes or spermatids to identify the twelve stages of the seminiferous epithelium (Appendix F, Figure 38).

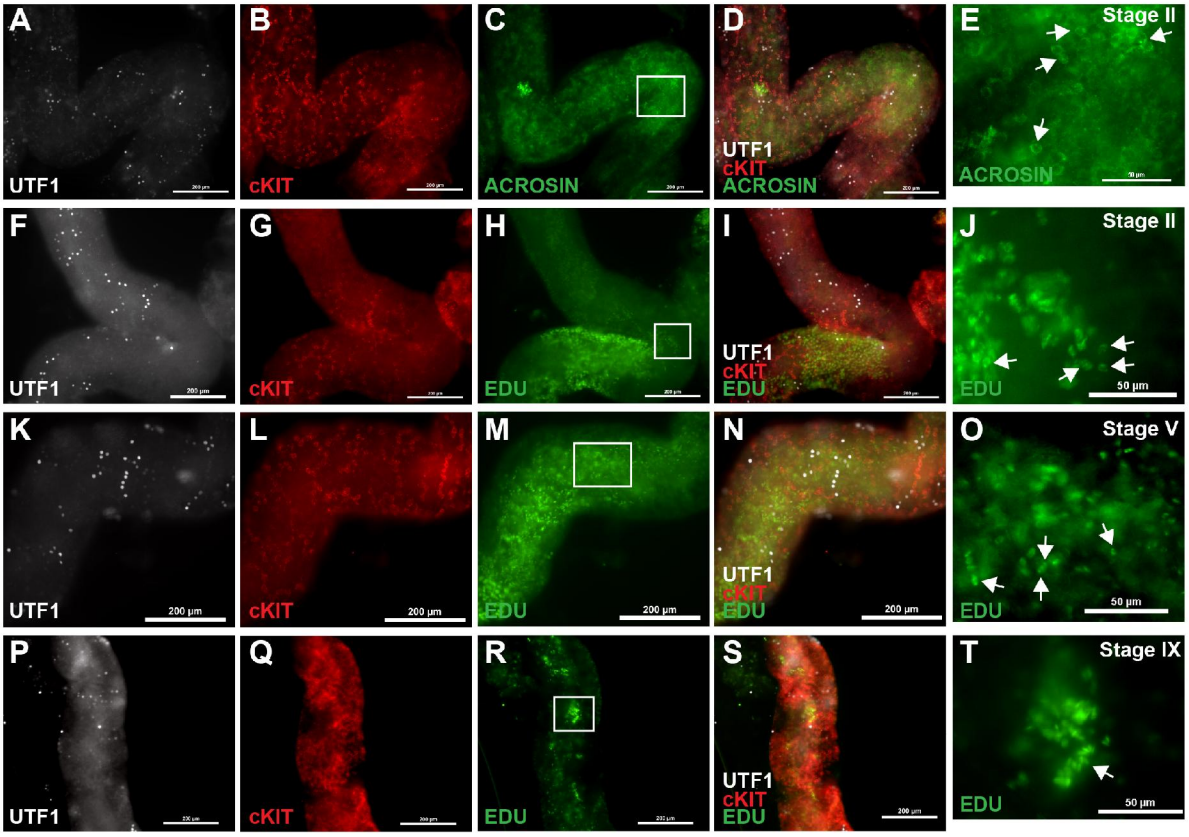

Co-staining of UTF1 (A) and cKIT (B) with ACROSIN (C) enabled us not just to identify double positive cells and their clone sizes (D), but also to identify round spermatids with unique morphology that characterize the stage of the seminiferous epithelium (E). Similarly, co-staining of UTF1(F, K, P) and cKIT (G, L, Q) with EDU (H, M, R) helped to identify and characterize clonal distributions of UTF1+ and/or cKIT+ cells (I, N, S) in stages of seminiferous epithelium as revealed by the morphology of unique round (J, O) and elongated (T) spermatids. Scale bar- 200µm (A-D, F-I, K-N, P-S), 50µm (E, J, O, T)

Figure 18: Staging seminiferous tubules in whole mount using Acrosin and EDU

3.3.8 Clonal dynamics of differentiating spermatogonia in stages of seminiferous epithelium

Next, by co-staining UTF1, cKIT and EDU in adult Rhesus testis we evaluate the distribution and dynamics of undifferentiated and differentiating clones across stages of seminiferous epithelium in whole mount. Due to variations in the length of different stages of seminiferous epithelium and consequently, variation in frequency of observation in each stage; we normalize our observations to total observation made in that stage of the seminiferous epithelium. First, we evaluate whether the distribution or dynamics of cKIT+ cells of clone sizes 1 and 2 are stage-dependent. Following our staining, we unexpectedly observed cKIT+, differentiating spermatogonia with clone sizes 1 or 2 stages X to VI of the seminiferous epithelium. These clone sizes are the most frequent cKIT+ clones during steady-state spermatogenesis. (Figure 19A). cKIT+ cells of larger clone sizes (3-8) appear to be present more in the early stages (I-VI) than the late stages (IX-XII). Due to high density of cKIT+ cells in stages VII and IX (Appendix G, Figure 39), objectively quantifiable clone sizes were only characterized (Figure 19A). Proportionate distribution of cKIT+ spermatogonia of clone sizes greater than 2 appears to be random with no break-out pattern in the proportion of cells with clone sizes 3-8 (Figure 19A).

To better understand the dynamics and/or origin of cKIT+ cells with clone size lesser or equal to 8, we evaluate the distribution of transitioning (UTF1+/cKIT+) cells during steady-state spermatogenic lineage development in the Rhesus testis. Since the frequency of cKIT+ cells appear “infinite”, we normalized the proportion of transition cells as a proportion of UTF1+ cells in that stage. We found that most of the transitioning cells are of clone sizes 1 and 2, and their distribution is spread across the stages of seminiferous epithelium (Figure 19B). Proportionate

distribution of transitioning cells of clone sizes 3-8 also appears to be more in the earlier stages than in latter stages (Figure 19B). We observed subpopulation of UTF1+/cKIT+ cells, which we call “seed cells”, in a continuous association (as revealed by intercytoplasmic bridges) with larger, sometimes unquantifiable cKIT+ cells of a different morphology (Appendix H, Figure 40). Notably, “seed cells” did not incorporate EDU while the attaching cKIT+ clones of different morphology did (Appendix H, Figure 40). This is different when UTF1+ cells are seen as clones of 1, 2, 3 or 4 (Appendix H, Figure 40). We quantified the frequency of the clone size of “seed cells”, we found that 48.6% are singles, 29.7% are paired, 7.1% and 8.7% have clone size 3 and 4 respectively, while 5.9% have clone size greater than 4 (Table 3). We further assessed whether pattern of distribution of EDU+ /cKIT+ cells will enhance our understanding of the development dynamics of cKIT+ cells. We found that cKIT+ cells of all clone sizes incorporate EDU and these EDU+/cKIT+ cells were relatively more frequently found in the early stages (I-VI) (Appendix I, Figure 41).

Table 3: Frequency of observed transitioning "seed cells "

Clone size	**1**	**2**	**3**	**4**	**>4**
Count	157	96	23	28	19
Proportion of total observation (%)	48.6	29.7	7.1	8.7	5.9

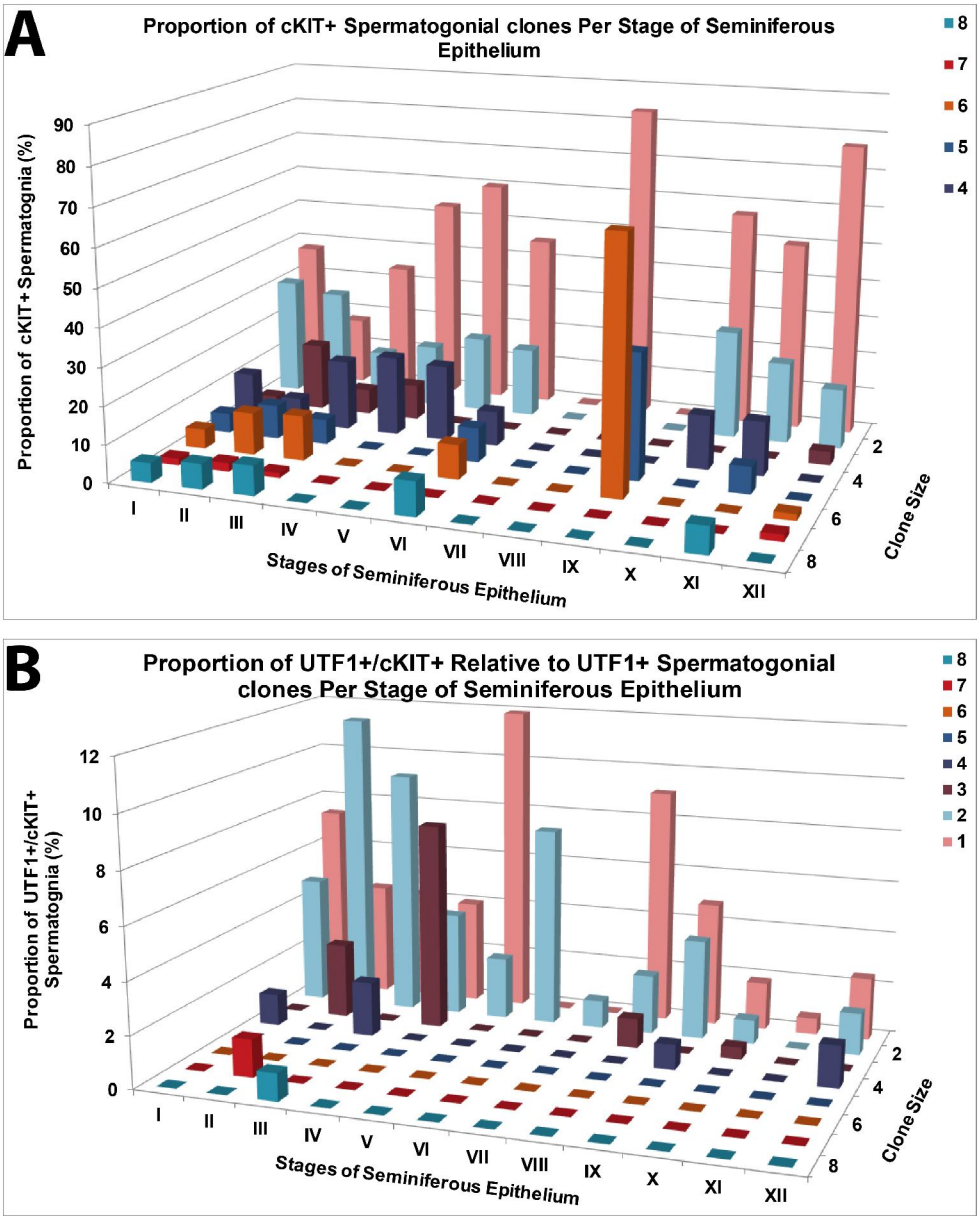

Expression of cKIT was used to quantify the proportion of differentiating clones in each stage of the seminiferous epithelium during steady-state spermatogenesis (A). Expressions and overlapping of UTF1 and cKIT were used to quantify the proportion of transitioning (UTF1+/cKIT+) clones in each stage of the seminiferous epithelium during steady-state spermatogenesis. Events in 5 microscopic field were analyzed for each stage of the seminiferous epithelium.

Figure 19: Clonal dynamics of differentiating spermatogonia in stages of seminiferous epithelium

3.3.9 Clonal dynamics of undifferentiated spermatogonia in stages of seminiferous epithelium

Next, we ask whether transitioning cells of clone sizes 1-8 directly arise from UTF1+ cells or they are products of asymmetric division and/or fragmented clones. To address this, and to understand the clonal distribution of undifferentiated spermatogonia in Rhesus whole mount testis; we assess the distribution and self-renewing dynamics of UTF1+ cell during steady-state spermatogenesis. Following characterization of UTF1+ spermatogonial clones across stages of seminiferous epithelium, we found that UTF1+ cells are more often seen as spermatogonia with clone sizes 1, 2 or 4 in all stages of the seminiferous epithelium (Figure 20A). This suggest that the undifferentiated, UTF1+ spermatogonia mostly undergo symmetric division during steady-state spermatogenesis. Across the stages, there appears to be a trend characterized by inverse relationship between the proportion of UTF1+ spermatogonia with clone size 1 and 2. The proportion of single UTF1+ cells peaked by stages VII and XI to I while the proportion of the paired cells peaked by stages IV and IX. This suggest that the proportion of cells with clone size 2, at least partly, originate from cells of clone size 1, and vice versa.

To further understand the dynamics of mitotic divisions by UTF1+ cells, we evaluate the clonal distribution of UTF1+/EDU+ cells across stages of seminiferous epithelium. We found that the proportion of UTF1+/EDU+ cell of clone size 1 decreases from stage I to IV, which follows the trend of UTF1+/EDU+ cell of clone size 2 after their initial elevation from stage I to II (Figure 20A). These trends are simultaneously accompanied by decline in the proportion of UTF1, and increase in the proportion of UTF1+ cells of clone size 2 (Figure 20A). Trend of events also suggests that single UTF1+ cells divide to become paired UTF1+ cells from stage I to IV of the seminiferous epithelium (Figure 20A and B). Dynamics of proportion of labeled

cells suggest that paired UTF1+ cells divide to replenish the single UTF1+ cell population between stages V-VIII (Figure 20A and B). Single UTF1+ cells that had incorporated EDU increases from stage IX to XII (Figure 20A and B), which suggest preparation of single UTF1+ cells for the next division that will repopulate single and/or paired cells. Trend of paired UTF1+/EDU+ cells as well as trend of UTF1+ cells from stages IX to XII (Figure 20A and B) suggest that some decisions that deplete the population of paired UTF1+ cells are being made during these stages. Observations in our data suggest that one of the decisions is to divide into UTF1+ cells of clone size four from stage X-XII (Figure 20B). It's unclear from our trends if there is a cyclical pattern that drive emergence of UTF1+ cells of clone size 4 (Figure 20A and B). Taken together, our results indicate that single UTF1+ cells become paired cells between stages I-IV; paired cells replenish the single cell population between stages V-VIII; paired cells make other decisions in spermatogenic development, possibly including further symmetric division to cells of clone size 4 beginning from, but not limited, to stage IX-XII.

Next, we asked whether apoptosis play a role in the regulation of UTF1+ spermatogonial clones. To do this, we co-stained activated caspase 3 with UTF1 and EDU in whole mount seminiferous tubules of Rhesus macaques. The observed UTF1+ clones are mostly negative for activated caspase 3. However, rare instances of caspase 3-positive, paired UTF1+ cells were observed (Appendix I, Figure 41). These results indicate that, on rare occasion, apoptosis could also be a fate of paired UTF1+ spermatogonia.

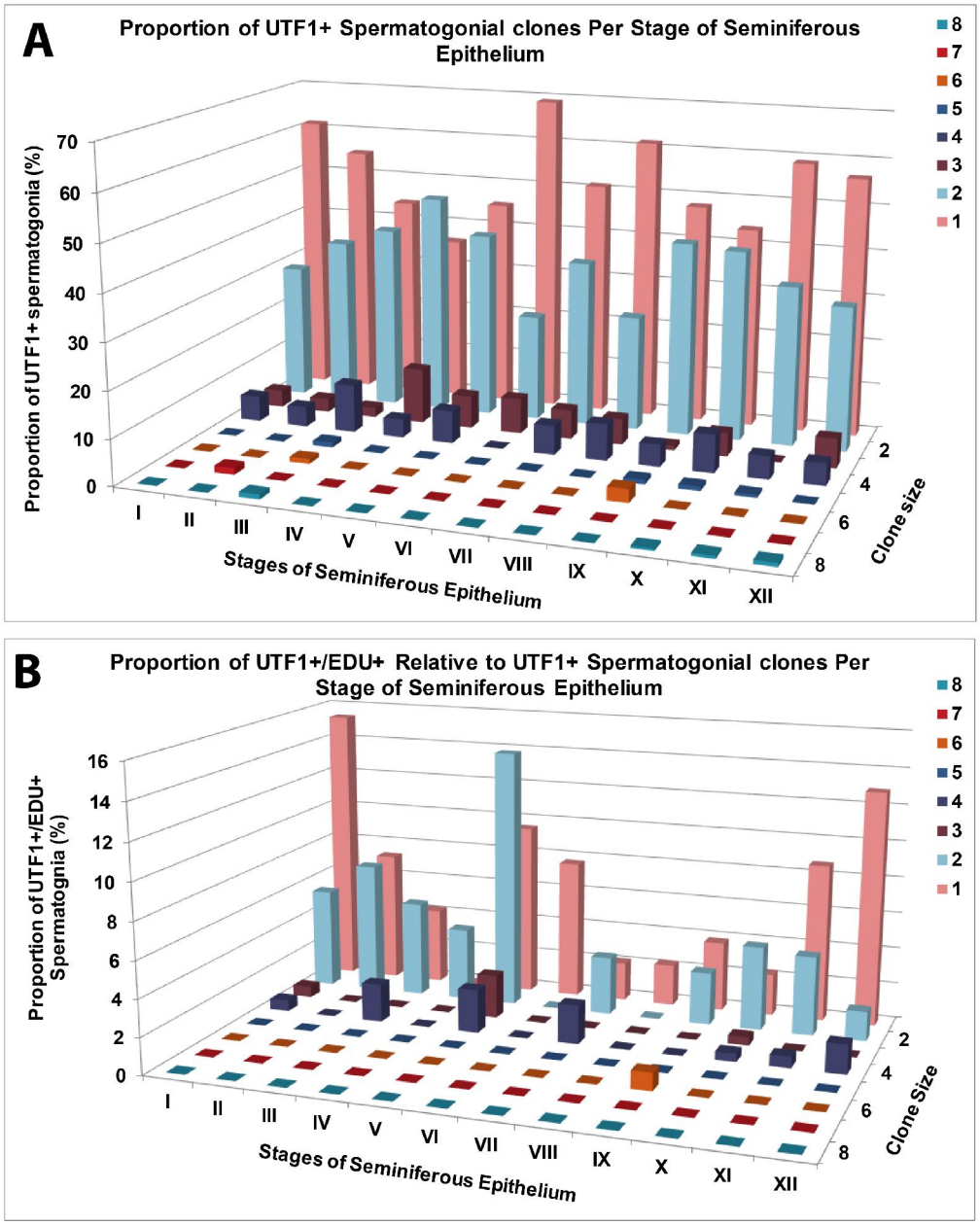

Expression of UTF1 was used to quantify the proportion of undifferentiated spermatogonia clones in each stage of the seminiferous epithelium during steady-state spermatogenesis (A). Expressions and overlapping of UTF1 and EDU were used to quantify the proportion of cycling UTF1+ (UTF1+/EDU+) clones in each stage of the seminiferous epithelium during steady-state spermatogenesis. Events in 5 microscopic field were analyzed for each stage of the seminiferous epithelium.

Figure 20: Clonal dynamics of undifferentiated spermatogonia in stages of seminiferous epithelium

3.4 DISCUSSION

This study provides a framework; first to correlate nuclear descriptions of primate undifferentiated spermatogonia (A_{dark} and A_{pale}) and differentiating spermatogonia (B-type) to molecular markers; and to use the markers to characterize the clonal dynamics of undifferentiated and differentiating spermatogonia in the Rhesus testis. This approach, using UTF1 and cKIT, revealed clonal dynamics of undifferentiated and differentiating spermatogonia that is different from rodent's. Our use of Rhesus monkey as a model of primate spermatogenic development opened the opportunity to label cells in spermatogenic development with an S-phase labeling molecule and to explore their labeling or morphological appearance in dissecting clonal spermatogenic lineage development in the primate testis. This is line with how the undifferentiated and differentiating spermatogonia were characterized as A_s, A_{pr} and A_{al},using different molecular markers including GFRA1, PLZF, SALL4, LIN28, NANOS2 and NGN3 in rodent (Buaas et al., 2004a; Costoya et al., 2004; Gassei & Orwig, 2013; Grasso et al., 2012; Sada et al., 2009; Yoshida et al., 2004). The approach helped us to learn about the molecular pathways and/or functional role of some of these markers in rodent spermatogenic development (Costoya et al., 2004; Hobbs et al., 2012; Lovelace et al., 2016; Naughton et al., 2006). This study provides the initial knowledge gaps needed to dissect primate spermatogenic lineage development using molecular markers, upon which subsequent functional studies can be built.

This present study demonstrates that UTF1, ENO2 and UCHL1 are markers of undifferentiated spermatogonia that is also conserved in the Rhesus testis. Detection of these markers in neonatal testis around the time that SSCs are established from gonocytes (Culty, 2009), suggest that these markers are expressed by cells that included the stem cells. Our study further shows that these markers are expressed by the undifferentiated spermatogonial pool. We

also revealed that each of these markers was expressed by subpopulations of A_{dark} and A_{pale} (undifferentiated) spermatogonia during development and in adult primate testis. The expression pattern of UTF1 and ENO2 indicates that the marker is expressed by A_{dark} and A_{pale} and turned-off in B-type spermatogonia. Expression pattern of UCHL1 indicates that this marker is also expressed by A_{dark} and A_{pale}; minimally expressed in B-type spermatogonia and turned-off in spermatocytes. We also demonstrate that A_{dark} rarely express cKIT, while A_{pale} (~22%) sometimes do, which is similar to previous observation of the proportion of A_{pale} spermatogonia expressing cKIT in Rhesus testis (Hermann et al., 2009). However, more than 95% of B-type spermatogonia and preleptotene spermatocyte (which are the other cell-types on the basement membrane) are cKIT+. These indicate that as the expressions of UTF1, ENO2 and UCHL1 are being turned-off; the expression of cKIT is coming up.

We used immunofluorescence co-staining to further demonstrate that while there are minimal overlaps between these markers and cKIT, the markers clearly characterize a population of cKIT- cells on the basement membrane of the seminiferous tubules, which is consistent with the molecular characteristics and physical location of undifferentiated (stem and progenitor) spermatogonia in the primate testis, respectively (Valli et al., 2014b). Although expression of cKIT broadly overlap with UCHL1 expression, results from our co-staining of UTF1 or ENO2 with cKIT reveal that the number/proportion of differentiating spermatogonia on the basement membrane is relatively more than the number/proportion of undifferentiated spermatogonia on the basement membrane of the Rhesus testis. This observation is in contrast to the relative distribution of undifferentiated and differentiating spermatogonia in human testis (Valli et al., 2014b). While 48.7% overlap exist between the expression of UTF1 and ENO2, the proportion of cells expressing only either of the marker indicates the presence of heterogeneous

undifferentiated spermatogonial pool in the Rhesus testis. This is similar to previous observation in another primate species (Valli et al., 2014b) and rodent (Hermann et al., 2015; Suzuki et al., 2009). Heterogeneous population of undifferentiated spermatogonia including the A_s spermatogonia is a subject of active research in the field.

By co-staining UTF1 with cKIT in whole mount, we dissect the clonal dynamics of undifferentiated and differentiating spermatogonia in the Rhesus testis. We demonstrate that, similar to rodent's, Rhesus spermatogonia develop in interconnected clones of cells and increased clone size is associated with increased spermatogonial differentiation. However, unlike rodent, the frequency of differentiating (cKIT) spermatogonia of clone sizes 1 and 2 are high, and clones greater than two appear as odd and even clones without a clear pattern. There are at least two possibilities for this observation- 1) cKIT+ cells of clone sizes 1 and 2 develop from transitioned, previously UTF1+ spermatogonia of clone sizes 1 and 2 respectively, while greater clones divide asymmetrically. 2) cKIT+ cells of clone sizes 1 and 2 emerge from highly frequent clone fragmentation events of greater clones. Based on the frequency of these single and paired cKIT+ cells vis a vis the frequency of UTF1+ and UTF1+/cKIT+ clones of 1 and 2, the first theory is plausible. We cannot rule out the possibility of a highly regulated process that differentially prioritize emergence of cKIT+ cells with clone size 1 and or 2 following fragmentation. In which case, the second theory could hold. High frequency of single and paired clones of cKIT+ cells have also been demonstrated in human testis (Di Persio et al., 2017).

Classically, we demonstrate that A_{dark} spermatogonia rarely express cKIT, and that almost all B-type spermatogonia are cKIT+. This study and a previous one (Hermann et al., 2009), have shown that ~22% of A_{pale} are cKIT+. Further evidence from previous observations (van Alphen et al., 1988) indicate that more A_{pale} than A_{dark} were seen as single spermatogonia.

Since A_{dark} and A_{pale} are almost equally represented on the basement of the seminiferous tubules (Clermont & Leblond, 1959; Marshall & Plant, 1996), and ten times more A_{pale} express cKIT than A_{dark}, then, we can speculate that 92% of cKIT+ cells of clone sizes 1 and 2 are from differentiating A_{pale}. We could not determine whether the previously reported A_{pale} spermatogonia of clone size 4 (Ehmcke et al., 2005a; van Alphen et al., 1988) are cKIT+ or cKIT-. We made these observations using UTF1, which is only expressed by ~50% of A_{pale}.

Our results suggest at least three sources of cKIT+ cells of clone sizes 1 and/or 2: (1) From transitioned UTF1+ cells, and (2) from dividing cKIT+ cells of lesser clone size (applicable to cells of clone size 2). Our results also suggest that decision to differentiate, characterized by the expression of cKIT, are made mostly in cells of clone sizes 1 and 2. However, cKIT+ cells of higher clone sizes (3-8) could arise from transiting cells of other clone sizes but the frequency of this decision is much lesser. Decision to differentiate (characterized by cKIT expression) is seen more frequently in cells in the earlier stages (I-VI) than those in the latter stages (VII-XII).

Notably, we observed and reported how cKIT+ cells of larger clones might develop from UTF1+/cKIT+ cells of a different morphology. We observed that mostly single and paired, or sometimes transitioning cells of 3, 4 or greater act as “seed cells” from which ostensibly cKIT+ cells of longer chains develop. In a study of X-irradiated testis, de Rooij and others observed that B-type spermatogonia develop as a continuous cluster of A_{dark} and A_{pale} spermatogonia (van Alphen et al., 1988). While we cannot comment on the classical phenotype of the “seed cells”, these observations are paradigm shift on how we need to think about the development of differentiating spermatogonia during steady-state spermatogenesis. It’s becoming clearer that some aspects of rodent spermatogenic development model did not fit into the existing data from

Rhesus testis. In a similar study in human testis, Vicini and others observed that UTF1+ cells are mitotically quiescent (Di Persio et al., 2017). We demonstrate here that UTF1+, undifferentiated spermatogonia may or may not be labeled with EDU, but as far as we observed, the "seed cells" (UTF1+/cKIT+), were not labeled even when the adjacent (cKIT+) cells were. Since almost all B-type spermatogonia and preleptotene spermatocytes are cKIT+, which is similar to the expression of cKIT by differentiating A_1-A_4 spermatogonia in rodent (Schrans-Stassen et al., 1999); then it is reasonable to opine that cKIT+ cells of higher clones are mostly of B-type and preleptotene spermatocytes.

Unlike the differentiating cells, the undifferentiated (UTF1+/cKIT-) spermatogonia were observed more frequently as singles and pairs, less frequently as cells with 3 or 4 aligned cells and clone sizes greater than 4 was rarely seen. Evaluating the dynamics of the clonal distribution of undifferentiated, UTF1+ cells across the stage of seminiferous epithelium gave a clearer picture on possible self-renewing scheme used by these cells. Presence of UTF1+ cells of clone sizes 1, 2 and 4 in every stage of the seminiferous epithelium suggest that the UTF1+ mostly undergo one to two symmetric divisions. While few UTF1+ cells of clone size 3 were sometimes seen, higher frequency of cells with clone size 4 relative to cells with clone size 3, suggests that cells become aligned as 4 cells first before the clone size gets reduced to 3, probably through clone fragmentation. This suggests that Rhesus has fewer (one to two) transit amplifying divisions in the pool of undifferentiated spermatogonia than rodent's (four to five). This observation raised question on the differences in the mechanisms that drive undifferentiated spermatogonial self-renewal in primate and rodent.

We found two peaks in the proportion of single and paired UTF1+ cells across the stages. The proportion of the clone size that incorporated EDU helped us to dissect the dynamics of their

self-renewing division. We explored understanding the expected trends during spermatogenic development as one pool of cells arise from another. For instance, four trends are expected in stages that single UTF1+/EDU+ cells divide to become cell of clone size 2: (1) Proportion of UTF1+/EDU+ cells of clone size 1 should decline; (2) proportion of UTF1+ cells of clone size 1 should also decrease; (3) proportion of UTF1+/EDU+ cells of clone size 2 should be initially elevated (as the paired cells are still strongly labeled with EDU), and decline later; (4) proportion of UTF1+/ EDU+cells of clone size 2 should decline as EDU labeling declines. Applying these logic to our observations, we infer that single UTF1+ cells divide to become paired UTF1+ cells from stage I to IV of the seminiferous epithelium; paired UTF1+ cells divide to replenish the single UTF1+ cell population between stages V-VIII; single UTF1+ cells prepare for the next division that will repopulate paired cells by stages IX-XII and decisions on the fate of paired UTF1+ cells are also being made during these stages (IX-XII). Based on our data, these include division into UTF1+ cells of clone size four and apoptotic regulation on rare occasion.

Data from this study further suggest that one of the decisions made by UTF1+ cells is transition to cKIT+ cells, which impact the trend of transitioning UTF1+/cKIT+ cells from stage XI. This peaks by stage II, and declines up to stage V. This transitioning might also contribute to elevated proportion of cKIT+ cells by stage I and II, as would dividing EDU+/cKIT+ cells of clone size 1 and II. Indeed, UTF1+ cells of clone sizes 3, 4 and beyond also form “seed cells”, at a relatively high frequency. If the pattern of differentiation decision for terminal undifferentiated spermatogonia in rodent is conserved in primate, we speculate that UTF1+ cells of clone sizes 3 or greater are late progenitors that enter the differentiation pipeline. We cannot rule out the existence of undifferentiated spermatogonia of greater clone sizes that might be revealed by another marker. We unsuccessfully attempted to characterize the clonal dynamics of

undifferentiated and differentiating spermatogonia in the seminiferous epithelium using ENO2 and GFRA1. Future studies will explore the use of other markers (preferably with broader coverage of the A_{dark} and A_{pale} pool) to validate the description of distribution and dynamics of undifferentiated and differentiating spermatogonia reported in this study. These observations should be cautiously correlated to the clonal dynamics of A_{dark} and A_{pale} during steady-state spermatogenesis.

In conclusion, using Rhesus macaque as a model of primate spermatogenic development, we demonstrate that three molecular markers (UTF1, ENO2 and UCHL1), which are conserved in human, are also expressed in Rhesus testis during development and in adult life. We demonstrated that these markers partially overlap with A_{dark} and A_{pale} during neonatal, juvenile and adult life. We used co-staining of UTF1 and cKIT, with novel EDU staining, to dissect the clonal distribution and dynamics during steady-state spermatogenesis. We propose new schemes for renewal of undifferentiated spermatogonial clones as revealed by UTF staining.

4.0 ISOLATION, ENRICHMENT AND SURVIVAL OF PRIMATE SPERMATOGONIAL STEM CELLS IN CULTURE

The study described in this chapter is being prepared for submission in Journal of "Stem Cell Research".

4.1 INTRODUCTION

Chemotherapy and radiation treatments for cancer and other conditions can cause permanent infertility (Green et al., 2010; Levine et al., 2010; Meistrich, 2009; Wallace et al., 2005). Adult patients have the option of cryopreserving semen before these therapies, which they can use in the future to achieve pregnancy through assisted reproductive technologies (Goossens et al., 2013; Valli et al., 2015a). Unfortunately, this option is not available to prepubertal boys who are yet to produce sperm cells in their semen (Goossens et al., 2013; Valli et al., 2015a). However, these boys have spermatogonial stem cells (SSCs) in their testes which are poised to initiate spermatogenesis at puberty and they can be obtained through testicular tissue biopsy (Onofre et al., 2016; Paniagua & Nistal, 1984; Valli et al., 2015a). Several academic centers around the world are already freezing testicular tissues for boys undergoing these gonadotoxic treatments in anticipation that SSCs in the testis tissue would be used to regenerate spermatogenesis later (Ginsberg et al., 2010; Keros et al., 2007; Valli et al., 2015a; Wyns et al., 2011).

Spermatogonial stem cell transplantation, which is the proof of principle for this approach was pioneered by Raph Brinster in 1994 (Brinster & Avarbock, 1994; Brinster & Zimmermann, 1994). Subsequently, this approach has been used to regenerate spermatogenesis with donor-derived sperm cells, embryo or progeny in mice (Ogawa et al., 2000), rats (Brinster et al., 2003), dog (Kim et al., 2008), goats (Honaramooz et al., 2003b) and sheep (Herrid et al., 2009). Previously, we used this approach to restore fertility with donor-derived embryo in a nonhuman primate model of cancer survivorship (Hermann et al., 2012). However, there are challenges that need to be addressed before SSCs transplantation can be efficiently translated to the clinic. One of these is that small tissue biopsies obtained from prepubertal boys have very few stem cells that may be insufficient to regenerate robust spermatogenesis after transplantation (Goossens et al., 2013; Valli et al., 2015a). Therefore, there is need to develop techniques for isolation, enrichment and in vitro amplification of stem cells recovered from primate testicular tissue.

Successful in vitro expansion of rodent SSCs involves natural enrichment of stem cells by using cells from young animals (Hamra et al., 2008; Kubota et al., 2004a, 2004b; Ryu et al., 2004). Also, identifying and using cell surface markers to further isolate and enrich SSCs in the germ cell population, while removing somatic cells that can overpopulate the culture. These are critical steps before rodent SSCs culture was established (Kubota et al., 2004a; Nagano et al., 1998; Shinohara et al., 1999). Rodent SSCs express surface markers including alpha-6-integrin (ITGA6) which is not restricted to SSCs, but can be used to isolate and enrich SSCs using fluorescence-activated or magnetic-activated cell sorting (FACS and MACS, respectively) approaches (Kubota et al., 2003b; Shinohara et al., 1999). These techniques facilitate effective separation of spermatogonia from more advanced germ cells and somatic cells of the testis

(Kubota et al., 2004a; Nagano et al., 1998). Other critical steps for culturing rodent SSCs include addition of growth factors (glial cell-derived neurotrophic factor (GDNF) and basic fibroblast growth factor (bFGF)) and use of feeders (for example, STO) or feederless (for example, laminin) layer on which SSCs' population was maintained and expanded in number (Kubota & Brinster, 2008). However, unlike in the rodents, optimum conditions for in vitro, long-term expansion of primate spermatogonial stem cells (SSCs) are yet to be determined despite multiple progress made in different studies (Guo et al., 2014; Guo et al., 2015; Langenstroth et al., 2014; Liu et al., 2011; Medrano et al., 2016; Sadri-Ardekani et al., 2009; Zheng et al., 2014), and it is not known whether culturing primate SSCs enriched with ITGA6 can help to replicate success achieved in rodents. Evaluating these possibilities using nonhuman primate model (Rhesus macaques) is particularly important because regenerative capacity of isolated, enriched, cultured and transplanted primate SSCs to produce functional sperm cells (through fertilization) can be assessed (Hermann et al., 2007; Hermann et al., 2012), an experiment that is presently ethically difficult in human.

However, since the proportion of undifferentiated spermatogonia in Rhesus testis (~4% of germ cell population) is relatively low (Marshall & Plant, 1996; Plant et al., 2005; Ramaswamy et al., 2000), we hypothesize that ITGA6-based enrichment approach that isolate subpopulation of testis cells as a fraction with higher concentration of SSCs would help to improve the establishment of primate SSC culture. Therefore, the objectives of this study are to 1) evaluate the concentration of transplantable stem cell pool in the Rhesus testis during development, 2) use ITGA6 to enrich primate SSCs in subpopulation of sorted testis cells, 3) evaluate the survival of enriched spermatogonial stem and progenitor cells in culture.

4.2 MATERIALS AND METHODS

4.2.1 Experimental animal

Experiments that involve the use of Rhesus macaques' tissues and cells were approved by the Institutional Animal care and Use Committee of Magee-Womens Research Institute and the University of Pittsburgh and performed according to the National Institutes of Health's *Guide for the Care and Use of Laboratory Animals*. Adults (Age=72-168 months), juvenile (Age=14-18 months) and neonatal (Age=1-2 days) Rhesus macaques used in this study were housed in the Nonhuman Primate Vivarium of Magee-Womens Research Institute under a 12-hour cycle of light and darkness.

4.2.2 Preparation of single cell suspension from Rhesus testis tissue

Testis was collected from monkeys by castration. Tunica was then removed and testicular parenchyma cut into small pieces in collagenase solution (Collagenase IV (Worthington, LS004188, Lakewood, NJ): 1 mg/ml in Hank's Balanced Salt Solution (HBSS) (ThermoFisher Scientific, 24020-117, Grand Island, NY). Sample was then incubated at 37°C in shaker (at 250 rpm) for 5 mins. Sample was then removed and manually shaken vigorously 50-100 times. The tubules were then separated from the supernatant after spinning at 1400rpm for 5 mins. They were then washed twice with HBSS. Pre-prepared, filtered DNAse solution (DNase I (Sigma-Aldrich, DN-25, St Louis, MO); 7mg/ml in HBSS) was then added to the sample and this was quickly followed by the addition of equal volume of 0.25%Trypsin/EDTA (ThermoFisher Scientific, 25200-114, Grand Island, NY). Sample was then vigorously triturated 3-5 times

followed by incubation at 37°C for 5 minutes. Trituration was then repeated 10 times and the enzymatic digestion was terminated with 10% volume of fetal bovine serum (FBS) (HyClone, SH30070.03, Logan, UT) after rapid microscopic evaluation of cells in solution revealed cells as single cells.

4.2.3 Rhesus-to-mouse xenotransplantation

A biological replicate is defined by the donor testis cells. Transplantable stem cells in each Rhesus donor testis cells were evaluated by transplanting cells from each biological replicate into at least six rodent testes. Single cell suspension containing Rhesus testis cells was transplanted into the efferent ducts of infertile nude mice. Infertile nude mice preparation and management as well as transplantation approach were as previously described (Medrano et al., 2014). After 2 months, testis was collected from each recipient mouse and colonizing activity of stem cell was evaluated through whole mount immunofluorescent staining.

4.2.4 Whole mount immunofluorescent staining

Following tunica removal, testis was simultaneously digested enzymatically using 1mg/ml Collagenase type IV (Worthington, LS004188, Lakewood, NJ) and 1mg/ml of DNase I (Sigma-Aldrich, DN-25, St Louis, MO), and mechanically teased apart under a dissection microscope until the seminiferous tubules were observed as free strands. Tubules were then fixed overnight in 4% Paraformaldehyde (PFA) (ThermoFisher Scientific, T353-500, Grand Island, NY), followed by permeabilization with 0.1% Triton-X (ThermoFisher Scientific, BP 151, Grand Island, NY) in Dulbecco's phosphate buffer saline (D-PBS) (ThermoFisher Scientific, 14200-

166, Grand Island, NY). Tissues were then blocked with blotto milk (Santa Cruz, SC-2324, Dallas, TX) solution (20 mg of blotto dry powder milk/ml of D-PBS + 0.05%Triton-X). They were then stained with rabbit anti-Rhesus (1:200, Orwig lab) primary antibody overnight at 4°C. Excess primary antibody was removed by washing with blotto milk solution 1hr × 3 times. Donkey anti-rabbit IgG AlexaFluor488, 1:200 (ThermoFisher Scientific, A21206, Grand Island, NY) was then used to detect the primary antibody in an overnight incubation at 4°C. VectaShield mounting media containing DAPI (Vector Laboratories, H-1200, Burlingame, CA) was then used to mount the seminiferous tubules on slides.

4.2.5 Fluorescence-activated cell sorting

Cells in single cell suspension with predetermined concentration were stained with PE-conjugated rat anti-human ITGA6 (BD Pharmagen, 555736, Franklin Lakes, NJ) or PE-conjugated rat IgG2a (BD Pharmagen, 555844, Franklin Lakes, NJ) at 10µl/10^6 cells for 20 min at 4°C. They were then washed 3 × 3 mins with serum supplemented D-PBS (DPBS-S). The DPBS-S solution comprised of 10% FBS in Dulbecco's PBS (ThermoFisher Scientific, 14200-166, Grand Island, NY). They were then re-suspended in DPBS-S media containing propidium iodide (5ul/ml). Finally, cell suspension was transferred into 5ml Falcon® tubes (Corning, 352054, Corning, NY) and taken to the Flow cytometry and FACS core, Magee-Womens Research Institute, Pittsburgh, for sorting.

4.2.6 Magnetic-activated cell sorting

Following cell number determination, cells were stained with PE-conjugated rat anti-human ITGA6 (BD Pharmagen, 555736, Franklin Lakes, NJ) at 10µl/10^6 cells for 20 min at 4°C. Cells were then washed twice in DPBS-S. They were then re-suspended in 8ul of DPBS-S per 10^6 cells, and 2ul/10^6 cells of anti-PE microBeads (Miltenyl biotech, 130-048-801, Auburn, CA) was then added and incubated for 25 min at 4°C. Cells were again washed twice with DPBS-S. They were then put into MACS® separation columns (Miltenyl biotech, 130-042-401, Auburn, CA). While the negative fraction flows through, the positive fraction is eluted with 10% FBS in MEMα (Gibco®, life technologies, NY) after the removal of the column from magnetic field.

4.2.7 Culture of Rhesus spermatogonial stem and progenitor cells

Mitomycin-treated STO and C166 cells were seeded about 24 hours before culturing spermatogonia, while plates were coated with 2ug/cm^2 laminin from Engelbreth-Holm-Swarm murine sarcoma basement membrane (Sigma-Aldrich, L2020, St Louis, MO) or 100ug/cm^2 Corning® Matrigel® growth factor reduced basement membrane marix (ThermoFisher Scientific, CB-40230, Grand Island, NY) 3-4 hours before the introduction of ITGA6+ cells. ITGA6+ cells were plated and cultured in mouse serum free media, MSFM (Kubota & Brinster, 2008) that included 20ng/ml of glial cell line-derived neurotrophic factor-GDNF (Peprotech, 450-10, Rocky Hill, NJ) and 1ng/ml of basic fibroblast growth factor-bFGF (ThermoFisher Scientific, 354060, Grand Island, NY). Cells were incubated at 37°C and 20% Oxygen. Media was replaced every 48hours. By the 7^{th} day of culture, media was removed and the cells were taken off the plate through low (0.05%) trypsin digestion (ThermoFisher Scientific, 25200114, Grand Island, NY)

that was halted by the addition of 10% fetal bovine serum (ThermoFisher Scientific, 10082147, Grand Island, NY). Cells were collected into 15ml tube and spinned down at 2500rpm for 7 minutes. Cells were then re-suspended in minimum essential medium alpha, MEMα (ThermoFisher Scientific, 11120052, Grand Island, NY). Aliquot was taken for counting and a fraction was also spotted on slide for immunocytochemistry. The remaining cells were then re-suspended in MSFM after spinning down (as above). GDNF and bFGF were then added (as above) to the cells and they were re-plated on previously plated mitomycin-treated STO, mouse yolk sac endothelial cell line (C166), precoated laminin or Matrigel.

4.2.8 In-well staining of cultured cells

Media were carefully removed from cultured cells. Known volume of D-PBS, followed by equal volume of 4% PFA were added to the cells, and left on the bench for 2 mins. Cells were further fixed with 2% PFA for 15 mins. Cells were then washed (3 × 3 mins) with D-PBS, and non-specific antigenic sites were blocked with donkey blocking buffer for 30 mins. Cells were then stained with 1:100 dilution of Mouse anti-human GFRA1 (R&D systems, MAB 7141, Minneapolis, MN). After washing with DPBS-T (3 × 3 mins), drops of donkey anti-mouse Alexa® 488 (ThermoFisher Scientific, A21202, Grand Island, NY) diluted in donkey blocking buffer (1:200) was then used to detect the primary antibody. Secondary antibody was incubated for 30 mins at room temperature. After washing with DPBS-T (3 × 3 mins) and DPBS (1 × 3 mins), cells were viewed under brightfield and fluorescent microscopy.

4.2.9 Immunocytochemistry of Rhesus testis cells

Testis cells suspension (5-10ul) was spotted on glass slide and equal volume of fixative (50% methanol (MEOH) and 50% Acetone) was added to the cells. After 3 minutes, twice the volume of fixative was further added. Cells were then left on the bench to dry completely. Drops of PBS were added to rehydrate cells for 3-5 minutes. Donkey blocking buffer was then used to block non-specific antigenic sites for 30 minutes at room temperature. Primary antibody (Mouse anti-human GFRA1, 1:100, R&D systems, MAB 7141, Minneapolis, MN) was diluted in donkey blocking buffer and added to fixed cells on slide for 90 minutes at room temperature. Mouse normal IgG at similar concentration was used as substitute primary antibody in negative controls. Slides were then washed in 0.1% tween 20 (Sigma-Aldrich, P5927, St Louis, MO) in DPBS (DPBS-T) for 3 × 3 mins to remove excess antibody. Donkey anti-mouse Alexa® 488 (ThermoFisher Scientific, A21202, Grand Island, NY) was diluted in donkey blocking buffer (1:1000) and used to detect primary antibody on cells. Secondary antibody was incubated for 45 mins at room temperature. Cells were then rinsed with DPBS-T (3 × 3 mins) and DPBS (1 × 3 mins). Vectashield mounting medium with DAPI (Vector Laboratories, H-1200, Burlingame, CA) was used for mounting.

4.2.10 Data and Statistical Analyses

Quantification of colony with stem cell activity was performed under fluorescence microscopy in whole mount seminiferous tubules of recipient mice testes following previously described guidelines (Hermann et al., 2007). Following Immunocytochemistry experiments, data points were acquired by simultaneously counting at least 1000 DAPI-positive (cells), and the number of

GFRA1-positive cells in the count. For culture data points, the total number of GFRA1-positive cells put into or recovered from culture was determined as a product of the proportion of GFRA1+ cells in spotted cells during ICC multiplied by the total number of cells put into or recovered from culture respectively.

Quantitative observations from biological replicates are presented as mean ± standard error of the mean (SEM). Quantitative variables were compared with one-way analysis of variance (ANOVA) method. If significantly different F-value was obtained (*-$P<0.05$; **-$P<0.01$), multiple paired-wise comparison was then performed, by simultaneously using Scheffé multiple comparison test, Tukey's honest significant difference (HSD) test and Bonferroni and Holm's multiple comparison test, to identify variables with relative significant difference. All statistical analyses were performed using freely available online (as at 03/30/2018) statistical tool at http://astatsa.com/OneWay_Anova_with_TukeyHSD/.

4.3 RESULTS

4.3.1 Transplantable cells in Rhesus testis during development

Since rodent's SSCs isolation and enrichment involves the use of testis cells from pups (Hamra et al., 2008; Kubota et al., 2004a, 2004b; Ryu et al., 2004), we hypothesized that transplantable stem cells mostly reside in the neonatal Rhesus testis during development. To test this hypothesis, we examined the relative stem cell activity in neonatal, juvenile and adult testes cells of Rhesus macaque. While primate-to-primate SSC transplantation as a routine biological assay is not practicable due to cost, variability and logistics (Hermann et al., 2010; Hermann et al.,

2007), primate-to-mouse xenotransplantation as a quantitative assay of stem cell activity in the primate (including Rhesus macaque) testis is well established (Hermann et al., 2007; Hermann et al., 2009; Nagano et al., 2001; Nagano et al., 2002). Cells from enzymatically-digested testis tissue of neonatal, juvenile and adult monkeys were collected and injected into the seminiferous tubules of infertile nude mice. Two months later, patches of spermatogonia-like colonies from injected primate testis cells were seen in the mouse seminiferous tubules (Figure 21A). Following our previously published strict criteria for identifying and analyzing region of colonization by xenotrasplanted stem cell (Hermann et al., 2007), quantification revealed that the concentration of transplantable stem cells was higher in cells from neonatal testis (36.7 colonies/10^6 cells) than in juvenile (7.1 colonies/10^6 cells) and adult (13.2 colonies/10^6 cells) testes (Figure 21B). Similarly, when compared with testis cells recovered per gram of juvenile (395.8±88.0 million cells) and adult (224.0±32.7 million cells) testes, higher (897.9±222.3 million cells) transplantable cells were recovered per gram of testis from neonatal testis (Figure 21C). However, due to the difference in testis size during development, the overall number of transplantable cells was much higher in adult testis (4101.4±1144.6 million per testis) than juvenile (184±114 million per testis) or neonatal (39±20 million per testis) testes (Figure 21D).

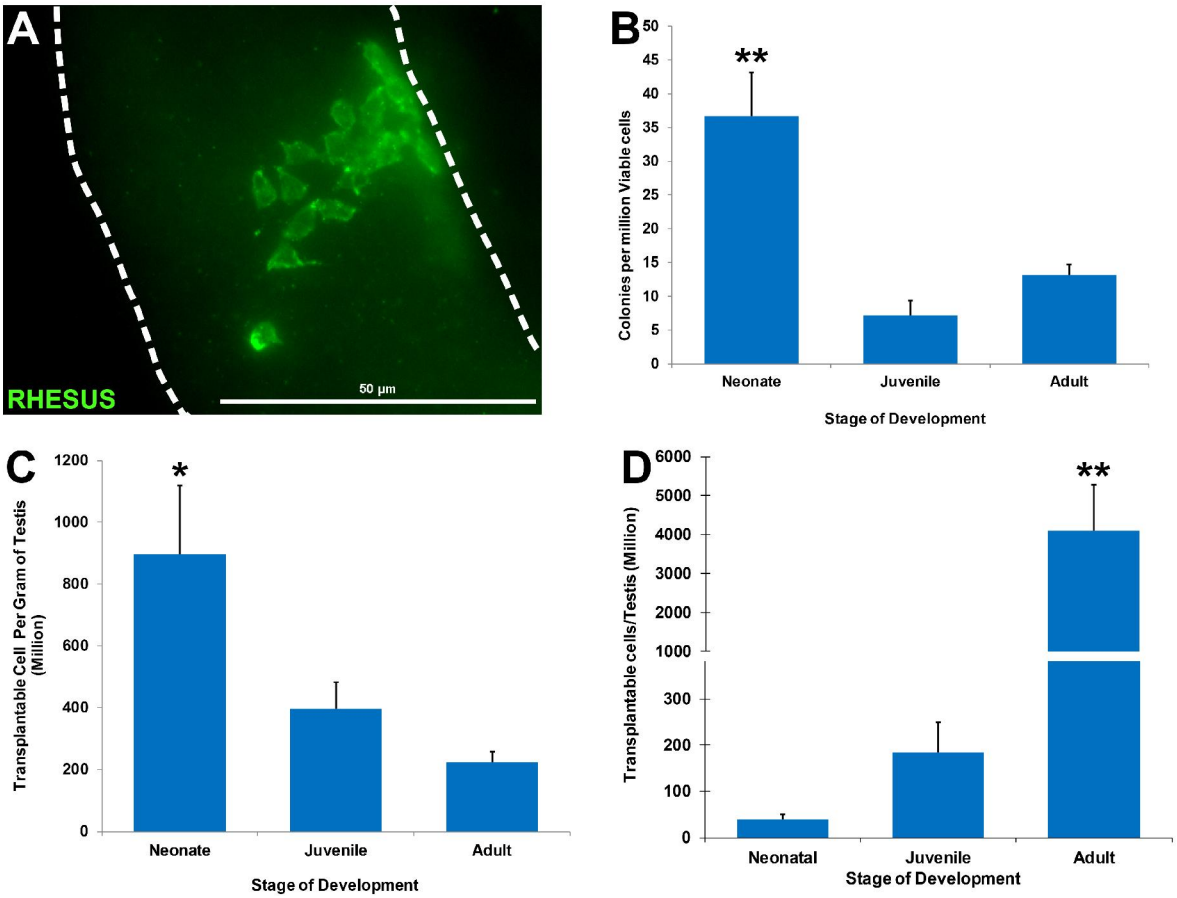

Two months after transplantation, Rhesus testis cells were detected as colonies of spermatogonia-like cells in the mouse seminiferous epithelium (A). Colonies of spermatogonia-like cells were higher in neonate compare to juvenile and adult per million of viable cells that was transplanted (B). The number of recovered transplantable cell per gram of testis was greater in neonate than in juvenile and adult testes (C). However, transplantable cells per testis is greater in adult than juvenile and neonatal testis (D). Bar graph expressed as Mean ± Standard error of the mean, Scale bar= 50µm, n=5. Data were statistically compared with one-way ANOVA, followed by multiple paired wise comparison test, * = P<0.05, ** = P<0.01

Figure 21: Transplantable cells in Rhesus testis during development

4.3.2 ITGA6 mediates enrichment of GFRA1-postive cells following FACS experiment

Since spermatogonial stem and progenitor cells are located on the basement membrane (Shinohara et al., 1999), we hypothesized that cell surface marker expressed by cells on the basement membrane could be used to isolate the stem and progenitor cell population from the germ-cell pool and to enrich the stem cell population. The stem and progenitor (undifferentiated) spermatogonia are described as A_{dark} and A_{pale} in the primate (Clermont, 1963, 1969) and we previously reported that glial cell-derived neurotrophic factor (GDNF) family receptor alpha-1 (GFRA1) is expressed by all A_{dark} and A_{pale} spermatogonia in Rhesus testis (Hermann et al., 2009). Maki et al. previously demonstrated that integrin alpha-6 (ITGA6), a cell surface marker, is expressed by germ cells on the basement membrane of Rhesus testis (Maki et al., 2009). We used ITGA6 in a fluorescent-activated cell sorting (FACS) experiment and used GFRA1 expression to characterize the stem and progenitor cells population in the unsorted (Figure 22A), positive (Figure 22B) and negative (Figure 22C) fractions. Quantification analysis revealed that GFRA1+ cells were significantly enriched (46.1±2.9%) in the ITGA6+ relative to GFRA1+ cells in the unsorted (2.5±1.3%) and negative (0.26±0.1%) fractions (Figure 22D). This result shows that ITGA6-mediated FACS experiment leads to the enrichment of spermatogonial stem and progenitor cells in the Rhesus testis.

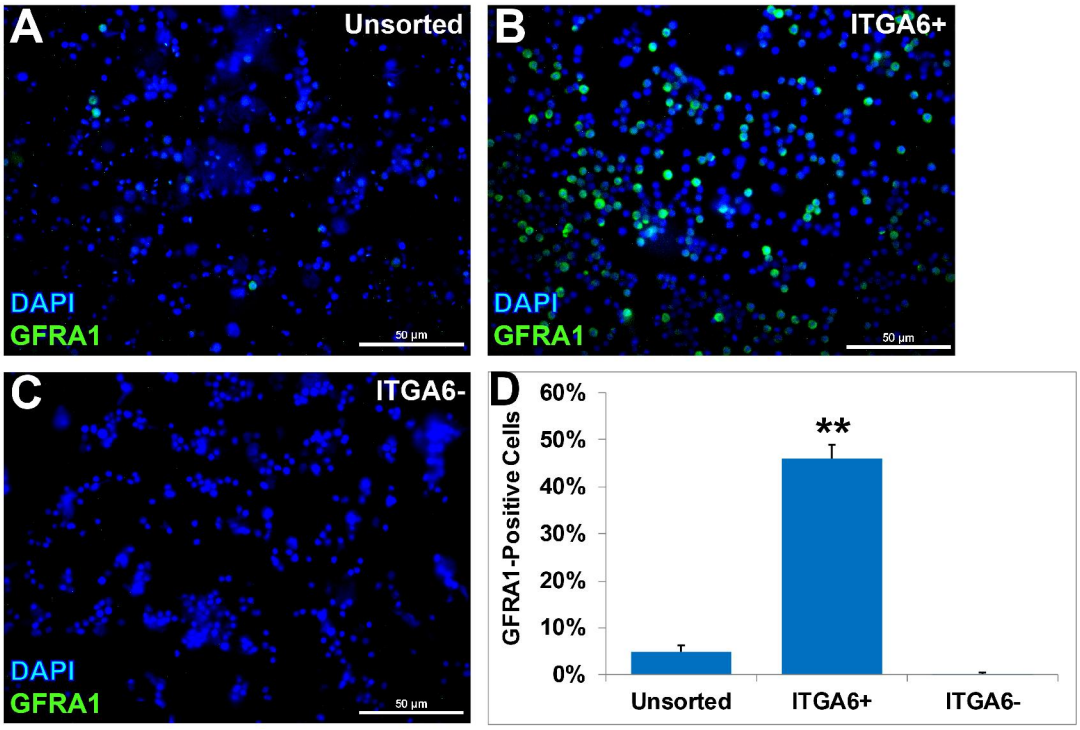

Immunocytochemistry staining for GFRA1 in cells from the unsorted (A), ITGA6-postive (B) and ITGA6-negative (C) fractions revealed about 18-fold enrichment in the ITGA6-postive, with almost all GFRA1-postive cells in the positive fraction (D). (Bar graph expressed as Mean ± SEM, Scale bar= 50µm, n=3, ** = P<0.01)

Figure 22: ITGA6 mediates enrichment of GFRA1-postive cells following FACS experiment

4.3.3 ITGA6 mediates enrichment of spermatogonial stem cells following MACS experiment

Due to the limited number of throughput cells, slow processing and the need for specialized equipment and skilled operator during FACS experiments, routine use of FACS to collect large number (>30millions cells/day) of cells for cell culture or other use might not be very efficient (Valli et al., 2014b). Therefore, we next used ITGA6 in magnetic activated cell sorting (MACS) experiment to isolate and enrich GFRA1+ cells from Rhesus testis cells (Figure 23A-C). Quantification of GFRA1 expression in the unsorted (Figure 23A), ITGA6+ (Figure 23B) and ITGA6- (Figure 23C) fractions revealed a 9-fold enrichment in the ITGA6+ (31.1±3.7%) relative to the unsorted (3.5±1.0%) fraction while 2.2±1.0% of cells in the ITGA6- fraction still express GFRA1+ cells (Figure 23D). This result demonstrates that ITGA6-mediated MACS approach also enriched the spermatogonial stem and progenitor population.

Next, enrichment of SSCs in the ITGA6+ fraction was demonstrated through primate-to-nude mouse xenotransplantation. Transplantation of ITGA6-mediated, MACS-sorted and unsorted cells revealed colonizing activity of Rhesus transplantable stem cells in mouse seminiferous epithelium (Figure 23E). Colonies of spermatogonia-like cells of Rhesus origin were enriched 5-fold in the MACS-separated ITGA6+ (4470.5±1107.5 per million) cells compared to the processed, unsorted (905.9±320.8 per million) cells (Figure 23F). Colonizing activity of transplantable stem cells was rare (38.6±16.6 per million) in the ITGA6- cells (Figure 23F). This result indicates that ITGA6-mediated, MACS experiment facilitates the enrichment of SSC population in the Rhesus testis.

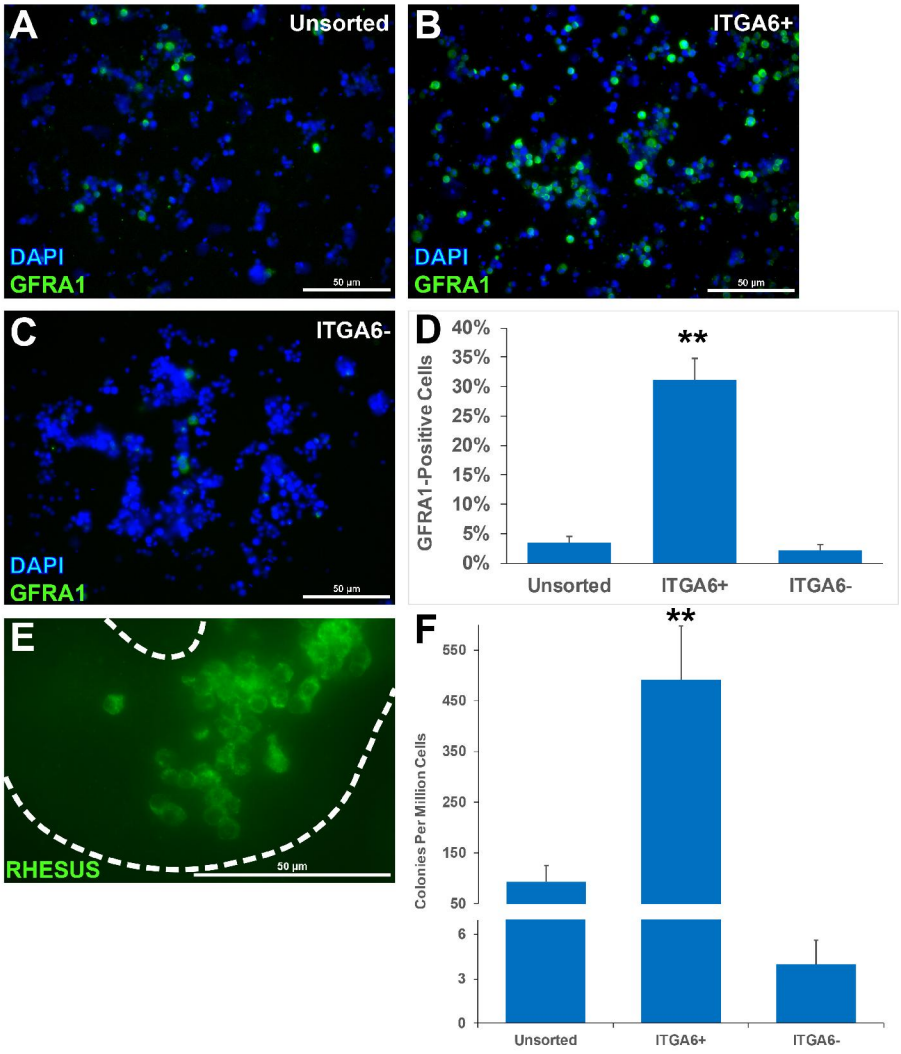

Immunocytochemistry staining for GFRA1 in cells from the unsorted (A), ITGA6-postive (B) and ITGA6-negative (C) fractions revealed about 9-fold enrichment of GFRA1-positive cells in the ITGA6-postive relative to the unsorted fraction (D). Two months after transplantation of unsorted, ITGA6-positive and ITGA6-negative fractions from adult Rhesus testis cells into mouse seminiferous tubules, colonies of spermatogonial-like cells were detected with anti-Rhesus antibody (E). Quantification analysis reveals 5-fold enrichment of cells with stem cell activity in the positive fraction relative to the unsorted fraction. (Bar graph expressed as Mean ± SEM, Scale bar= 50µm, n=6, ** = P<0.01).

Figure 23: ITGA6 mediates enrichment of spermatogonial stem cells following MACS experiment

4.3.4 ITGA6-positive cells survive in culture

Based on these preliminary observations, we are developing primate SSC culture condition, in which MACS-mediated ITGA6+ cells, enriched in SSCs are isolated from adult Rhesus testis. ITGA6+ cells were maintained on mouse yolk sac-derived endothelial cell (C166) feeders (Kubota et al., 2011) or laminin-coated plates (Kanatsu-Shinohara et al., 2011) in a standard previously described mouse serum free media (Kubota et al., 2004a). ITGA6+ cells appear to grow during the first 3 days, producing colonies with "grape-like" appearance (Figure 24A and B), which are similar to the appearance of cultured rodent SSCs in culture. By the 5^{th} day, bigger colonies of ITGA6+ cells were seen in culture (Fig 24C) and the cell density began to decline by the 7^{th} day of culture (Figure 24D). However, some of the cells in cluster were GFRA1+ (Figure 24E and F), indicating survival of spermatogonial stem and progenitor (GFRA1+) cells in this culture up to 7 days.

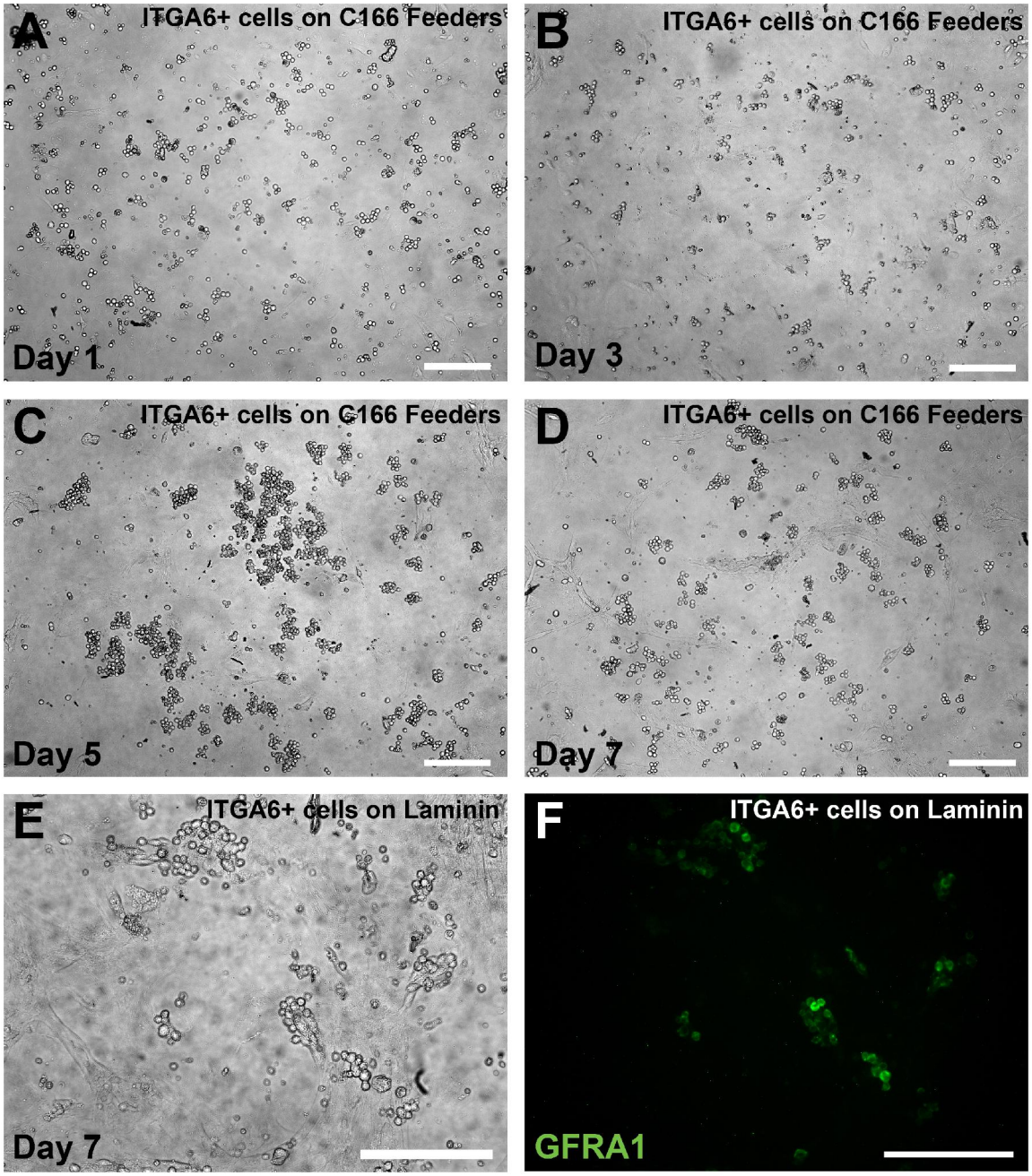

ITGA6-positive cells plated on C166 survive in culture after 1 (A), 3 (B), 5 (C) and 7 (D) days. ITGA6-positive cells plated on laminin(E) maintains the expression of GFRA1 after 7 days in culture (F). (Scale bar= 200µm)

Figure 24: ITGA6-positive cells survive in culture

4.3.5 Subpopulation of GFRA1-positive cells survive in culture up to 14 days

Next, we quantify the survival of spermatogonial stem and progenitor cells in culture. Since counting the feeder cell population could skew the total cell population invariably influencing the quantified proportion of stem and progenitor cells in the culture, we evaluated the number of GFRA1+ cells that is maintained/recovered from ITGA6-positive cells cultured for 7 or 14 days either on SIM mouse embryo-derived thioguanine and ouabain resistant (STO) (Kubota et al., 2004a) or C166 (Kubota et al., 2011) feeders, and on laminin (Kanatsu-Shinohara et al., 2011)- or Matrigel (Choi et al., 2014)-coated plates relative to the number of GFRA1+ cells at the beginning of culture. Irrespective of the culture condition, we observed significant decrease ($P<0.01$) in the number of GFRA1+ cells recovered from cells by the 7^{th} and 14^{th} day of culture (Figure 25). By the 14^{th} day in culture, lesser GFRA1+ cells ($P<0.05$) were recovered from ITGA6+ cells cultured on laminin and Matrigel conditions compared to the recovered GFRA1+ from C166 condition (Figure 25).

Taken together, these results demonstrate that enriched primate stem and progenitor cells are depleted in standard mouse culture condition used in this study.

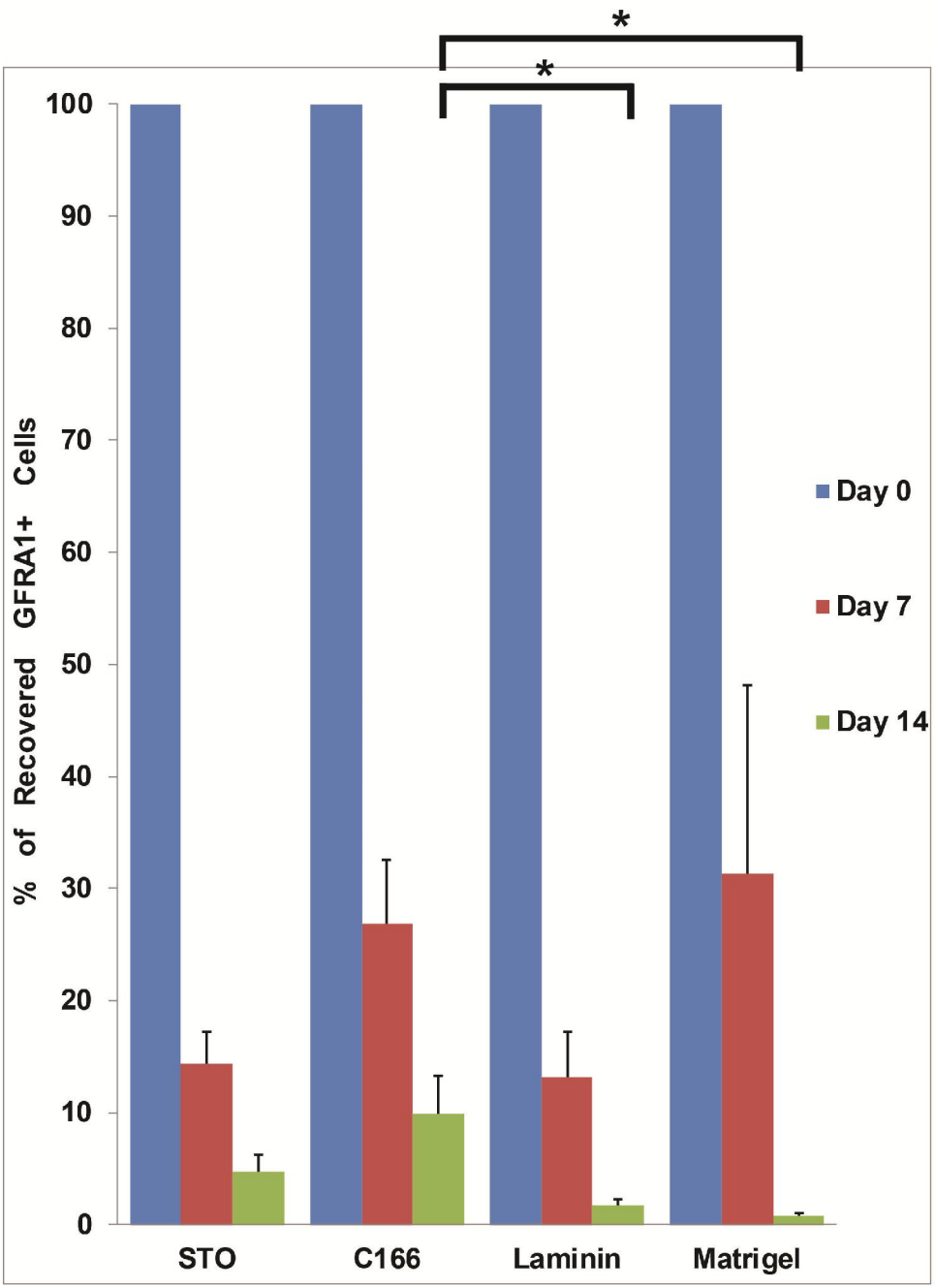

Recovered number of GFRA1+ cells (by days 7 amd 14) were expressed as percentage of total GFRA1+ cells put in culture by Day 0. (Bar expressed as Mean ± SEM, n=5, * = P<0.05)

Figure 25: Subpopulation of GFRA1-positive cells survive in culture up to 14 days

4.4 DISCUSSION

The presence of Rhesus-derived spermatogonia-like colonies in the mouse seminiferous epithelium indicates that the transplanted cells survived and migrated to the basement membrane of the mouse seminiferous tubules (Hermann et al., 2007; Nagano et al., 1999; Nagano et al., 2001), where individual transplantable SSC initiate mitotic division which is later detected as colony of spermatogonia-like cells (Hermann et al., 2007). This is similar to previous observations following transplantation of testis cells from other primate species including human (Nagano et al., 2002; Valli et al., 2014b), baboon (Nagano et al., 2001), marmoset (Langenstroth et al., 2014) and Rhesus (Hermann et al., 2007; Hermann et al., 2009) into mouse seminiferous tubules. Unlike in rodent-to-rodent transplantation where complete spermatogenesis is recovered following SSC transplantation (Brinster & Avarbock, 1994; Brinster & Zimmermann, 1994; Clouthier et al., 1996), colonies in primate-to-mouse xenotransplantation is known to be arrested at the early stage (Nagano et al., 2001; Nagano et al., 2002). This is ostensibly due to the (~65-85million years of) evolutionary gap between rodent and primates (Eizirik et al., 2001; Kumar & Hedges, 1998).

The concentration of xenotranplantable stem cells as well as the number of transplantable cells per gram of testis was higher in neonatal testes, which is expected. Based on the number of transplantable stem cell per million testis cells, we estimate an average of ~1400 transplantable stem cells per testis of Rhesus neonate, ~1300 transplantable stem cells per juvenile testis and ~54100 transplantable stem cells per testis of Adult Rhesus. These values did not reflect the total stem cell population in the testis as how efficiently transplanted cells can colonize SSC niche following transplantation (homing efficiency) and how efficiently Rhesus SSC can engraft into mouse seminiferous epithelium may influence the transplantable stem cell pool number (Nagano,

2003). If these factors were constant during development, it's tempting to postulate that while some spermatogonial cell divisions take place in the juvenile testis, the goal was not to directly expand the stem cell pool. It is not impossible for either or both factors to vary during development. Also, varying ratio of putative SSCs: germ cells: other testis cells (mainly Sertoli cells) at different stages of development may alter the concentration of putative stem cells in the transplantable testis cells. For instance, if we assume that the putative regenerative SSC pool reside in the A_{dark} and A_{pale} population in Rhesus testis, using the formula and parameters for calculating total number of (Sertoli and germ (A_{dark} and A_{pale})) cells during development as proposed by Marshall and Plant (Marshall & Plant, 1996), we estimated the ratio of A_{dark}: A_{pale}: Sertoli cell per gram of testis cells as 1:1:31 in neonate, 1:1.7:34.6 in Juvenile and 1:1:6.8 in adult. A_{dark} and A_{pale} are the germ-cell types present in neonatal and juvenile testis and they comprise ~4% of germ cells in adult testis (Marshall & Plant, 1996; Ramaswamy et al., 2000). Therefore, the ratio of putative SSCs: germ cells: Sertoli cells is 1:1:15.5 in neonates, 1:1:12.8 in Juveniles and 1:11.5:3.4 in adult Rhesus testis cells.

Availability of high number of testis cells for sorting, cell culture and downstream analysis informed our decision to use adult testis cells for our subsequent experiments. Use of ITGA6 in FACS results in efficient enrichment of spermatogonial stem and progenitor cells into the positive fraction. This observation is similar to previous report (Maki et al., 2009). We further demonstrate that this isolation approach did not result in the loss of spermatogonial stem and progenitor cells in the negative fraction. ITGA6-mediated FACS enrichment approach result in ~200% enrichment of GFRA+ cells compare to MACS's enrichment. Although GFRA1+ cells were not completely depleted in MACS's ITGA6-negative fraction, comparative advantage of ~9-fold enrichment of spermatogonial stem and progenitor cells in positive fraction following

sorting made this a technique of choice to isolate cells for transplantation and culture. Xenotransplantation data revealed that ITGA6-mediated MACS result in almost complete isolation of transplantable stem cells from the unsorted fraction to the positive fraction. Since only ~5-fold enrichment of transplantable stem cells was observed in the xenotransplanted ITGA6-positive fraction, our results indicate that the cell population representing the stem and progenitor (GFRA1+) cells are disproportionately more than stem cells in the transplanted cell population. Therefore, relative to the unsorted fraction, since the fold of stem cell enrichment is roughly half of the GFRA1+ enrichment, our observations suggest that stem cell pool is roughly 50% of GFRA1+ cells is Rhesus testis.

Since culture condition for amplifying primate SSCs is yet to be optimized, we cultured ITGA6+ cells in standard mouse culture condition, which is known to have worked for mouse spermatogonial proliferation (Kubota et al., 2004a). Whether mouse serum-free media or feeders (STO and C166) and feeder-free (laminin and Matrigel) layers are required to maintain and amplify enriched ITGA6-positive cells in culture is still an open question. Although, the initial observation of grape-like colonies from cultured ITGA6+ cells which appear to increase over time suggest cell proliferation during the first few days of culture. However, subsequent depletion of GFRA1+ cells over time suggest 1) progressive differentiation and/or apoptosis of GFRA1+ cells and/or 2) lack of self-renewing proliferation of GFRA1+ cells following differentiation of some cohort of GFRA1+ cells. While the subpopulation and doubling time of cell-types in the GFRA1+ spermatogonial population is not known, it is apparent that the cell population was decreasing after day 5. Future studies will assess the rate of proliferation, differentiation and apoptosis in the ITGA6+ cells maintained for short and long-term in culture.

Identification and inclusion of ligands of growth factor receptors in culture may also be critical to establish primate SSCs in culture.

This study provides basic information required before the establishment of SSCs in culture including the relative stem cell pool in the Rhesus testis during development, techniques for high throughput enrichment of SSCs, and preliminary outcomes in the iterative process of establishing primate SSC culture. The tools presented in this study can facilitate pre-clinical development of stem cell technologies including in vitro maintenance of spermatogonial stem cells, platform for rapid gene editing and easier functional assay in the primate testis cells.

5.0 PREGNANCY ESTABLISHED AFTER AUTOLOGOUS GRAFTING OF CRYOPRESERVED TESTICULAR TISSUE FROM PREPUBERTAL RHESUS MACAQUES

This chapter is being submitted as a research paper to "Science Translational Medicine".

5.1 INTRODUCTION

Infertility affects 10-15% of couples in the United States (Hamada et al., 2012) and 50% of these cases is partly or wholly caused by male factors (Farhi & Ben-Haroush, 2011; Hamada et al., 2012; Irvine, 1998). Chemotherapy and radiation treatment for cancer and other conditions can deplete the spermatogonial stem cells (SSCs) resulting in infertility (Green et al., 2010; Levine et al., 2010; Meistrich, 2009; Wallace et al., 2005). While the adult men have the options of cryopreserving their semen or embryo from their semen, which may be used later in life to achieve pregnancy, the prepubertal boys do not have these options (Goossens et al., 2013; Valli et al., 2014a). However, they do have SSCs in their testes which are poised to initiate spermatogenesis at puberty (Onofre et al., 2016; Paniagua & Nistal, 1984). Several academic centers in the world are presently cryopreserving testicular biopsy from these boys in anticipation that this tissue may be used for cell-based and/or tissue-based therapies to restore patient's fertility in the future (Ginsberg et al., 2010; Keros et al., 2007; Valli et al., 2015a; Wyns

et al., 2011). This is important because event-free survival rate of children that were treated for cancer is about 80-85% (Hudson, 2010), and 30% of them would be azoospermic during adult life (Thomson et al., 2002).

Spermatogonial stem cells are at foundation of spermatogenesis and they may have application for the treatment of infertility caused by gonadotoxic, cancer treatments (Kubota & Brinster, 2006; Phillips et al., 2010; Valli et al., 2015a). Following the initial demonstration that SSCs could be isolated and transplanted to regenerate spermatogenesis in infertile mice by Ralph Brinster and colleagues (Brinster & Avarbock, 1994; Brinster & Zimmermann, 1994), the technique has been demonstrated in the rat, dog, pig, cattle, sheep, goat and monkey with donor derived sperm in rat, dog, pig, goat, sheep and monkey (Hermann et al., 2012; Herrid et al., 2009; Honaramooz et al., 2003a; Izadyar et al., 2003; Kim et al., 2008; Mikkola et al., 2006; Ogawa et al., 1999).

As we approach translating this technique to the clinic, potential limitations on the use of this (cell-based) approach to restore robust spermatogenesis in human patients include 1) SSCs are rare cell-type in the testis, 2) specific approach or markers that can identify and isolate all the cells that constitute the SSC pool in the testis is yet to be reported and 3) the integrity of SSC niche is important for continuous, regulated steady-state spermatogenesis (Aponte, 2015; Hermann et al., 2015; Oatley & Brinster, 2012; Smith et al., 2014; Valli et al., 2014a). Moreover, testicular samples from prepubertal cancer patients are being collected and cryopreserved as tissues (Ginsberg et al., 2010; Keros et al., 2007; Valli et al., 2015a; Wyns et al., 2011). Therefore, tissue-based options are being evaluated as alternative approach for fertility preservation and restoration (Ehmcke et al., 2011; Jahnukainen et al., 2012; Jahnukainen et al., 2006; Luetjens et al., 2008a; Orwig & Schlatt, 2005; Rathi et al., 2008; Schlatt et al., 2009;

Schlatt et al., 2006). Grafting of testicular tissue is a potential viable option because tissue integrity is preserved while SSCs are kept in their physiological niche and in contact with the supporting cells that are important in normal spermatogenesis (Goossens et al., 2013). Also, cell viability is higher in cryopreserved testicular tissue than the cells (Pacchiarotti et al., 2013).

In 2002, testicular tissue grafting as an option for fertility preservation became very likely when Schlatt and colleagues reported complete spermatogenesis from xenografted goat and pig fetal testis tissues (Honaramooz et al., 2002). Subsequently, this success has been repeated using immature donor testis in hamster (Schlatt et al., 2002b), rabbit (Shinohara et al., 2002), dog (Abrishami et al., 2010), cat (Kim et al., 2007; Snedaker et al., 2004), horse (Rathi et al., 2006) and cattle (Huang et al., 2008; Oatley et al., 2004; Oatley et al., 2005; Rathi et al., 2005). While there is yet to be any report of complete spermatogenesis from xenografted human testis tissue as far as we know (Geens et al., 2006; Sato et al., 2010; Schlatt et al., 2006; Skakkebaek et al., 1974; Van Saen et al., 2011; Wyns et al., 2008; Yu et al., 2006), important progress in the primates is evident by the attainment of complete spermatogenesis from xenografted prepubertal testis tissue (Arregui et al., 2008; Ehmcke et al., 2011; Honaramooz et al., 2004b; Liu et al., 2016) with functional sperm in Rhesus macaque (Honaramooz et al., 2004b) and live-baby in Cynomolgus monkey (Liu et al., 2016).

Since infertility is not life-threatening and fertility treatments are elective, best fertility treatment practice would consider the risk of cancer re-introduction after transplantation (Valli et al., 2015a). Therefore, xenografting of prepubertal boys testis tissue is potentially valuable when the tissue to be grafted could harbor occult malignant cells especially in patients with leukemia (Valli et al., 2015a). Malignant cells have been detected in the testis tissue of 20% of patients before the onset of oncologic treatment (Kim et al., 1981) and these cells could be effectively

transmitted through testis transplantation (Jahnukainen et al., 2001). Gonadotoxic (chemotherapy and radiation) treatments are also used to treat non-malignant, life-threatening conditions including those requiring hematopoietic stem cell transplantation or patients with severe autoimmune disease requiring high dose chemotherapy (Onofre et al., 2016). Autologous grafting of testicular tissue is a potential option of fertility preservation in the latter group of patients. This approach also eliminates exposure to xenobiotic risks (Gassei & Orwig, 2016; Kimsa et al., 2014).

Progress towards the development of a nonhuman primate model of autologous grafting of prepubertal testicular tissue has been made in 3 known studies (Jahnukainen et al., 2012; Luetjens et al., 2008a; Wistuba et al., 2006a). Following their initial recovery of ectopic (back) testicular tissue grafts with meiotic arrest (Wistuba et al., 2006a), Wistuba and co-workers recovered spermatozoa from fresh tissue grafted into orthotopic site in Cynomolgus monkey (Luetjens et al., 2008a). This success (of spermatozoa recovery) has been repeated from frozen and thawed testis tissue grafted into the subcutaneous area of Rhesus scrotum (Jahnukainen et al., 2012). However, the recovered sperm were not functionally evaluated. Also, complete spermatogenesis was not observed from fresh or frozen-thawed testis tissue grafted to other areas of the body including the back (Cynomolgus monkey), arm and shoulder (Rhesus monkey) (Jahnukainen et al., 2012; Luetjens et al., 2008a). While 20-64% of grafted fresh tissue was recovered in cynomolgus monkey studies (Luetjens et al., 2008a; Wistuba et al., 2006a), none of the grafted frozen-thawed tissue was recovered (Luetjens et al., 2008a). This was also similar to Jahnukainen et al.'s 5% recovery after "large amount" of frozen and thawed testicular tissue was grafted into Rhesus macaque (Jahnukainen et al., 2012). While it is not known how and if fresh testis tissue grafts would behave similar to frozen-thawed tissue in Rhesus macaque, there is

potential concern on how and if recovery of sperm cells would indeed be achievable from very small, frozen-thawed testis tissue of prepubertal patients. It is not clear if grafted testicular tissue loss is due to freezing and thawing of tissue, lack of vascularization leading to tissue ischemia and necrosis or other factors (Jahnukainen et al., 2012; Luetjens et al., 2008a). Similar phenomenon of loss of frozen-thawed ovarian tissue xenografted into mouse was prevented by grafting into angiogenic granulation tissue to improve vascularization (Israely et al., 2006; Liu et al., 2002). We speculate that direct attachment of testicular tissue grafts to the subcutis, with high functional capillary density (Rucker et al., 1998), would facilitate recovery of tissue grafts. Therefore, the objectives of this study are to 1) evaluate graft recovery and spermatogenic development outcomes in prepubertal testicular tissue grafts sutured to the subcutis, and to evaluate if the outcomes are different in (a) fresh versus frozen-thawed tissue, (b) graft with substance that can facilitate angiogenesis-Matrigel (Donovan et al., 2001) versus plain graft and (c) graft placed in subcutis of back versus scrotal area in Rhesus macaques. 2) We also aim to functionally evaluate the recovered sperm cells from autologously grafted prepubertal testis tissue of primate using Rhesus macaque as a model.

5.2 MATERIALS AND METHODS

5.2.1 Experimental animal

The use of nonhuman primate tissues and Rhesus macaques in our experiments were approved by the Institutional Animal Care and Use Committee of Magee-Womens Research Institute and the University of Pittsburgh. Experiments were performed in accordance to the National

Institutes of Health's *Guide for the Care and Use of Laboratory Animals*. Five prepubertal Rhesus macaques (Age= 38-40 months, 39.2 ± 0.5 months; body weight = 4.0-4.6kg, 4.3±0.1kg) were used in this study. Monkeys were housed in the nonhuman primate vivarium of Magee-Womens Research Institute in a (12-hour) cycle of light and darkness.

5.2.2 Testis collection, processing and grafting

Monkeys were sedated with Ketamine (10mg/kg)-Xylazine (0.7mg/kg), and the scrotal area was aseptically prepared. Testis from previously hemicastrated monkeys were exteriorized from the scrotum through an incision on the scrotal wall and excised from the spermatic cord following triple ligation of the cord. Scrotal incision was closed by 1 layer inverting subcutaneous suture. Testis was immediately placed in Hank's balanced salt solution, HBSS (ThermoFisher Scientific, 24020-117, Grand Island, NY) at room temperature for holding and transportation. Testicular tissues were then processed (tunica removed), weighed (1.612-2.175gm, 1.882±0.162gm) and cut into small pieces (2-5mm^3) in a sterile chamber. Samples from cut tissue were randomly selected for weight estimation. Cut testicular tissue pool were then divided into two, to be grafted as fresh or frozen-thawed sample. Four pieces of tissue were grafted into each site. Fresh or frozen-thawed (see freezing-thawing of testicular section below) tissues were sutured to the sub cutis of the back skin (3 fresh and 3 frozen) and the scrotal area (1 fresh and 1 frozen) with a simple interrupted approach using non-absorbable 6.0 silk suture (Fisher Scientific, NC9917567, Hampton, NH). 300ul of Corning® Matrigel® growth factor reduced basement membrane marix, Matrigel (ThermoFisher Scientific, CB-40230, Grand Island, NY) was added to each of four sites on the back (2 fresh and 2 frozen) and both scrotal sites. Two sites on the back were grafted without Matrigel addition.

5.2.3 Freezing and thawing of testicular tissue

Testicular tissues were slowly frozen using previously described protocol (Keros et al., 2007) with slight modification. Briefly, six to ten testis tissue pieces held in HBSS at room temperature were transferred into 2.0ml cryovials which was followed immediately by the addition of 1.5ml of cryoprotectant media. The cryoprotectant media comprised of 5% fetal bovine serum (FBS) and 5% dimethyl sulfoxide (DMSO) in MEMα. Cryovials containing tissue were then placed in 4^{o}C to equilibrate for 30 mins. They were then cooled from 4^{o}C at the rate of -1^{o} C per minute until 0^{o}C. They were then held at 0^{o}C for 5 mins. This was followed by cooling at -0.5^{o}C per mins until -8^{o}C. The cryovials were manually seeded while being held at this temperature for 10mins. They were then cooled to -40^{o}C at -0.5^{o}C per minutes, and held at this temperature for 10mins. Tissues were then cooled to -80.0^{o}C at the rate of -1. 5^{o}C. Tissues were then plunged into liquid nitrogen at the end of the cycle. After retrieval from liquid nitrogen, cryovials containing testicular tissue samples were quickly transferred into water bath at 37^{o}C until completely thawed. Thawed tissues were transferred into a sterile dish and washed in HBSS.

5.2.4 Measurement of graft volume

Previously published methods of testis volume measurement (Arslan et al., 1993; Marshall et al., 1983; Simorangkir et al., 2009b) were modified for measuring graft volume. Two-dimensional length of graft's height and width along the vertical and horizontal axis respectively were measured with calipers by only one individual throughout the period of experimentation.

5.2.5 Testosterone and follicle stimulating hormone assay

Testosterone assay was performed using KIR1709 testosterone assay kit (Immuno-Biological laboratories, Inc, MN). The detection limit of the assay was 0.05ng/ml. Serum follicle stimulating hormone (FSH) radioimmunoassay was performed by the Endocrine Technologies Support Core (ETSC) at the Oregon National Primate Research Center (ONPRC; Beaverton, OR) using reagents from Dr. Albert Parlow at the National Hormone and Peptide Program (NHPP, Harbor-UCLA Medical Center, Los Angeles). This was a homologous cynomolgus macaque assay with recombinant cynomolgus FSH (AFP- 6940A) for both iodination and standards. The rabbit anticynomolgus FSH (AFP-782594) was used at a final dilution of 1:1,038,462. The standard curve ranged between 0.005 and 10 ng/tube and the sensitivity of the assay at 87.5%, binding was 0.1 ng/ml. The intra-assay variation for this assay ranged from 6.9-11.7% and the inter-assay variation was 14.6%.

5.2.6 Graft retrieval, sperm recovery and analysis

Grafts were recovered for analysis after 8-10 months. Recovered grafts from each graft site were briefly teased apart in whole mount under a dissection microscope to expose sperm cells. They were then weighed and part of the tissue was either fixed in 4% paraformaldehyde (PFA) or enzymatically digested to release more sperm cells.

Sperm cells recovered from either mechanically disrupted tubules in wet mount or from enzymatically digested tissue were quantified by putting 10ul of sperm cell suspension in hemocytometer chamber. Sperm cells in two of the four large quadrants of the chamber were then counted and the average of the obtained count was multiplied by the dilution factor and a

constant factor (10^4) to determine the concentration of the sperm cells. Total sperm cell count was determined by multiplying the concentration value with the volume of sperm cell suspension. Final total sperm cell count comprised of the addition of counted sperm cells from enzymatic digestion and mechanical manipulation.

5.2.7 Immunofluorescence staining

Cut tissue sections (5µm each) from PFA-fixed testis grafts were deparaffinized in xylene (15 mins × 2 times) and rehydrated in graded ethanol series (100% × 2 times for 10 min each, 95% for 5 mins, 80% for 5 mins, 70% for 5 mins, 50% for 5 mins, 25% for 5 mins) and washed in 1X Dulbecco's phosphate buffer saline-DPBS (Life technologies, Grand Island, NY) for 3 mins. Sections were then incubated in sodium citrate buffer (10 mM Sodium Citrate, 0.05% Tween-20, pH 6) at 97.5°C for 30 min to retrieve antigenic sites. Sections on slides were cooled and washed twice in DBPS-T (0.1% Tween-20 in 1X DPBS) for 2 min each. Donkey buffer (1 × DPBS containing 3% bovine serum albumin, 0.1% Triton X-100 and 5% normal donkey serum) was then used to block non-specific antigenic sites in tissue sections for 30 min at room temperature. Primary antibodies (VASA: Goat anti-human VASA, 1:300, R&D systems, AF2030, Minneapolis, MN; ACROSIN: Rabbit anti-ACROSIN, 1:300, Novus Biologicals, NBP1-85407, Littleton, CO; Mouse anti-human GFRA1 1:200, R&D systems, MAB7141, Minneapolis, MN) were diluted in Donkey blocking buffer and added to tissue sections for 90 min at room temperature. Either of mouse (BD Bioscience, BDB557273, Franklin Lakes, NJ), rabbit (BD Bioscience, BDB550875, Franklin Lakes, NJ) or goat (R&D, AB-108-C, Minneapolis, MN) normal IgG at similar concentration as primary antibody was used as substitute of primary antibody in negative controls. After washing (3 × 5 mins in 1XDPBS), drops of diluted (1:200)

secondary antibody (Alexa fluoro® Donkey anti-mouse 647: A31571, Alexa fluoro® anti-rabbit 488: A21206 and Alexa fluoro® anti-goat 568: A11057; Life technologies Inc, Eugene, OR) was added to tissue section for 45 mins at room temperature. After rinsing in DPBS-T (3 × 5 mins) and DPBS (1 × 5 min), tissue sections were mounted with DAPI containing vectashield mounting medium (Vector Laboratories, H-1200, Burlingame, CA).

5.2.8 Hematoxylin and Eosin staining

Cut tissue sections (5µm each) from PFA-fixed testis grafts were deparaffinized and rehydrated in graded ethanol series with final hydration in water. Sections on slides were then stained in hematoxylin 560 (Leica biosystems Inc, 3801575, Buffalo grove, IL) for 5 mins and rinsed in running tap water (1 min). Sections were then placed in Define MX-aq (Leica biosystems Inc, 3803595, Buffalo grove, IL) for 1 min also followed by rinsing in running tap water for 1 min. This was followed by placement of sections in blue buffer (Leica biosystems Inc, 3802915, Buffalo grove, IL) for 1 min and rinsing in tap water for 1 min. Sections were then dipped in 70% alcohol 3 times and counterstained in Eosin with phloxine (Leica biosystems Inc, 3801606, Buffalo grove, IL) for 30 secs. Sections were then dehydrated, cleared and mounted.

5.2.9 Evaluation of most-advanced germ-cell type

Seminiferous tubules cross sections of hematoxylin- and eosin-stained sections were evaluated for the most advanced germ-cell type. Individual cross section was evaluated for absence of germ cells (Sertoli-cell only) or presence of germ cells which include sections with only spermatogonia (spermatogonia-most advanced germ cell), spermatogonia and spermatocytes

(spermatocytes-most advanced germ cell), and spermatogonia, spermatocytes and spermatids (spermatids-most advanced germ cell). Tubular cross section with each phenotype was quantified across the testis tissue section on slide. Frequency of individual phenotype of the most advanced germ cell was expressed as a percentage of the total cross sections that was counted.

5.2.10 Enzymatic digestion of graft tissue

Testicular tissue was cut into small pieces and placed in pre-constituted, filter-sterilized, warm enzymatic media. The enzymatic media was based on modified human tubal fluid (MHTF) (Irvine Scientific, 90126, Santa Ana, CA) containing 10% serum substitute supplement (SSS) (Irvine Scientific, 99193, Santa Ana, CA) with the addition of 25μg/ml DNase (Worthington, LS002147, Lakewood, NJ), 4.08mg/ml collagenase (Sigma-Aldrich, C5138, St Louis, MO) and 1.6mM $CaCl_2$ (Sigma-Aldrich, C7902, St Louis, MO). Tissue was minced in media until it became moderately slurry. Solution containing minced tissue was then transferred into 15ml tube and vortexed for 1 minute. Solid, unminced tissue was then picked out after the tissue suspension was allowed to set at room temperature. The supernatant was discarded and the slurry tissue was washed with MHTF. Washed, slurry tissue was then transferred into tube containing enzymatic media, and digested in a rocking incubator at 37^{o}C for 45 mins. Tube containing tissue was taken out and shaken vigorously every 15 mins during incubation. Undigested debris were removed from the bottom of tubes after centrifuging at 1300 revolution per minute (rpm) for 5 mins. Supernatant was evaluated for sperm cells.

5.2.11 Sperm processing and storage for ICSI

Testicular graft fragments were shipped overnight to the Oregon national primate research center (ONPRC) in Beaverton, Oregon at ambient temperature in a 15mL conical tube containing 15 mL of MHTF. Upon arrival, a small 10 µL sample was observed under bright field and subjectively evaluated for sperm quality and viability. The supernatant was aspirated off the settled graft fragments and centrifuged for 7 minutes at 300g to pellet the sperm and accompanying cells. Supernatant was discarded and the remaining pellet was suspended in 300µL of HEPES-buffered Tyrode albumin lactate pyruvate (TALP) media with 3 mg/mL of bovine serum albumin (TH media) at ambient temperature as previously described (Tachibana et al., 2010). To this, 300 µL of TEST-yolk buffer (TYB) extender (Irvine Scientific, 90129, Santa Ana, CA) was added dropwise and the suspension was gently mixed again. Sperm cells were maintained in the media during intracytoplasmic sperm injection (ICSI).

5.2.12 Regulation of animal use at the Oregon National Primate Research Center

All Rhesus monkeys were managed and cared for in strict accordance with the guidelines set forth by the National Institute of Health's *Guide for the Care and Use of Laboratory Animals* and all experiments were performed only following approval by the Oregon Health & Science University Institutional Animal Care and Use Committee (IACUC).

5.2.13 Ovarian follicle stimulation and oocyte recovery

Rhesus macaque oocytes were obtained by laparoscopic aspiration of antral follicles following a 10-day controlled ovary stimulation (COS) protocol as previously described (Wolf et al., 1990). Briefly, within the first four days at the onset of menses, 30 IU of recombinant human follicle stimulating hormone (r-hFSH) was administered intramuscularly (IM) b.i.d. on days 1-8 with 30 IU of recombinant human luteinizing hormone (r-hLH) given IM b.i.d. on days 8-9. Estradiol and progesterone concentrations were evaluated daily in blood serum samples via electrochemiluminescent immune assay to verify a response to gonadotropin treatment. When serum estradiol exceeded 200 pg/ml, 1 mg/kg of a GnRH antagonist was administered subcutaneously to prevent an endogenous LH surge and premature ovulation. On day 8, 1000 IU human chorionic gonadotropin (hCG) was supplied IM and antral follicles were aspirated via laparoscopy 36 hours later into TH supplemented with 5 IU/mL of heparin at 37°C. Oocytes were isolated out of follicular aspirate and washed with fresh TH. Surrounding cumulus granulosa cells were removed by repeated pipetting through a fine bore tip and stage of oocyte meiosis was evaluated based on nuclear configuration. Mature, metaphase II (MII) arrested ova with homogenous cytoplasm and an extruded polar body were washed three times through pre-equilibrated Global medium (Life Global Group, LGGG, Guilford, CT) with 10% protein supplement (PS) (Life Global Group, LGPS, Guilford, CT). This was maintained in 100 μL drops under oil at 37°C in 5% CO_2 humidified air until use. Immature recovered oocytes were similarly treated and cultured for 22 hours in Global media and PS, as above, to allow time for completion of meiosis to MII arrest.

5.2.14 Intracytoplasmic sperm injection (ICSI) and embryo culture

Sperm preparations for ICSI were made by pipetting 5µL of settled pellet directly from the TYB extended sample onto a 60mm petri dish. Three successive 1:20 dilutions were made into adjacent drops of fresh TH warmed to 37°C. An additional 20 µL drop of TH was added to the dish to which MII ova were transferred before the plate was flooded with oil to cover all drops. Sperm injections were performed on a Zeiss Axiovert A1 inverted microscope using Narashigi 3-axis hydraulic manipulators. Suction was applied through a glass holding micropipette with a 120 µm outer diameter, 30 µm inner diameter, and a 30° angled bend to hold the ova in place. Sperm of normal morphology and with twitching flagellar movement were selected from the diluted sample drops and injected into the oocyte cytoplasm using a spiked glass pipette with a 5 µm inner diameter, 10 µm bevel, and a 30° angled bend. Following completion of injections, oocytes were transferred to fresh Global media + 10% PS and cultured at 37°C in 5% CO_2 in humidified air with complete medium changes every 48 hours.

5.3 RESULTS

5.3.1 Grafted testicular tissue has phenotype of prepubertal testis tissue

To evaluate the spermatogenic outcome of secured autologous prepubertal testis tissue grafts in Rhesus macaque; first, collected testes tissue were cut into small pieces under sterile condition (Figure 26A). For each grafting site, 4 testicular tissue grafts were secured in the subcutaneous layer of the back or scrotal area with a simple interrupted knot using non-absorbable suture

material (Figure 26B). Estimation of cut testis tissue piece by measuring the weight of randomly selected grafts revealed that the tissues were between 10.54-22.48mg (15.34±1.54mg).

We used Hematoxylin and Eosin staining to evaluate the most advanced germ-cell type in the cross sections of pre-grafted fresh (Figure 26C) and frozen-thawed (Figure 26D) testis tissue while tissue from adult cross section was used as control (Figure 26E). Quantification of this assessment revealed that spermatogonia were the most advanced germ-cell type seen in the cross sections of four (13-022: 100% of 678; 13-024: 100% of 665; 13-026: 100% of 401; 13-030: 100% of 678) monkeys while spermatogonia were found in 99.2% and spermatocytes were found in only 6 of 747 seminiferous tubule cross sections (0.8%) of the fifth (13-008) monkey. Taken together, we demonstrate that immature fresh and frozen-thawed testicular tissue were grafted into each of the monkey.

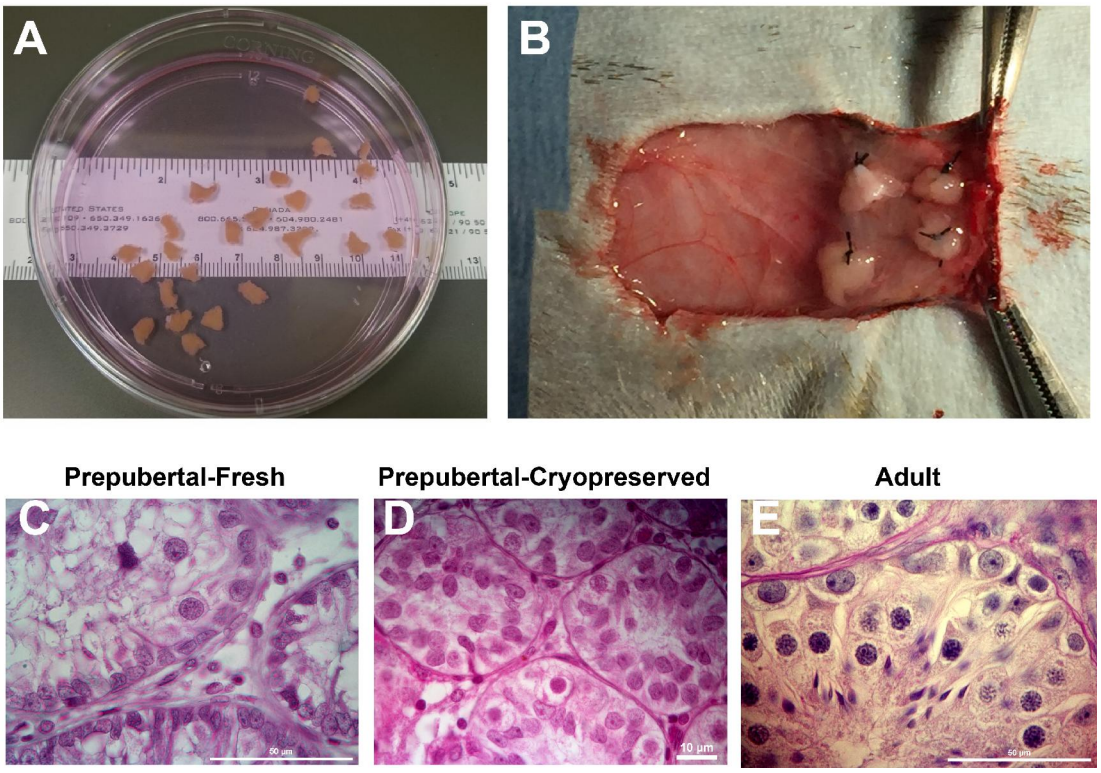

Testis tissue of bilaterally castrated Rhesus macaque was collected and cut into small tissue pieces (A). Four testis tissues were grafted to the subcutis of each grafting site (B). Hematoxylin and Eosin staining reveals spermatogonia which are yet to be established on the basement membrane in the grafted testis tissue (C, D), while multiple types and layers of germ cell were seen in adult testis section (E). n=5. Scale bar=50um (C, E) Scale bar=10um (D).

Figure 26: Grafted testicular tissue has phenotype of prepubertal testis tissue

5.3.2 Immunofluorescence staining confirms prepubertal phenotype

Next, to demonstrate that the germ cells in the grafted tissues were undifferentiated spermatogonia, and not post-meiotic germ cells, we used immunofluorescence staining to evaluate the stage of spermatogenic development in the pre-grafting testis tissue. We previously demonstrated that expressions of VASA, a pan germ-cell marker and GFRA1, a marker of undifferentiated spermatogonia are conserved in Rhesus macaque (Hermann et al., 2009). It has also been shown that expression of ACROSIN, a marker of spermatid, is conserved in Rhesus macaque (Moreno et al., 2000). We co-stained VASA, GFRA1 and ACROSIN in immunofluorescence experiment to dissect the molecular phenotype of germ cells before grafting. VASA+ cells that have not completely migrated to the basement membrane of the seminiferous tubules were observed in the pre-grafted fresh (Figure 27A) and frozen-thawed (Figure 27B) testes tissues, and the pattern of expression is different from that of mature testis cross section from adult animal in which multiple layers of VASA+ cells were seen (Figure 27C). GFRA1+ cells which are yet to be established on the basement membrane were observed in the pre-grafted fresh (Figure 27D) and frozen-thawed (Figure 27E) testes tissues, and the pattern of expression is different from that of GFRA1+ cells in mature/adult testis cross section which are already established on the basement membrane of the seminiferous tubules (Figure 27F). Cells in the pre-grafted fresh (Figure 27G) and frozen-thawed (Figure 27H) testis tissues were negative for the post-meiotic, spermatid marker-ACROSIN. However, post-meiotic, ACROSIN+ cells were present very close to the lumen of seminiferous tubules in the adult testis cross section (Figure 27I). Overlay of VASA, GFRA1 and ACROSIN expressions revealed that VASA+ and GFRA1+ cells overlap in the pre-grafted fresh (Figure 27J) and frozen-thawed (Figure 27K) testes tissue sections. Only few VASA+ cells found on the basement membrane

overlap with GFRA1+ cells while all ACROSIN+ cells found close to the lumen of the seminiferous epithelium overlap with VASA+ cells in the adult cross-section (Figure 27L).

Taken together, these results demonstrate that the grafted fresh and frozen-thawed testicular tissue were from prepubertal monkey.

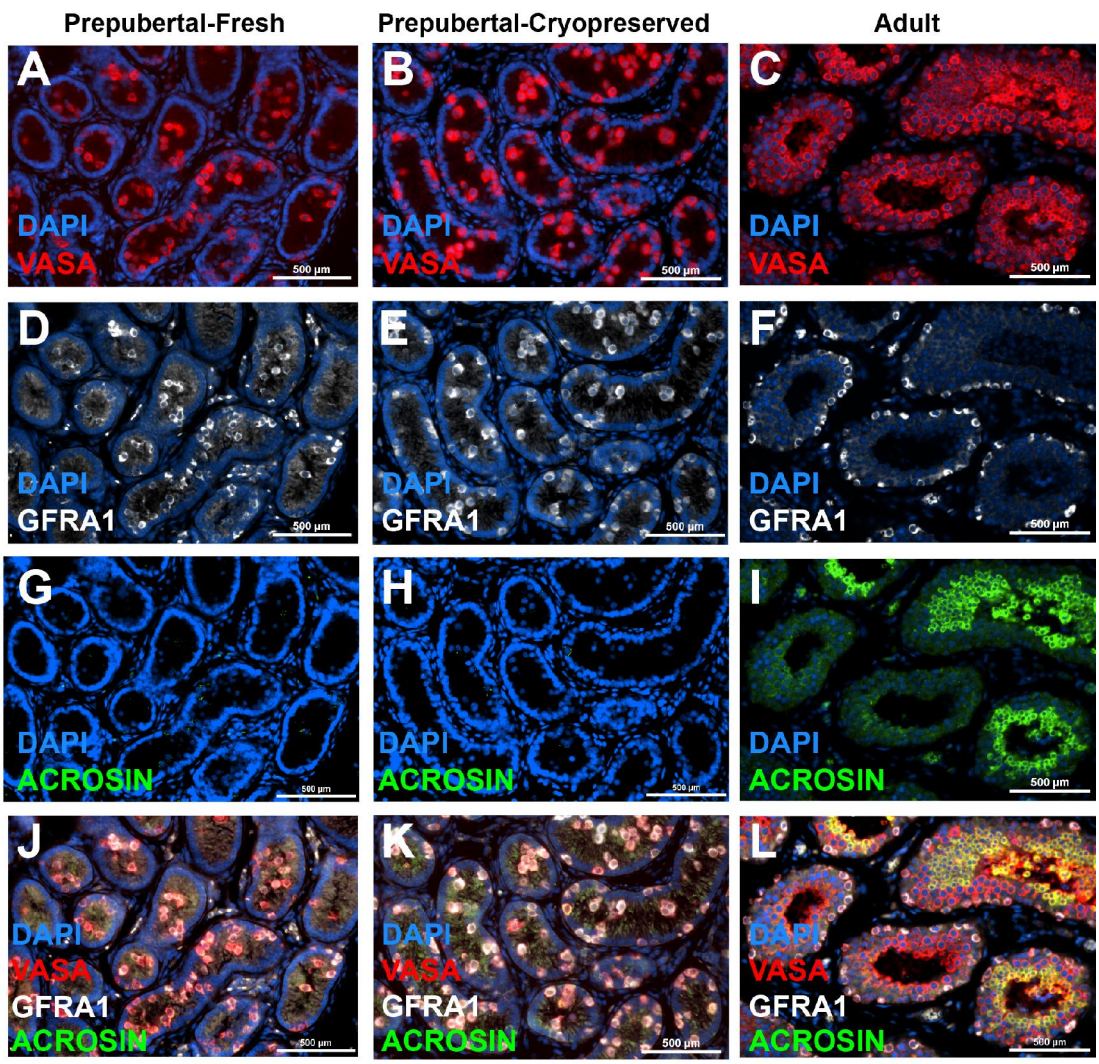

Immunofluorescence staining reveals that few VASA+ cells are seen in the cross section of grafted fresh (A) and frozen-thawed (B) testis sections, which are in contrast with multiple layer of concentric VASA+ cells in adult testis sections (C). Cells in cross sections of grafted testis tissue express GFRA1 (D, E), while GFRA1+ cells are only restricted to the basement membrane of seminiferous tubules in adult testis (F). Cells in the grafted testicular tissue are ACROSIN- (G, H), while ACROSIN+ cells are found close to the lumen of seminiferous epithelium in adult testis section (I). Merged panel reveals that VASA+/GFRA1+/ACROSIN- cells were in the grafted fresh (J) and frozen-thawed (K) testis tissue; unlike the few VASA+/GFRA1+/ACROSIN- cells on the basement membrane and VASA+/GFRA1-/ACROSIN+ cells close to the lumen of seminiferous tubules in adult testis (L). Scale bar=500um

Figure 27: Immunofluorescence staining reveals prepubertal phenotype of pre-grafted testis tissue

5.3.3 Increasing graft volume indicate tissue growth in graft sites

Four to seven months after testicular tissue grafting on the monkeys, clear "bumps" suggesting tissue growth in graft sites were observed for grafts on the back (Figure 28A) and for those in scrotal area (Figure 28B). We used graft volume measurement, which commenced in the middle of the experiment, to evaluate the progression of graft growth. We first observed visible "bumps" suggesting tissue growth in grafts placed in the scrotal area (Figure 28B) and the measurement commenced earlier. Testicular graft volume measurement was taken during 4 or 8 different time points for tissues grafted in the back or scrotal area respectively (Figure 28C). Relative to the first graft volume measurement, there was significant increase ($P<0.01$) in the volume of testicular tissue grafts placed on the back and in scrotal area as the experiment progressed (Figure 28C). Due to variation in the thickness of back skin compared to that of the scrotal area, we did not compare graft volume from these two locations statistically. However, data of graft volume from the scrotal area over time, relative to first measurement, revealed significant graft volume increase ($P<0.01$) in the matrigel-treated fresh and matrigel-treated frozen-thawed testicular tissue grafts (Figure 28D). However, for each time point, there was no significant difference ($P>0.05$) in the graft volume of fresh versus frozen-thawed tissue (Figure 28D). Similarly, over the period of graft volume measurement, there was relative increase ($P<0.05$) in the volume of frozen-thawed testicular tissue grafts on the back (Figure 28E) but the relative growth of fresh graft ($P>0.05$) was not statistically significant. Also, for each time point, there was no difference ($P>0.05$) in the graft volume of fresh versus frozen-thawed tissue on the back (Figure 28E). Our data further indicate that, relative to first graft volume measurement, volume of matrigel-treated as well as plain (untreated) testis tissue grafts on the back increased ($P<0.01$) over time (Figure 28F); and there was no difference ($P>0.05$) in the graft volume of back grafts

treated with matrigel when compared with plain grafts for each of the time point (Figure 28F). Taken together, these data indicate that the graft volume of testicular tissue grafts increased during grafting.

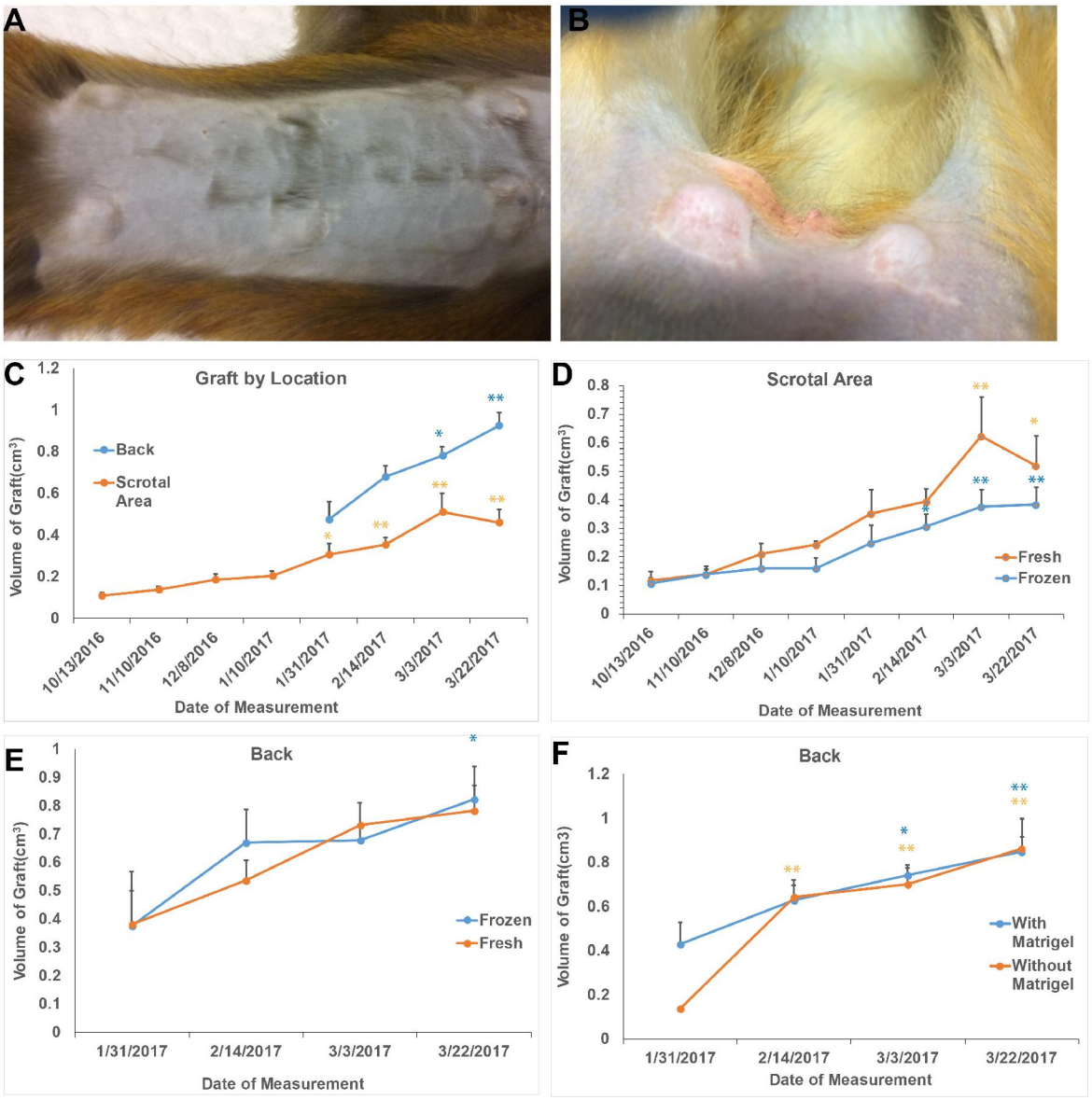

"Bumps" suggesting tissue growth were seen on the back (A) and in scrotal area (B) of Rhesus monkey. Graft volume measurement reveals that tissues grafted to the back and scrotal area increases significantly over time (C). While there was no difference in the growth rate of fresh versus frozen-thawed tissue grafted to the scrotal area (D) or back (E), average graft volume increases over time (D-E). Similarly, addition of matrigel did not influence the growth rate of grafted testicular tissue while the average graft volume of grafts treated with Matrigel and those not increased over time (F). Data point are presented as mean ± standard error of the mean.

Figure 28: Increasing graft volume suggests tissue growth in graft site

5.3.4 Hormonal assay demonstrates intact hypothalamus-pituitary-gonadal axis

In primates, rapid increase in testicular volume is one of the indicators of pubertal development (Mattison et al., 2011; Morris et al., 2009), a stage that is regulated and characterized by the re-appearance of pulsatile gonadotropins releasing hormone (GnRH), which results in elevated production of gonadotropins (FSH and LH) (Plant et al., 2005). LH mediates testosterone (T) production (Plant et al., 2005). Therefore, we next evaluated the endocrine (FSH, Testosterone) profile of prepubertal Rhesus macaques before and during testicular tissue grafting. Levels of FSH and T were respectively monitored in 13-008 (Figure 29A and 29B), 13-022 (Figure 29C and 29D), 13-024 (Figure 29E and 29F), 13-026 (Figure 29G and 29H) and 13-030 (Figure 29I and 29J) before or after testicular tissue grafting. Hormonal assay revealed relative elevation of FSH (Figure 29A, C, E, G and I) and T (Figure 29B, D, F, H and J) levels in each of the monkeys few weeks after testicular tissue grafting. Although, there were variabilities from one biological replicate to another, the trend, however, appears to be consistent. Taken together, our FSH and Testosterone data suggest that the hypothalamus-pituitary-gonadal axis in the Rhesus macaque is intact following testicular tissue grafting while the Testosterone levels indicate pubertal development weeks after testicular tissues were grafted into the monkeys.

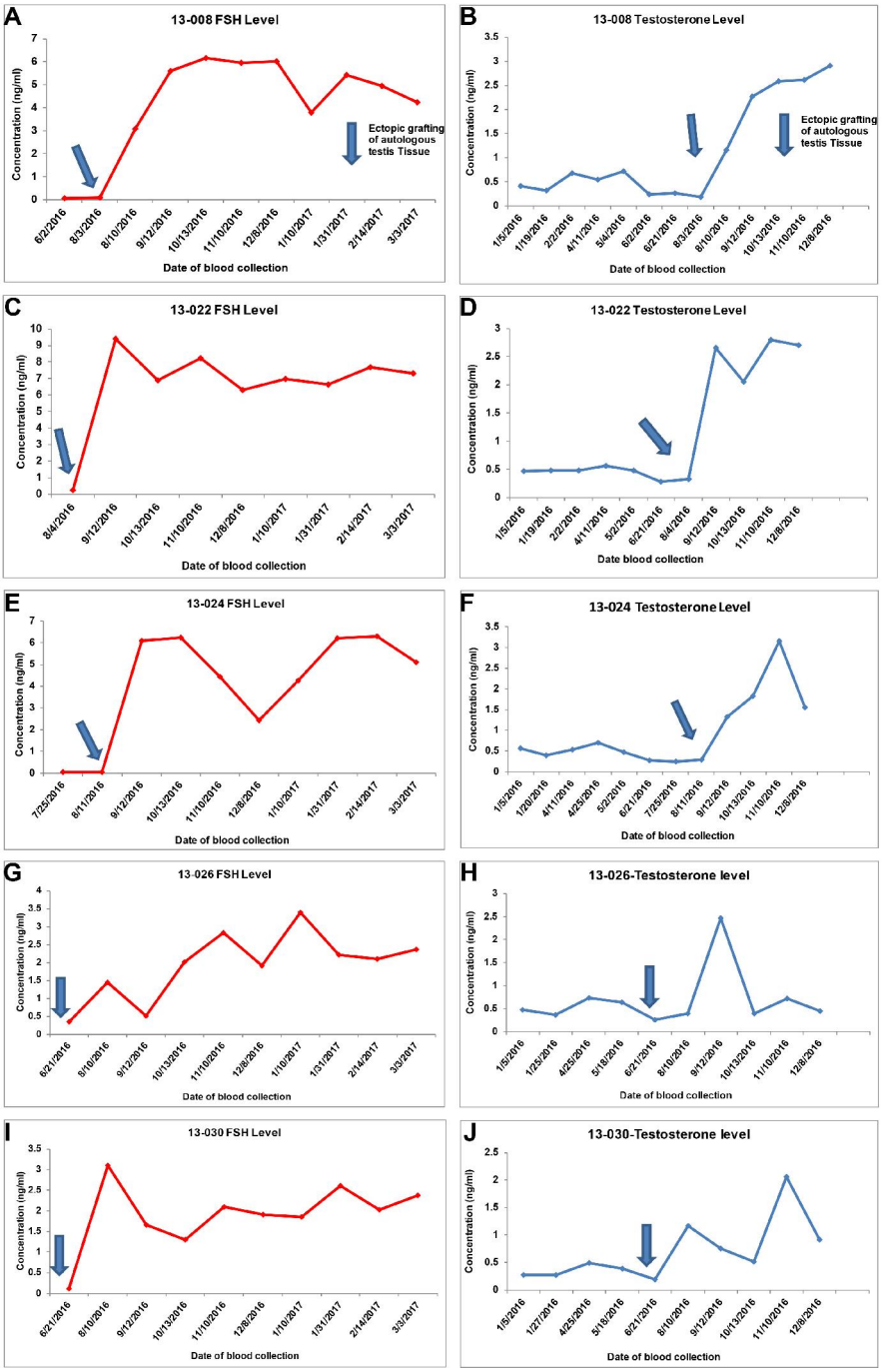

Elevated FSH and testosterone levels were respectively seen in 13-008 (A-B), 13-022 (C-D), 13-024 (E-F), 13-026 (G-G), and 13-030 (I-J) after bilateral castration and tissue grafting. Blue arrow indicates time of testicular tissue collection and grafting.

Figure 29: Hormonal assay demonstrates intact hypothalamus-pituitary-gonadal axis

5.3.5 Sperm cells from recovered testicular tissue grafts

After eight to ten months of grafting, testicular tissues were recovered from 100% of the graft sites but usually as single, fused testis tissue (Figure 30A). Following the teasing apart of this tissue, spermatozoa were seen on wet mount slide viewed under the microscope (Figure 30B). Weight of testicular tissue grafts recovered from the scrotal area is greater ($P<0.01$) than the weight of grafts from the back's subcutis (Figure 30C). However, there is no difference ($P>0.05$) in the weight of recovered back's fresh versus frozen-thawed testicular tissue grafts (Figure 30D). Similarly, weight of testicular tissue grafts on the back treated with Matrigel are not different ($P>0.05$) from the weight of plain, untreated tissue grafts (Figure 30E). Following enzymatic digestion of testicular tissue grafts, recovered sperm cells from tissues grafted to the back as well as scrotal area were quantified (Figure 30F). While millions of sperm cells where recovered from testicular tissue grafts in each grafting sites per treatment group (Figure 30F), the differences in the total sperm count from one treatment group to another was not statistically significant. These data demonstrate that developing, sperm cells-producing testicular tissue grafts can be recovered from grafted autologous, fresh as well as frozen-thawed tissues.

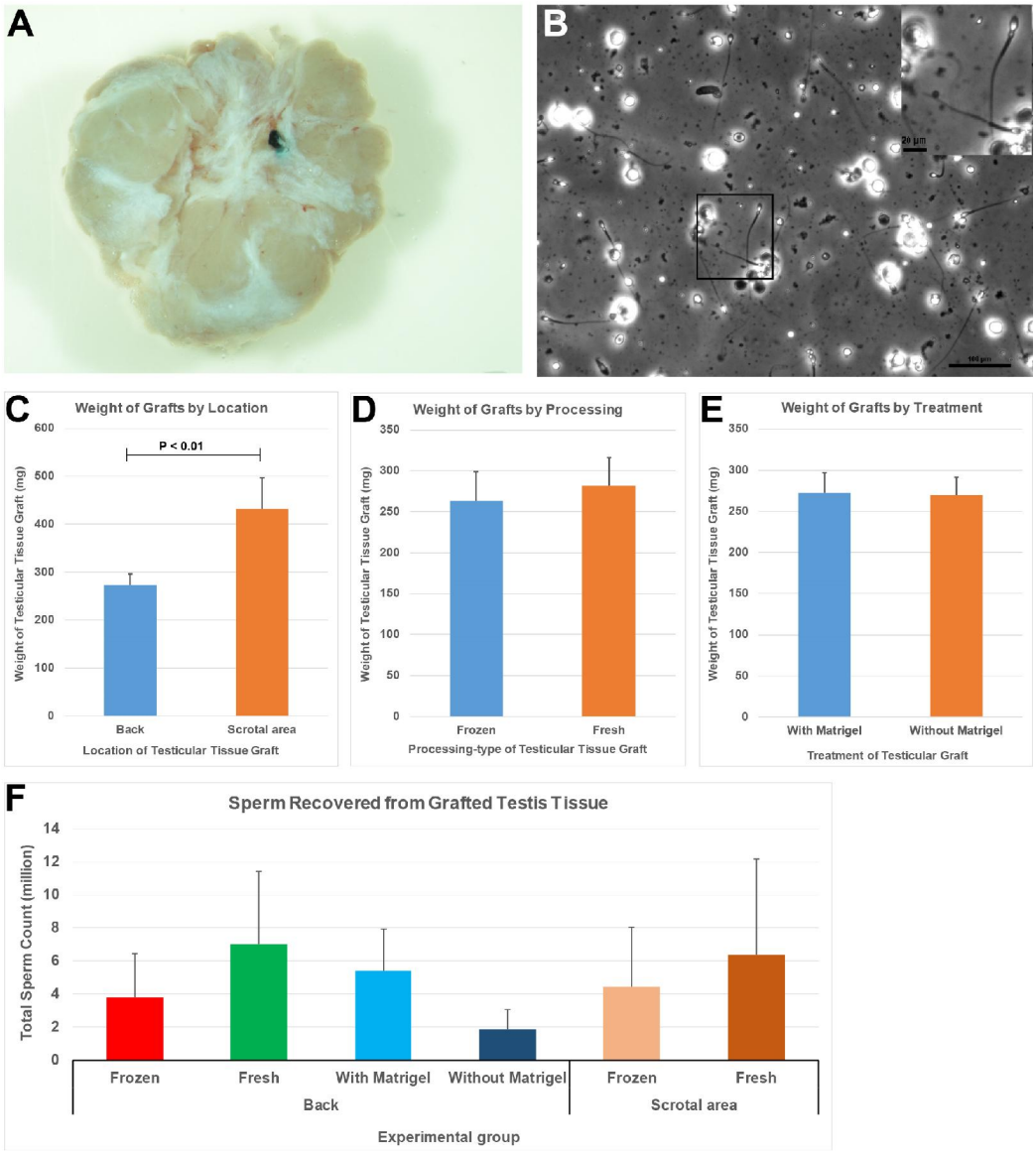

Grafted tissues were recovered as one fused testis tissue (A) and sperm cells were found following mechanical disruption of the tissue (B). While the weight of recovered graft from scrotal area was heavier than graft from the back (C), there was no difference in the weight of recovered grafts from fresh versus frozen-thawed grafts (D). Similarly, addition of matrigel did not influence the weight of recovered testis tissue from grafted testicular tissue (E). Irrespective of the experimental group, millions of sperm cells per graft were recovered from the grafted tissues (F). Bar graph are presented as mean ± standard error of the mean

Figure 30: Sperm cells from recovered testicular tissue graft

5.3.6 Most-advanced germ cell type in the recovered Tissue

Next, through immunofluorescence staining of fixed tissues from the recovered grafts, we demonstrate that cells in the cross-section of the tissue are VASA+, germ cells (Figure 31A); and ACROSIN staining was used to show that ACROSIN+, post-meiotic spermatids are arranged in concentric pattern very close to the lumen of the seminiferous epithelium (Figure 31B) in a pattern similar to what was seen in adult seminiferous tubules cross section (Figure 27I). Because ACROSIN+, post-meiotic (spermatids) cells are present and detected in the germ-cell (VASA+) population (Figure 31C), complete spermatogenesis took place in the recovered testicular tissue grafts. This was further confirmed through Hematoxylin and Eosin staining of tissue from the recovered grafts (Figure 31D). Spermatogonia, spermatocytes, round and elongated spermatids as well as sperm cells were seen in each of the cross sections of tissue grafts irrespective of graft location or treatment group (Figure 31D to G). Quantitatively, absence of germ cell (Sertoli cell only phenotype) as well as the proportion of the most advanced germ-cell phenotype (Spermatids/Sperm cells, spermatocytes, spermatogonia) in cross section of recovered tissue grafts treated with Matrigel is similar ($P>0.05$) to those not treated (Figure 31E). The proportion of seminiferous tubules with Sertoli-cell only, spermatogonia, spermatocytes or spermatids/sperm cells phenotype in the grafted fresh tissue is similar ($P>0.05$) to those of recovered frozen-thawed tissue (Figure 31F) from the back. This observation is similar in tissues recovered from scrotal area. Also, the proportion of seminiferous epithelium with Sertoli cell only or spermatogonia, spermatocytes and spermatids/sperm cells as the most advanced germ cell is not different ($P>0.05$) in the grafts placed on the back or in scrotal area (Fig 31G).

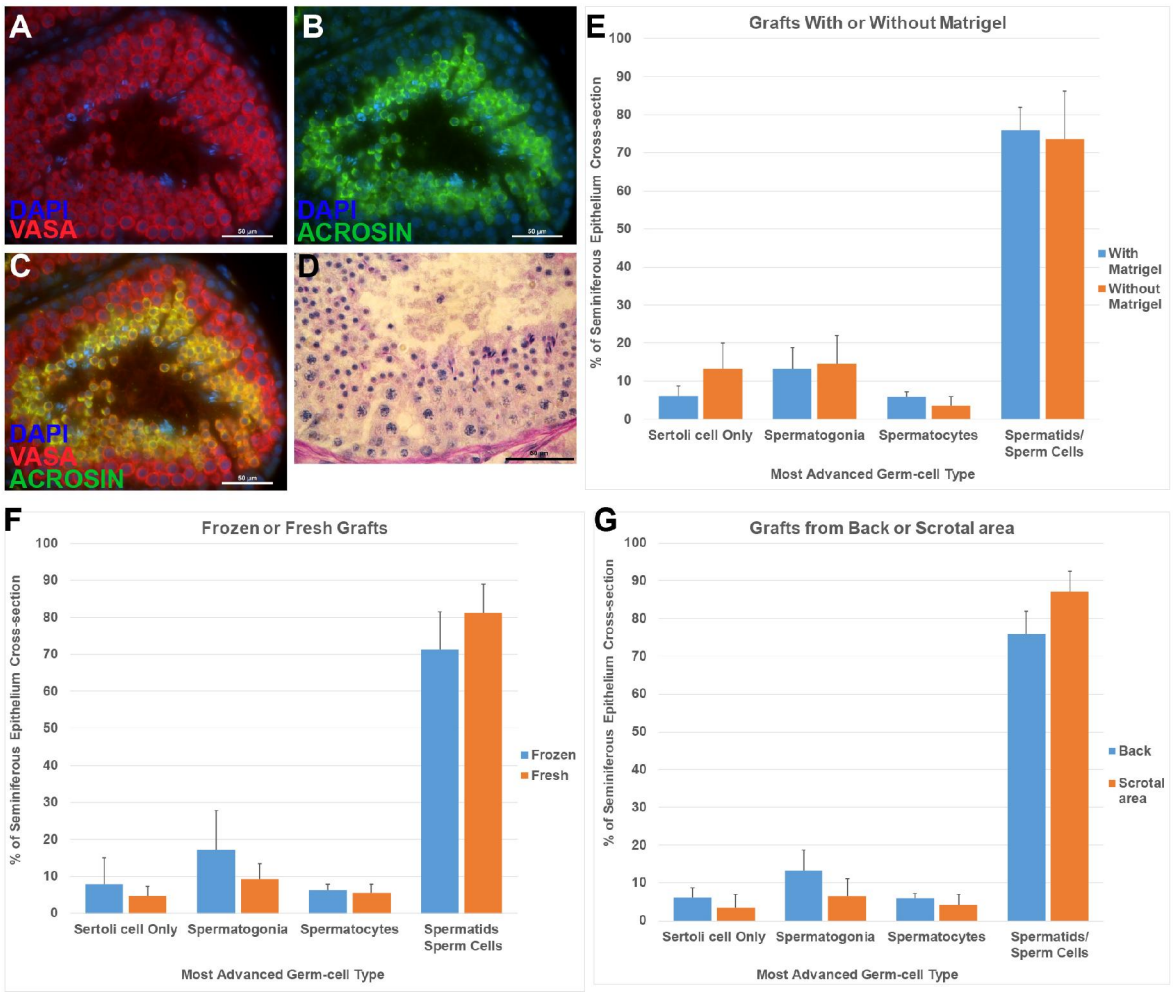

Immunofluorescence staining revealed of recovered grafted tissue revealed multiple layer of concentric VASA+ cells (A) with ACROSIN+ cells close to the lumen of seminiferous tubules (B), and the ACROSIN+ cells overlap with the VASA+ cells (C) in the recovered tissue graft. Hematoxylin and Eosin staining revealed complete spermatogenesis (presence of spermatids/sperm cells) in cross section of seminiferous tubules (D). Quantification reveals that more than 70% of cross sections of seminiferous tubules have complete spermatogenesis (E-G), and there was no difference between the proportion of most-advanced germ cells in tissue grafted with Matrigel when compared with those that were not (E). Similarly, there was no difference in the proportion of most-advanced germ cells from grafted fresh tissue when compared with the frozen-thawed samples (F). Also, we did not observe any difference in the proportion of most-advanced germ cells from grafts placed in the back when compared with those placed in scrotal area (G). Bar graph are presented as mean ± standard error of the mean.

Figure 31. Most-advanced germ cell type in the recovered tissue

5.3.7 Pregnancy from graft-derived sperm cells

Sperm samples were obtained through enzymatic digestion or mechanical disruption of testicular tissue grafts and they contain mature, fully formed sperm of normal morphology (Figure 30B). Approximately 5% of sperm cells still displayed flagellar twitching without forward progression following overnight shipment to ART facility. A total of 58 Rhesus macaque's oocytes were recovered following controlled ovarian stimulation (COS) and follicle aspiration. Of these, n=16 were at MII (*in vivo* matured) and immediately used for intracytoplasmic sperm injection (ICSI) (Figure 32A). Of the remaining oocytes, n=30 had resumed meiosis but were in metaphase I (MI) and n=12 had not yet initiated meiosis resumption as indicated by retained germinal vesicle (GV). MI and GV oocytes were allowed to mature *in vitro* overnight from which n=3 more MII ova were produced and used for ICSI (Figure 32A). Development of the resulting zygotes was maintained and monitored in vitro. Embryo development proceeded through the two-cell stage 1 day after fertilization (Figure 32B). Two days post-fertilization, embryo development was at eight-cell stage (Figure 32C) and they reached morula stage of development by day 5-6 (Figure 32D). Cavitation of embryo, which is indicative of blastocoel formation was observed 10 days after fertilization (Figure 32E), and the blastocyst began to hatch by day 11 post-fertilization (Figure 32F). Blastocysts were transferred into surrogate Rhesus female which results in pregnancy (Figure 32F). Evaluation of fetal development is ongoing.

Sperm cells from grafted testis tissue were used to fertilize Rhesus oocytes through ICSI (A). Cultured developing Rhesus embryo attained 2-cell embryonic stage by day 1 (B) and 8-cell embryonic stage by day 2 (C). Developing Rhesus embryo attained Morula stage by day 6 (D), and blastocoel was visible in the blastocyst embryo by day 10 (E). The blastocyst hatches by 11^{th} day in culture (F). Transferred blastocysts result in pregnancy in surrogate Rhesus (G).

Figure 32: Pregnancy from graft-derived sperm cells

5.4 DISCUSSION

We demonstrate that sperm cells, which can result in the establishment of pregnancy after fertilization, can be recovered from autologous, immature/prepubertal testicular tissue grafts placed in the subcutis of the back/scrotal area in a non-human primate model of fertility preservation. We also show that complete spermatogenesis occurs in the fresh or frozen-thawed testicular tissue grafts placed in skin's subcutis with non-absorbable suture. This observation is consistent for grafts placed on the back or scrotum. Our data further indicate that grafted testicular tissues respond to hypothalamic-pituitary-gonadal axis control of testis and spermatogenic development, which is characterized by elevated serum levels of FSH and testosterone, increased graft volume and completion of spermatogenesis with recovery of sperm cells in grafts. Based on our results, while testicular tissue grafts placed in the subcutaneous layer in scrotal area grow bigger than those on the back, relatively reduced growth size of tissue grafted to the back was not due to failure of spermatogenic development and sperm cell recovery. Similarly, our data reveal that freezing of immature testicular tissues as well as the addition of Matrigel to testicular tissue grafts has no impact on tissue growth, spermatogenic development and recovery of sperm cells.

In this study, immature testicular tissues, with spermatogonia as the most-advanced germ cell (in four monkeys) were grafted to generate complete spermatogenesis in graft sites. Based on previous studies (Jahnukainen et al., 2012; Luetjens et al., 2008b; Wistuba et al., 2006b), the role of donor age in autologous testicular tissue grafts of non-human primate model is not clear. However, xenografting of immature testis tissue grafts gives better developmental outcomes (complete spermatogenesis) than adult's in hamster (Schlatt et al., 2002b), cat (Kim et al., 2007),

dog (Abrishami et al., 2010), horse (Rathi et al., 2006), goat (Arregui et al., 2008; Honaramooz et al., 2002) and others as previously reviewed (Arregui & Dobrinski, 2014). While prepubertal age in Rhesus macaques can be up to 48 months (Honaramooz et al., 2004a), prepubertal Rhesus in our colony are late-maturing and the ones used in this study are not more than 40 months old. Their body weight and testis weight/volume are similar to those of other prepubertal Rhesus raised in our facility (Simorangkir et al., 2012; Verhagen et al., 2014). The presence of undifferentiated spermatogonia (GFRA1+ cells) as the germ (VASA+) cell-type in the grafted tissue couple with the location of germ cells away from the basement membrane of the seminiferous tubule are characteristic phenotype of prepubertal testis cross section, which is similar to what was observed in other studies (Hermann et al., 2009; Marshall & Plant, 1996). Although, spermatocytes were seen in 0.8% of seminiferous tubules cross-section of one monkey, the frequency and the presence of spermatogonia at the middle of the same cross sections and not on the basement membrane (unpublished data) suggests a possibility of spermatocytes development being due to haphazard, loosely regulated progression to spermatocyte development in few regions of the seminiferous epithelium rather than due to pubertal development. This is similar to transient appearance of primary spermatocytes in prepubertal boys between ages 3-5 (Huff et al., 2001; Huff et al., 1993; Huff et al., 1989).

Testicular tissue volume is an indicator of testicular function (Sakamoto et al., 2008). Since only small testicular biopsy can be obtained from prepubertal patients, growth and recovery of grafted testicular tissue are important data points in the development of nonhuman primate model of fertility preservation. In this study, through the measurement of graft volume, we observed progressive tissue growth in all experimental conditions. Grafting a fresh or frozen-thawed tissue or the addition of matrigel to tissue grafts did not appear to influence the viability

and growth of testicular tissue as revealed by graft volume measurement. The increasing graft volume was not due to inflammation, irritation or abscess formation as we did not observe any sign of these pathological conditions when the grafts were on the monkey or during removal (unpublished data). Due to apparent variation in the thickness of back and scrotal skin, we did not statistically compare the graft volume for each time point.

Testicular tissue grafts were recovered from all (100% of) the grafting site, and the combined weight of the grafts is much higher than the collective weight of the tissue grafted in each case. Although instances of fibrosis were observed in the recovered tissue but fibrosis is not the reason for tissue fusion as it is not all inseparable tissues that were fibrotic (unpublished data). On the average, recovered weight (>270mg/graft site) were more than four-fold of the estimated average weight of tissue grafted to each site. Grafted testis tissues were recovered from all grafting sites with fresh or frozen-thawed tissue. This observation is at variance with previous studies that recovered 0% (after 10 months) or 5% (after 5 months) from frozen-thawed tissues grafted to cynomolgus and Rhesus monkeys respectively (Jahnukainen et al., 2012; Luetjens et al., 2008a). This result suggests that the previously reported loss of grafted frozen-thawed tissue is probably at best partly due to the freeze-thawing cycle; other factors might have contributed to the outcome. Similar event of follicle loss in ovarian tissue grafts is caused by "burn out" due to follicular growth which is more rapid in frozen-thawed tissue than in fresh tissue (Gavish et al., 2014).

Physical dimension of grafts is a variable that influences transplantation success (Gavish et al., 2014). Thinner ovarian tissue graft, whether fresh or frozen-thawed, also initiate follicular growth faster than the thicker ones, which "burn out" faster. This phenomenon occurs due to hypoxia arising from tissue ischemia during the first few days of grafting until blood vessels

reconnects to the tissue (Gavish et al., 2014). If germ cell development in grafted male and female gonads are similar in behavior, then variation in the thickness of grafted testicular tissue (2-5mm^3) in our study compared with the (0.5mm-1mm^3) size grafted in other studies (Jahnukainen et al., 2012; Luetjens et al., 2008a; Wistuba et al., 2006a) might play a role in the survival and growth of autologous testis tissue grafts in primate.

Since we utilized grafting approach that placed the tissue grafts in direct contact with capillaries at the subcutis, the surface area to volume ratio of tissue in contact with the capillary network in subcutis is relatively high and this helps to reduce/prevent the impact of apoptosis or necrosis due to hypoxia (Gavish et al., 2008; Gavish et al., 2014). This is one possibility for the higher rate of graft survival and growth observed in this study. However, it appears that this survival and growth of testicular tissue grafts are not primarily influenced by matrigel addition. This indicates that other factors might impact tissue survival and growth more directly than matrigel addition.

Our result further demonstrates that the location of graft placement (subcutis of back or scrotal area) plays a role in determining how big a graft grows. Higher frequency of sweat glands on scrotal skin (than in other regions of the body) is important for testicular thermoregulation and it facilitates optimum temperature for robust spermatogenesis (Blazquez et al., 1988; Kastelic et al., 1996; Rahman et al., 2011). We speculate that this is a factor for the heavier testicular weight of recovered grafts from this location. Heavier scrotal testicular tissue grafts could also be associated to the presence of more than twice skin layers in the back than in genital area, which might make the back skin more resistant to expansion due to tissue growth (Pierard, 1999; Ya-Xian et al., 1999). Our observations here are similar to previous studies which observed complete spermatogenesis from autologous testicular tissue grafted into the scrotum or

scrotal area, a feat that was absent in tissue grafted in other locations of the body (Jahnukainen et al., 2012; Luetjens et al., 2008a). Nevertheless, weight of recovered testicular grafts from the back in this study, does not appear to be unimportant. Generally, grafting accelerates testicular growth and the process is driven by endogenous gonadotropins secretion in primates (Honaramooz et al., 2004b; Mattison et al., 2011).

Pulsatile gonadotropins-releasing hormone (GnRH), which is secreted from hypothalamus at puberty, drives pubertal development in primates (Plant et al., 2005). Active pulsatile release of GnRH appears to be absent during the initial few weeks preceding testicular grafting as indicated by basal levels of FSH and testosterone in this study. We speculate that the observed elevation of FSH level after castration and grafting is due to the response of the anterior pituitary to produce more FSH due to the absence and/or reduced negative feedbacks from gonadal hormones. While we did not assay the LH levels, testosterone levels indicate active communication between the circulating LH and the Leydig cells in the testis. These results indicate that the hypothalamic-pituitary-gonadal axis is intact and monkeys precociously attain puberty following removal and grafting of testicular tissue (Honaramooz et al., 2004b). Here, we accessed pubertal maturity of hypothalamic-pituitary axis with FSH response, and pituitary-gonadal axis with testosterone response. While we did not know of any other studies that evaluated hypothalamic-pituitary axis with FSH in primate model of autologous testis tissue grafts, this response is similar to previous observation of elevated chorionic gonadotropins (CG)level, a pituitary hormone with luteinizing activity in cynomolgus monkey, following autologous testis tissue grafts (Wistuba et al., 2006a). Unlike in previous studies where testosterone level was low in grafted, fully castrated cynomolgus monkey (Luetjens et al., 2008a; Wistuba et al., 2006a), grafted testicular tissues served as the only source of testosterone in our

bilaterally castrated Rhesus. In this study, testosterone level was up to 2ng/ml at some point in all animals. This is similar to pubertal and adult testosterone levels in intact Rhesus macaque (Mattison et al., 2011; Plant et al., 2005) despite of our collection of circulating blood in the morning when testosterone level in Rhesus are relatively low due to diurnal GnRH pulsatility (Plant, 1981). In the primate testis, FSH and testosterone are important for testicular growth as well as proliferation and differentiation of spermatogonia (Arslan et al., 1993; Simorangkir et al., 2009a) while testosterone is important for complete spermatogenesis (Marshall et al., 1986; Marshall et al., 1983; Weinbauer et al., 1988).

Presence of sperm cells in wet mount following teasing apart of recovered tissue grafts, as well as the presence and frequency of spermatids and sperm cells as the most-advanced germ cell histologically, indicate that complete spermatogenesis took place in the grafts during grafting. Following the initial proliferation of Sertoli cells, testicular and spermatogenic development in pubertal primates involves proliferation of undifferentiated spermatogonia with accompanying production of large number of differentiated spermatogonia (Plant et al., 2005). The latter cell-type becomes spermatocytes when they enter meiosis, and after two meiotic divisions, they give rise to spermatids (Phillips et al., 2010). Thus, presence of seminiferous tubules cross-section with Sertoli-cell only, spermatogonia, spermatocytes, spermatids and sperm cells phenotype indicate that spermatogenesis is at different stages in the grafts. Our data indicate that spermatogenesis is complete in most tubules in the grafts as spermatids and/or sperm cells are found in more than 70% of the seminiferous tubules cross section. Neither grafting of fresh or frozen-thawed tissue, nor addition of matrigel and location of graft placement (subcutis of back or scrotal area) significantly influences the extent and frequency of spermatogenic

development in the grafts. This is also consistent with our recovery of millions of sperm cells from tissue grafts irrespective of the treatment conditions.

However, the proportion of motile sperm from testicular grafts was small and this is similar to proportion of motile sperm cells in samples obtained from men through testicular sperm extractions (TESE) for use in ICSI (Omurtag et al., 2013). Sperm motility does not affect fertilization or pregnancy rate following IVF/ICSI (Moghadam et al., 2005), and the fertilization rate of sperm cells extracted from testicular tissue grafts is within the range of previously reported fertilization rate (10%-81%) in Rhesus macaques (Hewitson et al., 1998; Mitalipov et al., 2002; Wolf, 2004; Wolf et al., 2004). The resulting embryo progressed in development at a similar rate as Rhesus embryos in other studies: normal cleavage divisions reaching 8-cell stage by day 2, formation of compacted mass of cells (morula) by day 6 and hatching blastocyst by the 11^{th} day after ICSI. (Hewitson et al., 1998; Wolf, 2004; Wolf et al., 2004). Embryo development also appeared to be consistently normal *in vivo*. As at the time of going to press during the mid-third trimester of gestation, no sign of abnormal fetal development has been detected while the fetus has been sexed to be a female and named Grady (Graft-derived baby).

In summary, this study demonstrates that grafting of tissue to the wall of the subcutis could help in the recovery of frozen-thawed testis tissue. We also demonstrate that the recovered tissue could grow more than four-fold of the initial grafts. Our results further revealed that millions of sperm could be recovered from testicular tissue grafts placed in the back or scrotal sites, and these sperm cells are fertilization-competent. Therefore, as grafting of autologous prepubertal testicular tissue nears translation into fertility clinic, potential significance of our results to patients includes: 1) Potential approach to recovering testicular tissue grafts from frozen and thawed tissue that is grafted on the patient, 2) potential fertility preservation through

small testicular tissue biopsy grafted into ectopic sites and 3) Possibility of recovering millions of sperm cells, which are fertilization-competent, from grafted testicular tissue biopsy. However, unlike in this study, most prepubertal patients would still have their testicles intact, so, future studies using our approach of testicular tissue grafting on nonhuman primate animal model with intact testis need to be performed. Also, there is need to evaluate the postnatal development and reproductive potential of baby derived from nonhuman primate before translating this approach to the clinic.

In conclusion, we produce functional sperm cells from fresh and frozen-thawed prepubertal testis tissue that was autologously grafted on Rhesus macaque, a non-human primate model of fertility preservation for prepubertal patients.

6.0 CONCLUSION

Spermatogonial stem cells (SSCs) are at the foundation of spermatogenesis and may have application for treating some cases of male infertility. High dose chemotherapy treatments for cancer and other non-malignant conditions can cause infertility associated with azoospermia, and this may be due to a depletion of the SSC pool (Valli et al., 2015a). If that is the case and the testicular environment (SSC niche) is functionally intact, then SSC transplantation may constitute a cell-based therapy for restoring fertility in male cancer survivors. Theoretically, SSCs can be isolated via biopsy and cryopreserved prior to cancer treatment and then reintroduced into the testis after cure to regenerate spermatogenesis. Alternatively, SSCs can be left in their niche, and the collected tissue can be used to preserve fertility, which is a tissue-based therapy. However, before these options can be practically explored by patients in fertility clinic, there are two broad knowledge gaps that need be filled: (A) Functional evaluation of the potential risk and success of these fertility preservation options in nonhuman primate model before translation to human and (B) understanding the identity of primate SSC and how they drive steady state spermatogenic development. If we understand how SSCs and other spermatogonia behave endogenously, then we can predict their behavior following transplantation and take steps to achieve optimum fertility restoration. Understanding SSCs behavior may also provide knowledge that can lead to the development of male contraceptives. This study has contributed to revealing some of the unknowns using Rhesus macaque, which has

similar testis anatomy and physiology as human, as a model of primate spermatogenic development and fertility preservation.

The SSC pool in the primate testis are described as A_{dark} and A_{pale} spermatogonia, but the relative regenerative potential of the pool during development and adult life is unknown. All A_{dark} and A_{pale} expressed GFRA1, a marker of undifferentiated spermatogonia (Hermann et al., 2009). Using xenotransplantation, we demonstrate that the concentration of xenotranplantable stem cells in neonatal testis was 5-fold higher than in juvenile and 3-fold higher than in adult testes. The paradox of higher concentration of stem cells in adult testis cells than juvenile is worth exploring. Based on the estimated ratio of SSCs:germ cell ratio of 1:1 in juvenile testis, compared to similar ratio of 1:11.5 in adult testis, there is an 18-fold decline in the potential of transplanted stem cells of juvenile testis to initiate stem cell activity. Unlike in neonates and adult human and Rhesus, testicular secretion of testosterone is at the basal level during juvenile stage of development. This, alongside FSH level, which is also at basal level are sufficient to precociously drive steady-state spermatogenesis in juvenile Rhesus (Plant et al., 2005). The role of testosterone and FSH in spermatogenesis has been reviewed elsewhere (Ramaswamy & Weinbauer, 2014; Walker & Cheng, 2005) and the observed impact may be due to immature Sertoli cells that have not been triggered to initiate and regulate steady-state stem cell activity. This observation may have implication for prepubertal boys who are presently cryopreserving their testicular tissues in anticipation that the stem cells in the tissue can be used to restore fertility later in life. A potential treatment option is to prime the Sertoli cell of the juvenile donors with testosterone and/or FSH treatment. However, for clinical and experimental purposes, sourcing stem cells from adult testis is better as access to tissue sample is easier, overall number

of transplantable cells is higher due to the testis size and the Sertoli cells are already primed during puberty to support steady-state stem cell activity.

We speculate that the influence of testosterone and/or FSH was beneficial for the successful grafting and production of sperm from our prepubertal testis tissue. The initial removal of testosterone source, which typically negatively regulate gonadotropins secretion would trigger high production and release of gonadotropins (Resko et al., 1977), including FSH as observed at the beginning of this study. The sustained, high FSH level in circulation will eventually benefit the Sertoli cells once tissue re-vascularization is established. LH activity in the circulation also played a role in synthesis of testosterone, which is important for completion of meiosis and spermiogenesis (Walker, 2010). Obviously, communication was established between the hypothalamus, pituitary and the grafts, which eventually lead to testosterone production through LH activity. Levels of FSH and testosterone in circulation have negative feedback on the release of gonadotropins (Dubey et al., 1987). Clinically, temporarily removing/obliterating other sources of testosterone and/or FSH source may be helpful for graft survival.

Since successful initiation and maintenance of spermatogenesis in the tissue grafts is dependent on the hormonal signal discussed above, how quickly the grafts become re-vascularized and reconnect to systemic circulation is another critical factor for initiation and completion of spermatogenesis. Grafting in granulation tissues and addition of human menopausal gonadotrophins (HMG) have been used to achieve this in xenografted ovarian tissue (Israely et al., 2006; Wang et al., 2012). We attempted to enhance this by adding matrigel to our tissue without any difference statistically or in the spermatogenic development and output. This suggest we did something else right. We created skin flap before suturing our grafts in-place. The former action might not directly influence the migration of inflammatory cells to the fascia

and subcutis. We speculate that directly suturing our tissue in place might be helpful for initiating intense inflammatory response that also attracts cells that are important for vascular remodeling. Clinically, it may be beneficial to consider grafting testicular tissue in place by using suture materials that trigger moderate inflammatory response.

We also demonstrate that ITGA6-mediated isolation and enrichment of GFRA1+ (spermatogonial stem and progenitor or A_{dark} and A_{pale}) by FACS results in 200% enrichment compared to MACS using adult Rhesus testis cells. We established by xenotransplantation that Rhesus stem cells are absent in ITGA6- fraction. This is a potential tool to avoid loss of rare stem cells during enrichment or sorting experiments. Based on these initial results, we established foundational primate SSC culture conditions using SSCs in ITGA6-postive, MACS-isolated cells from adult Rhesus testis. ITGA6+ cells produced colonies with "grape-like" appearance in culture, which is similar to the appearance of cultured rodent SSCs. ITGA6+ cells retain phenotype of stem and progenitor cells (GFRA1 expression) up to 14 days in culture with C166 feeders providing the best platform for retaining GFRA1 expression in culture. Roughly 26% of GFRA1+ cells were preserved in this condition for 7 days and 10% preserved for 14 days in culture. GFRA1+ cells do not reflect the stem cell population put in culture. Since, the precise stem cell population in the A_{dark} and A_{pale} (or GFRA1+) spermatogonia is presently unknown; we can speculate that it will be a subpopulation of the GFRA1 pool. We also know that roughly 22% of A_{pale} are cKIT+, which means they have lost their stem cell potential. Thus, since the population of A_{dark} and A_{pale} are almost equal in the Rhesus testis, then 89% of GFRA1+ cells represent cKIT- stem and progenitor cells. If stem cells in Rhesus testis behave in vitro as stem cells in rodent, which divides once every 2.7-4.7 days in vitro (Kanatsu-Shinohara et al., 2006; Kanatsu-Shinohara et al., 2003) as it does in vivo, which is 3 days (Huckins & Oakberg, 1978b),

then A_{dark} (50% of GFRA1+ stem and progenitor cells in culture) are also slow cycling cells while A_{pale} (39% of GFRA1+ stem and progenitor cells in culture) divide more frequently in vitro. Since only 55.5% of A_{pale} were labeled after BrdU administration for 3 weeks, assuming A_{pale} comprise of one population of cell that behave similarly, the cell cycle duration, or time that it will take to label 100% of A_{pale} can be estimated to be 5.5 weeks or 38 days. Using the same logic, estimated cell cycle time for A_{dark} is 25.6 weeks or 179 days. Therefore, while it may be presently challenging to expect amplification/multiplication of GFRA1+ cells in short-term culture, this tool provides a platform to manipulate primate stem and progenitor cells for mechanistic studies.

While there may be several steps ahead of us before cell-based SSCs transplantation can be used to achieve fertility, use of testicular tissue for fertility preservation appears to be much closer. In this study, we used autologous grafting of prepubertal testicular tissue to generate sperm cells in ectopic sites, and achieved third-trimester pregnancy from the sperm. The location of testicular tissue grafts may impact how big the tissue eventually becomes but not spermatogenic development in the tissue. This beckons on what is the best option for a patient. In the future, patients who desire to have their testicular tissue grafted in the "privacy" of their private areas are confident of a potential outcome as indicated in this study, and those that want it grafted for adventurous ecstasy are potentially assured of equal outcome, which is production of millions of sperm cells in the tissue. Questions on the health and development of babies that will born using the sperm cells generated from grafted testicular tissue are yet to be answered.

Fertility preservation and restoration leading to production of sperm cells are dependent on the activity of SSCs. SSCs are defined by their ability to self-renew for the replenishment of stem cell pool, and/or to undergo transit amplifying division with the emergence of

differentiating cell-types that supports continuous spermatogenesis (de Rooij & Grootegoed, 1998). They are involved in continuous, well-synchronized, tightly-regulated divisions with the objective of producing millions of sperm cells per day (Phillips et al., 2010). Most of what we know about SSCs and how they drive spermatogenic development leading to production of sperm cells are learnt from rodent. However, while there are similarities in the beginning (SSCs activity) and ending of spermatogenesis (production of mature sperm cell) in primate and rodent, there are differences in (1) the nomenclature used to describe SSCs and their functions, (2) the SSC pool, (3) dynamics of SSCs and their progenitors in spermatogenic development, (4) the clone size and mitotic divisions of progenitor spermatogonial pool, and (5) spermatogenic output (Hermann et al., 2010). While each of the above 5 concepts are extensively studied and understood in the rodent, the first four of the concepts are vaguely studied and understood in the primate testis, ostensibly, due to limitations in tools availability and accessibility to experimental samples and/or subjects. We used Rhesus macaques to elucidate some aspects of the first four concepts listed above.

This study challenged the "dogma" of describing primate SSCs, A_{dark} and A_{pale}, as "reserve" and "active" stem cells, respectively. We used long-term BrdU administration to demonstrate that A_{dark} are mitotically active, slow-cycling, label-retaining SSCs during steady-state spermatogenesis, with mitotic frequency similar in prepubertal Rhesus as adult. We demonstrate that at any moment in time, only 2.4-2.6% of A_{dark} are cycling. All A_{dark} are quiescent during stages V-VIII of the seminiferous epithelium, which covers 46% of the seminiferous cycle (de Rooij et al., 1986). Our data also showed that subpopulations of both A_{dark} and A_{pale} are label-retaining cells with evidence of self-renewal and differentiation in these cell-types, thereby, fulfilling the classical definition of stem cells. Our findings further reveal that

all A_{pale}, like A_{dark} do not divide during every cycle of the seminiferous epithelium. A_{dark} and A_{pale} cells can be targeted for (minor) apoptotic regulation of spermatogenic development. However, major apoptotic regulation of spermatogenic development occurs in the pachytene and round spermatids in a stage-dependent manner. One of the limitations of classical studies is that we are blindsided by how our observations could correlate to lessons learnt from rodent studies. Also, there is no opportunity for mechanistic /functional studies to influence SSCs for fertility or contraceptive purposes.

We went further to correlate the classical description of dark and pale with molecular markers. We demonstrate that subpopulation of A_{dark} and A_{pale} express UTF1, ENO2 and UCHL1 during development and in adulthood (steady state). We demonstrate that these markers are markers of undifferentiated spermatogonia in Rhesus testis. We used UTF1 expression, co-stained with cKIT to reveal the clonal distribution of undifferentiated and differentiating spermatogonia in Rhesus testis during steady state. We found that undifferentiated spermatogonia exist more frequently as clones of single and paired cells, clones of 3 or 4 are less frequently observed, clones greater than 4 are rare. This suggest that primate undifferentiated spermatogonia undergo fewer transit amplifying division than rodents'. Surprisingly, frequency of single and paired differentiating spermatogonia is high and this raise the question on the mechanism that drives the development of differentiating spermatogonia during steady-state spermatogenesis. Our findings indicate that undifferentiated spermatogonia divide once or twice symmetrically, with data suggesting clone fragmentation in cells of clone size 4. We identified that single undifferentiated spermatogonia divides to become paired cells between stage I-IV, while the paired cells complete their cytokinesis to replenish the single cell pool by stage V-VIII. Single cells begin to incorporate EDU, preparing for their next division from stage IX-XII. Also

during this stage, paired cells make decisions on their fate. We identified that some undergo further mitotic divisions to give rise to cells of clone size four, which becomes obvious beginning from stage X-XII. Other paired undifferentiated spermatogonia begin to transit towards differentiation which becomes noticeable from stage XI. On rare occasion, paired undifferentiated spermatogonia are targeted for apoptosis around stage X. We also found that differentiating asymmetric cells develop from "seed cells", which are usually single or paired double-positive cells that are quiescent while their adjacent cells, connected to them by intercytoplasmic bridge, are cycling. "Seed cells" of 3 or 4 clone sizes are less frequent, and those greater than 4 are rare.

The above description captures the dynamic of $A_{pale,}$ which is found more as single cells than A_{dark} (van Alphen et al., 1988). Our approach relies on trend to identify pattern of events, it cannot capture unchanged basal factor that might not interfere with the dynamics one way or the other. A_{dark} are rarely in cell cycle. ~2.4-2.6% at any time, compare to 18.9% A_{pale}. After labeling for 2 cycles of the seminiferous epithelium, only ~11.7% of A_{dark} had gone through S-phase compared to ~55.5% of A_{pale}. This suggest that A_{pale} cycle 5-8 times faster than A_{dark}. A_{dark} is quiescent between stages I-IV, when single cells divide to become paired cells. More A_{pale} are seen in cell cycle, and the proportion increases from stage V-VIII as revealed by Ki67 staining. A_{pale} begins to transit to B1 from stage IX, and this continues until stage XII. Few paired A_{pale} divides to form clone of 4 that may become "seed cells" or undergo clone fragmentation to release a single cell that "boost" its population of single cells. Some single A_{pale} are cKIT+. Twenty five percent and 20% of single and paired cells respectively are cKIT+. The cKIT+ single and paired cells are 11 times more of A_{pale} than A_{dark} as A_{dark} rarely express cKIT. This

indicates almost all cKIT+ cells of larger clone sizes are A_{pale}, B-type and preleptotene spermatocytes.

Incomplete capturing of the A_{dark} and A_{pale} population is a limitation in the interpretation of this molecular marker-based dissection of primate spermatogenic lineage development. On the average, only ~12% of A_{dark} and A_{pale} combined are cKIT+, while only 65% of them are UTF1+. Use of molecular markers left ~23% of these cells uncharacterized. Nonetheless, this limitation is not unique to this study. Markers of stem and progenitor cells in rodent rarely completely overlap. In fact, known markers that are restricted to A_s (ID4, BMI1, PAX7 and EOMES), only labeled subpopulations of the cell-type (Fayomi et al., 2018).

This study has redefined what stem cells are in the primate testis; dissected the dynamics of the stem and progenitor cells during steady-state spermatogenesis using classical and contemporary approaches; and demonstrated potential options for the use of primate stem cells for fertility preservation and/or restoration. Progresses made in this thesis are springboards for understanding human spermatogenic development and for efficient use and translation of stem cell-based therapy to human fertility clinics.

APPENDIX A

MITOTICALLY ACTIVE GERM CELLS IN ADULT TESTIS

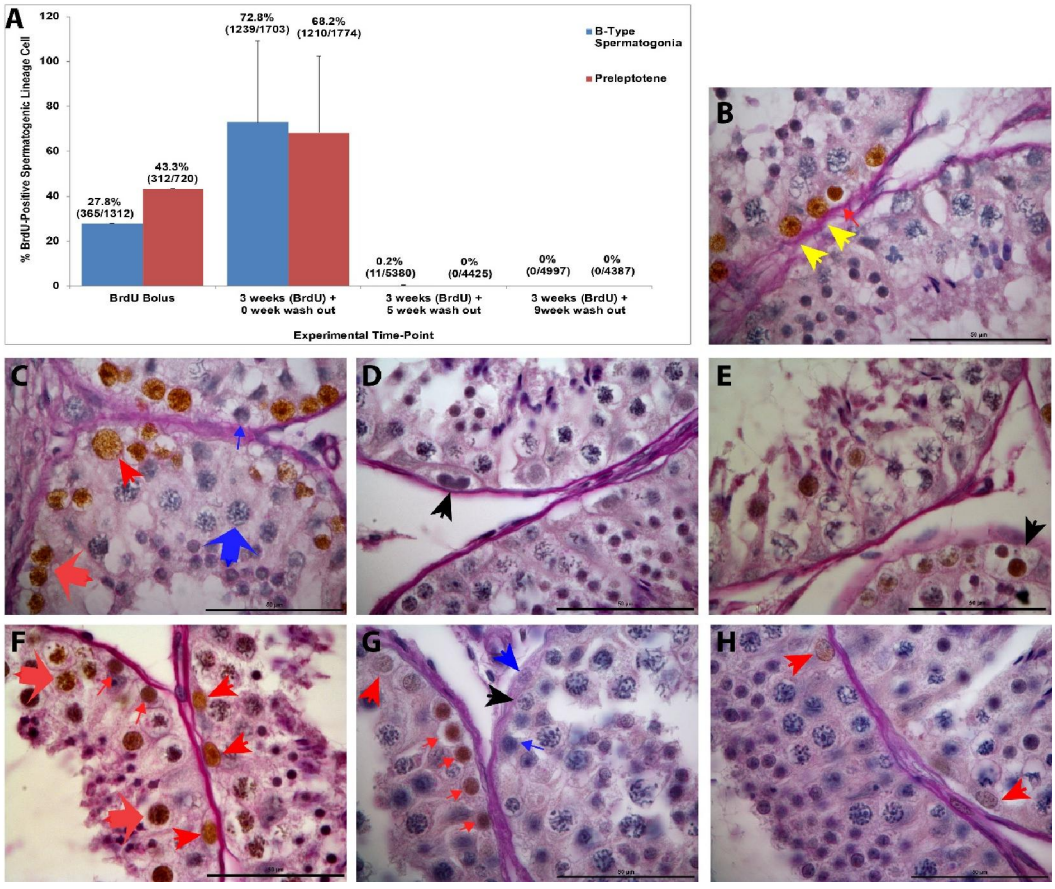

Figure 33: Mitotically active germ cells

Appendix A: Quantification of BrdU-labeled germ cells (A). Following a bolus of BrdU, labeled germ cells including the B-type spermatogonia (yellow big arrow), A_{dark} spermatogonia (red small arrow) (B), preleptotene spermatocytes (very big red arrow), A_{pale} spermatogonia and unlabeled germ cells including A_{dark} (blue small arrow) and pachytene spermatocytes (very big blue arrow) were observed. Phenomenon of mitotically active A_{dark} spermatogonia at telophase (big black arrow) (D and E). After 3 weeks of BrdU administration, spermatogonia including A_{dark} (small red arrow) and A_{pale} (big red arrow) alongside spermatocytes (very big red arrow) were labeled (F). BrdU staining also revealed label-retaining A_{dark} (red small arrow) with unlabeled A_{dark} (blue small arrow) as well as label-retaining A_{pale} (red big arrow) with unlabeled A_{pale} (blue big arrow) after administration of BrdU for 3 weeks followed by 5 weeks of wash out. See also unlabeled B-type spermatogonia (black big arrow) (G-H). Quantification analysis was normalized from animal to animal by counting cells in 500 cross sections of seminiferous epithelium. Scale bar=50um

APPENDIX B

KI67 AND CKIT EXPRESSION BY GERM CELLS ACROSS STAGES OF SEMINIFEROUS EPITHELIUM

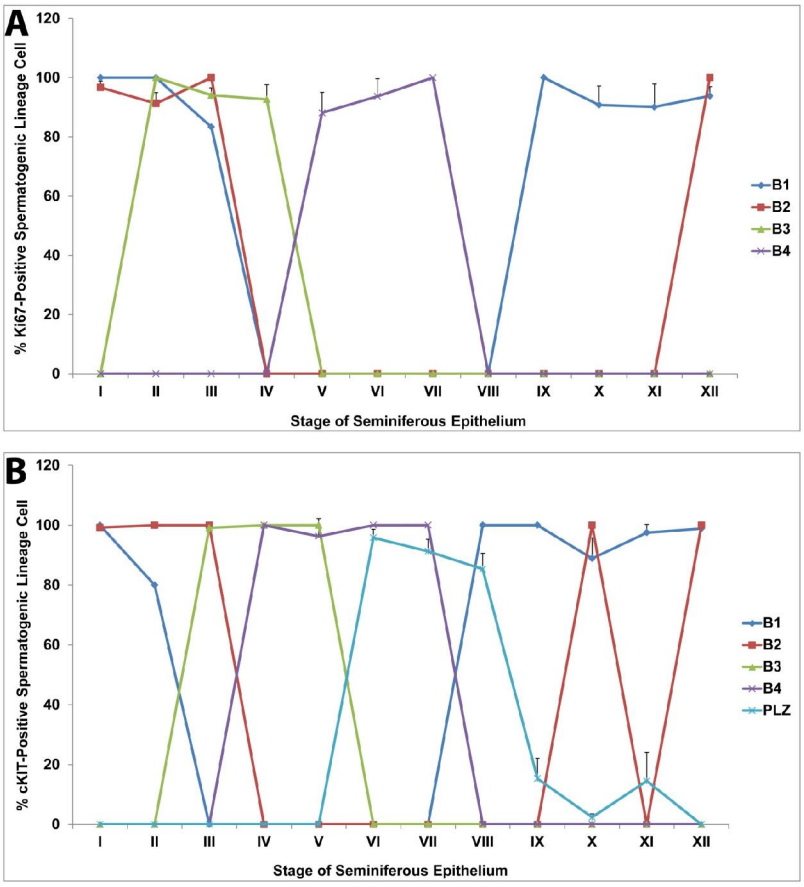

Figure 34: Proliferating and Differentiating germ cells

Appendix B: Proportion of Ki67-postive cells in differentiated spermatogonia and spermatocytes across the stages of the seminiferous epithelium (A). Proportion of cKIT-postive cells in B-type spermatogonia and spermatocytes in stages of seminiferous epithelium (B).

APPENDIX C

PROLIFERATING AND DIFFERENTIATING SPERMATOGONIA IN ADULT RHESUS TESTIS

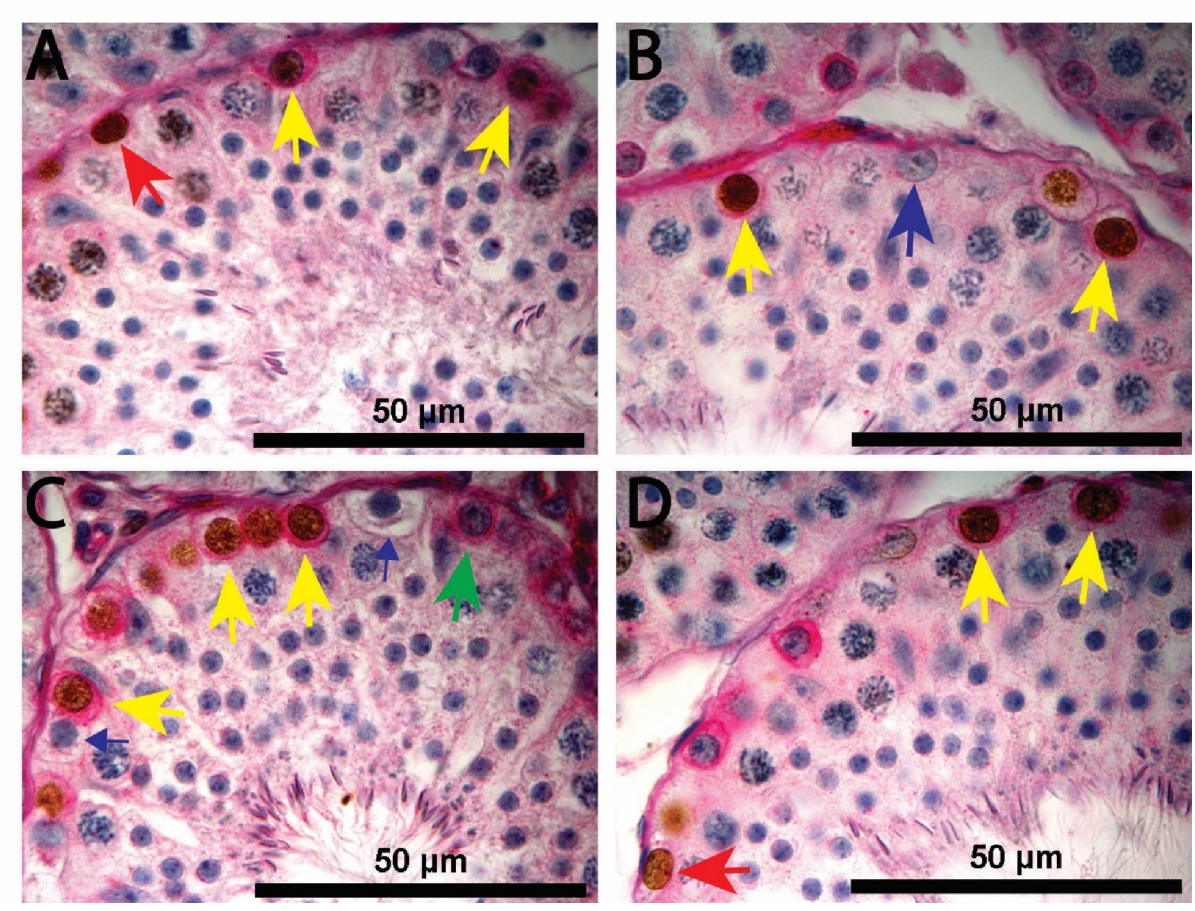

Figure 35: Proliferating and differentiating spermatogonia in adult testis cross-section

Appendix C: Colorimetric PAS-H staining for BrdU and cKIT reveals many BrdU-postive, cKIT-postive A_{pale} (big yellow arrow) (A-D). However, BrdU-postive, cKIT-negative A_{pale} (big red arrow) (A and D), BrdU-negative, cKIT-negative A_{pale} (big blue arrow) (B) as well as BrdU-negative, cKIT-postive A_{pale} spermatogonia (big green arrow) (C) were also seen. Note the BrdU-negative, cKIT-negative A_{dark} (small blue arrow) in the cross section (C). Scale bar=50µm.

APPENDIX D

UTF1 IS EXPRESSED IN ALL STAGES OF SEMINIFEROUS EPITHELIUM

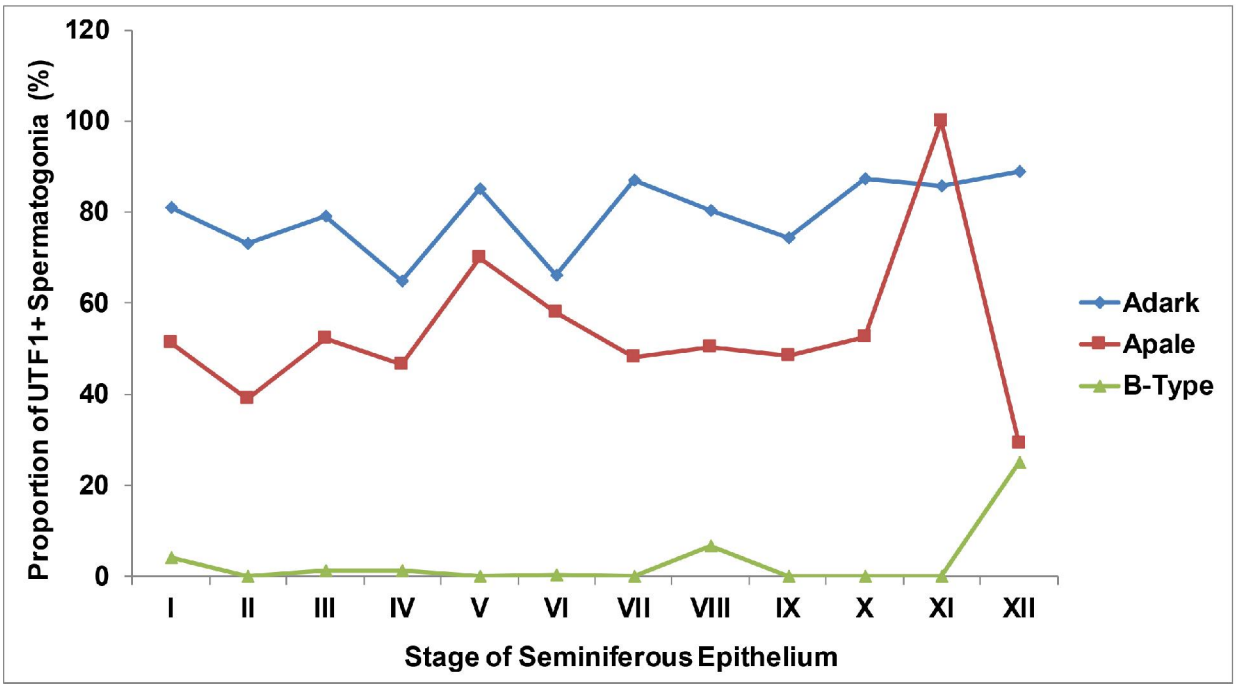

Figure 36: Expression of UTF1 in stages of seminiferous epithelium

Appendix D: Colorimetric PAS-H staining followed by quantitative analysis revealed the proportion of A_{dark}, A_{pale} and B-type spermatogonia that expressed UTF1 across the stages of the seminiferous epithelium. Observations were normalized by counting events across a section of testis tissue. n=3, pooled observation from the replicates is reported.

APPENDIX E

UNDIFFERENTIATED AND DIFFRENTIATING SPERMATOGONIA IN WHOLE MOUNT SEMINIFEROUS EPITHELIUM

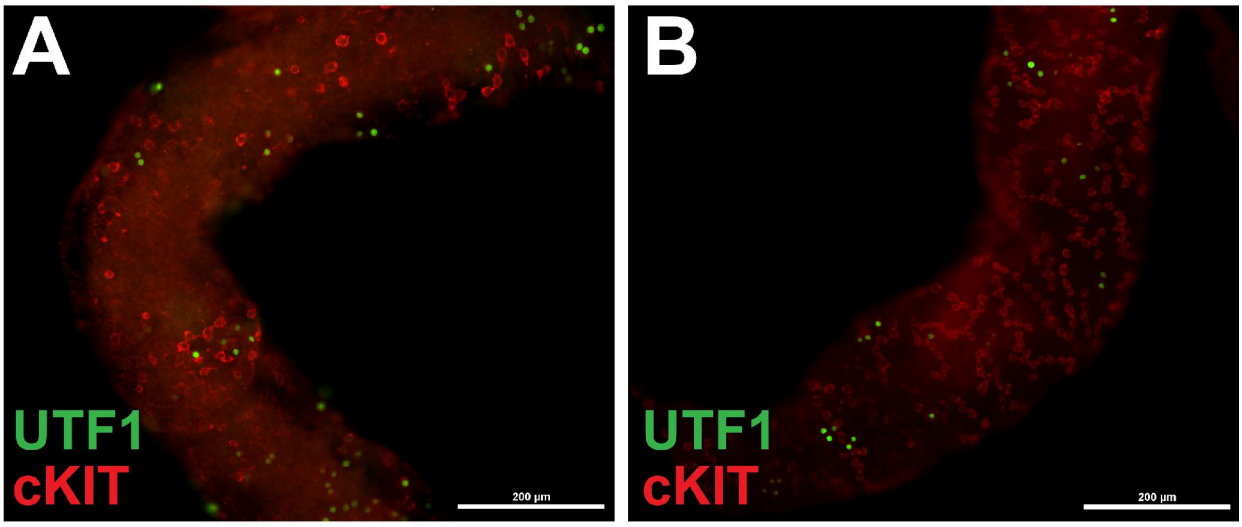

Figure 37: Clonal distribution of UTF1 and cKIT in seminiferous epithelium

Appendix E: Co-staining of UTF1and cKIT in whole mount seminiferous epithelium revealed UTF1+ and cKIT+ clones of few (A) and large clone sizes (B).

APPENDIX F

SCHEMATICS OF UNIQUE CELL MORPHOLOGIES THAT DEFINE EACH STAGE

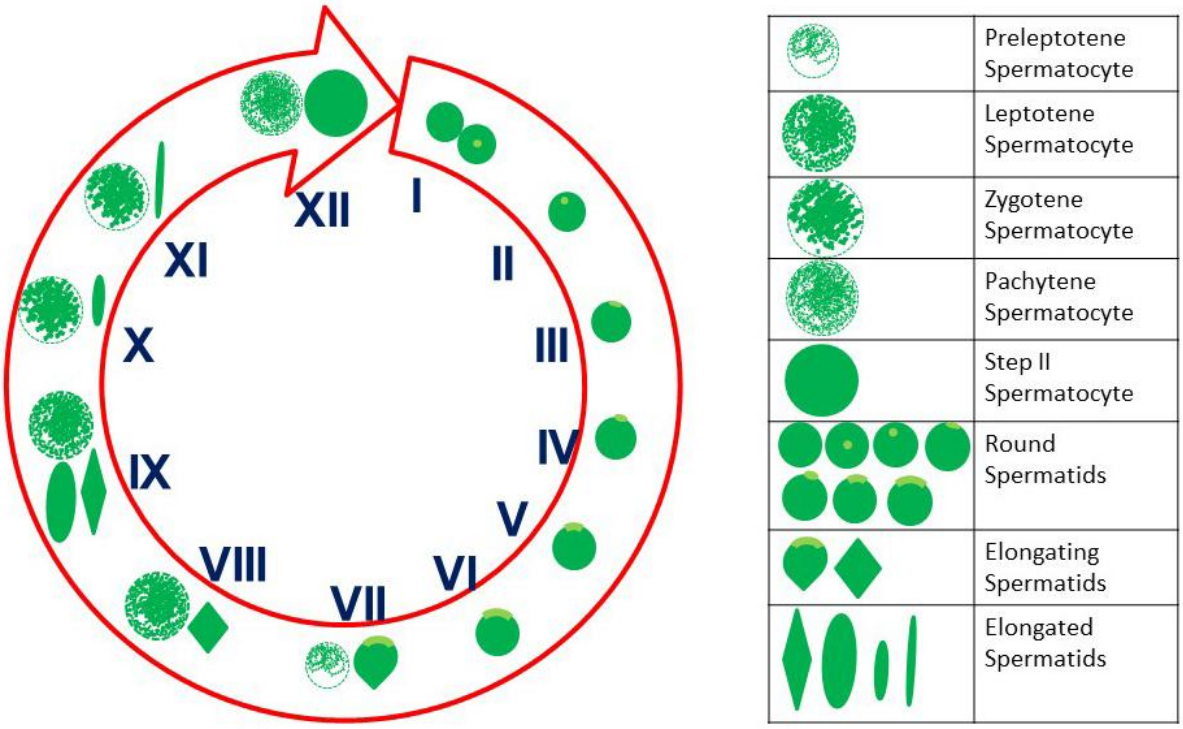

Figure 38: Schematics of unique cell morphology used in staging seminiferous epithelium

Appendix F: EDU staining in whole mount seminiferous epithelium revealed unique morphology that helped to uniquely identify the 12 stages of the seminiferous epithelium in the Rhesus testis.

APPENDIX G

DENSE DIFFERENTIATING CELLS IN STAGE VII OF THE SEMINIFEROUS EPITHELIUM

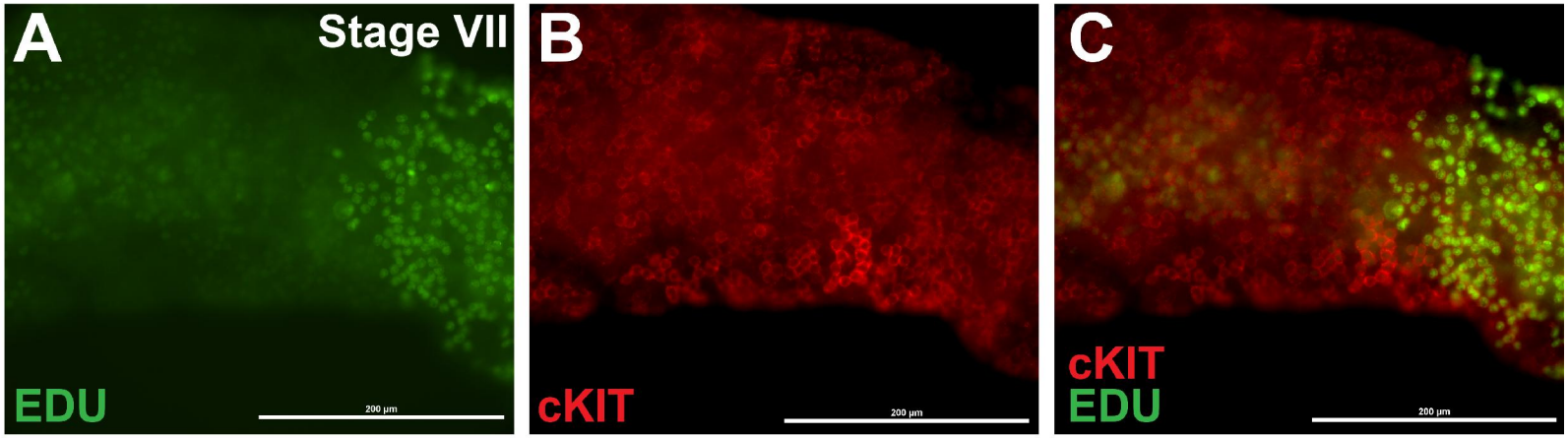

Figure 39: Dense differentiating cells at stage VII of seminiferous epithelium

Appendix G: EDU staining revealed a stage VII seminiferous epithelium (A) in which the clonal distribution of cKIT+ cells in very dense or “infinite” (B). Overlaying the two channels revealed that the cKIT+ cells are in S-phase at different time point.

APPENDIX H

MITOTIC UNDIFFERENTIATED AND DIFFERENTIATING SPERMATOGONIA

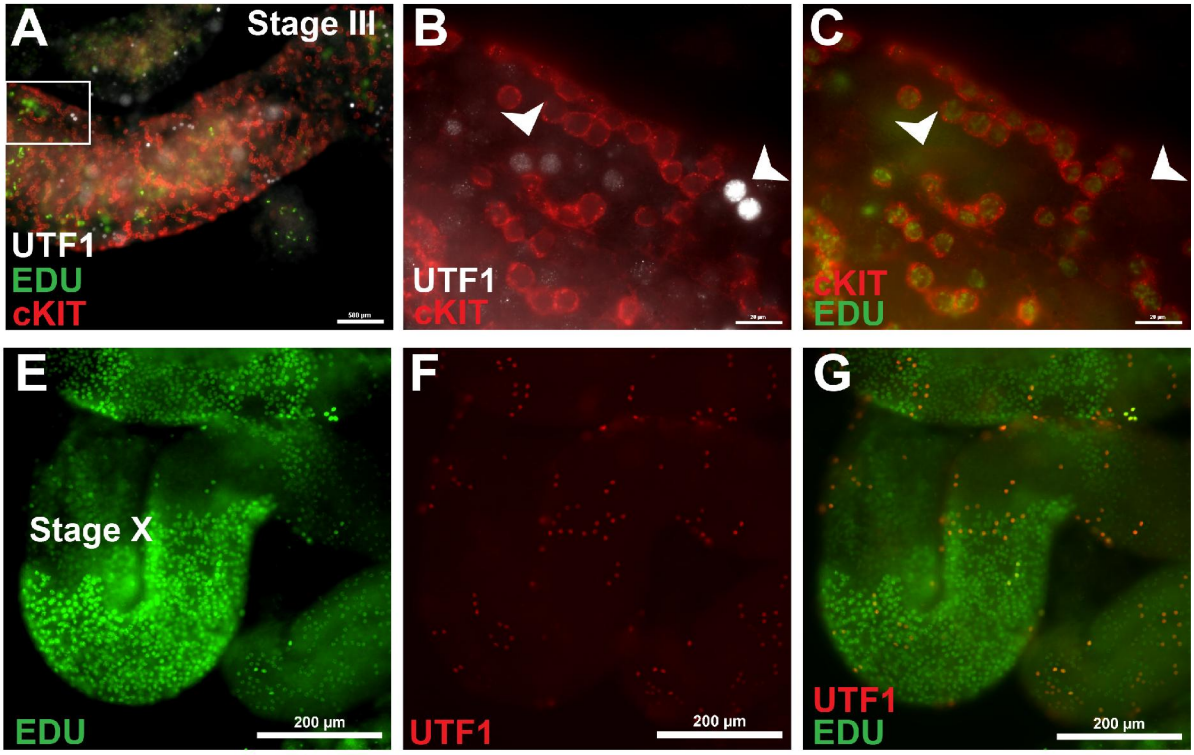

Figure 40: UTF1+ cells selectively incorporate EDU

Appendix H: Co-staining of UTF1, cKIT and EDU revealed the clone sizes of undifferentiated (UTF1+), transitioning (UTF1+/cKIT+) and differentiating (cKIT+) cells in Rhesus seminiferous epithelium during steady state (A). Transitioning "seed cells" (B, white arrow) have distinct morphology that is different from that of their adjacent cells connected by intercytoplasmic bridge. During S-phase, "seed cells" do not incorporate EDU (C, white arrow) but other adjacent cKIT+ cells uniformly incorporated EDU (C). EDU was detected in late zygotenes and early pachytenes at stage X (E). UTF1+ expression was also detected in cell clones in whole mount (F). Overlaying of E and F revealed that UTF1+ cells of different clone sizes at this stage incorporated EDU.

APPENDIX I

DIFFERENTIATING CELLS AT S-PHASE DURING STAGES OF SEMINIFEROUS EPITHELIUM

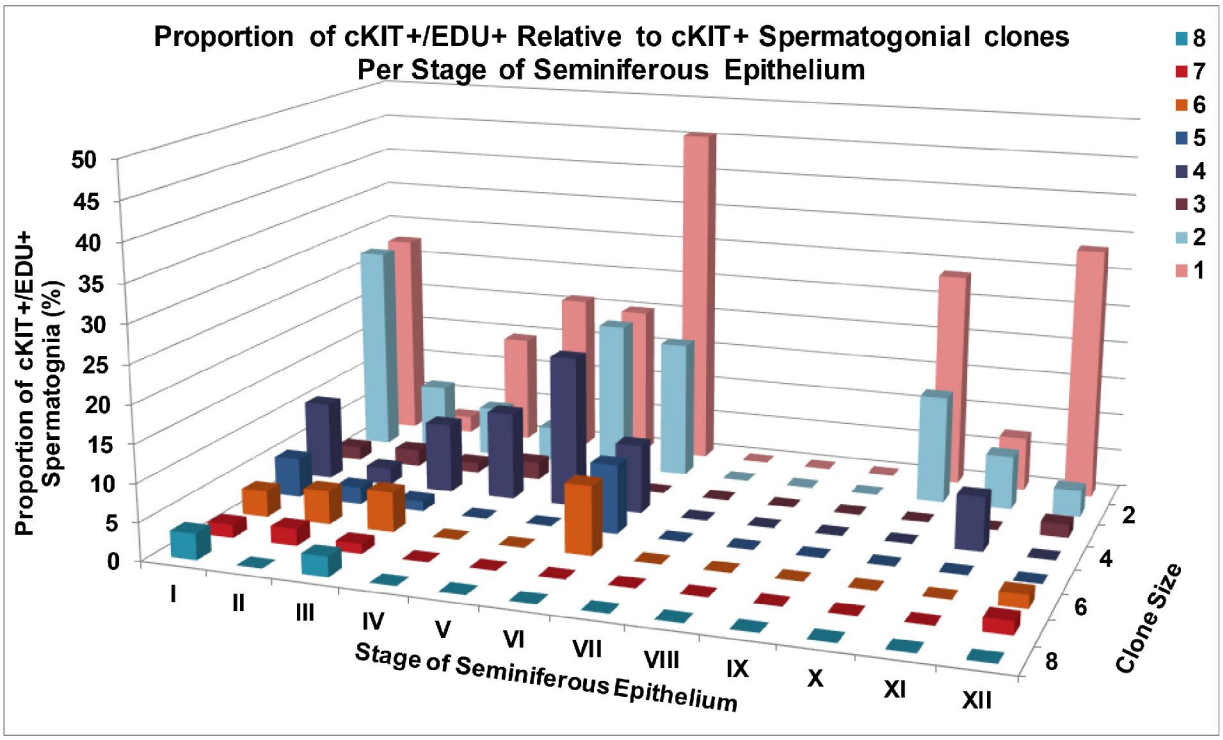

Figure 41: cKIT-positive cells at S-phase

Appendix I: Detection and overlapping of EDU and cKIT were used to quantify the proportion of cycling cKIT+ (cKIT+/EDU+) clones in each stage of the seminiferous epithelium during steady-state spermatogenesis. Cycling cKIT+ cells are more frequent in early stages (I-VI). Events in 5 microscopic field were analyzed for each stage of the seminiferous epithelium.

APPENDIX J

APOPTOSIS IN TESTIS CELLS IN WHOLE MOUNT

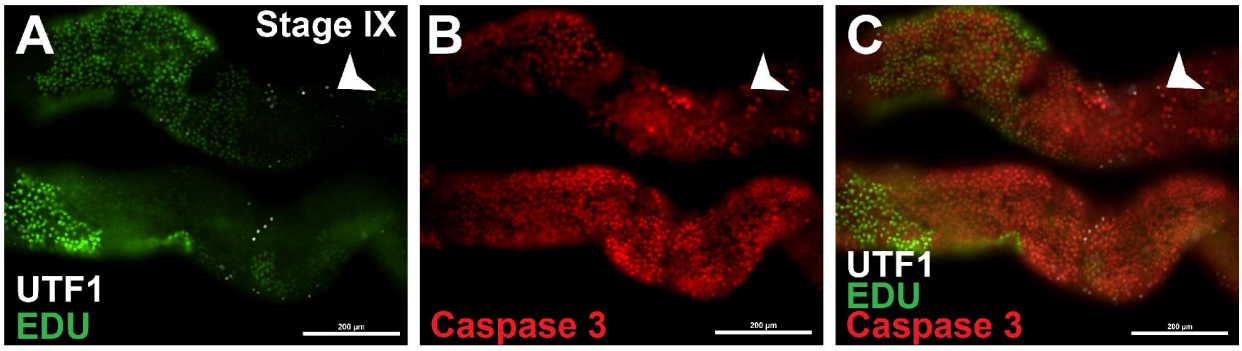

Figure 42: Rare caspase 3-positive UTF1-positive cells

Appendix J: Co-staining of UTF1 and EDU revealed the clone sizes of undifferentiated (UTF1+) spermatogonia in stage IX seminiferous epithelium (A). Activated caspase 3 staining revealed apoptotic germ cells in the seminiferous epithelium at stage IX (B). Overlaying A and B showed that activated caspase 3 is not expressed by most of the undifferentiated spermatogonia but paired, UTF1+ cells expressing activated caspase 3 cells were rarely observed (A-C, white arrow).

BIBLIOGRAPHY

Abrishami, M., Abbasi, S., & Honaramooz, A. (2010). The effect of donor age on progression of spermatogenesis in canine testicular tissue after xenografting into immunodeficient mice. *Theriogenology, 73*(4), 512-522. doi:10.1016/j.theriogenology.2009.09.035

Aeckerle, N., Drummer, C., Debowski, K., Viebahn, C., & Behr, R. (2015). Primordial germ cell development in the marmoset monkey as revealed by pluripotency factor expression: suggestion of a novel model of embryonic germ cell translocation. *Molecular Human Reproduction, 21*(6), 552. doi:10.1093/molehr/gav016

Aeckerle, N., Eildermann, K., Drummer, C., Ehmcke, J., Schweyer, S., Lerchl, A., . . . Behr, R. (2012). The pluripotency factor LIN28 in monkey and human testes: a marker for spermatogonial stem cells? *Molecular Human Reproduction, 18*(10), 477-488. doi:10.1093/molehr/gas025

Aflatoonian, B., & Moore, H. (2006). Germ cells from mouse and human embryonic stem cells. *Reproduction, 132*(5), 699-707. doi:10.1530/REP-06-0022

Alison, M. R., & Islam, S. (2009). Attributes of adult stem cells. *J Pathol, 217*(2), 144-160. doi:10.1002/path.2498

Almeida, C., Cunha, M., Ferraz, L., Silva, J., Barros, A., & Sousa, M. (2011). Caspase-3 detection in human testicular spermatozoa from azoospermic and non-azoospermic patients. *Int J Androl, 34*(5 Pt 2), e407-414. doi:10.1111/j.1365-2605.2011.01151.x

Aloisio, G. M., Nakada, Y., Saatcioglu, H. D., Pena, C. G., Baker, M. D., Tarnawa, E. D., . . . Castrillon, D. H. (2014). PAX7 expression defines germline stem cells in the adult testis. *J Clin Invest, 124*(9), 3929-3944. doi:10.1172/JCI75943

Aponte, P. M. (2015). Spermatogonial stem cells: Current biotechnological advances in reproduction and regenerative medicine. *World J Stem Cells, 7*(4), 669-680. doi:10.4252/wjsc.v7.i4.669

Arregui, L., & Dobrinski, I. (2014). Xenografting of testicular tissue pieces: 12 years of an in vivo spermatogenesis system. *Reproduction, 148*(5), R71-84. doi:10.1530/REP-14-0249

Arregui, L., Rathi, R., Zeng, W., Honaramooz, A., Gomendio, M., Roldan, E. R., & Dobrinski, I. (2008). Xenografting of adult mammalian testis tissue. *Anim Reprod Sci, 106*(1-2), 65-76. doi:10.1016/j.anireprosci.2007.03.026

Arslan, M., Weinbauer, G. F., Schlatt, S., Shahab, M., & Nieschlag, E. (1993). FSH and testosterone, alone or in combination, initiate testicular growth and increase the number of spermatogonia and Sertoli cells in a juvenile non-human primate (Macaca mulatta). *J Endocrinol, 136*(2), 235-243.

Bendel-Stenzel, M., Anderson, R., Heasman, J., & Wylie, C. (1998). The origin and migration of primordial germ cells in the mouse. *Semin Cell Dev Biol, 9*(4), 393-400. doi:10.1006/scdb.1998.0204

Berthold, A. A. (1894). Transplantation der Hoden. *Archiv für Anat., Physiol. und wiss. Med.*, 5.

Blazquez, N. B., Mallard, G. J., & Wedd, S. R. (1988). Sweat glands of the scrotum of the bull. *J Reprod Fertil, 83*(2), 673-677.

Braun, R. E., Sharma, M., Srivastave, A., Fairfield, H. E., & Bergstrom, D. E. (2017). *Identification of Slow-Cycling Long-Term Spermatogonial Stem Cells and Their Regulation by PLZF*. Paper presented at the Society for the Study of Reproduction, Washington DC. Symposium retrieved from http://www.ssr.org/sites/ssr.org/files/uploads/attachments/node/482/ssr2017abstracts.pdf

Brinster, C. J., Ryu, B. Y., Avarbock, M. R., Karagenc, L., Brinster, R. L., & Orwig, K. E. (2003). Restoration of fertility by germ cell transplantation requires effective recipient preparation. *Biology of Reproduction, 69*(2), 412-420. doi:10.1095/biolreprod.103.016519

Brinster, R. L. (2007). Male germline stem cells: from mice to men. *Science, 316*(5823), 404-405. doi:10.1126/science.1137741

Brinster, R. L., & Avarbock, M. R. (1994). Germline transmission of donor haplotype following spermatogonial transplantation. *Proc Natl Acad Sci U S A, 91*(24), 11303-11307.

Brinster, R. L., & Zimmermann, J. W. (1994). Spermatogenesis following male germ-cell transplantation. *Proc Natl Acad Sci U S A, 91*(24), 11298-11302.

Browman, L. G. (1937). Testicular heterotransplantation in rats and mice. *Journal of Experimental Zoology, 75*(2), 29. doi:10.1002/jez.1400750207

Buaas, F. W., Kirsh, A. L., Sharma, M., McLean, D. J., Morris, J. L., Griswold, M. D., . . . Braun, R. E. (2004a). Plzf is required in adult male germ cells for stem cell self-renewal. *Nat Genet, 36*(6), 647-652. doi:Doi 10.1038/Ng1366

Buaas, F. W., Kirsh, A. L., Sharma, M., McLean, D. J., Morris, J. L., Griswold, M. D., . . . Braun, R. E. (2004b). Plzf is required in adult male germ cells for stem cell self-renewal. *Nat Genet, 36*(6), 647-652. doi:10.1038/ng1366

Cevelotto, G. (1909). Uber Verpfanzungen und Gefueungen der Hoden *Frank. Zeitschr.Path., 3*, 7.

Chan, F., Oatley, M. J., Kaucher, A. V., Yang, Q.-E., Bieberich, C. J., Shashikant, C. S., & Oatley, J. M. (2014). Functional and molecular features of the Id4+ germline stem cell population in mouse testes. *Genes & Development, 28*(12), 1351-1362. doi:10.1101/gad.240465.114

Chapman, K. M., Medrano, G. A., Chaudhary, J., & Hamra, F. K. (2015). NRG1 and KITL signal downstream of retinoic acid in the germline to support soma-free syncytial growth of differentiating spermatogonia. *Cell Death Discovery, 1*, 15018. doi:10.1038/cddiscovery.2015.18

Chemes, H. E., Gottlieb, S. E., Pasqualini, T., Domenichini, E., Rivarola, M. A., & Bergada, C. (1985). Response to acute hCG stimulation and steroidogenic potential of Leydig cell fibroblastic precursors in humans. *J Androl, 6*(2), 102-112.

Chen, L. Y., Brown, P. R., Willis, W. B., & Eddy, E. M. (2014). Peritubular myoid cells participate in male mouse spermatogonial stem cell maintenance. *Endocrinology, 155*(12), 4964-4974. doi:10.1210/en.2014-1406

Chen, L. Y., Willis, W. D., & Eddy, E. M. (2016). Targeting the Gdnf Gene in peritubular myoid cells disrupts undifferentiated spermatogonial cell development. *Proc Natl Acad Sci U S A, 113*(7), 1829-1834. doi:10.1073/pnas.1517994113

Chen, S. R., & Liu, Y. X. (2015). Regulation of spermatogonial stem cell self-renewal and spermatocyte meiosis by Sertoli cell signaling. *Reproduction, 149*(4), R159-167. doi:10.1530/REP-14-0481

Cheng, C. Y., & Mruk, D. D. (2002). Cell junction dynamics in the testis: Sertoli-germ cell interactions and male contraceptive development. *Physiol Rev, 82*(4), 825-874. doi:10.1152/physrev.00009.2002

Choi, N. Y., Park, Y. S., Ryu, J. S., Lee, H. J., Arauzo-Bravo, M. J., Ko, K., . . . Scholer, H. R. (2014). A novel feeder-free culture system for expansion of mouse spermatogonial stem cells. *Mol Cells, 37*(6), 473-479. doi:10.14348/molcells.2014.0080

Clermont, Y. (1963). The cycle of the seminiferous epithelium in man. *Am J Anat, 112*, 35-51. doi:10.1002/aja.1001120103

Clermont, Y. (1966). Renewal of spermatogonia in man. *Am J Anat, 118*(2), 509-524. doi:10.1002/aja.1001180211

Clermont, Y. (1969). Two classes of spermatogonial stem cells in the monkey (Cercopithecus aethiops). *Am J Anat, 126*(1), 57-71. doi:10.1002/aja.1001260106

Clermont, Y. (1972). Kinetics of spermatogenesis in mammals: seminiferous epithelium cycle and spermatogonial renewal. *Physiol Rev, 52*(1), 198-236.

Clermont, Y., & Antar, M. (1973). Duration of the cycle of the seminiferous epithelium and the spermatogonial renewal in the monkey Macaca arctoides. *Am J Anat, 136*(2), 153-165. doi:10.1002/aja.1001360204

Clermont, Y., & Bustos-Obregon, E. (1968). Re-examination of spermatogonial renewal in the rat by means of seminiferous tubules mounted "in toto". *Am J Anat, 122*(2), 237-247. doi:10.1002/aja.1001220205

Clermont, Y., & Leblond, C. P. (1959). Differentiation and renewal of spermatogonia in the monkey, Macacus rhesus. *Am J Anat, 104*, 237-273. doi:10.1002/aja.1001040204

Clermont, Y., & Perey, B. (1957). Quantitative study of the cell population of the seminiferous tubules in immature rats. *Am J Anat, 100*(2), 241-267. doi:10.1002/aja.1001000205

Clouthier, D. E., Avarbock, M. R., Maika, S. D., Hammer, R. E., & Brinster, R. L. (1996). Rat spermatogenesis in mouse testis. *Nature, 381*(6581), 418-421. doi:10.1038/381418a0

Codesal, J., Regadera, J., Nistal, M., Regadera-Sejas, J., & Paniagua, R. (1990). Involution of human fetal Leydig cells. An immunohistochemical, ultrastructural and quantitative study. *J Anat, 172*, 103-114.

Cortes, D., Muller, J., & Skakkebaek, N. E. (1987). Proliferation of Sertoli cells during development of the human testis assessed by stereological methods. *Int J Androl, 10*(4), 589-596.

Costoya, J. A., Hobbs, R. M., Barna, M., Cattoretti, G., Manova, K., Sukhwani, M., . . . Pandolfi, P. P. (2004). Essential role of Plzf in maintenance of spermatogonial stem cells. *Nat Genet, 36*(6), 653-659. doi:10.1038/ng1367

Crisler, G. (1929). THE HETEROGENEOUS TESTIS TRANSPLANT PROBLEM AS APPLIED TO WHITE RATS AND MICE. *American Journal of Physiology, 90*(3), 8. doi:10.1152/ajplegacy.1929.90.3.623

Culty, M. (2009). Gonocytes, the forgotten cells of the germ cell lineage. *Birth Defects Res C Embryo Today, 87*(1), 1-26. doi:10.1002/bdrc.20142

Dameron, J. T. (1951). The anterior chamber of the eye for investigative purposes; a site for transplantation of fetal endocrine tissues and cancer, and for the study of tissue reaction. *Surgery, 30*(5), 787-799.

De Miguel, M. P., Arnalich Montiel, F., Lopez Iglesias, P., Blazquez Martinez, A., & Nistal, M. (2009). Epiblast-derived stem cells in embryonic and adult tissues. *Int J Dev Biol, 53*(8-10), 1529-1540. doi:10.1387/ijdb.072413md

de Rooij, D. G. (1973). Spermatogonial stem cell renewal in the mouse. I. Normal situation. *Cell Tissue Kinet, 6*(3), 281-287.

de Rooij, D. G. (1998). Stem cells in the testis. *Int J Exp Pathol, 79*(2), 67-80.

de Rooij, D. G., & Griswold, M. D. (2012). Questions About Spermatogonia Posed and Answered Since 2000. *J Androl, 33*(6), 1085-1095. doi:10.2164/jandrol.112.016832

de Rooij, D. G., & Grootegoed, J. A. (1998). Spermatogonial stem cells. *Curr Opin Cell Biol, 10*(6), 694-701.

De Rooij, D. G., & Lok, D. (1987). Regulation of the density of spermatogonia in the seminiferous epithelium of the Chinese hamster: II. Differentiating spermatogonia. *Anat Rec, 217*(2), 131-136. doi:10.1002/ar.1092170204

de Rooij, D. G., & Russell, L. D. (2000). All you wanted to know about spermatogonia but were afraid to ask. *J.Androl, 21*(6), 776-798.

de Rooij, D. G., van Alphen, M. M., & van de Kant, H. J. (1986). Duration of the cycle of the seminiferous epithelium and its stages in the rhesus monkey (Macaca mulatta). *Biology of Reproduction, 35*(3), 587-591.

de Sousa Lopes, S. M., Roelen, B. A., Monteiro, R. M., Emmens, R., Lin, H. Y., Li, E., . . . Mummery, C. L. (2004). BMP signaling mediated by ALK2 in the visceral endoderm is necessary for the generation of primordial germ cells in the mouse embryo. *Genes Dev, 18*(15), 1838-1849. doi:10.1101/gad.294004

Di Persio, S., Saracino, R., Fera, S., Muciaccia, B., Esposito, V., Boitani, C., . . . Vicini, E. (2017). Spermatogonial kinetics in humans. *Development, 144*(19), 3430-3439. doi:10.1242/dev.150284

Donovan, D., Brown, N. J., Bishop, E. T., & Lewis, C. E. (2001). Comparison of three in vitro human 'angiogenesis' assays with capillaries formed in vivo. *Angiogenesis, 4*(2), 113-121.

Dubey, A. K., Zeleznik, A. J., & Plant, T. M. (1987). In the rhesus monkey (Macaca mulatta), the negative feedback regulation of follicle-stimulating hormone secretion by an action of testicular hormone directly at the level of the anterior pituitary gland cannot be accounted for by either testosterone or estradiol. *Endocrinology, 121*(6), 2229-2237. doi:10.1210/endo-121-6-2229

Ehmcke, J., Gassei, K., Westernstroer, B., & Schlatt, S. (2011). Immature rhesus monkey (Macaca mulatta) testis xenografts show increased growth, but not enhanced seminiferous differentiation, under human chorionic gonadotropin treatment of nude mouse recipients. *Int J Androl, 34*(5 Pt 2), e459-467. doi:10.1111/j.1365-2605.2011.01179.x

Ehmcke, J., Luetjens, C. M., & Schlatt, S. (2005a). Clonal organization of proliferating spermatogonial stem cells in adult males of two species of non-human primates, Macaca mulatta and Callithrix jacchus. *Biology of Reproduction, 72*(2), 293-300. doi:10.1095/biolreprod.104.033092

Ehmcke, J., & Schlatt, S. (2006). A revised model for spermatogonial expansion in man: lessons from non-human primates. *Reproduction, 132*(5), 673-680. doi:10.1530/rep.1.01081

Ehmcke, J., Simorangkir, D. R., & Schlatt, S. (2005b). Identification of the starting point for spermatogenesis and characterization of the testicular stem cell in adult male rhesus monkeys. *Hum Reprod, 20*(5), 1185-1193. doi:10.1093/humrep/deh766

Ehmcke, J., Wistuba, J., & Schlatt, S. (2006). Spermatogonial stem cells: questions, models and perspectives. *Hum Reprod Update, 12*(3), 275-282. doi:10.1093/humupd/dmk001

Eildermann, K., Aeckerle, N., Debowski, K., Godmann, M., Christiansen, H., Heistermann, M., . . . Behr, R. (2012). Developmental Expression of the Pluripotency Factor Sal-Like Protein 4 in the Monkey, Human and Mouse Testis: Restriction to Premeiotic Germ Cells. *Cells Tissues Organs, 196*, 206-220. doi:10.1159/000335031

Eizirik, E., Murphy, W. J., & O'Brien, S. J. (2001). Molecular dating and biogeography of the early placental mammal radiation. *J Hered, 92*(2), 212-219.

Farhi, J., & Ben-Haroush, A. (2011). Distribution of causes of infertility in patients attending primary fertility clinics in Israel. *Isr Med Assoc J, 13*(1), 51-54.

Fayomi, A., David, S., Doungkamchan, C., & Orwig, K. E. (2018). Spermatogonia. In *Reference Module in Biomedical Sciences*: Elsevier.

Fayomi, A. P., & Orwig, K. E. (In Press). Spermatogonial Stem Cells and Spermatogenesis in Mice, Monkeys and Men. *Stem Cell Research*.

Fouquet, J. P., & Dadoune, J. P. (1986). Renewal of spermatogonia in the monkey (Macaca fascicularis). *Biology of Reproduction, 35*(1), 199-207.

Fouquet, J. P., & Raynaud, F. (1985). Renewal of Leydig cells in the neonatal and adult monkey: a radioautographic study. *Biol Cell, 54*(2), 187-190.

Garbuzov, A., Pech, M. F., Hasegawa, K., Sukhwani, M., Zhang, R. J., Orwig, K. E., & Artandi, S. E. (2018). Purification of GFRα1+ and GFRα1− Spermatogonial Stem Cells Reveals a Niche-Dependent Mechanism for Fate Determination. *Stem Cell Reports*. doi:https://doi.org/10.1016/j.stemcr.2017.12.009

Gassei, K., Ehmcke, J., Dhir, R., & Schlatt, S. (2010). Magnetic activated cell sorting allows isolation of spermatogonia from adult primate testes and reveals distinct GFRa1-positive subpopulations in men. *J Med Primatol, 39*(2), 83-91. doi:10.1111/j.1600-0684.2009.00397.x

Gassei, K., & Orwig, K. E. (2013). SALL4 expression in gonocytes and spermatogonial clones of postnatal mouse testes. *PLoS ONE, 8*(1), e53976. doi:10.1371/journal.pone.0053976

Gassei, K., & Orwig, K. E. (2016). Experimental methods to preserve male fertility and treat male factor infertility. *Fertil Steril, 105*(2), 256-266. doi:10.1016/j.fertnstert.2015.12.020

Gavish, Z., Ben-Haim, M., & Arav, A. (2008). Cryopreservation of whole murine and porcine livers. *Rejuvenation Res, 11*(4), 765-772. doi:10.1089/rej.2008.0706

Gavish, Z., Peer, G., Roness, H., Cohen, Y., & Meirow, D. (2014). Follicle activation and 'burn-out' contribute to post-transplantation follicle loss in ovarian tissue grafts: the effect of graft thickness. *Hum Reprod, 29*(5), 989-996. doi:10.1093/humrep/deu015

Geens, M., De Block, G., Goossens, E., Frederickx, V., Van Steirteghem, A., & Tournaye, H. (2006). Spermatogonial survival after grafting human testicular tissue to immunodeficient mice. *Human Reproduction, 21*(2), 390-396. doi:10.1093/humrep/dei412

Ginsberg, J. P., Carlson, C. A., Lin, K., Hobbie, W. L., Wigo, E., Wu, X., . . . Kolon, T. F. (2010). An experimental protocol for fertility preservation in prepubertal boys recently diagnosed with cancer: a report of acceptability and safety. *Hum Reprod, 25*(1), 37-41. doi:10.1093/humrep/dep371

Ginsburg, M., Snow, M. H., & McLaren, A. (1990). Primordial germ cells in the mouse embryo during gastrulation. *Development, 110*(2), 521-528.

Goossens, E., Van Saen, D., & Tournaye, H. (2013). Spermatogonial stem cell preservation and transplantation: from research to clinic. *Human Reproduction, 28*(4), 897-907. doi:10.1093/humrep/det039

Grasso, M., Fuso, A., Dovere, L., de Rooij, D. G., Stefanini, M., Boitani, C., & Vicini, E. (2012). Distribution of GFRA1-expressing spermatogonia in adult mouse testis. *Reproduction, 143*(3), 325-332. doi:10.1530/REP-11-0385

Green, D. M., Kawashima, T., Stovall, M., Leisenring, W., Sklar, C. A., Mertens, A. C., . . . Robison, L. L. (2010). Fertility of male survivors of childhood cancer: a report from the Childhood Cancer Survivor Study. *J Clin Oncol, 28*(2), 332-339. doi:10.1200/JCO.2009.24.9037

Grisanti, L., Falciatori, I., Grasso, M., Dovere, L., Fera, S., Muciaccia, B., . . . Vicini, E. (2009). Identification of spermatogonial stem cell subsets by morphological analysis and prospective isolation. *Stem Cells, 27*(12), 3043-3052. doi:10.1002/stem.206

Griswold, M. D. (1998). The central role of Sertoli cells in spermatogenesis. *Semin Cell Dev Biol, 9*(4), 411-416. doi:10.1006/scdb.1998.0203

Griswold, M. D., & Oatley, J. M. (2013). Concise review: Defining characteristics of mammalian spermatogenic stem cells. *Stem Cells, 31*(1), 8-11. doi:10.1002/stem.1253

Guo, J., Grow, E. J., Yi, C., Mlcochova, H., Maher, G. J., Lindskog, C., . . . Cairns, B. R. (2017). Chromatin and Single-Cell RNA-Seq Profiling Reveal Dynamic Signaling and Metabolic Transitions during Human Spermatogonial Stem Cell Development. *Cell Stem Cell, 21*(4), 533-546.e536. doi:https://doi.org/10.1016/j.stem.2017.09.003

Guo, Y., Hai, Y., Gong, Y., Li, Z., & He, Z. (2014). Characterization, isolation, and culture of mouse and human spermatogonial stem cells. *J Cell Physiol, 229*(4), 407-413. doi:10.1002/jcp.24471

Guo, Y., Liu, L., Sun, M., Hai, Y., Li, Z., & He, Z. (2015). Expansion and long-term culture of human spermatogonial stem cells via the activation of SMAD3 and AKT pathways. *Exp Biol Med (Maywood), 240*(8), 1112-1122. doi:10.1177/1535370215590822

Gupta, G., Maikhuri, J. P., Setty, B. S., & Dhar, J. D. (2000). Seasonal variations in daily sperm production rate of rhesus and bonnet monkeys. *J Med Primatol, 29*(6), 411-414.

Haimoto, H., Takahashi, Y., Koshikawa, T., Nagura, H., & Kato, K. (1985). Immunohistochemical localization of gamma-enolase in normal human tissues other than nervous and neuroendocrine tissues. *Lab Invest, 52*(3), 257-263.

Hamada, A. J., Montgomery, B., & Agarwal, A. (2012). Male infertility: a critical review of pharmacologic management. *Expert Opin Pharmacother, 13*(17), 2511-2531. doi:10.1517/14656566.2012.740011

Hamilton, D. (1986). The Monkey glad affair. *Medical History, 32*(1), 2.

Hamra, F. K., Chapman, K. M., Wu, Z., & Garbers, D. L. (2008). Isolating highly pure rat spermatogonial stem cells in culture. In S. X. Hou & S. R. Singh (Eds.), *Germline Stem Cells* (Vol. 450, pp. 163-179). Totowa, NJ: Humana Press.

Hanley, N. A., Hagan, D. M., Clement-Jones, M., Ball, S. G., Strachan, T., Salas-Cortes, L., . . . Wilson, D. I. (2000). SRY, SOX9, and DAX1 expression patterns during human sex determination and gonadal development. *Mech Dev, 91*(1-2), 403-407.

Hara, K., Nakagawa, T., Enomoto, H., Suzuki, M., Yamamoto, M., Simons, B. D., & Yoshida, S. (2014). Mouse Spermatogenic Stem Cells Continually Interconvert between Equipotent Singly Isolated and Syncytial States. *Cell Stem Cell, 14*(5), 658-672. doi:10.1016/j.stem.2014.01.019

Heller, C. G., & Clermont, Y. (1963). Spermatogenesis in man: an estimate of its duration. *Science, 140*, 184-186.

Helsel, A. R., Yang, Q. E., Oatley, M. J., Lord, T., Sablitzky, F., & Oatley, J. M. (2017). ID4 levels dictate the stem cell state in mouse spermatogonia. *Development, 144*(4), 624-634. doi:10.1242/dev.146928

Hermann, B. P., Mutoji, K. N., Velte, E. K., Ko, D., Oatley, J. M., Geyer, C. B., & McCarrey, J. R. (2015). Transcriptional and translational heterogeneity among neonatal mouse spermatogonia. *Biology of Reproduction, 92*(2), 54. doi:10.1095/biolreprod.114.125757

Hermann, B. P., Phillips, B. T., & Orwig, K. E. (2011). The elusive spermatogonial stem cell marker? *Biology of Reproduction, 85*(2), 221-223. doi:10.1095/biolreprod.111.093146

Hermann, B. P., Sukhwani, M., Hansel, M. C., & Orwig, K. E. (2010). Spermatogonial stem cells in higher primates: are there differences from those in rodents? *Reproduction, 139*(3), 479-493. doi:REP-09-0255 [pii]

10.1530/REP-09-0255

Hermann, B. P., Sukhwani, M., Lin, C. C., Sheng, Y., Tomko, J., Rodriguez, M., . . . Orwig, K. E. (2007). Characterization, cryopreservation, and ablation of spermatogonial stem cells in adult rhesus macaques. *Stem Cells, 25*(9), 2330-2338. doi:10.1634/stemcells.2007-0143

Hermann, B. P., Sukhwani, M., Simorangkir, D. R., Chu, T., Plant, T. M., & Orwig, K. E. (2009). Molecular dissection of the male germ cell lineage identifies putative spermatogonial stem cells in rhesus macaques. *Hum Reprod, 24*(7), 1704-1716. doi:10.1093/humrep/dep073

Hermann, B. P., Sukhwani, M., Winkler, F., Pascarella, J. N., Peters, K. A., Sheng, Y., . . . Orwig, K. E. (2012). Spermatogonial stem cell transplantation into rhesus testes regenerates spermatogenesis producing functional sperm. *Cell Stem Cell, 11*(5), 715-726. doi:10.1016/j.stem.2012.07.017

Herrid, M., Olejnik, J., Jackson, M., Suchowerska, N., Stockwell, S., Davey, R., . . . Hill, J. R. (2009). Irradiation enhances the efficiency of testicular germ cell transplantation in sheep. *Biology of Reproduction, 81*(5), 898-905. doi:10.1095/biolreprod.109.078279

Hewitson, L., Takahashi, D., Dominko, T., Simerly, C., & Schatten, G. (1998). Fertilization and embryo development to blastocysts after intracytoplasmic sperm injection in the rhesus monkey. *Hum Reprod, 13*(12), 3449-3455.

Hobbs, R. M., Fagoonee, S., Papa, A., Webster, K., Altruda, F., Nishinakamura, R., . . . Pandolfi, P. P. (2012). Functional antagonism between Sall4 and Plzf defines germline progenitors. *Cell Stem Cell, 10*(3), 284-298. doi:10.1016/j.stem.2012.02.004

Holstein, A. F., Wartenberg, H., & Vossmeyer, J. (1971). [Cytology of the prenatal development of human gonads. 3. Development of leydig cells in the testis of embryos and fetuses]. *Z Anat Entwicklungsgesch, 135*(1), 43-66.

Honaramooz, A., Behboodi, E., Blash, S., Megee, S. O., & Dobrinski, I. (2003a). Germ cell transplantation in goats. *Mol Reprod Dev, 64*(4), 422-428. doi:10.1002/mrd.10205

Honaramooz, A., Behboodi, E., Megee, S. O., Overton, S. A., Galantino-Homer, H., Echelard, Y., & Dobrinski, I. (2003b). Fertility and germline transmission of donor haplotype following germ cell transplantation in immunocompetent goats. *Biology of Reproduction, 69*(4), 1260-1264. doi:10.1095/biolreprod.103.018788

Honaramooz, A., Li, M. W., Penedo, M. C., Meyers, S., & Dobrinski, I. (2004a). Accelerated maturation of primate testis by xenografting into mice. *Biol Reprod, 70*(5), 1500-1503. doi:10.1095/biolreprod.103.025536

Honaramooz, A., Li, M. W., Penedo, M. C. T., Meyers, S., & Dobrinski, I. (2004b). Accelerated maturation of primate testis by xenografting into mice. *Biology of Reproduction, 70*(5), 1500-1503. doi:DOI 10.1095/biolreprod.103.025536

Honaramooz, A., Snedaker, A., Boiani, M., Scholer, H., Dobrinski, I., & Schlatt, S. (2002). Sperm from neonatal mammalian testes grafted in mice. *Nature, 418*(6899), 778-781. doi:10.1038/nature00918

Huang, S., Sartini, B. L., & Parks, J. E. (2008). Spermatogenesis in testis xenografts grafted from pre-pubertal Holstein bulls is re-established by stem cell or early spermatogonia. *Anim Reprod Sci, 103*(1-2), 1-12. doi:10.1016/j.anireprosci.2006.11.018

Huckins, C. (1971a). The spermatogonial stem cell population in adult rats. I. Their morphology, proliferation and maturation. *Anat Rec, 169*(3), 533-557. doi:10.1002/ar.1091690306

Huckins, C. (1971b). The spermatogonial stem cell population in adult rats. III. Evidence for a long-cycling population. *Cell Tissue Kinet, 4*(4), 335-349.

Huckins, C. (1978a). The morphology and kinetics of spermatogonial degeneration in normal adult rats: an analysis using a simplified classification of the germinal epithelium. *Anat Rec, 190*(4), 905-926. doi:10.1002/ar.1091900410

Huckins, C. (1978b). Spermatogonial intercellular bridges in whole-mounted seminiferous tubules from normal and irradiated rodent testes. *Am J Anat, 153*(1), 97-121. doi:10.1002/aja.1001530107

Huckins, C., & Oakberg, E. F. (1978a). Morphological and quantitative analysis of spermatogonia in mouse testes using whole mounted seminiferous tubules, I. The normal testes. *Anat Rec, 192*(4), 519-528. doi:10.1002/ar.1091920406

Huckins, C., & Oakberg, E. F. (1978b). Morphological and quantitative analysis of spermatogonia in mouse testes using whole mounted seminiferous tubules. II. The irradiated testes. *Anat Rec, 192*(4), 529-542. doi:10.1002/ar.1091920407

Hudson, M. M. (2010). Reproductive outcomes for survivors of childhood cancer. *Obstet Gynecol, 116*(5), 1171-1183. doi:10.1097/AOG.0b013e3181f87c4b

Huff, D. S., Fenig, D. M., Canning, D. A., Carr, M. G., Zderic, S. A., & Snyder, H. M., 3rd. (2001). Abnormal germ cell development in cryptorchidism. *Horm Res, 55*(1), 11-17. doi:10.1159/000049957

Huff, D. S., Hadziselimovic, F., Snyder, H. M., 3rd, Blythe, B., & Ducket, J. W. (1993). Histologic maldevelopment of unilaterally cryptorchid testes and their descended partners. *Eur J Pediatr, 152 Suppl 2*, S11-14.

Huff, D. S., Hadziselimovic, F., Snyder, H. M., 3rd, Duckett, J. W., & Keating, M. A. (1989). Postnatal testicular maldevelopment in unilateral cryptorchidism. *J Urol, 142*(2 Pt 2), 546-548; discussion 572.

Ikami, K., Tokue, M., Sugimoto, R., Noda, C., Kobayashi, S., Hara, K., & Yoshida, S. (2015). Hierarchical differentiation competence in response to retinoic acid ensures stem cell maintenance during mouse spermatogenesis. *Development, 142*(9), 1582-1592. doi:10.1242/dev.118695

Irvine, D. S. (1998). Epidemiology and aetiology of male infertility. *Hum Reprod, 13 Suppl 1*, 33-44.

Israely, T., Nevo, N., Harmelin, A., Neeman, M., & Tsafriri, A. (2006). Reducing ischaemic damage in rodent ovarian xenografts transplanted into granulation tissue. *Hum Reprod, 21*(6), 1368-1379. doi:10.1093/humrep/del010

Izadyar, F., Den Ouden, K., Stout, T. A., Stout, J., Coret, J., Lankveld, D. P., . . . De Rooij, D. G. (2003). Autologous and homologous transplantation of bovine spermatogonial stem cells. *Reproduction, 126*(6), 765-774.

Izadyar, F., Wong, J., Maki, C., Pacchiarotti, J., Ramos, T., Howerton, K., . . . Copperman, A. (2011). Identification and characterization of repopulating spermatogonial stem cells from the adult human testis. *Hum Reprod, 26*(6), 1296-1306. doi:10.1093/humrep/der026

Jahnukainen, K., Ehmcke, J., Nurmio, M., & Schlatt, S. (2012). Autologous ectopic grafting of cryopreserved testicular tissue preserves the fertility of prepubescent monkeys that receive sterilizing cytotoxic therapy. *Cancer Res, 72*(20), 5174-5178. doi:10.1158/0008-5472.CAN-12-1317

Jahnukainen, K., Ehmcke, J., Quader, M. A., Saiful Huq, M., Epperly, M. W., Hergenrother, S., . . . Schlatt, S. (2011). Testicular recovery after irradiation differs in prepubertal and pubertal non-human primates, and can be enhanced by autologous germ cell transplantation. *Hum Reprod, 26*(8), 1945-1954. doi:10.1093/humrep/der160

Jahnukainen, K., Ehmcke, J., Soder, O., & Schlatt, S. (2006). Clinical potential and putative risks of fertility preservation in children utilizing gonadal tissue or germline stem cells. *Pediatr Res, 59*(4 Pt 2), 40R-47R. doi:10.1203/01.pdr.0000205153.18494.3b

Jahnukainen, K., Hou, M., Petersen, C., Setchell, B., & Soder, O. (2001). Intratesticular transplantation of testicular cells from leukemic rats causes transmission of leukemia. *Cancer Res, 61*(2), 706-710.

Jameson, S. A., Natarajan, A., Cool, J., DeFalco, T., Maatouk, D. M., Mork, L., . . . Capel, B. (2012). Temporal transcriptional profiling of somatic and germ cells reveals biased lineage priming of sexual fate in the fetal mouse gonad. *PLoS Genet, 8*(3), e1002575. doi:10.1371/journal.pgen.1002575

Jeanes, A., Wilhelm, D., Wilson, M. J., Bowles, J., McClive, P. J., Sinclair, A. H., & Koopman, P. (2005). Evaluation of candidate markers for the peritubular myoid cell lineage in the developing mouse testis. *Reproduction, 130*(4), 509-516. doi:10.1530/rep.1.00718

Kanatsu-Shinohara, M., Inoue, K., Lee, J., Miki, H., Ogonuki, N., Toyokuni, S., . . . Shinohara, T. (2006). Anchorage-independent growth of mouse male germline stem cells in vitro. *Biology of Reproduction, 74*(3), 522-529. doi:10.1095/biolreprod.105.046441

Kanatsu-Shinohara, M., Inoue, K., Ogonuki, N., Morimoto, H., Ogura, A., & Shinohara, T. (2011). Serum- and feeder-free culture of mouse germline stem cells. *Biology of Reproduction, 84*(1), 97-105. doi:10.1095/biolreprod.110.086462

Kanatsu-Shinohara, M., Ogonuki, N., Inoue, K., Miki, H., Ogura, A., Toyokuni, S., & Shinohara, T. (2003). Long-term proliferation in culture and germline transmission of mouse male germline stem cells. *Biology of Reproduction, 69*(2), 612-616. doi:10.1095/biolreprod.103.017012

Kashimada, K., & Koopman, P. (2010). Sry: the master switch in mammalian sex determination. *Development, 137*(23), 3921-3930. doi:10.1242/dev.048983

Kastelic, J. P., Cook, R. B., Coulter, G. H., & Saacke, R. G. (1996). Insulating the scrotal neck affects semen quality and scrotal/testicular temperatures in the bull. *Theriogenology, 45*(5), 935-942.

Keros, V., Hultenby, K., Borgstrom, B., Fridstrom, M., Jahnukainen, K., & Hovatta, O. (2007). Methods of cryopreservation of testicular tissue with viable spermatogonia in pre-pubertal boys undergoing gonadotoxic cancer treatment. *Hum Reprod, 22*(5), 1384-1395. doi:10.1093/humrep/del508

Kim, T. H., Hargreaves, H. K., Brynes, R. K., Hawkins, H. K., Lui, V. K., Woodard, J., & Ragab, A. H. (1981). Pretreatment testicular biopsy in childhood acute lymphocytic leukaemia. *Lancet, 2*(8248), 657-658.

Kim, Y., Selvaraj, V., Pukazhenthi, B., & Travis, A. J. (2007). Effect of donor age on success of spermatogenesis in feline testis xenografts. *Reprod Fertil Dev, 19*(7), 869-876.

Kim, Y., Turner, D., Nelson, J., Dobrinski, I., McEntee, M., & Travis, A. J. (2008). Production of donor-derived sperm after spermatogonial stem cell transplantation in the dog. *Reproduction, 136*(6), 823-831. doi:10.1530/REP-08-0226

Kimsa, M. C., Strzalka-Mrozik, B., Kimsa, M. W., Gola, J., Nicholson, P., Lopata, K., & Mazurek, U. (2014). Porcine endogenous retroviruses in xenotransplantation--molecular aspects. *Viruses, 6*(5), 2062-2083. doi:10.3390/v6052062

Kluin, P. M., & Derooij, D. G. (1981). A Comparison between the Morphology and Cell-Kinetics of Gonocytes and Adult Type Undifferentiated Spermatogonia in the Mouse. *Int J Androl, 4*(4), 475-493.

Kluin, P. M., Kramer, M. F., & de Rooij, D. G. (1983). Testicular development in Macaca irus after birth. *Int.J.Androl, 6*(1), 25-43.

Komai, Y., Tanaka, T., Tokuyama, Y., Yanai, H., Ohe, S., Omachi, T., . . . Ueno, H. (2014). Bmi1 expression in long-term germ stem cells. *Sci Rep, 4*, 6175. doi:10.1038/srep06175

Kristensen, D. M., Nielsen, J. E., Skakkebaek, N. E., Graem, N., Jacobsen, G. K., Rajpert-De Meyts, E., & Leffers, H. (2008). Presumed pluripotency markers UTF-1 and REX-1 are expressed in human adult testes and germ cell neoplasms. *Hum Reprod, 23*(4), 775-782. doi:10.1093/humrep/den010

Kubota, H., Avarbock, M. R., & Brinster, R. L. (2003a). Spermatogonial stem cells share some, but not all, phenotypic and functional characteristics with other stem cells. *Proc.Natl.Acad.Sci.U.S.A., 100*(11), 6487-6492.

Kubota, H., Avarbock, M. R., & Brinster, R. L. (2003b). Spermatogonial stem cells share some, but not all, phenotypic and functional characteristics with other stem cells. *Proc Natl Acad Sci U S A, 100*(11), 6487-6492. doi:10.1073/pnas.0631767100

Kubota, H., Avarbock, M. R., & Brinster, R. L. (2004a). Culture conditions and single growth factors affect fate determination of mouse spermatogonial stem cells. *Biology of Reproduction, 71*(3), 722-731. doi:10.1095/biolreprod.104.029207

Kubota, H., Avarbock, M. R., & Brinster, R. L. (2004b). Growth factors essential for self-renewal and expansion of mouse spermatogonial stem cells. *Proc Natl Acad Sci U S A, 101*(47), 16489-16494. doi:10.1073/pnas.0407063101

Kubota, H., & Brinster, R. L. (2006). Technology Insight: in vitro culture of spermatogonial stem cells and their potential therapeutic uses. *Nature Clinical Practice Endocrinology & Metabolism, 2*(2), 99-108. doi:DOI 10.1038/ncpendmet0098

Kubota, H., & Brinster, R. L. (2008). Culture of rodent spermatogonial stem cells, male germline stem cells of the postnatal animal. *Methods Cell Biol, 86*, 59-84. doi:10.1016/S0091-679X(08)00004-6

Kubota, H., Wu, X., Goodyear, S. M., Avarbock, M. R., & Brinster, R. L. (2011). Glial cell line-derived neurotrophic factor and endothelial cells promote self-renewal of rabbit germ

cells with spermatogonial stem cell properties. *FASEB J, 25*(8), 2604-2614. doi:10.1096/fj.10-175802

Kumar, S., & Hedges, S. B. (1998). A molecular timescale for vertebrate evolution. *Nature, 392*(6679), 917-920. doi:10.1038/31927

Kurihara, L. J., Kikuchi, T., Wada, K., & Tilghman, S. M. (2001). Loss of Uch-L1 and Uch-L3 leads to neurodegeneration, posterior paralysis and dysphagia. *Hum Mol Genet, 10*(18), 1963-1970.

Kurimoto, K., Yamaji, M., Seki, Y., & Saitou, M. (2008). Specification of the germ cell lineage in mice: a process orchestrated by the PR-domain proteins, Blimp1 and Prdm14. *Cell Cycle, 7*(22), 3514-3518. doi:10.4161/cc.7.22.6979

Langenstroth, D., Kossack, N., Westernströer, B., Wistuba, J., Behr, R., Gromoll, J., & Schlatt, S. (2014). Separation of somatic and germ cells is required to establish primate spermatogonial cultures. *Human Reproduction, 29*(9), 2018-2031. doi:10.1093/humrep/deu157

Lawson, K. A., Dunn, N. R., Roelen, B. A., Zeinstra, L. M., Davis, A. M., Wright, C. V., . . . Hogan, B. L. (1999). Bmp4 is required for the generation of primordial germ cells in the mouse embryo. *Genes Dev, 13*(4), 424-436.

Leblond, C. P., & Clermont, Y. (1952). Definition of the stages of the cycle of the seminiferous epithelium in the rat. *Ann N Y Acad Sci, 55*(4), 548-573.

Lee, J., Kanatsu-Shinohara, M., Inoue, K., Ogonuki, N., Miki, H., Toyokuni, S., . . . Shinohara, T. (2007). Akt mediates self-renewal division of mouse spermatogonial stem cells. *Development, 134*(10), 1853-1859. doi:10.1242/dev.003004

Leitch, H. G., Tang, W. W., & Surani, M. A. (2013). Primordial germ-cell development and epigenetic reprogramming in mammals. *Curr Top Dev Biol, 104*, 149-187. doi:10.1016/B978-0-12-416027-9.00005-X

Lespinasse, V. D. (1913). TRANSPLANTATION OF THE TESTICLE. *Journal of American Medical Association, 61*(21), 2. doi:10.1001/jama.1913.04350220013004

Levine, J., Canada, A., & Stern, C. J. (2010). Fertility preservation in adolescents and young adults with cancer. *J Clin Oncol, 28*(32), 4831-4841. doi:10.1200/JCO.2009.22.8312

Li, L., & Bhatia, R. (2011). Stem cell quiescence. *Clin Cancer Res, 17*(15), 4936-4941. doi:10.1158/1078-0432.CCR-10-1499

Lim, J., Goriely, A., Turner, G. D., Ewen, K. A., Jacobsen, G. K., Graem, N., . . . Rajpert-De Meyts, E. (2011). OCT2, SSX and SAGE1 reveal the phenotypic heterogeneity of spermatocytic seminoma reflecting distinct subpopulations of spermatogonia. *J Pathol, 224*(4), 473-483. doi:10.1002/path.2919

Liu, J., Van der Elst, J., Van den Broecke, R., & Dhont, M. (2002). Early massive follicle loss and apoptosis in heterotopically grafted newborn mouse ovaries. *Hum Reprod, 17*(3), 605-611.

Liu, S., Tang, Z., Xiong, T., & Tang, W. (2011). Isolation and characterization of human spermatogonial stem cells. *Reprod Biol Endocrinol, 9*, 141. doi:10.1186/1477-7827-9-141

Liu, Z., Nie, Y.-H., Zhang, C.-C., Cai, Y.-J., Wang, Y., Lu, H.-P., . . . Sun, Q. (2016). Generation of macaques with sperm derived from juvenile monkey testicular xenografts. *Cell Res, 26*(1), 139-142. doi:10.1038/cr.2015.112

Lovelace, D. L., Gao, Z., Mutoji, K., Song, Y. C., Ruan, J., & Hermann, B. P. (2016). The regulatory repertoire of PLZF and SALL4 in undifferentiated spermatogonia. *Development, 143*(11), 1893-1906. doi:10.1242/dev.132761

Luetjens, C. M., Stukenborg, J.-B., Nieschlag, E., Simoni, M., & Wistuba, J. (2008a). Complete Spermatogenesis in Orthotopic But Not in Ectopic Transplants of Autologously Grafted Marmoset Testicular Tissue. *Endocrinology, 149*(4), 1736-1747. doi:10.1210/en.2007-1325

Luetjens, C. M., Stukenborg, J. B., Nieschlag, E., Simoni, M., & Wistuba, J. (2008b). Complete spermatogenesis in orthotopic but not in ectopic transplants of autologously grafted marmoset testicular tissue. *Endocrinology, 149*(4), 1736-1747. doi:10.1210/en.2007-1325

Lydston, G. F. (1914). Transplantation of a testicle from the dead to the living body. *New York Medical Journal*.

Maki, C. B., Pacchiarotti, J., Ramos, T., Pascual, M., Pham, J., Kinjo, J., . . . Izadyar, F. (2009). Phenotypic and molecular characterization of spermatogonial stem cells in adult primate testes. *Hum Reprod, 24*(6), 1480-1491. doi:10.1093/humrep/dep033

Manku, G., & Culty, M. (2015). Mammalian gonocyte and spermatogonia differentiation: recent advances and remaining challenges. *Reproduction, 149*(3), R139-157. doi:10.1530/REP-14-0431

Manova, K., Nocka, K., Besmer, P., & Bachvarova, R. F. (1990). Gonadal Expression of C-Kit Encoded at the W-Locus of the Mouse. *Development, 110*(4), 1057-1069.

Marshall, G. R., Jockenhovel, F., Ludecke, D., & Nieschlag, E. (1986). Maintenance of complete but quantitatively reduced spermatogenesis in hypophysectomized monkeys by testosterone alone. *Acta Endocrinol (Copenh), 113*(3), 424-431.

Marshall, G. R., & Plant, T. M. (1996). Puberty occurring either spontaneously or induced precociously in rhesus monkey (Macaca mulatta) is associated with a marked proliferation of Sertoli cells. *Biology of Reproduction, 54*(6), 1192-1199.

Marshall, G. R., Wickings, E. J., Ludecke, D. K., & Nieschlag, E. (1983). Stimulation of spermatogenesis in stalk-sectioned rhesus monkeys by testosterone alone. *J Clin Endocrinol Metab, 57*(1), 152-159. doi:10.1210/jcem-57-1-152

Mattison, D. R., Plant, T. M., Lin, H. M., Chen, H. C., Chen, J. J., Twaddle, N. C., . . . Morris, S. M. (2011). Pubertal delay in male nonhuman primates (Macaca mulatta) treated with methylphenidate. *Proc Natl Acad Sci U S A, 108*(39), 16301-16306. doi:10.1073/pnas.1102187108

McCarrey, J. R. (1993). Development of the germ cell. In C. Desjardins & L. L. Ewing (Eds.), *Cell and Molecular Biology of the Testis* (pp. 58-89). New York: Oxford University Press. (Reprinted from: NOT IN FILE).

McLaren, A. (2003). Primordial germ cells in the mouse. *Dev Biol, 262*(1), 1-15.

Meachem, S. J., Ruwanpura, S. M., Ziolkowski, J., Ague, J. M., Skinner, M. K., & Loveland, K. L. (2005). Developmentally distinct in vivo effects of FSH on proliferation and apoptosis during testis maturation. *J Endocrinol, 186*(3), 429-446. doi:10.1677/joe.1.06121

Medrano, J. V., Martinez-Arroyo, A. M., Sukhwani, M., Noguera, I., Quinonero, A., Martinez-Jabaloyas, J. M., . . . Simon, C. (2014). Germ cell transplantation into mouse testes procedure. *Fertil Steril, 102*(4), e11-12. doi:10.1016/j.fertnstert.2014.07.669

Medrano, J. V., Rombaut, C., Simon, C., Pellicer, A., & Goossens, E. (2016). Human spermatogonial stem cells display limited proliferation in vitro under mouse

spermatogonial stem cell culture conditions. *Fertil Steril*. doi:10.1016/j.fertnstert.2016.07.1065

Meistrich, M. L. (2009). Male gonadal toxicity. *Pediatr Blood Cancer, 53*(2), 261-266. doi:10.1002/pbc.22004

Meng, X., Lindahl, M., Hyvonen, M. E., Parvinen, M., de Rooij, D. G., Hess, M. W., . . . Sariola, H. (2000). Regulation of cell fate decision of undifferentiated spermatogonia by GDNF. *Science, 287*(5457), 1489-1493.

Mikkola, M., Sironen, A., Kopp, C., Taponen, J., Sukura, A., Vilkki, J., . . . Andersson, M. (2006). Transplantation of normal boar testicular cells resulted in complete focal spermatogenesis in a boar affected by the immotile short-tail sperm defect. *Reprod Domest Anim, 41*(2), 124-128. doi:10.1111/j.1439-0531.2006.00651.x

Mitalipov, S. M., Yeoman, R. R., Kuo, H. C., & Wolf, D. P. (2002). Monozygotic twinning in rhesus monkeys by manipulation of in vitro-derived embryos. *Biology of Reproduction, 66*(5), 1449-1455.

Moghadam, K. K., Nett, R., Robins, J. C., Thomas, M. A., Awadalla, S. G., Scheiber, M. D., & Williams, D. B. (2005). The motility of epididymal or testicular spermatozoa does not directly affect IVF/ICSI pregnancy outcomes. *J Androl, 26*(5), 619-623. doi:10.2164/jandrol.05018

Moore, C. R. (1924). The Behavior of the Germinal Epithelium in Testis Grafts and in Experimental Cryptorchid Testes (Rat and Guinea Pig). *Science, 59*(1515), 41-44. doi:10.1126/science.59.1515.41

Moreno, R. D., Ramalho-Santos, J., Chan, E. K., Wessel, G. M., & Schatten, G. (2000). The Golgi apparatus segregates from the lysosomal/acrosomal vesicle during rhesus spermiogenesis: structural alterations. *Dev Biol, 219*(2), 334-349. doi:10.1006/dbio.2000.9606

Morris, S. M., Dobrovolsky, V. N., Shaddock, J. G., Mittelstaedt, R. A., Bishop, M. E., Manjanatha, M. G., . . . Mattison, D. R. (2009). The genetic toxicology of methylphenidate hydrochloride in non-human primates. *Mutat Res, 673*(1), 59-66. doi:10.1016/j.mrgentox.2008.12.001

Muciaccia, B., Boitani, C., Berloco, B. P., Nudo, F., Spadetta, G., Stefanini, M., . . . Vicini, E. (2013). Novel stage classification of human spermatogenesis based on acrosome development. *Biology of Reproduction, 89*(3), 60. doi:10.1095/biolreprod.113.111682

Muller, T., Eildermann, K., Dhir, R., Schlatt, S., & Behr, R. (2008). Glycan stem-cell markers are specifically expressed by spermatogonia in the adult non-human primate testis. *Hum Reprod, 23*(10), 2292-2298. doi:10.1093/humrep/den253

Nagano, M., Avarbock, M. R., & Brinster, R. L. (1999). Pattern and kinetics of mouse donor spermatogonial stem cell colonization in recipient testes. *Biology of Reproduction, 60*(6), 1429-1436.

Nagano, M., Avarbock, M. R., Leonida, E. B., Brinster, C. J., & Brinster, R. L. (1998). Culture of mouse spermatogonial stem cells. *Tissue & Cell, 30*(4), 389-397.

Nagano, M., McCarrey, J. R., & Brinster, R. L. (2001). Primate spermatogonial stem cells colonize mouse testes. *Biology of Reproduction, 64*(5), 1409-1416.

Nagano, M., Patrizio, P., & Brinster, R. L. (2002). Long-term survival of human spermatogonial stem cells in mouse testes. *Fertil Steril, 78*(6), 1225-1233.

Nagano, M. C. (2003). Homing efficiency and proliferation kinetics of male germ line stem cells following transplantation in mice. *Biology of Reproduction, 69*(2), 701-707. doi:10.1095/biolreprod.103.016352

Nakagawa, T., Nabeshima, Y., & Yoshida, S. (2007). Functional identification of the actual and potential stem cell compartments in mouse spermatogenesis. *Dev Cell, 12*(2), 195-206. doi:10.1016/j.devcel.2007.01.002

Nakagawa, T., Sharma, M., Nabeshima, Y., Braun, R. E., & Yoshida, S. (2010). Functional hierarchy and reversibility within the murine spermatogenic stem cell compartment. *Science, 328*(5974), 62-67. doi:10.1126/science.1182868

Narisawa, S., Hecht, N. B., Goldberg, E., Boatright, K. M., Reed, J. C., & Millan, J. L. (2002). Testis-specific cytochrome c-null mice produce functional sperm but undergo early testicular atrophy. *Mol Cell Biol, 22*(15), 5554-5562.

Naughton, C. K., Jain, S., Strickland, A. M., Gupta, A., & Milbrandt, J. (2006). Glial cell-line derived neurotrophic factor-mediated RET signaling regulates spermatogonial stem cell fate. *Biology of Reproduction, 74*(2), 314-321. doi:10.1095/biolreprod.105.047365

Nel-Themaat, L., Vadakkan, T. J., Wang, Y., Dickinson, M. E., Akiyama, H., & Behringer, R. R. (2009). Morphometric analysis of testis cord formation in Sox9-EGFP mice. *Dev Dyn, 238*(5), 1100-1110. doi:10.1002/dvdy.21954

Nistal, M., Abaurrea, M. A., & Paniagua, R. (1982). Morphological and histometric study on the human Sertoli cell from birth to the onset of puberty. *J Anat, 134*(Pt 2), 351-363.

Oakberg, E. F. (1956a). A description of spermiogenesis in the mouse and its use in analysis of the cycle of the seminiferous epithelium and germ cell renewal. *Am J Anat, 99*(3), 391-413. doi:10.1002/aja.1000990303

Oakberg, E. F. (1956b). Duration of spermatogenesis in the mouse and timing of stages of the cycle of the seminiferous epithelium. *Am J Anat, 99*(3), 507-516. doi:10.1002/aja.1000990307

Oakberg, E. F. (1971). Spermatogonial stem-cell renewal in the mouse. *Anat.Rec., 169*(3), 515-531.

Oatley, J. M., Avarbock, M. R., Telaranta, A. I., Fearon, D. T., & Brinster, R. L. (2006). Identifying genes important for spermatogonial stem cell self-renewal and survival. *Proc Natl Acad Sci U S A, 103*(25), 9524-9529. doi:10.1073/pnas.0603332103

Oatley, J. M., & Brinster, R. L. (2006). Spermatogonial stem cells. *Methods Enzymol, 419*, 259-282. doi:10.1016/S0076-6879(06)19011-4

Oatley, J. M., & Brinster, R. L. (2012). The germline stem cell niche unit in mammalian testes. *Physiol Rev, 92*(2), 577-595. doi:10.1152/physrev.00025.2011

Oatley, J. M., de Avila, D. M., Reeves, J. J., & McLean, D. J. (2004). Spermatogenesis and germ cell transgene expression in xenografted bovine testicular tissue. *Biology of Reproduction, 71*(2), 494-501. doi:10.1095/biolreprod.104.027953

Oatley, J. M., Oatley, M. J., Avarbock, M. R., Tobias, J. W., & Brinster, R. L. (2009). Colony stimulating factor 1 is an extrinsic stimulator of mouse spermatogonial stem cell self-renewal. *Development, 136*(7), 1191-1199. doi:Doi 10.1242/Dev.032243

Oatley, J. M., Reeves, J. J., & McLean, D. J. (2005). Establishment of spermatogenesis in neonatal bovine testicular tissue following ectopic xenografting varies with donor age. *Biology of Reproduction, 72*(2), 358-364. doi:10.1095/biolreprod.104.030783

Oatley, M. J., Kaucher, A. V., Racicot, K. E., & Oatley, J. M. (2011). Inhibitor of DNA binding 4 is expressed selectively by single spermatogonia in the male germline and regulates the

self-renewal of spermatogonial stem cells in mice. *Biology of Reproduction, 85*(2), 347-356. doi:10.1095/biolreprod.111.091330

Ogawa, T., Dobrinski, I., Avarbock, M. R., & Brinster, R. L. (2000). Transplantation of male germ line stem cells restores fertility in infertile mice. *Nat Med, 6*(1), 29-34. doi:10.1038/71496

Ogawa, T., Dobrinski, I., & Brinster, R. L. (1999). Recipient preparation is critical for spermatogonial transplantation in the rat. *Tissue & Cell, 31*(5), 461-472.

Omurtag, K., Cooper, A., Bullock, A., Naughton, C., Ratts, V., Odem, R., & Lanzendorf, S. E. (2013). Sperm recovery and IVF after testicular sperm extraction (TESE): effect of male diagnosis and use of off-site surgical centers on sperm recovery and IVF. *PLoS ONE, 8*(7), e69838. doi:10.1371/journal.pone.0069838

Onofre, J., Baert, Y., Faes, K., & Goossens, E. (2016). Cryopreservation of testicular tissue or testicular cell suspensions: a pivotal step in fertility preservation. *Hum Reprod Update, 22*(6), 744-761. doi:10.1093/humupd/dmw029

Orwig, K. E., Ryu, B. Y., Master, S. R., Phillips, B. T., Mack, M., Avarbock, M. R., . . . Brinster, R. L. (2008). Genes involved in post-transcriptional regulation are overrepresented in stem/progenitor spermatogonia of cryptorchid mouse testes. *Stem Cells, 26*(4), 927-938. doi:10.1634/stemcells.2007-0893

Orwig, K. E., & Schlatt, S. (2005). Cryopreservation and transplantation of spermatogonia and testicular tissue for preservation of male fertility. *J Natl Cancer Inst Monogr, 34*(34), 51-56. doi:10.1093/jncimonographs/lgi029

Ostrer, H., Huang, H. Y., Masch, R. J., & Shapiro, E. (2007). A cellular study of human testis development. *Sex Dev, 1*(5), 286-292. doi:10.1159/000108930

Oulad-Abdelghani, M., Bouillet, P., Decimo, D., Gansmuller, A., Heyberger, S., Dolle, P., . . . Chambon, P. (1996). Characterization of a premeiotic germ cell-specific cytoplasmic protein encoded by Stra8, a novel retinoic acid-responsive gene. *J Cell Biol, 135*(2), 469-477.

Pacchiarotti, J., Ramos, T., Howerton, K., Greilach, S., Zaragoza, K., Olmstead, M., & Izadyar, F. (2013). Developing a Clinical-Grade Cryopreservation Protocol for Human Testicular Tissue and Cells. *BioMed Research International, 2013*, 10. doi:10.1155/2013/930962

Paniagua, R., & Nistal, M. (1984). Morphological and histometric study of human spermatogonia from birth to the onset of puberty. *J Anat, 139 (Pt 3)*, 535-552.

Parrish, A. B., Freel, C. D., & Kornbluth, S. (2013). Cellular mechanisms controlling caspase activation and function. *Cold Spring Harb Perspect Biol, 5*(6). doi:10.1101/cshperspect.a008672

Phillips, B. T., Gassei, K., & Orwig, K. E. (2010). Spermatogonial stem cell regulation and spermatogenesis. *Philos Trans R Soc Lond B Biol Sci, 365*(1546), 1663-1678. doi:10.1098/rstb.2010.0026

Pierard, G. E. (1999). EEMCO guidance to the in vivo assessment of tensile functional properties of the skin. Part 1: relevance to the structures and ageing of the skin and subcutaneous tissues. *Skin Pharmacol Appl Skin Physiol, 12*(6), 352-362. doi:10.1159/000029897

Plant, T. M. (1981). Time courses of concentrations of circulating gonadotropin, prolactin, testosterone, and cortisol in adult male rhesus monkeys (Macaca mulatta) throughout the 24 h light-dark cycle. *Biology of Reproduction, 25*(2), 244-252.

Plant, T. M. (2006). The male monkey as a model for the study of the neurobiology of puberty onset in man. *Mol Cell Endocrinol, 254-255*, 97-102. doi:10.1016/j.mce.2006.04.022

Plant, T. M. (2010). Undifferentiated primate spermatogonia and their endocrine control. *Trends Endocrinol Metab, 21*(8), 488-495. doi:10.1016/j.tem.2010.03.001

Plant, T. M., Ramaswamy, S., Simorangkir, D., & Marshall, G. R. (2005). Postnatal and pubertal development of the rhesus monkey (Macaca mulatta) testis. *Ann N Y Acad Sci, 1061*, 149-162. doi:10.1196/annals.1336.016

Povlsen, C. O., Skakkebaek, N. E., Rygaard, J., & Jensen, G. (1974). Heterotransplantation of human foetal organs to the mouse mutant nude. *Nature, 248*(445), 247-249.

Prince, F. P. (2001). The triphasic nature of Leydig cell development in humans, and comments on nomenclature. *J Endocrinol, 168*(2), 213-216.

Rahman, M. B., Vandaele, L., Rijsselaere, T., Maes, D., Hoogewijs, M., Frijters, A., . . . Van Soom, A. (2011). Scrotal insulation and its relationship to abnormal morphology, chromatin protamination and nuclear shape of spermatozoa in Holstein-Friesian and Belgian Blue bulls. *Theriogenology, 76*(7), 1246-1257. doi:10.1016/j.theriogenology.2011.05.031

Ramaswamy, S., Marshall, G. R., McNeilly, A. S., & Plant, T. M. (2000). Dynamics of the follicle-stimulating hormone (FSH)-inhibin B feedback loop and its role in regulating spermatogenesis in the adult male rhesus monkey (Macaca mulatta) as revealed by unilateral orchidectomy. *Endocrinology, 141*(1), 18-27.

Ramaswamy, S., Razack, B. S., Roslund, R. M., Suzuki, H., Marshall, G. R., Rajkovic, A., & Plant, T. M. (2014). Spermatogonial SOHLH1 nucleocytoplasmic shuttling associates with initiation of spermatogenesis in the rhesus monkey (Macaca mulatta). *Molecular Human Reproduction, 20*(4), 350-357. doi:10.1093/molehr/gat093

Ramaswamy, S., & Weinbauer, G. F. (2014). Endocrine control of spermatogenesis: Role of FSH and LH/ testosterone. *Spermatogenesis, 4*(2), e996025. doi:10.1080/21565562.2014.996025

Rathi, R., Honaramooz, A., Zeng, W., Schlatt, S., & Dobrinski, I. (2005). Germ cell fate and seminiferous tubule development in bovine testis xenografts. *Reproduction, 130*(6), 923-929.

Rathi, R., Honaramooz, A., Zeng, W., Turner, R., & Dobrinski, I. (2006). Germ cell development in equine testis tissue xenografted into mice. *Reproduction, 131*(6), 1091-1098.

Rathi, R., Zeng, W., Megee, S., Conley, A., Meyers, S., & Dobrinski, I. (2008). Maturation of Testicular Tissue from Infant Monkeys after Xenografting into Mice. *Endocrinology, 149*(10), 5288-5296. doi:10.1210/en.2008-0311

Resko, J. A., Quadri, S. K., & Spies, H. G. (1977). Negative feedback control of gonadotropins in male rhesus monkeys: effects of time after castration and interactions of testosterone and estradiol-17beta. *Endocrinology, 101*(1), 215-224. doi:10.1210/endo-101-1-215

Richter, C. P., Wislocki, G. B. (1928). Activity studies on castrated male and female rats with testicular grafts, in correlation with histopathological studies of grafts. *American Journal of Physiology, 86*, 10. doi:https://doi.org/10.1152/ajplegacy.1928.86.3.651

Roosen-Runge, E. C. (1962). The process of spermatogenesis in mammals. *Biol Rev Camb Philos Soc, 37*, 343-377.

Rucker, M., Roesken, F., Vollmar, B., & Menger, M. D. (1998). A novel approach for comparative study of periosteum, muscle, subcutis, and skin microcirculation by intravital fluorescence microscopy. *Microvasc Res, 56*(1), 30-42. doi:10.1006/mvre.1998.2077

Russell, L. D., Ettlin, R. A., SinhaHikim, A. P., & Clegg, E. D. (1990). *Histological and histopathological evaluation of the testis* (Vol. 1st). Clearwater, FL: Cache River Press.

Ryu, B. Y., Orwig, K. E., Kubota, H., Avarbock, M. R., & Brinster, R. L. (2004). Phenotypic and functional characteristics of spermatogonial stem cells in rats. *Dev Biol, 274*(1), 158-170. doi:10.1016/j.ydbio.2004.07.004

Sada, A., Suzuki, A., Suzuki, H., & Saga, Y. (2009). The RNA-Binding Protein NANOS2 Is Required to Maintain Murine Spermatogonial Stem Cells. *Science, 325*(5946), 1394-1398.

Sadri-Ardekani, H., Mizrak, S. C., van Daalen, S. K., Korver, C. M., Roepers-Gajadien, H. L., Koruji, M., . . . van Pelt, A. M. (2009). Propagation of human spermatogonial stem cells in vitro. *JAMA, 302*(19), 2127-2134. doi:10.1001/jama.2009.1689

Saitou, M. (2009). Germ cell specification in mice. *Curr Opin Genet Dev, 19*(4), 386-395. doi:10.1016/j.gde.2009.06.003

Sakamoto, H., Ogawa, Y., & Yoshida, H. (2008). Relationship between testicular volume and testicular function: comparison of the Prader orchidometric and ultrasonographic measurements in patients with infertility. *Asian J Androl, 10*(2), 319-324. doi:10.1111/j.1745-7262.2008.00340.x

Sand, K. (1919). Experiments on the internal secretion of the sexual glands, especially on experimental hermaphroditism. *Journal of Physiology, 53*(3-4), 7.

Sanzey, M., Abdul Rahim, S. A., Oudin, A., Dirkse, A., Kaoma, T., Vallar, L., . . . Niclou, S. P. (2015). Comprehensive analysis of glycolytic enzymes as therapeutic targets in the treatment of glioblastoma. *PLoS ONE, 10*(5), e0123544. doi:10.1371/journal.pone.0123544

Sato, Y., Nozawa, S., Yoshiike, M., Arai, M., Sasaki, C., & Iwamoto, T. (2010). Xenografting of testicular tissue from an infant human donor results in accelerated testicular maturation. *Human Reproduction, 25*(5), 1113-1122. doi:10.1093/humrep/deq001

Schlatt, S., Ehmcke, J., & Jahnukainen, K. (2009). Testicular stem cells for fertility preservation: preclinical studies on male germ cell transplantation and testicular grafting. *Pediatr Blood Cancer, 53*(2), 274-280. doi:10.1002/pbc.22002

Schlatt, S., Foppiani, L., Rolf, C., Weinbauer, G. F., & Nieschlag, E. (2002a). Germ cell transplantation into X-irradiated monkey testes. *Hum Reprod, 17*(1), 55-62.

Schlatt, S., Honaramooz, A., Ehmcke, J., Goebell, P. J., Rubben, H., Dhir, R., . . . Patrizio, P. (2006). Limited survival of adult human testicular tissue as ectopic xenograft. *Human Reproduction, 21*(2), 384-389. doi:DOI 10.1093/humrep/dei352

Schlatt, S., Kim, S. S., & Gosden, R. (2002b). Spermatogenesis and steroidogenesis in mouse, hamster and monkey testicular tissue after cryopreservation and heterotopic grafting to castrated hosts. *Reproduction, 124*(3), 339-346.

Schlatt, S., & Weinbauer, G. F. (1994). Immunohistochemical localization of proliferating cell nuclear antigen as a tool to study cell proliferation in rodent and primate testes. *Int J Androl, 17*(4), 214-222.

Scholzen, T., & Gerdes, J. (2000). The Ki-67 protein: from the known and the unknown. *J.Cell Physiol, 182*(3), 311-322.

Schrans-Stassen, B. H., van de Kant, H. J., de Rooij, D. G., & van Pelt, A. M. (1999). Differential expression of c-kit in mouse undifferentiated and differentiating type A spermatogonia. *Endocrinology, 140*(12), 5894-5900.

Setchell, B. P. (1990). The testis and tissue transplantation: historical aspects. *J Reprod Immunol, 18*(1), 1-8.

Sharpe, R. M. (1994). Regulation of Spermatogenesis. In E. Knobil & J. D. Neill (Eds.), *The Physiology of Reproduction* (pp. 1363-1434). New York: Raven Press, Ltd. (Reprinted from: NOT IN FILE).

Shen, Z., Pardington-Purtymun, P. E., Comeaux, J. C., Moyzis, R. K., & Chen, D. J. (1996). UBL1, a human ubiquitin-like protein associating with human RAD51/RAD52 proteins. *Genomics, 36*(2), 271-279. doi:10.1006/geno.1996.0462

Shima, J. E., McLean, D. J., McCarrey, J. R., & Griswold, M. D. (2004). The murine testicular transcriptome: characterizing gene expression in the testis during the progression of spermatogenesis. *Biology of Reproduction, 71*(1), 319-330. doi:10.1095/biolreprod.103.026880

Shinohara, T., Avarbock, M. R., & Brinster, R. L. (1999). beta1- and alpha6-integrin are surface markers on mouse spermatogonial stem cells. *Proc Natl Acad Sci U S A, 96*(10), 5504-5509.

Shinohara, T., Inoue, K., Ogonuki, N., Kanatsu-Shinohara, M., Miki, H., Nakata, K., . . . Ogura, A. (2002). Birth of offspring following transplantation of cryopreserved immature testicular pieces and in-vitro microinsemination. *Hum Reprod, 17*(12), 3039-3045.

Simorangkir, D. R., Marshall, G. R., Ehmcke, J., Schlatt, S., & Plant, T. M. (2005). Prepubertal expansion of dark and pale type A spermatogonia in the rhesus monkey (Macaca mulatta) results from proliferation during infantile and juvenile development in a relatively gonadotropin independent manner. *Biology of Reproduction, 73*(6), 1109-1115. doi:10.1095/biolreprod.105.044404

Simorangkir, D. R., Marshall, G. R., & Plant, T. M. (2009a). A re-examination of proliferation and differentiation of type A spermatogonia in the adult rhesus monkey (Macaca mulatta). *Hum Reprod, 24*(7), 1596-1604. doi:10.1093/humrep/dep051

Simorangkir, D. R., Ramaswamy, S., Marshall, G. R., Pohl, C. R., & Plant, T. M. (2009b). A selective monotropic elevation of FSH, but not that of LH, amplifies the proliferation and differentiation of spermatogonia in the adult rhesus monkey (Macaca mulatta). *Hum Reprod, 24*(7), 1584-1595. doi:10.1093/humrep/dep052

Simorangkir, D. R., Ramaswamy, S., Marshall, G. R., Roslund, R., & Plant, T. M. (2012). Sertoli cell differentiation in rhesus monkey (Macaca mulatta) is an early event in puberty and precedes attainment of the adult complement of undifferentiated spermatogonia. *Reproduction, 143*(4), 513-522. doi:10.1530/REP-11-0411

Sinha Hikim, A. P., Lue, Y., Diaz-Romero, M., Yen, P. H., Wang, C., & Swerdloff, R. S. (2003). Deciphering the pathways of germ cell apoptosis in the testis. *J Steroid Biochem Mol Biol, 85*(2-5), 175-182.

Skakkebaek, N. E., Jensen, G., Povlsen, C. O., & Rygaard, J. (1974). Heterotransplantation of human foetal testicular and ovarian tissue to the mouse mutant nude. A preliminary study. *Acta Obstet Gynecol Scand Suppl, 29*, 73-75.

Smith, B. E., & Braun, R. E. (2012). Germ cell migration across Sertoli cell tight junctions. *Science, 338*(6108), 798-802. doi:10.1126/science.1219969

Smith, J. F., Yango, P., Altman, E., Choudhry, S., Poelzl, A., Zamah, A. M., . . . Tran, N. D. (2014). Testicular niche required for human spermatogonial stem cell expansion. *Stem Cells Transl Med, 3*(9), 1043-1054. doi:10.5966/sctm.2014-0045

Snedaker, A. K., Honaramooz, A., & Dobrinski, I. (2004). A Game of Cat and Mouse: Xenografting of Testis Tissue From Domestic Kittens Results in Complete Cat Spermatogenesis in a Mouse Host. *J Androl, 25*(6), 926-930.

Stanley, L. L. (1920). Experiences in Testicle Transplantation. *Cal State J Med, 18*(7), 251-253.

Steger, K., Aleithe, I., Behre, H., & Bergmann, M. (1998). The proliferation of spermatogonia in normal and pathological human seminiferous epithelium: an immunohistochemical study using monoclonal antibodies against Ki-67 protein and proliferating cell nuclear antigen. *Molecular Human Reproduction, 4*(3), 227-233.

Steinach, E. (1910). Geschelchtstrieb und echtsekundare Geschelchtsmerkmale als folgender innersekretorischen Funktion der Keimdrusen. *Centrlbl. Physio, 24*, 16.

Suzuki, H., Ahn, H. W., Chu, T., Bowden, W., Gassei, K., Orwig, K., & Rajkovic, A. (2012). SOHLH1 and SOHLH2 coordinate spermatogonial differentiation. *Dev Biol, 361*(2), 301-312. doi:10.1016/j.ydbio.2011.10.027

Suzuki, H., Sada, A., Yoshida, S., & Saga, Y. (2009). The heterogeneity of spermatogonia is revealed by their topology and expression of marker proteins including the germ cell-specific proteins Nanos2 and Nanos3. *Dev Biol, 336*(2), 222-231. doi:10.1016/j.ydbio.2009.10.002

Svingen, T., & Koopman, P. (2013). Building the mammalian testis: origins, differentiation, and assembly of the component cell populations. *Genes Dev, 27*(22), 2409-2426. doi:10.1101/gad.228080.113

Tachibana, M., Sparman, M., & Mitalipov, S. (2010). Chromosome transfer in mature oocytes. *Nat Protoc, 5*(6), 1138-1147. doi:10.1038/nprot.2010.75

Tang, W. W., Kobayashi, T., Irie, N., Dietmann, S., & Surani, M. A. (2016). Specification and epigenetic programming of the human germ line. *Nat Rev Genet, 17*(10), 585-600. doi:10.1038/nrg.2016.88

Teerds, K. J., & Huhtaniemi, I. T. (2015). Morphological and functional maturation of Leydig cells: from rodent models to primates. *Hum Reprod Update, 21*(3), 310-328. doi:10.1093/humupd/dmv008

Tegelenbosch, R. A., & de Rooij, D. G. (1993). A quantitative study of spermatogonial multiplication and stem cell renewal in the C3H/101 F1 hybrid mouse. *Mutat Res, 290*(2), 193-200.

Thayer, K. A., Ruhlen, R. L., Howdeshell, K. L., Buchanan, D. L., Cooke, P. S., Preziosi, D., . . . vom Saal, F. S. (2001). Altered prostate growth and daily sperm production in male mice exposed prenatally to subclinical doses of 17a-ethinyl oestradiol. *Human Reproduction, 16*(5), 988-996.

Thomson, A. B., Campbell, A. J., Irvine, D. C., Anderson, R. A., Kelnar, C. J., & Wallace, W. H. (2002). Semen quality and spermatozoal DNA integrity in survivors of childhood cancer: a case-control study. *Lancet, 360*(9330), 361-367.

Tohonen, V., Ritzen, E. M., Nordqvist, K., & Wedell, A. (2003). Male sex determination and prenatal differentiation of the testis. *Endocr Dev, 5*, 1-23.

Tokuda, M., Kadokawa, Y., Kurahashi, H., & Marunouchi, T. (2007). CDH1 is a specific marker for undifferentiated spermatogonia in mouse testes. *Biol Reprod, 76*(1), 130-141. doi:10.1095/biolreprod.106.053181

Turner, C. D. (1938). Intra-ocular homotransplantation of prepuberal testes in the rat. *American Journal of Anatomy, 63*, 59. doi:10.1002/aja.1000630105

Valli, H., Gassei, K., & Orwig, K. E. (2015a). Stem cell therapies for male infertility: where are we now and where are we going? In D. T. Carrell, P. N. Schlegel, C. Racowsky, & L. Gianaroli (Eds.), *Biennial Review of Infertility* (Vol. 4, pp. 17-39). Switzerland: Springer International Publishing.

Valli, H., Phillips, B. T., Gassei, K., Nagano, M. C., & Orwig, K. E. (2015b). Spermatogonial Stem Cells and Spermatogenesis. In T. M. Plant & A. J. Zeleznik (Eds.), *Knobil and Neill's Physiology of Reproduction* (Fourth ed., Vol. 1, pp. 595-635). San Diego: Elsevier.

Valli, H., Phillips, B. T., Shetty, G., Byrne, J. A., Clark, A. T., Meistrich, M. L., & Orwig, K. E. (2014a). Germline stem cells: toward the regeneration of spermatogenesis. *Fertility and Sterility, 101*(1), 3-13. doi:10.1016/j.fertnstert.2013.10.052

Valli, H., Sukhwani, M., Dovey, S. L., Peters, K. A., Donohue, J., Castro, C. A., . . . Orwig, K. E. (2014b). Fluorescence- and magnetic-activated cell sorting strategies to isolate and enrich human spermatogonial stem cells. *Fertil Steril, 102*(2), 566-580. doi:10.1016/j.fertnstert.2014.04.036

van Alphen, M. M., & de Rooij, D. G. (1986). Depletion of the seminiferous epithelium of the rhesus monkey, Macaca mulatta, after X-irradiation. *Br J Cancer Suppl, 7*, 102-104.

van Alphen, M. M., van de Kant, H. J., & de Rooij, D. G. (1988). Repopulation of the seminiferous epithelium of the rhesus monkey after X irradiation. *Radiat Res, 113*(3), 487-500.

van Bragt, M. P., Roepers-Gajadien, H. L., Korver, C. M., Bogerd, J., Okuda, A., Eggen, B. J., . . . van Pelt, A. M. (2008). Expression of the pluripotency marker UTF1 is restricted to a subpopulation of early A spermatogonia in rat testis. *Reproduction, 136*(1), 33-40. doi:10.1530/REP-07-0536

van den Boom, V., Kooistra, S. M., Boesjes, M., Geverts, B., Houtsmuller, A. B., Monzen, K., . . . Eggen, B. J. (2007). UTF1 is a chromatin-associated protein involved in ES cell differentiation. *J Cell Biol, 178*(6), 913-924. doi:10.1083/jcb.200702058

Van Saen, D., Goossens, E., Bourgain, C., Ferster, A., & Tournaye, H. (2011). Meiotic activity in orthotopic xenografts derived from human postpubertal testicular tissue. *Human Reproduction, 26*(2), 282-293. doi:10.1093/humrep/deq321

Vergouwen, R. P., Jacobs, S. G., Huiskamp, R., Davids, J. A., & de Rooij, D. G. (1991). Proliferative activity of gonocytes, Sertoli cells and interstitial cells during testicular development in mice. *J Reprod Fertil, 93*(1), 233-243.

Verhagen, I., Ramaswamy, S., Teerds, K. J., Keijer, J., & Plant, T. M. (2014). Time course and role of luteinizing hormone and follicle-stimulating hormone in the expansion of the Leydig cell population at the time of puberty in the rhesus monkey (Macaca mulatta). *Andrology, 2*(6), 924-930. doi:10.1111/andr.275

von Kopylow, K., Kirchhoff, C., Jezek, D., Schulze, W., Feig, C., Primig, M., . . . Spiess, A. N. (2010). Screening for biomarkers of spermatogonia within the human testis: a whole genome approach. *Hum Reprod, 25*(5), 1104-1112. doi:10.1093/humrep/deq053

von Kopylow, K., Staege, H., Schulze, W., Will, H., & Kirchhoff, C. (2012a). Fibroblast growth factor receptor 3 is highly expressed in rarely dividing human type A spermatogonia. *Histochem Cell Biol, 138*(5), 759-772. doi:10.1007/s00418-012-0991-7

von Kopylow, K., Staege, H., Spiess, A. N., Schulze, W., Will, H., Primig, M., & Kirchhoff, C. (2012b). Differential marker protein expression specifies rarefaction zone-containing human Adark spermatogonia. *Reproduction, 143*(1), 45-57. doi:10.1530/REP-11-0290

Walker, W. H. (2010). Non-classical actions of testosterone and spermatogenesis. *Philos Trans R Soc Lond B Biol Sci, 365*(1546), 1557-1569. doi:10.1098/rstb.2009.0258

Walker, W. H., & Cheng, J. (2005). FSH and testosterone signaling in Sertoli cells. *Reproduction, 130*(1), 15-28. doi:10.1530/rep.1.00358

Wallace, W. H., Anderson, R. A., & Irvine, D. S. (2005). Fertility preservation for young patients with cancer: who is at risk and what can be offered? *Lancet Oncol, 6*(4), 209-218. doi:10.1016/S1470-2045(05)70092-9

Walls, G. V., Reed, A. A., Jeyabalan, J., Javid, M., Hill, N. R., Harding, B., & Thakker, R. V. (2012). Proliferation rates of multiple endocrine neoplasia type 1 (MEN1)-associated tumors. *Endocrinology, 153*(11), 5167-5179. doi:10.1210/en.2012-1675

Walter, C. A., Intano, G. W., McCarrey, J. R., McMahan, C. A., & Walter, R. B. (1998). Mutation frequency declines during spermatogenesis in young mice but increases in old mice. *Proc Natl Acad Sci U S A, 95*(17), 10015-10019.

Wang, Y., Chang, Q., Sun, J., Dang, L., Ma, W., Hei, C., . . . Jiang, X. (2012). Effects of HMG on revascularization and follicular survival in heterotopic autotransplants of mouse ovarian tissue. *Reprod Biomed Online, 24*(6), 646-653. doi:10.1016/j.rbmo.2012.02.025

Weinbauer, G. F., Gockeler, E., & Nieschlag, E. (1988). Testosterone prevents complete suppression of spermatogenesis in the gonadotropin-releasing hormone antagonist-treated nonhuman primate (Macaca fascicularis). *J Clin Endocrinol Metab, 67*(2), 284-290. doi:10.1210/jcem-67-2-284

Wen, Q., Cheng, C. Y., & Liu, Y. X. (2016). Development, function and fate of fetal Leydig cells. *Semin Cell Dev Biol, 59*, 89-98. doi:10.1016/j.semcdb.2016.03.003

Wen, Q., Zheng, Q. S., Li, X. X., Hu, Z. Y., Gao, F., Cheng, C. Y., & Liu, Y. X. (2014). Wt1 dictates the fate of fetal and adult Leydig cells during development in the mouse testis. *Am J Physiol Endocrinol Metab, 307*(12), E1131-1143. doi:10.1152/ajpendo.00425.2014

Wilkinson, K. D., Lee, K. M., Deshpande, S., Duerksen-Hughes, P., Boss, J. M., & Pohl, J. (1989). The neuron-specific protein PGP 9.5 is a ubiquitin carboxyl-terminal hydrolase. *Science, 246*(4930), 670-673.

Williams, R. G. (1949). Some responses of living blood vessels and connective tissue to testicular grafts in rabbits. *Anat Rec, 104*(2), 147-161.

Williams, R. G. (1950). Studies of living interstitial cells and pieces of seminiferous tubles in autogenous grafts of testis. *Am J Anat, 86*(3), 343-369. doi:10.1002/aja.1000860302

Wistuba, J., Luetjens, C. M., Wesselmann, R., Nieschlag, E., Simoni, M., & Schlatt, S. (2006a). Meiosis in autologous ectopic transplants of immature testicular tissue grafted to Callithrix jacchus. *Biology of Reproduction, 74*(4), 706-713. doi:10.1095/biolreprod.105.048793

Wistuba, J., Luetjens, C. M., Wesselmann, R., Nieschlag, E., Simoni, M., & Schlatt, S. (2006b). Meiosis in autologous ectopic transplants of immature testicular tissue grafted to Callithrix jacchus. *Biol Reprod, 74*(4), 706-713. doi:10.1095/biolreprod.105.048793

Wolf, D. P. (2004). Assisted reproductive technologies in rhesus macaques. *Reprod Biol Endocrinol, 2*, 37. doi:10.1186/1477-7827-2-37

Wolf, D. P., Thomson, J. A., Zelinski-Wooten, M. B., & Stouffer, R. L. (1990). In vitro fertilization-embryo transfer in nonhuman primates: the technique and its applications. *Mol Reprod Dev, 27*(3), 261-280. doi:10.1002/mrd.1080270313

Wolf, D. P., Thormahlen, S., Ramsey, C., Yeoman, R. R., Fanton, J., & Mitalipov, S. (2004). Use of Assisted Reproductive Technologies in the Propagation of Rhesus Macaque Offspring. *Biology of Reproduction, 71*(2), 486-493. doi:10.1095/biolreprod.103.025932

Wyns, C., Curaba, M., Petit, S., Vanabelle, B., Laurent, P., Wese, J. F., & Donnez, J. (2011). Management of fertility preservation in prepubertal patients: 5 years' experience at the Catholic University of Louvain. *Hum Reprod, 26*(4), 737-747. doi:10.1093/humrep/deq387

Wyns, C., Van Langendonckt, A., Wese, F. X., Donnez, J., & Curaba, M. (2008). Long-term spermatogonial survival in cryopreserved and xenografted immature human testicular tissue. *Human Reproduction, 23*(11), 2402-2414. doi:10.1093/humrep/den272

Ya-Xian, Z., Suetake, T., & Tagami, H. (1999). Number of cell layers of the stratum corneum in normal skin - relationship to the anatomical location on the body, age, sex and physical parameters. *Arch Dermatol Res, 291*(10), 555-559.

Yeh, J. R., Zhang, X., & Nagano, M. C. (2011). Wnt5a is a cell-extrinsic factor that supports self-renewal of mouse spermatogonial stem cells. *J Cell Sci, 124*(Pt 14), 2357-2366. doi:10.1242/jcs.080903

Ying, Y., Qi, X., & Zhao, G. Q. (2001). Induction of primordial germ cells from murine epiblasts by synergistic action of BMP4 and BMP8B signaling pathways. *Proc Natl Acad Sci U S A, 98*(14), 7858-7862. doi:10.1073/pnas.151242798

Yoshida, S., Sukeno, M., Nakagawa, T., Ohbo, K., Nagamatsu, G., Suda, T., & Nabeshima, Y. (2006). The first round of mouse spermatogenesis is a distinctive program that lacks the self-renewing spermatogonia stage. *Development, 133*(8), 1495-1505. doi:Doi 10.1242/Dev.02316

Yoshida, S., Takakura, A., Ohbo, K., Abe, K., Wakabayashi, J., Yamamoto, M., . . . Nabeshima, Y. (2004). Neurogenin3 delineates the earliest stages of spermatogenesis in the mouse testis. *Dev Biol, 269*(2), 447-458. doi:10.1016/j.ydbio.2004.01.036

Yoshinaga, K., Nishikawa, S., Ogawa, M., Hayashi, S. I., Kunisada, T., Fujimoto, T., & Nishikawa, S. I. (1991). Role of C-Kit in Mouse Spermatogenesis - Identification of Spermatogonia as a Specific Site of C-Kit Expression and Function. *Development, 113*(2), 689-699.

Yu, J., Cai, Z. M., Wan, H. J., Zhang, F. T., Ye, J., Fang, J. Z., . . . Ye, J. X. (2006). Development of neonatal mouse and fetal human testicular tissue as ectopic grafts in immunodeficient mice. *Asian J Androl, 8*(4), 393-403. doi:10.1111/j.1745-7262.2006.00189.x

Zhang, Z., Shao, S., & Meistrich, M. L. (2007). The radiation-induced block in spermatogonial differentiation is due to damage to the somatic environment, not the germ cells. *J Cell Physiol, 211*(1), 149-158. doi:10.1002/jcp.20910

Zheng, K., Wu, X., Kaestner, K., & Wang, P. (2009). The pluripotency factor LIN28 marks undifferentiated spermatogonia in mouse. *BMC Dev Biol, 9*(1), 38.

Zheng, Y., Thomas, A., Schmidt, C. M., & Dann, C. T. (2014). Quantitative detection of human spermatogonia for optimization of spermatogonial stem cell culture. *Hum Reprod, 29*(11), 2497-2511. doi:10.1093/humrep/deu232

Zhou, Q., Wang, M., Yuan, Y., Wang, X., Fu, R., Wan, H., . . . Zhou, Q. (2016). Complete Meiosis from Embryonic Stem Cell-Derived Germ Cells In Vitro. *Cell Stem Cell, 18*(3), 330-340. doi:10.1016/j.stem.2016.01.017